2001

The Flexural Response of Bolted Composite Panels at Elevated Temperature

Christopher Gary Malm

THE FLEXURAL RESPONSE OF BOLTED COMPOSITE PANELS AT ELEVATED TEMPERATURE

By

Christopher Gary Malm

B.S. University of Maine, 1999

A THESIS

Submitted in Partial Fulfillment of the

Requirements for the Degree of

Master of Science

(in Mechanical Engineering)

The Graduate School

The University of Maine

May 2001

Advisory Committee:

Vince Caccese, Associate Professor of Mechanical Engineering, Advisor

Donald Grant, Professor of Mechanical Engineering

Christine Valle, Assistant Professor of Mechanical Engineering

Roberto Lopez-Anido, Assistant Professor of Civil Engineering

THE FLEXURAL RESPONSE OF BOLTED COMPOSITE PANELS AT ELEVATED TEMPERATURE

By Christopher Gary Malm

Thesis Advisor: Dr. Vincent Caccese

An Abstract of the Thesis Presented
in Partial Fulfillment of the Requirements for the
Degree of Master of Science
(in Mechanical Engineering)
May, 2001

Carbon fiber/cyanate ester matrix composite panels with bolted connections to aluminum endplates were tested in four point bending at room and elevated temperatures. The specimens tested were subcomponents of the NASA X-38 Crew Return Vehicle. The X-38 is the proposed escape vehicle for the International Space Station, currently being constructed in Earth orbit. During reentry into the Earth's atmosphere, the composite aeroshell of the X-38 is expected to experience elevated temperatures, which makes accurate characterization of material properties at elevated temperature imperative to a sound design. Three varieties of specimens were tested: flat composite laminates, hat-stiffened composite laminates, and sandwich construction composite panels. Instrumentation was used to collect displacement, strain, load, and temperature data. The data were then used to characterize the effects of the elevated temperature environment on the stiffness, strength, and failure modes

of the composite material. After inspection of the results, the elevated temperature environment had a marked effect, lowering the stiffness and ultimate load capacity of the hat-stiffened and sandwich panels. The modes of failure for the hat-stiffened laminates were highly temperature dependent, while the effects of elevated temperature on the failure modes for the sandwich panels was not apparent from the data.

A simplified beam analysis, using strength of materials beam theory, was undertaken to characterize the joint stiffness in the room temperature experimental set-up. Results indicated a good correlation between the experimental deflected shape and the predicted deflected shape of the flat composite laminates, hat-stiffened laminates, and the composite sandwich panels.

Acknowledgements

The author would like to thank Dr. Vince Caccese for being a very supportive graduate advisor. The assistance of several undergraduate and graduate students, including Jean-Paul Kabche, Joshua Walls, Richard Mewer, and Thomas McNichols, is greatly appreciated. The assistance of Arthur Pete, the manager of the University of Maine Crosby Laboratories, is also appreciated. The author wants to thank the Maine Space Grant Consortium. Their generous funding paid for a large portion of the author's graduate education and his 5-week stay at NASA's Johnson Space Center during the summer of 2000. Also, the author would like to thank the members of his graduate committee, Dr. Donald Grant, Dr. Christine Valle, and Dr. Roberto Lopez-Anido, for their input and support. Finally, the author would like to thank his parents for their support.

Table of Contents

List of Tables

List of Figures

1. Overview

1.1 Introduction

The NASA X-38 Crew Return Vehicle is the proposed escape vehicle for the International Space System (ISS), which is now being constructed in Earth orbit. The geometry of the X-38 is based on the SV-5 lifting body shape, which was originally developed by the Air Force in the 1960s. The entire body of the craft is designed to produce lift, as opposed to most other aircraft where only the wings, and not the fuselage, contribute to the lift. A prototype X-38, known as vehicle 201, is currently being constructed at NASA's Lyndon B. Johnson Space Center (JSC) in Houston, Texas. The craft will be 28.5 feet (8.69 m) long, 14.5 feet (4.42 m) wide, will weigh about 16,000 pounds (71 kN), and be able to carry six passengers. The X-38 will eventually replace a Russian Soyuz spacecraft, which will serve as the space station's escape vehicle in its early years of construction and operation. Figure 1.1 is an artist's concept of the X-38 entering the Earth's atmosphere.

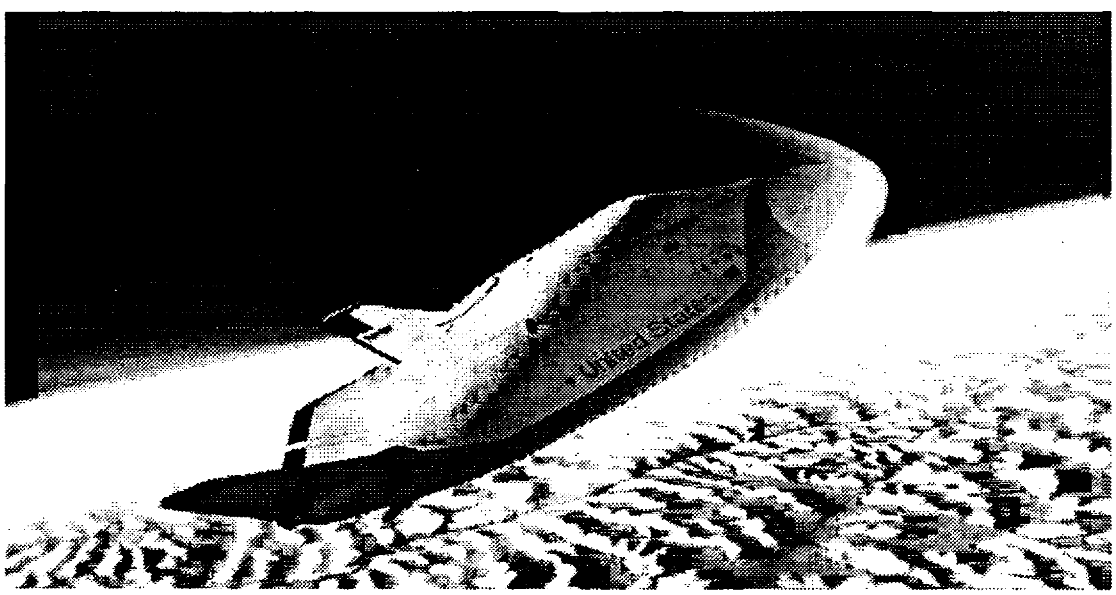

Figure 1.1 – Artist's Concept of the X-38 (picture courtesy of NASA)

The X-38 is designed to be released from the ISS and, with minimal directional thrusters, descend into the Earth's atmosphere. When the craft reaches an altitude of around 23,000 feet (7,000 m), a pilot chute followed by a drogue chute deploys, slowing the craft down before the deployment of the main parafoil at an altitude greater than 18,000 feet (5,500 m). The steerable parafoil is the largest parafoil ever made, covering an area of 7,500 square feet (697 m^2). It allows the X-38 to float gently to a desert landing on its landing skids. Approximate landing speeds are around 40 mph (64 kph). Figure 1.2 is a photograph of a scale model of the X-38 with its parafoil unfurled, taken during a drop test from a B-52.

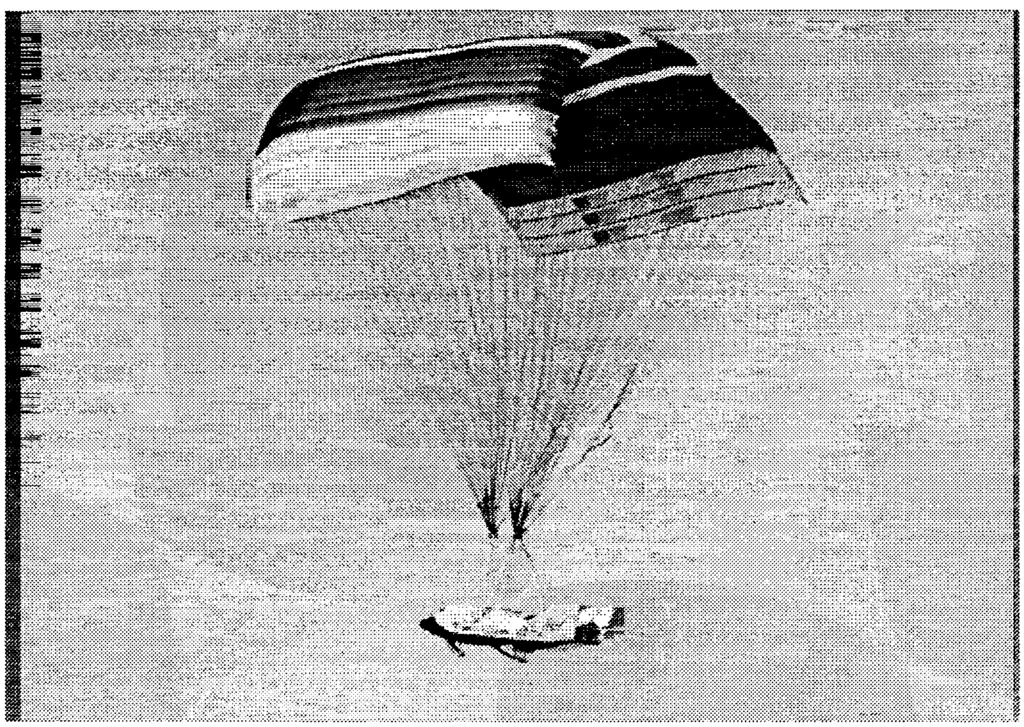

Figure 1.2 – Scale Model of X-38 During Drop Test From B-52 (photo courtesy of NASA)

Several drop tests have been conducted to date on scale models of the X-38 for design verification. Figure 1.3 is a graphical representation of a typical descent during a drop-test. Deployment from the ISS would follow a similar trajectory.

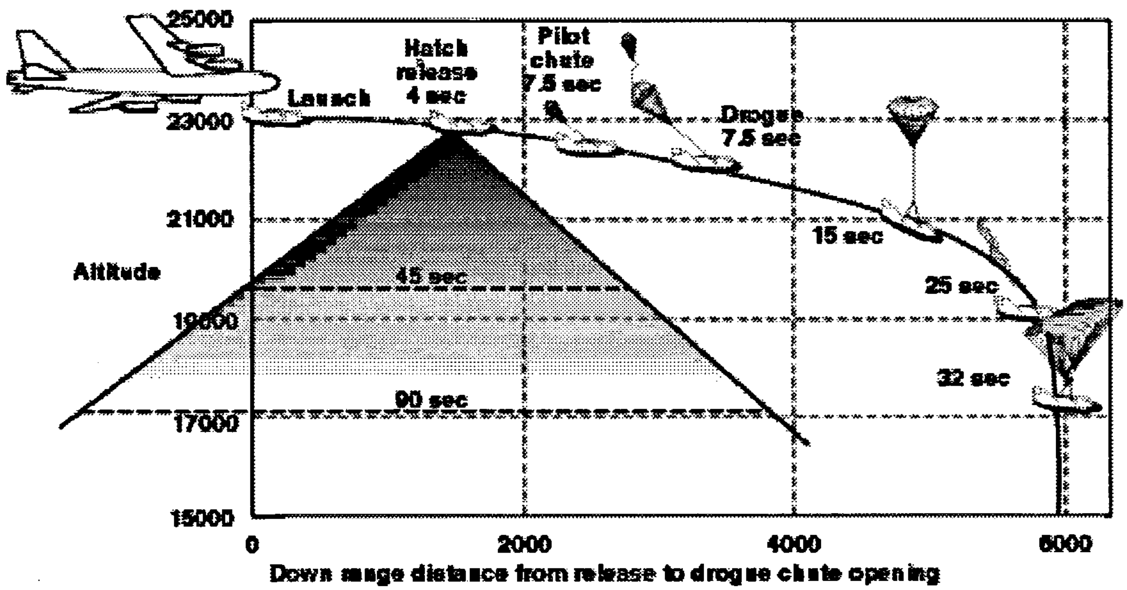

Figure 1.3 – Descent of X-38 (picture courtesy of NASA)

The X-38 is designed as a reusable vehicle, so it is ready for reuse after a small amount of service following a flight. Aside from being reusable, the most attractive aspect of the X-38 design is that it draws from proven technology, drastically reducing development costs.

1.2 Structure of the X-38

The structure of the X-38 consists of an aluminum subframe, a composite material aeroshell bolted to the subframe, and the thermal protection system covering the outer surface of the aeroshell. Figure 1.4 shows a portion of the aluminum subframe and the corresponding composite panels that attach to it.

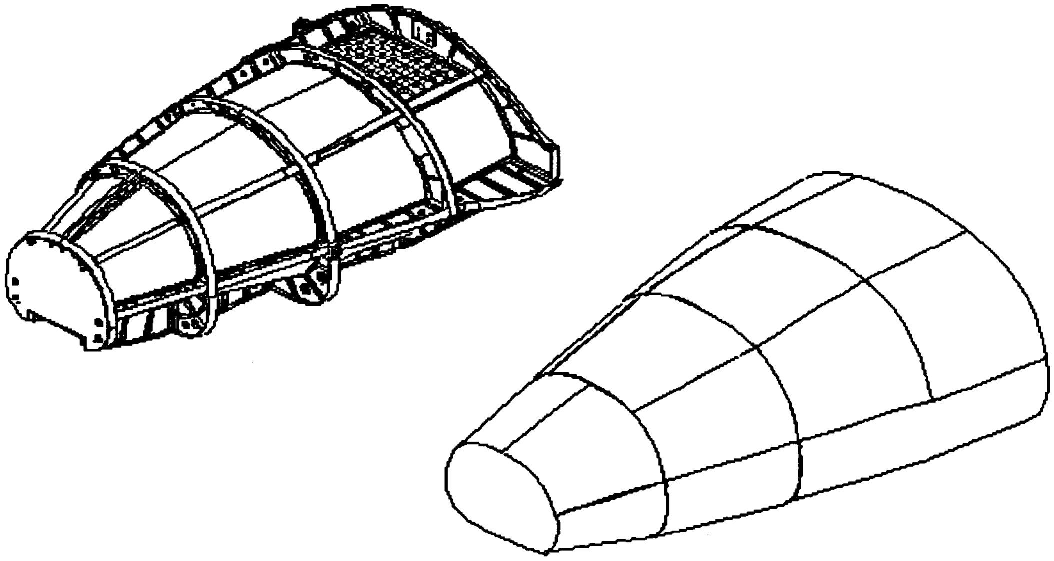

Figure 1.4 – Portion of X-38 Subframe and Panel Assembly (drawing courtesy JSC)

The main aeroshell of the X-38 is constructed from lightweight carbon fiber composites. These materials are essential for spacecraft design where weight is at a premium and a high strength-to-weight ratio is a necessity. The design requirements for the aeroshell panels are high and low temperature capability, sufficient strength at any design temperature in reaction to any design loading, and finally for panels with TPS tiles, deflections of less than 0.05 in/6 in arclength (0.127 cm/15.24 cm). The aeroshell panels will experience temperatures from –454°F (-270°C), which is the temperature in outer space, to 325°F (163°C), which is the design temperature for reentry. The X-38 was designed for load cases occurring during ground handling,

launch, in-orbit operations, re-entry, parafoil deployment, and landing with required factors of safety (Gafka and Baccus 2000).

Manufacturing of the composite aeroshell is currently being conducted at the NASA Johnson Space Center. Construction of each panel begins with a 3-D drawing created using Pro/Engineer™. The CAD drawing is then sent to a CNC 5-axis router which machines a tooling surface for the panel out of a stack of foam blocks. The tooling surface is then covered with dry fiberglass matting, injected with resin, and cured to create the tool face, or mold. The hand lay-up of the actual panel occurs next, which is where the carbon fiber/cyanate ester pre-pregs are laid onto the tooling face. A pre-preg is a layer of fibers impregnated with partially cured resin, which makes them flexible enough to lay in a mold. The entire panel is then enclosed in a vacuum bag. After drawing a vacuum and sealing the bag, the panel is cured and then post-cured in an autoclave.

The aeroshell panels of the X-38 are of three primary structural types: laminates, hat-stiffened laminates, and composite sandwich panels. The aeroshell is composed of curved shells and flat plates. Basic plate and shell theory shows that curved shells have a greater flexural rigidity than flat plates, making them stiffer in bending. Flat laminates are used in regions where the panels span small distances and loads induce flexural deformations within the desired range. Extra reinforcement is needed to resist bending under the aerodynamic design loads where the aeroshell spans substantial distances between supports. Two methods to reinforce a flat plate or moderately

curved shell are to add stiffeners stretching down its length, or to fabricate the plate using sandwich construction. A composite sandwich plate typically consists of two stiff outer facesheets with a lightweight core in between. The advantage of this type of construction is that it behaves much the same as an I-beam in that a greater bending stiffness is achieved by locating most of the material away from the neutral axis.

The focus of the work presented in this report is a study of the three types of aeroshell panels. Their strengths and stiffnesses under load was investigated at elevated temperature. The study was carried out using relatively inexpensive panel subcomponents, which use the same materials and joint details as in the X-38 prototype.

1.3 Objective

The objective of this study is to investigate the flexural response at elevated and room temperatures of the bolted composite panels being used in the aeroshell of the X-38 Crew Return Vehicle. Data from testing is used to assess strength, stiffness, and failure modes at room and elevated temperatures. The responses are also compared and correlated to simplified models. To accomplish the objectives, panels were tested in four-point bending at room temperature and 325°F (163°C), which is the maximum temperature that the engineers at NASA expect the aeroshell panels (beneath the thermal protection system) to experience during re-entry.

1.4 Scope of Work

This report will detail the experimental plan for testing of the X-38 panel sub-component in Section 2. This includes a general overview of the test program, detailed examination of the test specimens, explanation of experimental set-ups, and details of instrumentation. Section 3 presents the results of the room temperature and elevated temperature four-point bending tests. Included in the results are graphs of load versus displacement, load versus strain, and photographs showing modes of failure. Section 4 presents a simplified theoretical approach to analyzing the behavior of the panels using beam theory. This is followed by conclusions and recommendations in Section 5. Sections 6 and 7 are appendices, which include a portion of the temperature chamber computer code and a few sample MathCAD worksheets.

2. Description of Test Plan

2.1 Test Plan Overview

Three different configurations of composite panels (flat composite laminates, hat-stiffened composite laminates, and sandwich construction panels) were tested in four point bending at room temperature (RT), 74°F (23°C), and elevated temperature (ET), 325°F (163°C). Table 2.1 is a list of the specimens tested in this program, each panel's configuration (i.e. flat laminate, hat-stiffened laminate, composite sandwich), and the test temperature. The test program includes two flat laminates tested at elevated temperature, three hat-stiffened laminates tested at room temperature, and three hat-stiffened laminates tested at elevated temperature, all fabricated at the Johnson Space Center. Also, seven composite sandwich panels were tested at room temperature and two composite sandwich panels were tested at elevated temperature, all fabricated at Lockheed Martin Michoud Space Systems, New Orleans, LA.

The composite sandwich panels are labeled according to the following convention: **AA-TT-P##Y**. This is explained in Table 2.2. The nomenclature describes the type of loading condition, test temperature, the number of the larger panel that it was cut from, and its location on that panel. The loading condition refers to which sides of the panel the load was applied, inner mold line (IML), or outer mold line (OML). The OML side is the outermost surface of the panel when attached to the craft, and the inner mold line is the innermost surface on the craft.

Table 2.1 – Total Test Matrix

Panel Designation	Panel Configuration	Test Temperature
FI-RT-D5C	Sandwich (24")	RT
FI-RT-D5A	Sandwich (24")	RT
FI-RT-D3C	Sandwich (26")	RT
FI-RT-D3A	Sandwich (26")	RT
HSRT-01	HS	RT
HSRT-02	HS	RT
HSRT-03	HS	RT
FLHT-01	FL	ET
FLHT-02	FL	ET
FI-ET-D3B	Sandwich (24")	ET
FI-ET-D5B	Sandwich (26")	ET

RT = Room Temperature

ET = 325°F (163°C)

HS = Hat-Stiffened Laminate

FL = Flat Laminate

Table 2.2 – Sandwich Panel Nomenclature

AA indicates type of loading condition	**FI** = Flexure test with load on Inner Mold Line (IML) **FO** = Flexure test with load on Outer Mold Line (OML)
TT is test temperature	**RT** = Room temperature (73°F) **ET** = Elevated temperature (325°F)
P## is the panel number in the series	**P##** = P01 through P06
Y is the location on panel	**Y** = A through D

The flat laminates and hat-stiffened test specimens are labeled according to the following convention: **AABB - ##**. This is explained in Table 2.3. The nomenclature describes the type of panel (flat laminate or hat-stiffened), the test temperature (room or elevated), and the number of the panel in the series.

Table 2.3 – Flat Laminate and Hat-Stiffened Panel Nomenclature

AA indicates the specimen type	**FL** = Flat laminate **HS** = Hat-stiffened laminate
BB indicates the test temperature	**RT** = Room temperature **HT** = High Temperature (325°F)
## indicates the panel number in the series	## = 01 through 03

2.2 Bolted Connection

One main source of concern when designing a composite structure is the joining of composites together and the connections of composites with other metal structures. There are three types of composite connections: mechanical or bolted connections, adhesively bonded connections, and combinations of the two. Design criteria mandated that structural panels for the X-38 be removable, therefore bolted connections are the dominant type of connection. The composite aeroshell panels are bolted to the aluminum subframe. Figure 2.1 is a detailed drawing showing fabrication details of the bolted connection between the composite aeroshell and the aluminum subframe. Specifically, Figure 2.1 is a drawing of the connection for the composite sandwich panels. Practically speaking, the connection is identical for the

flat laminates and the hat-stiffened laminates. In developing geometries of sub-component test articles, it is essential to simulate the actual conditions as closely as possible.

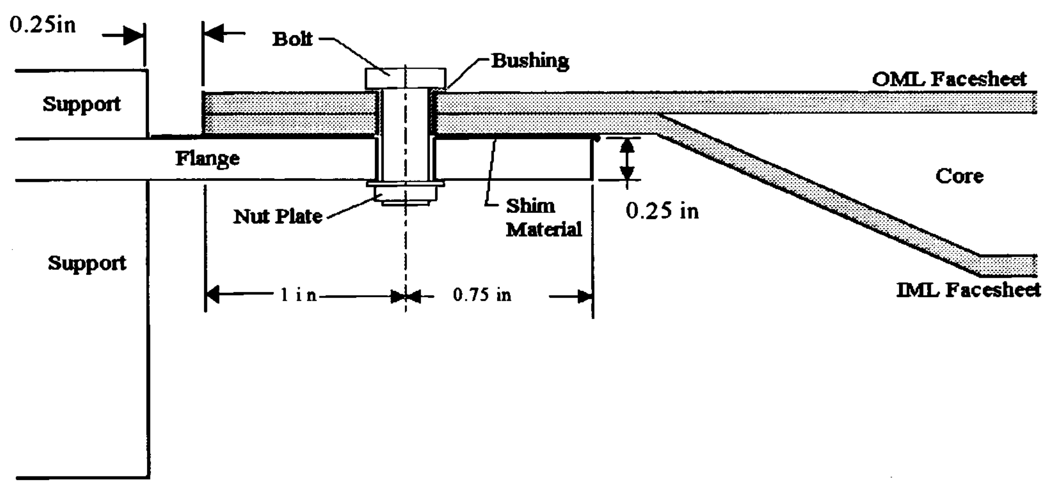

Figure 2.1 – Bolted Composite Connection

2.3 Test Specimens

2.3.1 Flat Laminates

Johnson Space Center of Houston, TX, supplied two flat laminate panels that were tested at the University of Maine. Figure 2.2 is a photograph of one of the flat composite laminates and Figure 2.3 is a detailed drawing of the flat laminate. The flat laminates have an isotropic, balanced, symmetric lay-up with the symmetric stacking sequence $[(0°/+45°/90°/-45°)_6]_S$. This results in forty-eight plies with a total thickness of 0.25-inch. Each individual lamina has a thickness of 0.0052-inch and is manufactured from a pre-preg tape with IM7 carbon fibers and cyanate ester resin. Each laminate is attached to two aluminum endplates. One laminate is attached to the

endplates with three permanent HLVAP10-8-8 titanium pins with HL70-8 aluminum collars, while the other article is fastened to the endplates with three NAS6404U9 titanium bolts with NAS1779 stainless steel nut plates. There is also a rubber shim (compound 14255) between the laminate and the endplates, which is held in place by an adhesive (manufactured by 3M) on both sides.

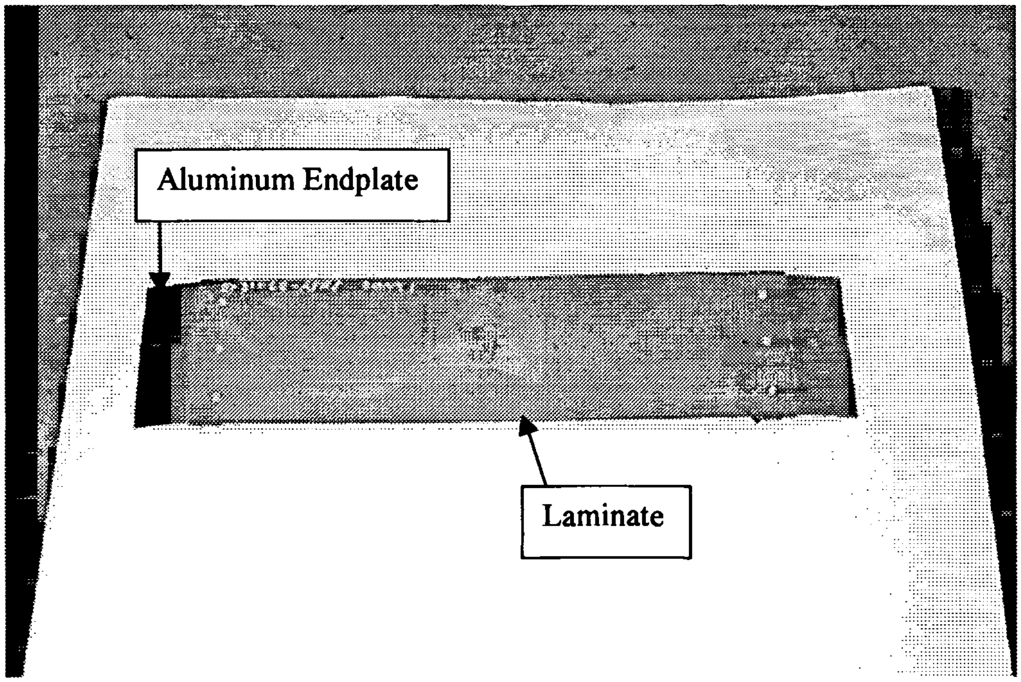

Figure 2.2 – Flat Composite Laminate

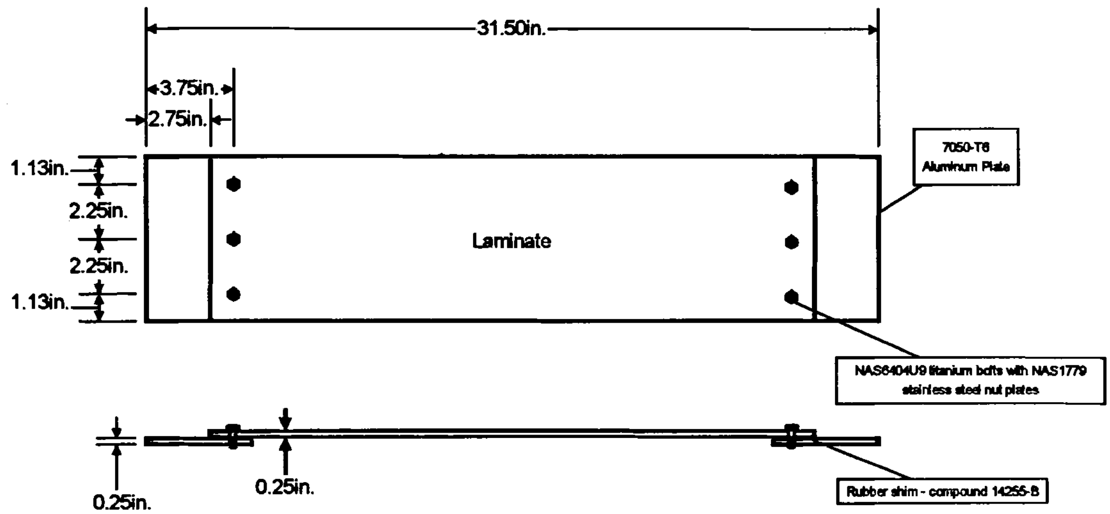

Figure 2.3 – Drawing of Flat Laminate

Table 2.4 outlines the materials used in the fabrication of the flat laminates. These included a pre-preg tape of IM7 carbon fibers impregnated with cyanate ester resin, titanium bolts, titanium and aluminum fasteners, aluminum endplates, and a rubber shim compound.

Table 2.4 – Summary of Laminate Materials

Material	Manufacturer/Dimensions	Properties
Prepreg Tape – IM7 fiber/cyanate ester resin	Hexcel, 0.005 in (0.013 cm) thick	E11 = 23.3 Msi (160.65 GPa) E22 = 1.12 Msi (7.72 GPa) ν12 = 0.30 G12 =500 ksi (3.45 GPa)
Titanium bolts – NAS6404U9 bolts with NAS1779 stainless steel nut plates	¼ in - 28 x 1in (0.635 cm x 2.54 cm)	$E_{titanium}$=15 ksi (100 GPa) $\nu_{titanium}$=0.33
Permanent fasteners – HLVAP10-8-8 titanium pin with an HL70-8 aluminum collar	10-32 thread, 0.75 in (1.91 cm) long	$E_{titanium}$=15 ksi (100 GPa) $\nu_{titanium}$=0.33
End plates – 7050-T6 aluminum	6.75 in x 4.5 in x 0.25 in (17.1 cm x 11.4 cm x 0.635 cm)	$E_{aluminum}$=10.4 ksi (72 GPa) $\nu_{aluminum}$=0.33
Rubber shim – Compound 14255-B	Mosites Corp. Approx. 1.75 in x 6.75 in x 0.030 in (4.44 cm x 17.1 cm x 0.076 cm)	

2.3.2 Hat-Stiffened Laminates

Johnson Space Center of Houston, TX, supplied the hat-stiffened laminates. The panels consisted of a flat carbon-fiber composite laminate, reinforced with a tapered carbon-fiber composite hat-stiffener. The hat-stiffened articles consist of a flat laminate with a reinforcing tapered hat stiffener attached down the length of the panel. The hat stiffener has a [0°/+45°/90°/-45°] symmetric lay-up while the flat laminate has

an identical lay-up to the plain flat laminates described in Section 2.3.1. The hat stiffener is made of a woven graphite fiber fabric and cyanate ester resin and is attached to the laminate with twelve HLVAP10-6-4 titanium pins with HL70-6 aluminum collars and NAS1587-3 stainless steel washers on either side of the laminate. The stiffener is also bonded to the laminate with a thin layer of AF191 adhesive. Each of the hat-stiffened panels is attached to two aluminum endplates with three NAS6404U9 titanium bolts with NAS1779 stainless steel nut plates. Figure 2.4 is a photograph of a hat-stiffened laminate and Figure 2.5 is a detailed drawing of a hat-stiffened laminate.

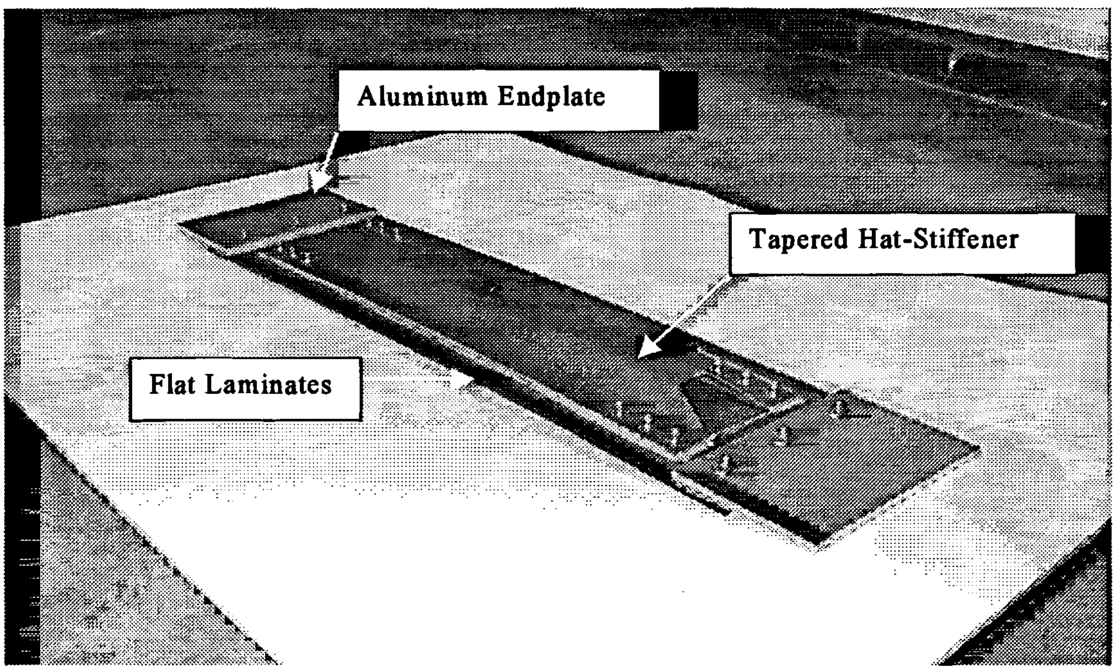

Figure 2.4 – Tapered Hat-Stiffened Laminate

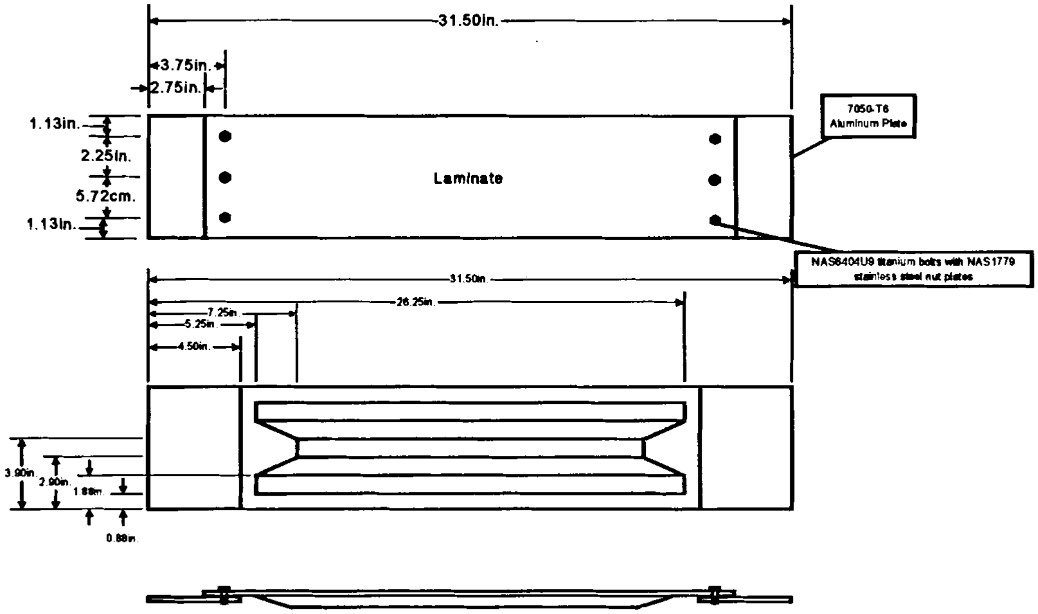

Figure 2.5 – Drawing of Hat-Stiffened Laminate

Table 2.5 outlines the materials used in the fabrication of the hat-stiffened laminates, including the pre-preg material, bolts, fasteners, endplates, and shim compound.

Table 2.5 – Summary of Hat-Stiffened Laminate Materials

Material	Manufacturer/Dimensions	Properties
Prepreg Tape – IM7 fiber/cyanate ester resin	Hexcel, 0.005 in (0.013 cm) thick	E11 =23.3 Msi (160.65 GPa) E22 = 1.12 Msi (7.72 GPa) ν12 = 0.30 G12 = 500 ksi (3.45 GPa)
Titanium bolts – NAS6404U9 bolts with NAS1779 stainless steel nut plates	¼ in - 28 x 1in (0.635 cm x 2.54 cm)	$E_{titanium}$=15 ksi (100 GPa) $\nu_{titanium}$=0.33
Stiffener fasteners – HLVAP10-6-4 titanium pin with an HL70-6 aluminum collar (also used an NAS1587-3L stainless steel washer on either side of the laminate)	10-32 thread, 0.75 in (1.91 cm) long	$E_{titanium}$=15 ksi (100 GPa) $\nu_{titanium}$=0.33
Stiffener adhesive – AF191	3M	
End plates – 7050-T6 aluminum	6.75 in x 4.5 in x 0.25 in (17.1 cm x 11.4 cm x 0.635 cm)	$E_{aluminum}$=10.4 ksi (72 GPa) $\nu_{aluminum}$=0.33
Rubber shim – Compound 14255-B	Mosites Corp. Approx. 1.75 in x 6.75 in x 0.030 in (4.44 cm x 17.1 cm x 0.076 cm)	

2.3.3 Tapered Composite Sandwich Construction Panels

Lockheed Martin Michoud Space Systems of New Orleans, LA, fabricated the composite sandwich construction panels. A photograph of two of the panels is shown in Figure 2.6, with the outer mold line (OML) side facing up. The panels are made of IM7 carbon fiber/cyanate ester matrix facesheets with a phenolic honeycomb core.

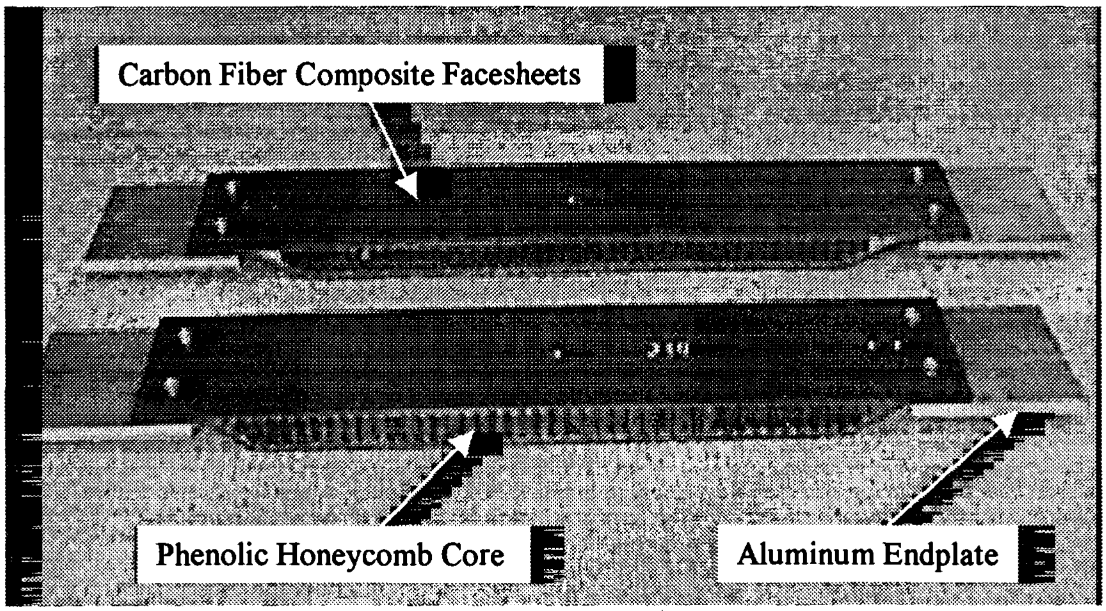

Figure 2.6 – Tapered Composite Sandwich Panels

Two different sizes were tested as part of this study and the previous study (Caccese and Malm 1999): 24 in (61 cm) in length with a 30° taper and 26 in (66 cm) in length with a 20° taper. Figure 2.7 and Figure 2.8 show the geometry of the 30° taper panels and the 20° taper panels, respectively. The sandwich panels are fabricated from carbon-fiber/ cyanate ester matrix laminate facesheets surrounding a 0.75 in (1.905 cm) Hexcel HRP/F50-4.5 phenolic honeycomb core. Figure 2.9 illustrates the various ply drop-offs in the facesheets down the length of the panel. Due to symmetry, only

half of the panel is shown. The facesheets are eight plies near the center of the panels, build up to eleven plies near the taper region, and total twenty-two plies at the flange.

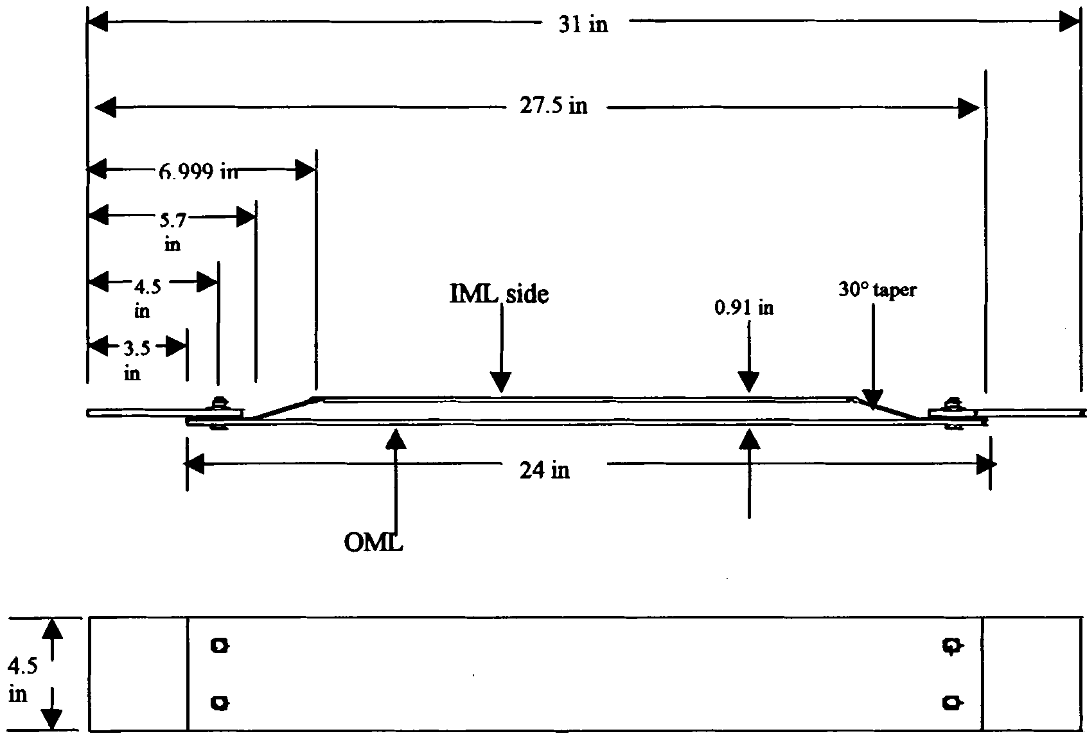

Figure 2.7 – 30° Taper Composite Sandwich Panel

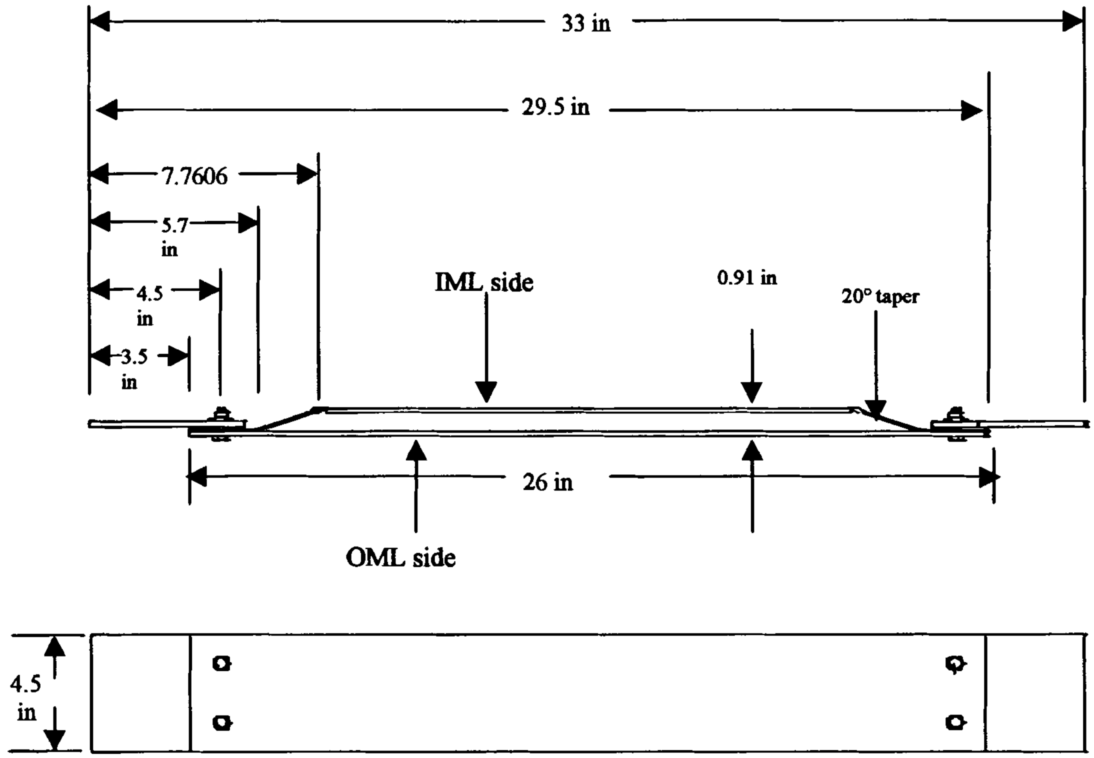

Figure 2.8 – 20° Taper Composite Sandwich Panel

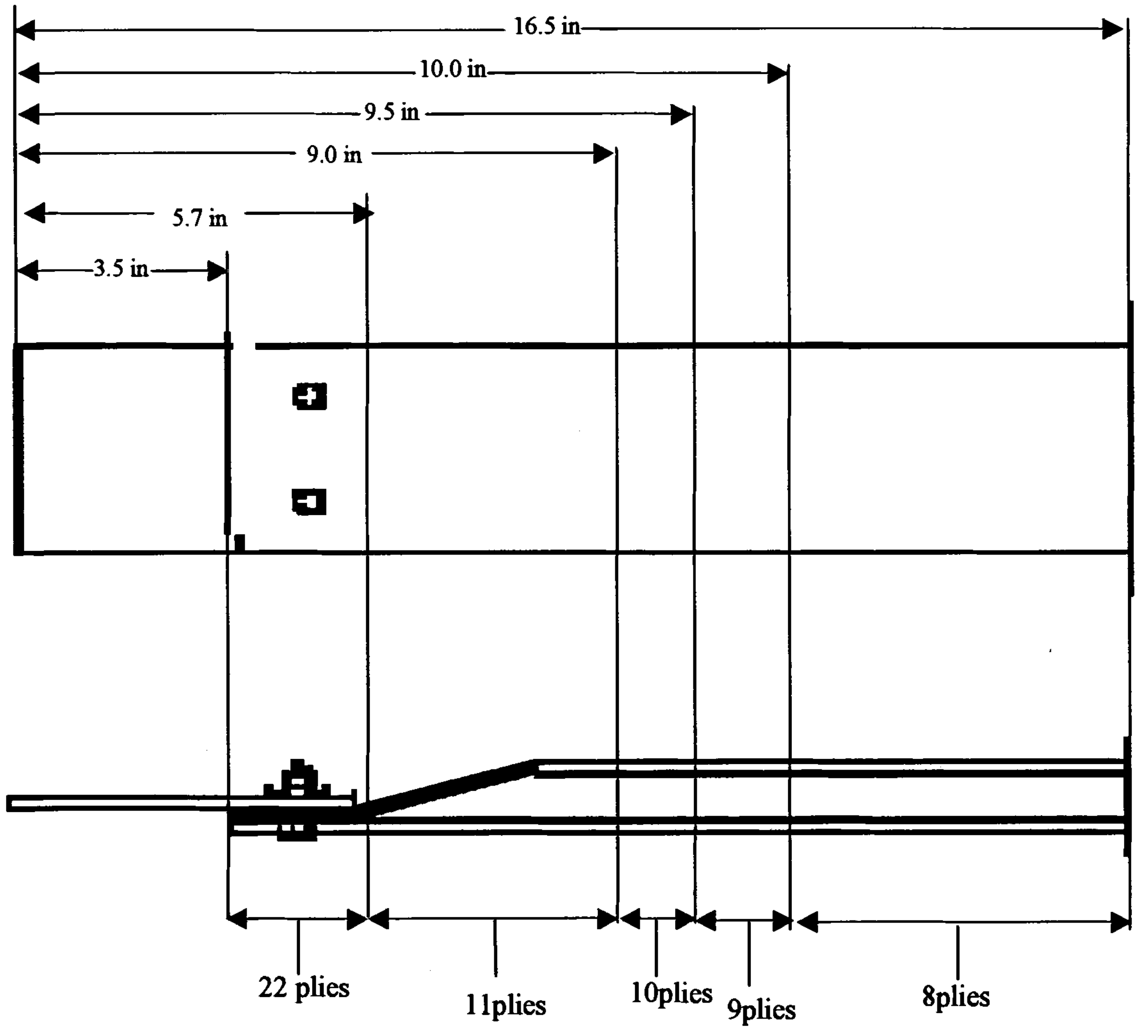

Figure 2.9 – Location of Ply Drop-Offs

Tables 2.6 outlines the material properties (moduli, strength, Poisson's ratio) for each individual lamina or ply. Table 2.7 outlines the properties of the composite laminates. The table is broken down to give the properties of each ply drop-off section of the sandwich panel. Table 2.8 outlines the moduli and strength properties of the phenolic honeycomb core.

Table 2.6 – Lamina Properties

Lamina Properties MSI/MPa			Lamina Strength (MSI/MPa)		
	English	SI		English	SI
$E_{1,t}$	21.99 Msi	151.62 GPa	F_{1tu}	295 ksi	2034 MPa
$E_{1,c}$	20.25 Msi	139.62 GPa	F_{1cu}	139.8 ksi	963.9 MPa
$E_{2,t}$	1.15 Msi	7.93 GPa	F_{2tu}	7.72 ksi	53.23 MPa
$E_{2,c}$	1.22 Msi	8.41 GPa	F_{2cu}	26.9 ksi	185.5 MPa
G_{12}	0.678 Msi	4.67 GPa	F_{su}	9.90 ksi	68.26 MPa
ν_{12}	0.326				
t_{ply}	0.01 in	0.254 cm			

Table 2.7 – Laminate Properties

# of Plies	Layup	E_x		E_y		G_{xy}		ν_{xy}
		English (MSI)	SI (GPa)	English (MSI)	SI (GPa)	English (MSI)	SI (GPa)	
22	{-45,0,90,45,90,0, 90,45,90,0,-45}$_s$	8.442	58.21	10.25	70.67	2.478	17.09	0.202
11	{-45,0,90,45,90,0)$_s$	8.442	58.21	10.25	70.67	2.478	17.09	0.202
10	{-45,0,90,45,90}$_s$	7.086	48.86	11.01	75.91	2.658	18.33	0.201
9	{-45,0,45,90$_2$,45,90, 0,-45}	7.587	52.31	9.68	66.74	2.835	19.55	0.246
9	{-45,0,90,45,90$_2$,45, 0,-45}	7.587	52.31	9.68	66.74	2.835	19.35	0.246
8	{-45,0,45,90}$_s$	8.274	57.05	8.274	57.05	3.155	21.75	0.311

Table 2.8 – Phenolic Honeycomb Core Properties

Hexcel-HRP/F50-4.5		English	SI
L-direction	Shear Modulus	25,000 psi	172.37 MPa
	Shear Strength	200 psi	1.38 MPa
		265 psi	1.83 MPa
W-direction	Shear Modulus	13,000 psi	89.63 MPa
	Shear Strength	100 psi	0.689 MPa
		140 psi	0.965 MPa
Thickness		0.75 in	1.88 cm

2.4 Room Temperature Testing of Composite Sandwich Panels

Destructive flexure inner mold line (IML) tests (load applied to the IML side) were conducted in a previous study at the University of Maine (Caccese and Malm 1999) on seven composite sandwich construction panels for Lockheed Martin Michoud Space Systems (LMMSS) of New Orleans, LA. These tests were in support of the LMMSS X-38 vehicle 201 Panel #13 subcomponent test program. The room temperature flexure IML tests are not described in detail but are included to compare the results with the elevated temperature flexure IML tests that were conducted as part of this current research effort. The test articles are identical to those described in Section 2.3.

2.5 Elevated Temperature Flexural Testing

Elevated temperature and room temperature destructive four point bending tests were conducted on hat-stiffened composite laminate panels, sandwich composite panels, and flat composite laminate panels at the University of Maine in Crosby Laboratory.

2.5.1 Environmental Test Chamber

The elevated temperature tests were conducted in a test chamber designed and constructed at the University of Maine (Mewer 2000). The elevated temperature test chamber fits into the MTS test frame (model 810), located in Crosby Laboratory, as shown in Figure 2.10. The MTS 810 has a total capacity of 110,000 lbf. For the purpose of this study, a 22,000 lbf capacity load cell was employed.

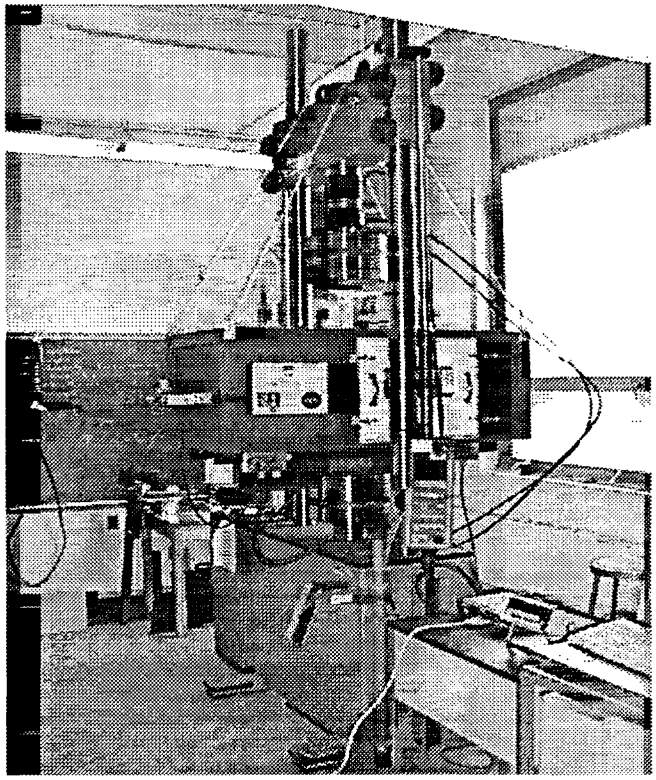

Figure 2.10 – Test Chamber Mounted in MTS 810 Load Frame

A cross-section of the elevated temperature test chamber is shown in Figure 2.11. The outer dimensions of the chamber are 26 in x 21 in x 50.375 in (66 cm x 53 cm x 128 cm). The top cover of the chamber is constructed of 0.25 in (0.635 cm) plywood insulated with 2.5 in (6.35 cm) Johns Manville 817 Spin-Glas insulation. The Spin-Glas insulation is covered with aluminum flashing to reflect the heat back into the interior. The bottom of the chamber is made of a 1 in (2.54 cm) board of Marinite P Structural Insulation, with a high compressive strength of 10,000 psi (68.95 MPa). The bottom also has a layer of Spin-Glas insulation placed over the Marinite and covered by aluminum flashing. A 6 in (15.24 cm) diameter fan is mounted on one end

of the chamber to create more uniform heat circulation. A standard 40-Watt lightbulb is installed in the oven to allow visual inspection of the specimen during testing. The door of the chamber is insulated with the Manville insulation and has a double pane glass window to allow for visual inspection during testing. The Marinite base of the chamber is bolted to a steel channel, which is bolted to a steel I-beam that fits into the bottom grips of the MTS 810 load frame.

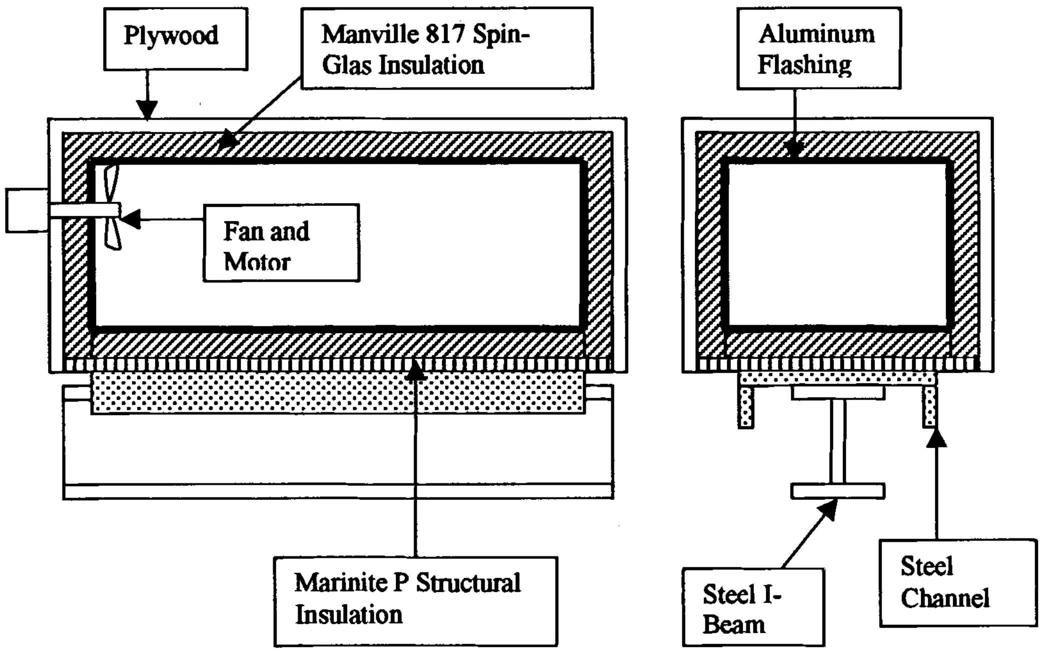

Figure 2.11 – Cross-Section of Elevated Temperature Test Chamber

The oven is heated by two 400 Watt, 20 Amp, cartridge heaters embedded in two 5-inch cubic steel blocks which rest on the 23.5 in x 47.875 in x 1 in (60 cm x 122 cm x 2.54 cm) Marinite structural insulation board. The Marinite board, manufactured by BNZ Materials Inc., was chosen for its high compressive strength of 10,000 psi (69

MPa). The chamber is also heated by 4 – 250 Watt infrared heat lamps spaced evenly about the interior of the chamber.

The chamber temperature is controlled by a Windows-based program written in Delphi 3, specifically for this application. Figures 2.12 and 2.13 are flowcharts illustrating the logic of the two main routines of the control program. The program is operated on a feedback control system with five type J thermocouples placed within the chamber, two of these to monitor the average temperature of the steel blocks and three to monitor the average air temperature.

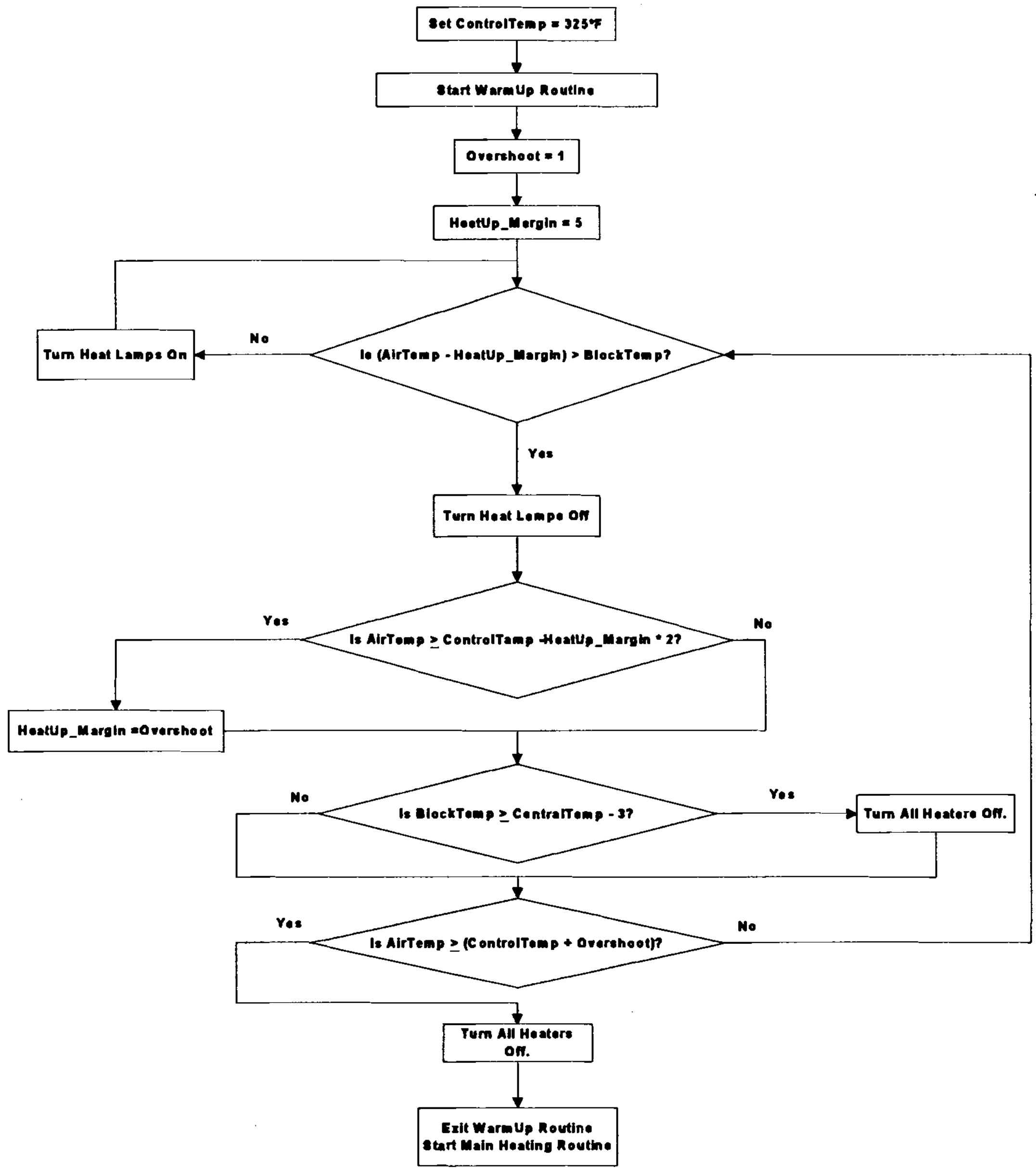

Figure 2.12 – Flowchart of Warm-Up control routine

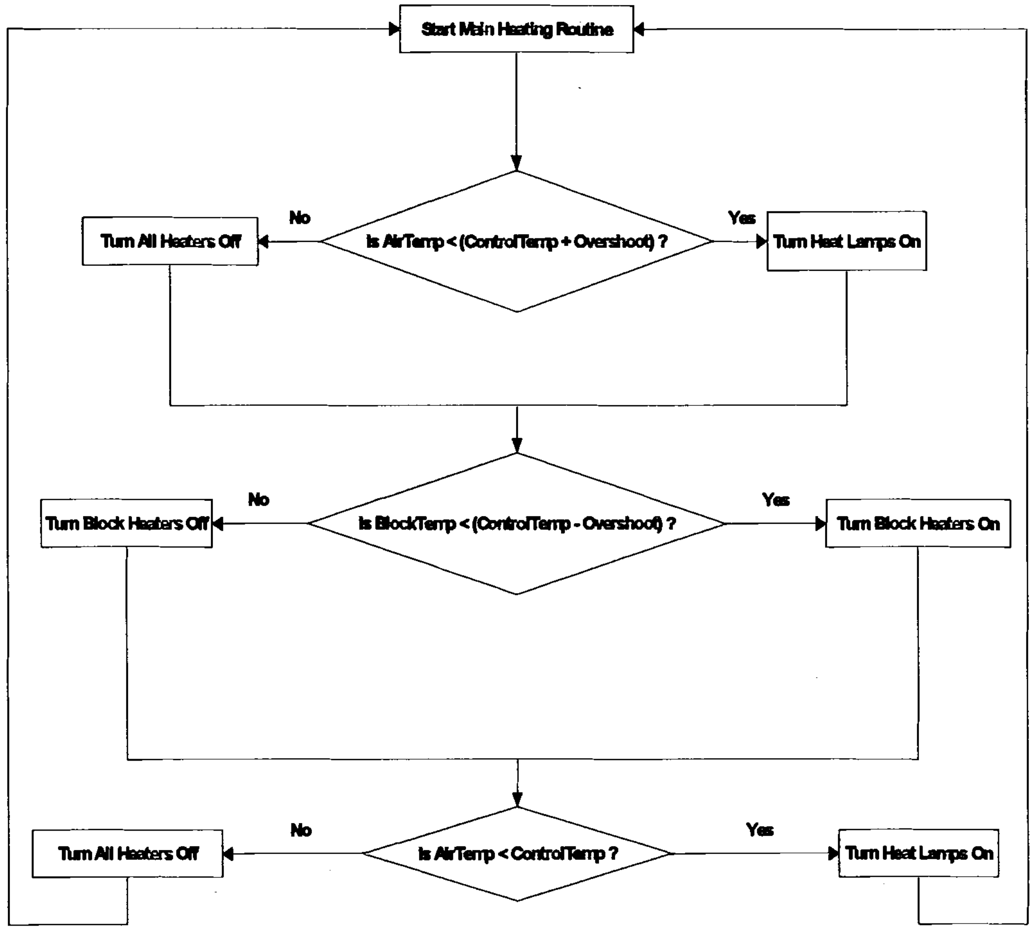

Figure 2.13 – Flowchart of Go Control routine

Type J thermocouples were chosen because of their broad temperature range, from 32°F to 1400°F. The thermocouples are connected to an IOTech Daqbook 100 data acquisition system, which is in turn connected to the PC running the Delphi temperature control program. Separate relay switches are wired in line with the heat lamps and the cartridge heaters. Figure 2.14 is a photograph of the electrical junction box, constructed at the University of Maine Crosby Laboratory, which houses the relay switches. The relay switches are connected to the Daqbook.

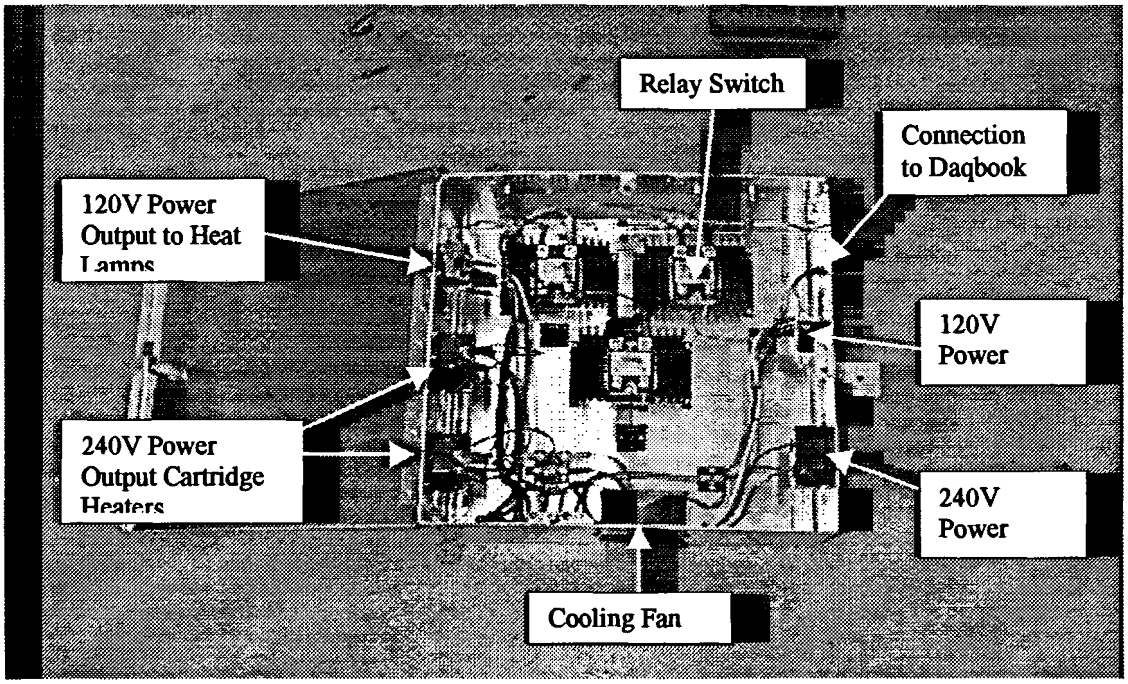

Figure 2.14 – Heating System Electrical Junction Box

Figure 2.15 is a screen capture from the HeatChamber program, which is used to control the temperature within the chamber. Because the steel blocks have a greater thermal mass than the air, the air in the oven heats up faster than the steel blocks, therefore the control program was configured to force the steel blocks and chamber environment to heat up at the same rate, creating a more efficient system. When the average air temperature exceeds the average block temperature by more than five degrees Fahrenheit, the heat lamps shut off but the block heaters remain on. When the air temperature and the blocks reach equilibrium, the heat lamps turn back on. This cycle continues until the target temperature is reached, and at that point the block heaters shut off and only the heat lamps are necessary to keep the chamber to temperature due to the high thermal capacity of the steel blocks. From a cold start, the

control system executes a Warm-Up routine, and after reaching temperature, the control program ceases the Warm-Up routine and launches the Go routine, which maintains the control temperature with only the heat lamps. The front-end of the heat control program was a WINDOWS™ application with a graphic user interface.

The program displays real-time temperature data and allows the user to log the data into a file at any sampling rate. Temperatures in air are recorded by three thermocouples and temperatures in the block heaters are recorded by two thermocouples. The program also displays the average air and block temperatures and all temperatures are displayed in both Centigrade and Fahrenheit by the program. The program also informs the user of which heater (cartridge heater or heat lamps) is operating. A portion of the computer code is given in Appendix A.

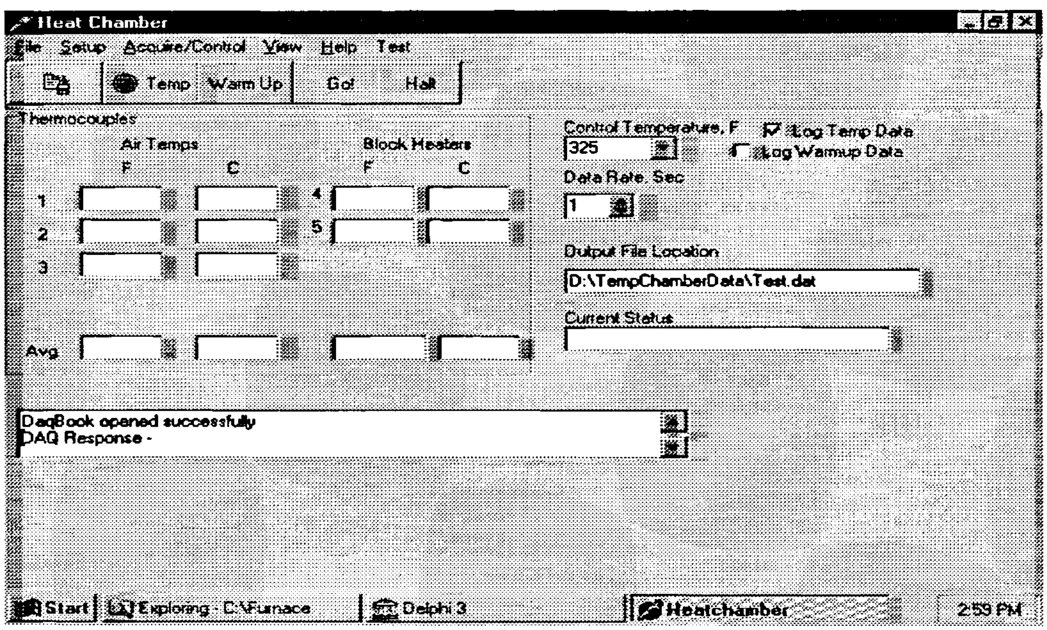

Figure 2.15 – Screen Capture of Heat Chamber program

Figure 2.16 is a graph of a typical heat-up cycle for the test chamber, with plots of the average air and block temperatures versus time. It takes the chamber approximately seventy-five minutes for the chamber to reach 325°F. The test chamber is able to maintain its control temperature with a variation of less than ±5°F.

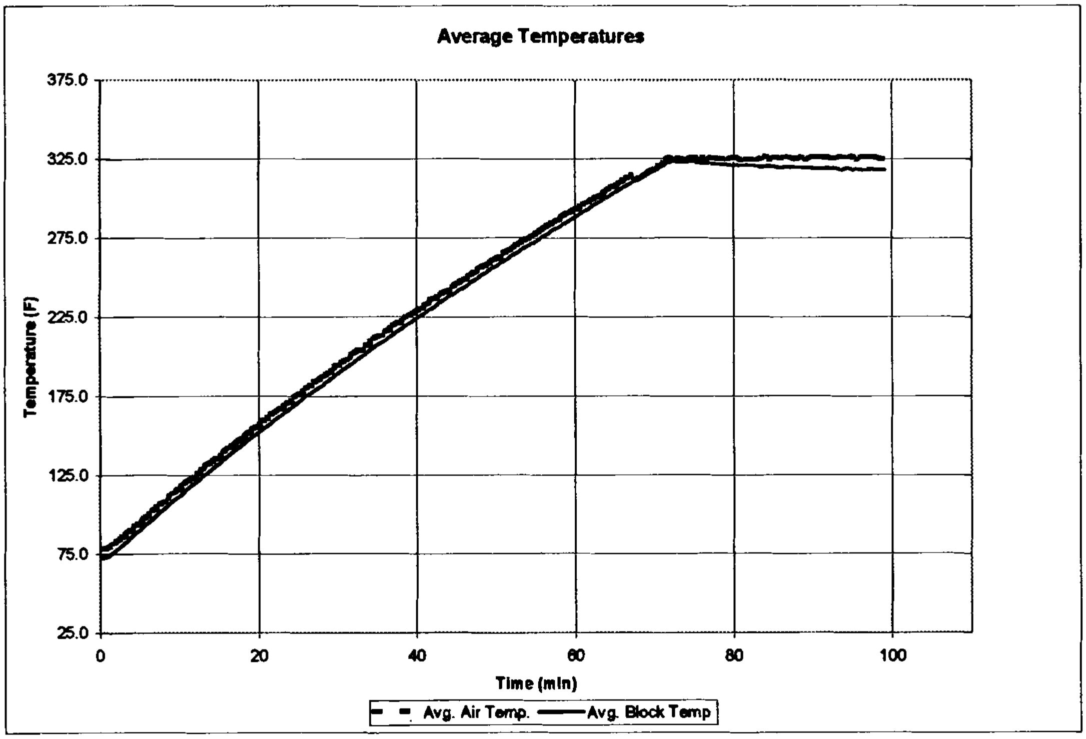

Figure 2.16 – Test Chamber Heat-Up Curve

The thermocouples were calibrated to the heat control program using a small oven. A type J thermocouple (iron/constantan) was connected to the appropriate channel on the Daqbook, and then inserted into the oven. A second type J thermocouple was also inserted into the oven, but connected to an OMEGA 10-channel Digicator thermocouple box with a digital display, capable of reading temperatures from Type J, K, T, R, S and B thermocouples. Temperatures were recorded from the thermocouple box with the corresponding outputs from the Daqbook. Data were collected over a

range from room temperature to over 325°F. Regression analysis was performed on the temperature versus output data, and the slope was entered back into the program to force the software to output calibrated temperatures.

2.5.2 Experimental Set-Up for Elevated Temperature Tests

During testing at elevated temperature, the test articles were spanned across the two steel blocks and were clamped into place with the 0.75 in (1.905 cm) steel plates and 0.5 in (1.27 cm) threaded rods, as shown in Figures 2.17 and 2.18. Originally, the two threaded rods at each end clamping the test articles in place extended only down into the Marinite of the chamber base. This was adequate for testing of the hat-stiffened laminates and the sandwich panels. However, this type of clamped end did not prove rigid enough for the very flexible flat laminates. Furthermore, this condition contributed to additional support flexibility during testing of the hat-stiffened and flat laminates. It is also noted that room temperature tests and elevated temperature tests of the hat-stiffened panels were all tested with this more flexible boundary condition. After a test was conducted on each of the flat laminates, it was noted that the steel blocks were rotating inward and both panels were allowed to flex excessively, thereby precluding failure before the displacement limits of the oven were reached. A second test was conducted on each flat laminate with 4 threaded rods at each end extending down through the steel channel, to strengthen the clamped end. This mitigated the end block rotation, forced the laminate to respond more as a clamped-clamped beam, and to resist more load. Both the room temperature and elevated temperature sandwich panels were all tested using the stiffened boundary condition.

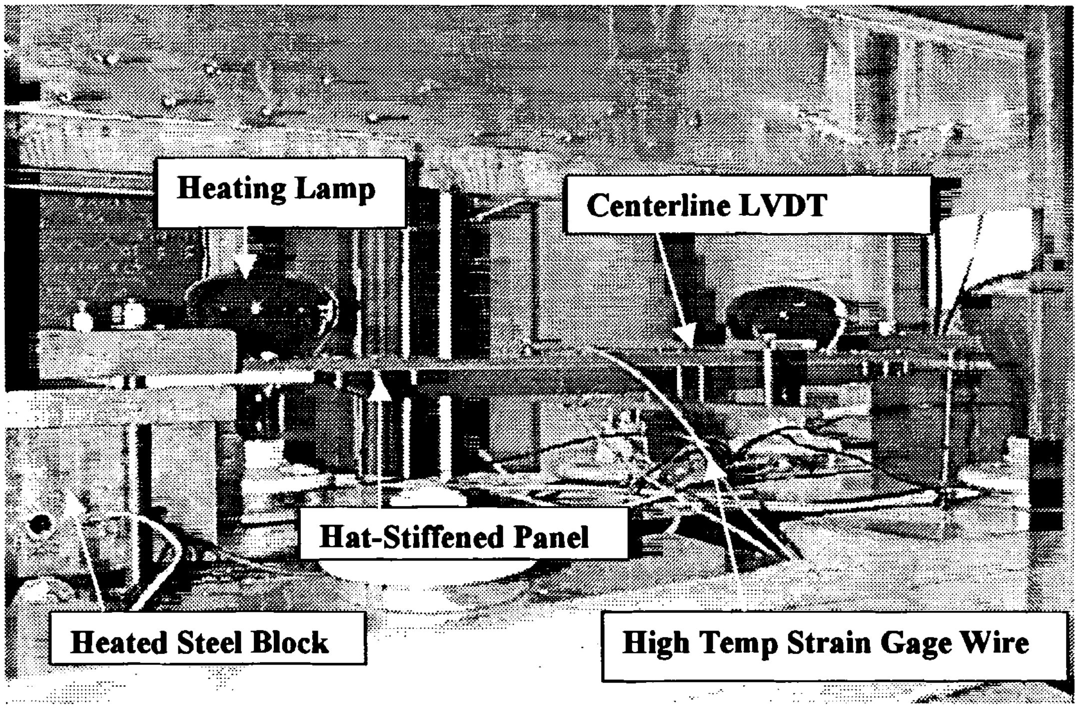

Figure 2.17 – Setup for Elevated Temperature Hat-Stiffened Panels

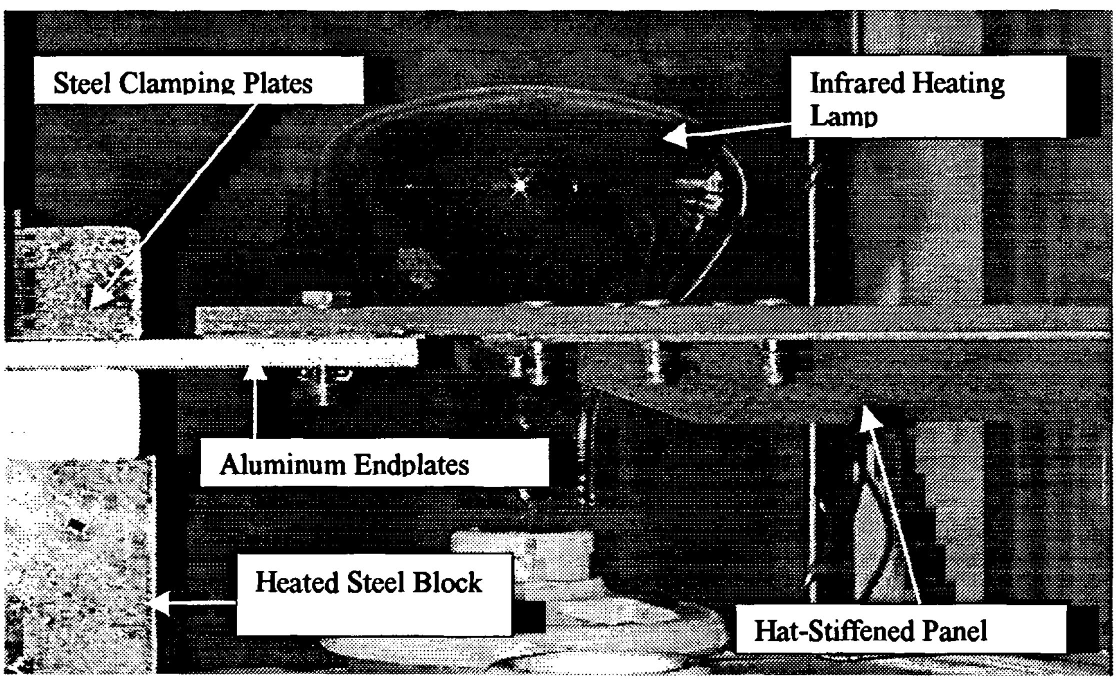

Figure 2.18 – Close-up of Joint Connection

During the flexure test, the lower cylinder of the MTS moves up at a constant rate of displacement, while in displacement control. This, in turn, moves the entire base of the oven up. A steel extension arm is held in the upper grips of the MTS. This is illustrated in Figure 2.19. The extension arm is necessary to prevent the entire crosshead from entering the oven. Bolted to the bottom of the extension arm are two pivoting aluminum cylinders spaced 5 in (12.7 cm) apart. The pivoting action ensures that there is no uneven loading. These two cylinders come in contact with the test panel by applying two line loads across the width of the panel, spaced at 5 inches (12.7 cm) apart.

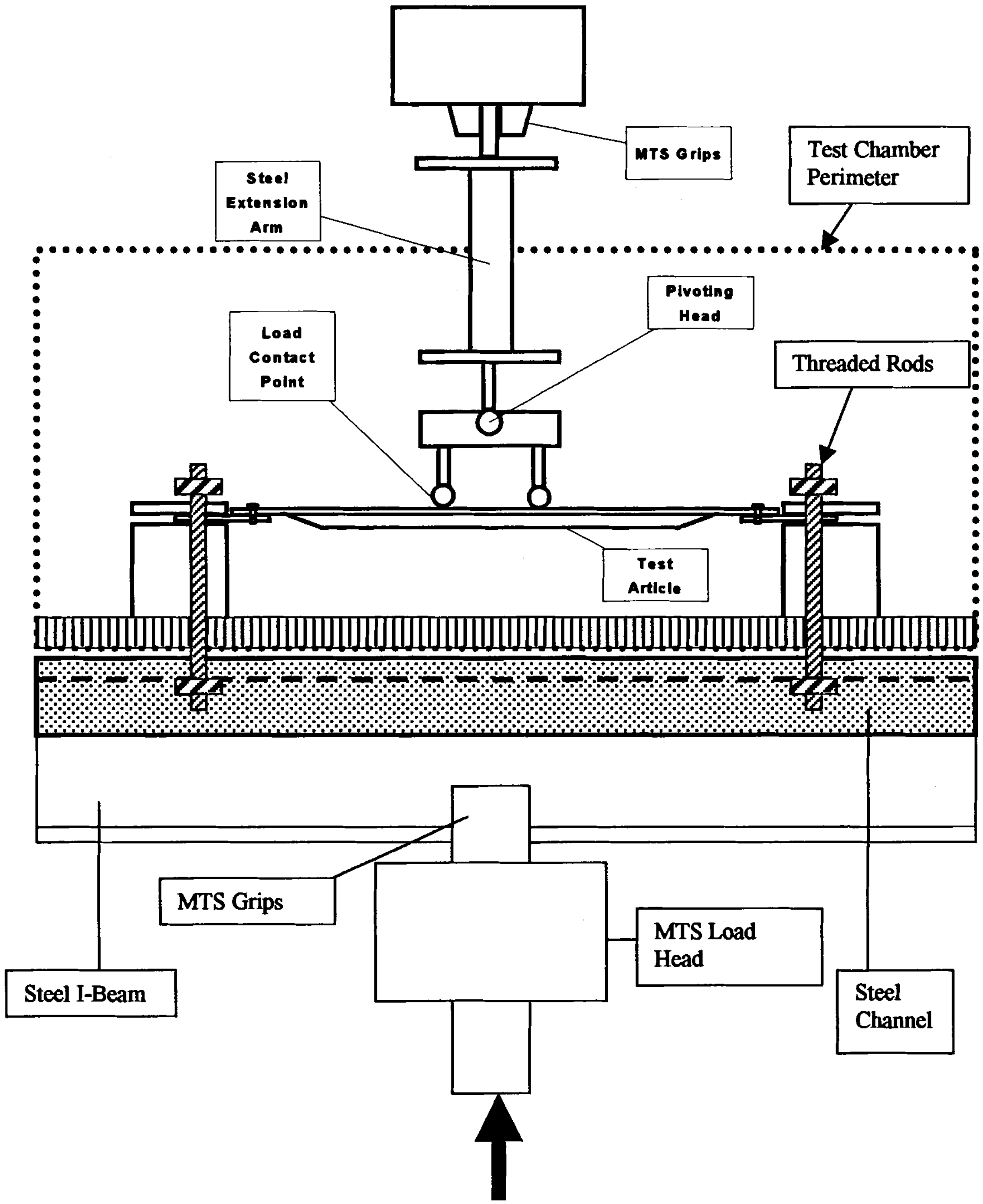

Figure 2.19 – Schematic of Load Application

2.5.3 Instrumentation

Instrumentation was configured to record strain, displacement, and load. Strains were monitored using bonded resistance strain gages, displacements were measured using linearly variable differential transducers (LVDTs), and loads were monitored using the MTS internal load cell.

All strain gages were obtained from Measurements Group, and were bonded to the test specimens according to the Student Manual for Strain Gage Technology (Measurements Group 1992). M-Bond 200 strain gage adhesive was used for bonding strain gages to the room temperature specimens. The elevated temperature tests required the use of M-Bond 600 strain gage adhesive. All strain gages bonded with M-Bond 600 had to be cured at 325°F in the test chamber for one hour to insure proper bonding between the strain gage and the specimen. All strain gages were wired in a quarter-bridge circuit through a Measurements Group eight channel Vishay model 2100 strain amplifier. Standard three-wire strain gage cable was used outside of the test chamber and spliced with high temperature strain gage wire, which was used in the interior of the chamber. RJ-11 connectors were used to connect the strain gages to the strain amplifier. The output from the strain amplifier was connected to an IOTECH Daqbook, configured to read up to sixteen channels at a sampling rate of 100 kHz.

Vertical displacements at various locations on the panels were measured using LVDTs obtained from Macro Sensors. Because the elevated temperatures could adversely

affect their performance, the LVDT cylinders were mounted on the top of the test chamber in spring-loaded fixtures. The LVDT cores were attached to a brass rod extender and then subsequently to a 1/4" steel rod, which extended into the chamber to contact the test specimens. The rods were spring-loaded (see Figure 2.20) to force contact between them and the specimens during a test.

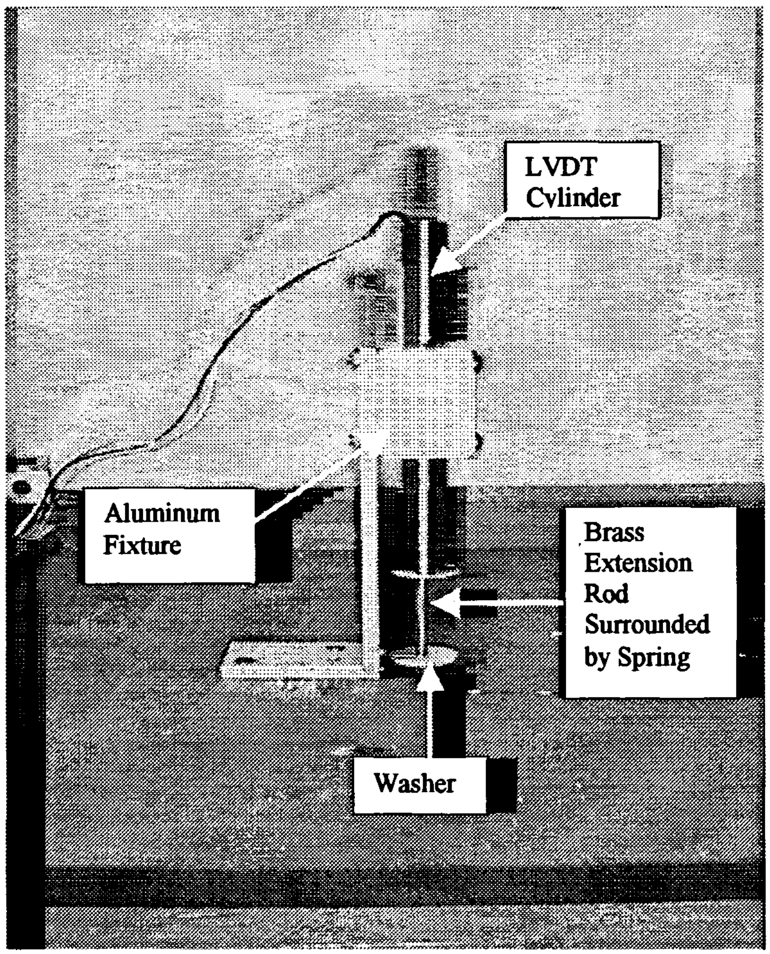

Figure 2.20 – LVDT Set-Up

Two LVDTs were used to measure the centerline deflection of the panels. One LVDT was positioned on top of the box to the left and the other to the right of the panel centerline. The extension rods came into the chamber and were attached to an

aluminum clamp (shown in Figure 2.17), which was tightened around the panels. Centerline deflection was taken as the average from these two LVDTs. All of the LVDTs were connected to the Daqbook. The outputs from the MTS LVDT and MTS Load cell were also connected to the Daqbook, but were first wired into a voltage divider, which cut the output voltage from the MTS in half. This was necessary because the output from the MTS has a range from $\pm$10V, and the Daqbook data acquisition hardware can only accept input voltages over the range of $\pm$5V. The Daqbook was connected to a 486 PC by way of the parallel port. Data acquisition of the strain, displacement, and load data was automated using DAQFI, a program written in Delphi 3 at the University of Maine. DAQFI allows the user to collect data at any sampling rate and store it in a file, which easily read by Microsoft Excel™.

2.5.3.1 Calibration

The eight channels of the strain amplifier, the LVDTs, the MTS load cell, and the MTS internal LVDT all output signals as voltage. To convert this voltage into meaningful data, they were all calibrated. The LVDTs were calibrated with an LVDT calibration table, as shown in Figure 2.20. The calibration table consists of a fixture to mount the LVDT, a screw-driven mechanism used to translate the LVDT core into the cylinder, and a Fowler Ultra-digit digital caliper to measure the displacement.

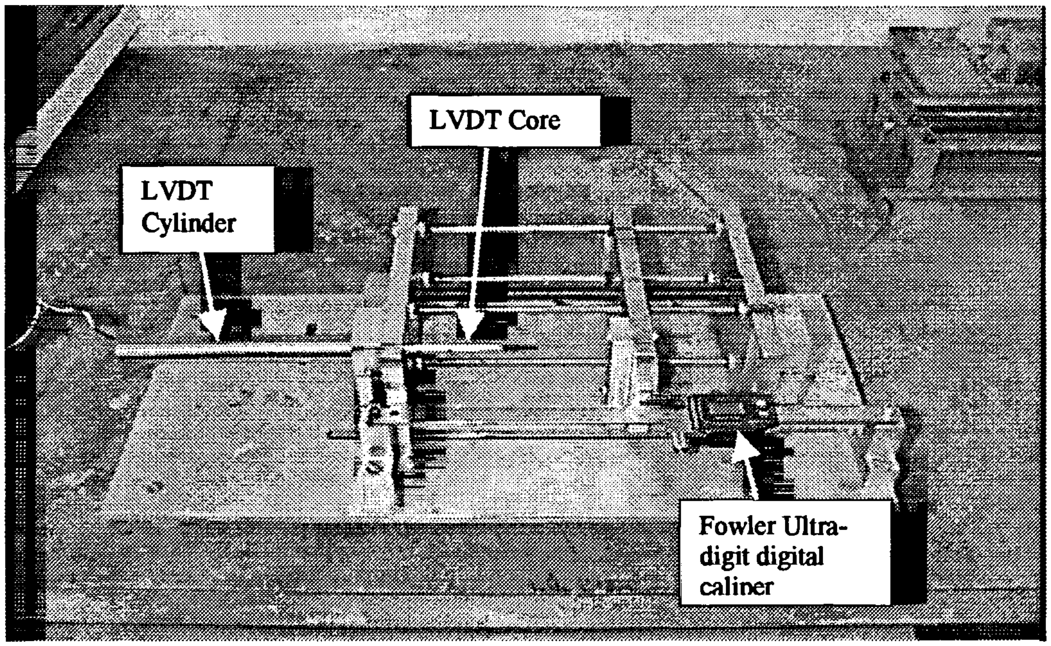

Figure 2.21 – LVDT Calibration Table

The calipers have a precision of ±0.0005 inch. Calibration is conducted by supplying power to the LVDT with a standard power supply and displacing the core into the LVDT cylinder. The output voltage of the LVDT is recorded with the use of a Hewlett-Packard Model 3111 Multimeter. Fitting a curve with a regression analysis through the voltage-displacement data will produce a slope that allows conversion from output voltage to displacement in inches.

Two different types of strain gages were used, 120Ω strain gages and 350Ω strain gages. Consequently, the channels of the strain amplifier had to be calibrated for both types. This was done with two different strain calibration boxes, both constructed at the University of Maine Crosby Laboratory. Each box has various combinations of resistors to simulate strain. The 120Ω strain gage calibration box is configured to simulate strains of 0, 100, 500, 1000, 2000, 3000, and 4000 microstrain from 120Ω

strain gages. The 350Ω strain gage calibration box is configured to simulate strains of 0, -100, -256, -500, -983, and –1992 microstrain from 350Ω strain gages. These strains were measured using a standard P3500 Strain System. Each box is connected to a channel on the strain amplifier, where a strain gage would normally be connected. After balancing the strain gage for zero strain, selecting different strains on the calibration box results in different outputs from the DAQFI program. This technique uses a through system calibration where a known strain goes through the entire test system to provide the calibration factors. Performing regression analysis through the strain versus output curve results in a slope that, when entered back into the DAQFI program, will convert the output from the strain gages into microstrain.

The MTS LVDT and the MTS Load Cell also required calibration factors for the DAQFI program. These were both calibrated before the test chamber was placed in the MTS load frame. A two-inch diameter steel rod was gripped in the MTS and pulled in tension. Output data were recorded from the output of the DAQFI program and the load-displacement data from the MTS digital display. A regression analysis through the data sets resulted in two slopes, one to convert the output voltage from the MTS LVDT into inches, and another to convert the output voltage from the MTS load cell into pounds force.

2.5.3.2 Flat Laminates Strain Gages

The flat laminate specimens (FLHT-01 and FLHT-02) each had four strain gages attached at the locations graphically shown in Figure 2.22. The relative coordinates of the strain gages are detailed in Tables 2.9 and 2.10:

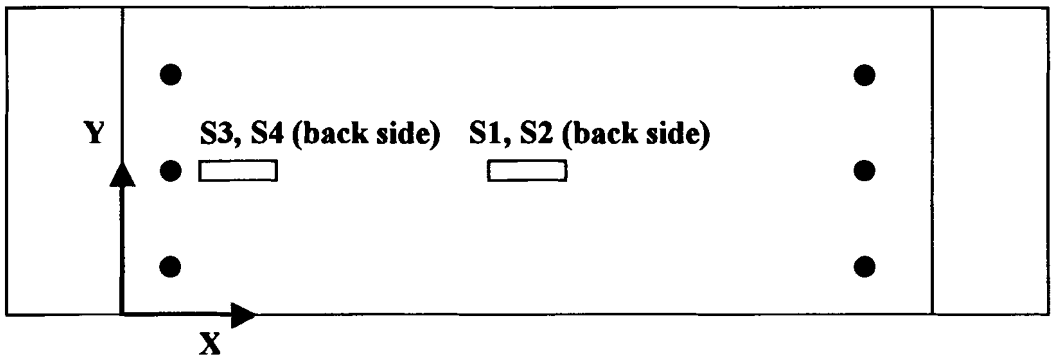

Figure 2.22 – Strain Gage Locations (FLHT-01 and FLHT-02)

Table 2.9 – Strain Gage Coordinates (FLHT-01)

Description	X	Y
S1 – Centerline OML*	13.0 in (33.02 cm)	3.375 in (8.57 cm)
S2 – Centerline IML*	13.0 in (33.02 cm)	3.375 in (8.57 cm)
S3 – Clamped End OML+	2.0 in (5.08 cm)	3.375 in (8.57 cm)
S4 – Clamped End IML+	2.0 in (5.08 cm)	3.375 in (8.57 cm)
*CEA-00-125UN-350		
+CEA-06-240UZ-120		

Table 2.10 – Strain Gage Coordinates (FLHT-02)

Description	X	Y
S1 – Centerline OML*	13.0 in (33.02 cm)	3.375 in (8.57 cm)
S2 – Centerline IML*	13.0 in (33.02 cm)	3.375 in (8.57 cm)
S3 – Clamped End OML*	2.0 in (5.08 cm)	3.375 in (8.57 cm)
S4 – Clamped End IML*	2.0 in (5.08 cm)	3.375 in (8.57 cm)
*CEA-00-125UN-350		

2.5.3.3 Flat Laminates LVDTs

Figure 2.23 gives a graphical representation of where the LVDTs were positioned for specimen FLHT-01, and Table 2.11 outlines the specific coordinates. After flat specimen FLHT-01 was tested, it was found that the centerline aluminum clamp interfered with the maximum deflection of the panel due to the flat specimens' inherent flexibility. During the second test on FLHT-01, the centerline clamp was removed. The centerline clamp was also removed for both tests conducted on flat specimen FLHT-02. The centerline deflection was only monitored by the MTS LVDT (D0). D1 through D3 represent Macro Sensor LVDTs mounted to the exterior of the chamber with steel and aluminum rods extending into the interior contacting the specimen.

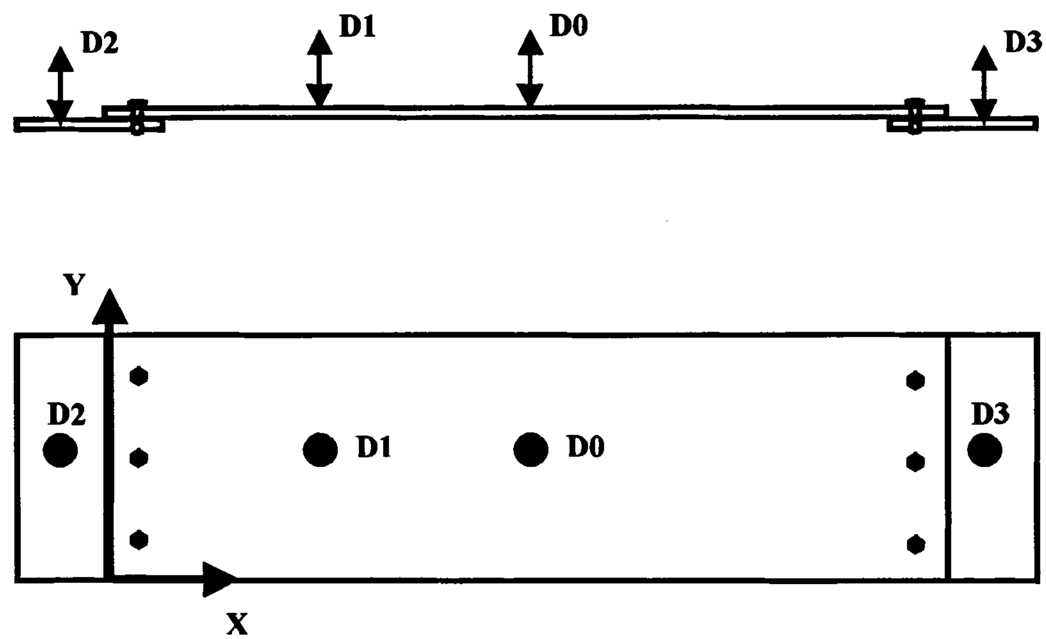

Figure 2.23 – LVDT Locations (Specimens FLHT-01 and FLHT-02)

Table 2.11 – LVDT Coordinates (Specimens FLHT-01 and FLHT-02)

Description	X	Y
D0 – MTS LVDT	13.0 in (33.02 cm)	3.375 in (8.57 cm)
D1 – Quarter-Length	6.5 in (16.51 cm)	3.375 in (8.57 cm)
D2 – Front-Clamped Edge	-0.75 in (-1.905 cm)	3.375 in (8.57 cm)
D3 – Rear Clamped Edge	26.75 in (67.945 cm)	3.375 in (8.57 cm)

2.5.3.4 Hat Stiffened Laminates Strain Gages

There were three strain gage lay-ups for the hat-stiffened panels, a two gage lay-up, six gage lay-up, and a twelve gage lay-up. Articles HSHT-01, HSHT-02, and HSRT-02 were instrumented with two strain gages. This is shown graphically in Figure 2.24 and the coordinates are given in Table 2.12, where gages are placed at the centerline only.

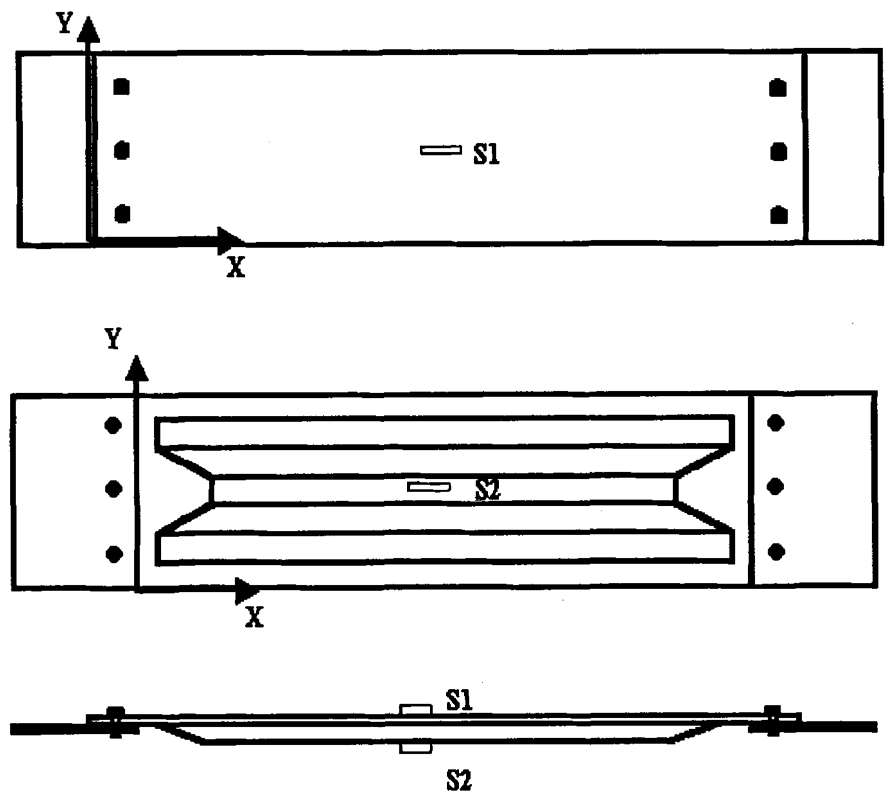

Figure 2.24 – Strain Gage Locations (Specimens HSHT-01, HSHT-02, and HSRT-02)

Table 2.12 – Strain Gage Coordinates (Specimen HSHT-01, HSHT-02, HSRT-02)

Description	X (in.)	Y (in.)
S1 – Centerline OML*	13.0	3.375
S2 – Centerline IML*	13.0	3.375
*CEA-00-125UW-350		

Test specimens HSRT-01 and HSHT-02 were instrumented with six strain gages. This is shown graphically in Figure 2.25 and the coordinates are given in Table 2.13.

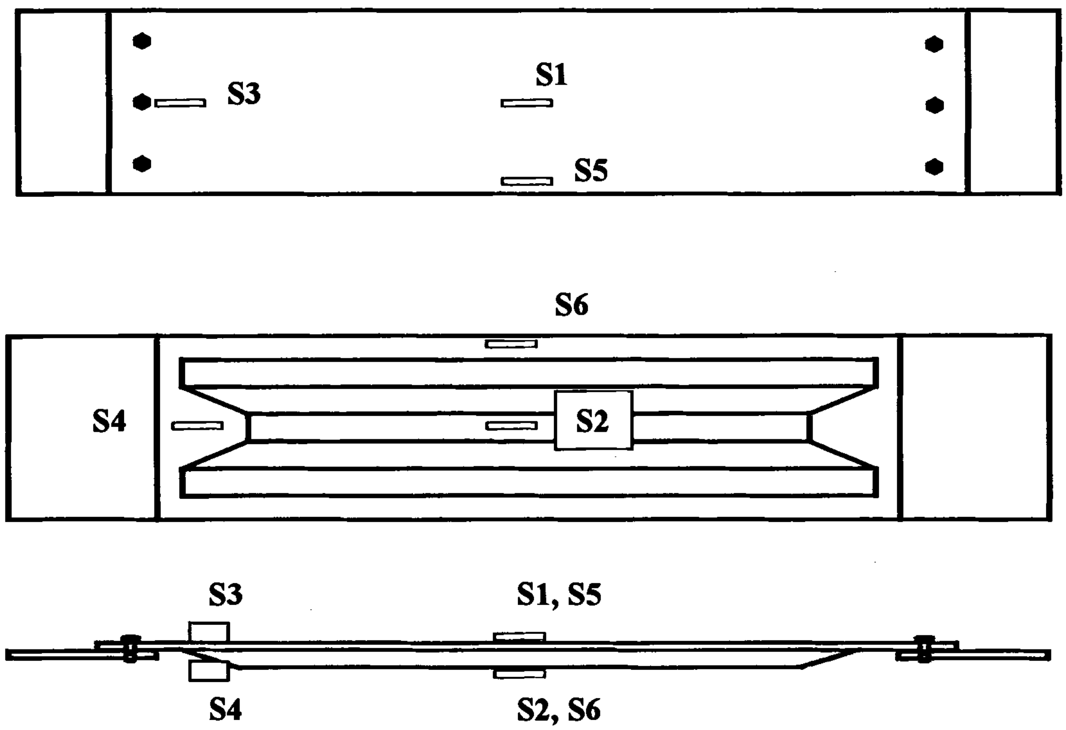

Figure 2.25 – Strain Gage Locations (Specimens HSRT-01 and HSHT-03)

Table 2.13 – Strain Gage Coordinates (Specimens HSRT-01 and HSHT-03)

Description	X	Y
S1 – Centerline OML*	13.0 in	3.375 in
S2 – Centerline IML*	13.0 in	3.375 in
S3 – Clamped End Center OML+	2.0 in	3.375 in
S4 – Clamped End Center IML+	2.0 in	3.375 in
S5 – Center Edge OML+	13.0 in	0.25 in
S6 – Center Edge IML+	13.0 in	0.25 in
*CEA-00-125UN-350		
+CEA-06-240UZ-120		

Specimen HSRT-03 was instrumented with twelve strain gages. This is shown graphically in Figure 2.26 and the coordinates are given in Table 2.14.

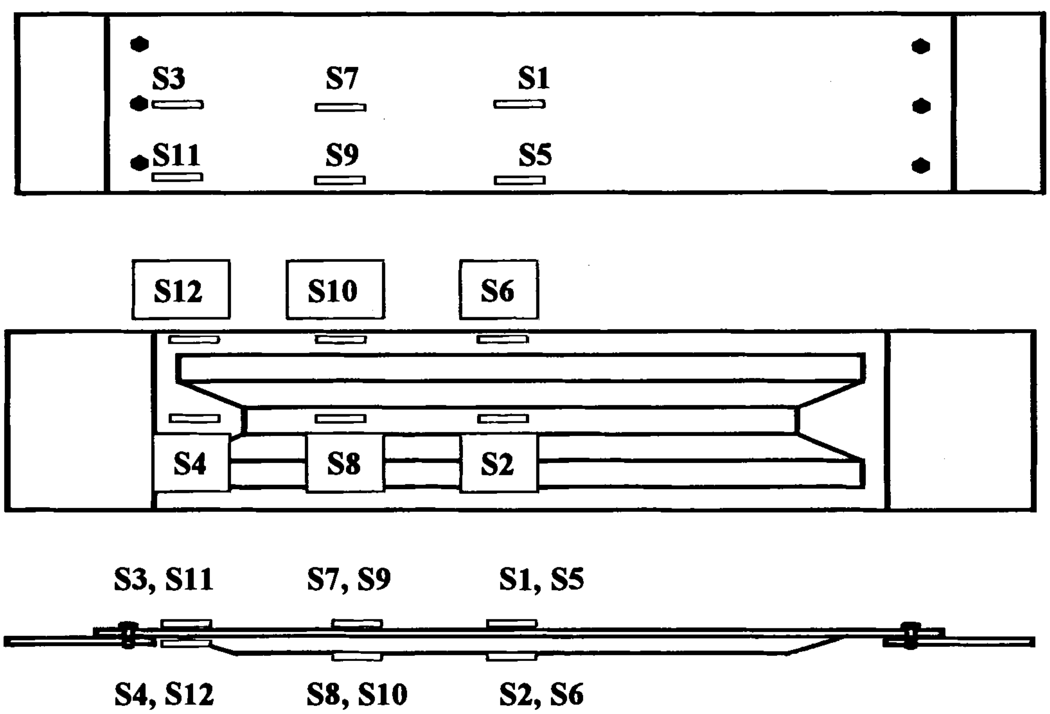

Figure 2.26 – Strain Gage Locations (Specimen HSRT-03)

Table 2.14 – Strain Gage Coordinates for HSRT-03

Description	X	Y
S1 – Centerline OML[*]	13.0 in	3.375 in
S2 – Centerline IML[*]	13.0 in	3.375 in
S3 – Clamped End Center OML[+]	2.0 in	3.375 in
S4 – Clamped End Center IML[+]	2.0 in	3.375 in
S5 – Center Edge OML[+]	13.0 in	0.25 in
S6 – Center Edge IML[+]	13.0 in	0.25 in
S7 – Quarter-Length Center OML[+]	6.5 in	3.375 in
S8 – Quarter-Length Center IML[+]	6.5 in	3.375 in
S9 – Quarter-Length Edge OML[+]	6.5 in	0.25 in
S10 – Quarter-Length Edge IML[+]	6.5 in	0.25 in
S11 – Clamped End Edge OML[+]	2.0 in	0.25 in
S12 – Clamped End Edge IML[+]	2.0 in	0.25 in
[*]CEA-00-125UN-350		
[+]CEA-06-240UZ-120		

2.5.3.5 Hat-Stiffened Laminates LVDTs

All of the hat-stiffened laminates were instrumented with LVDTs at the locations and coordinates shown in Figure 2.27 and Table 2.15. D0 represents the MTS LVDT, while D1 through D5 represent Macro Sensor LVDTs mounted to the exterior of the chamber with aluminum and steel rods extending into the interior to follow the specimen.

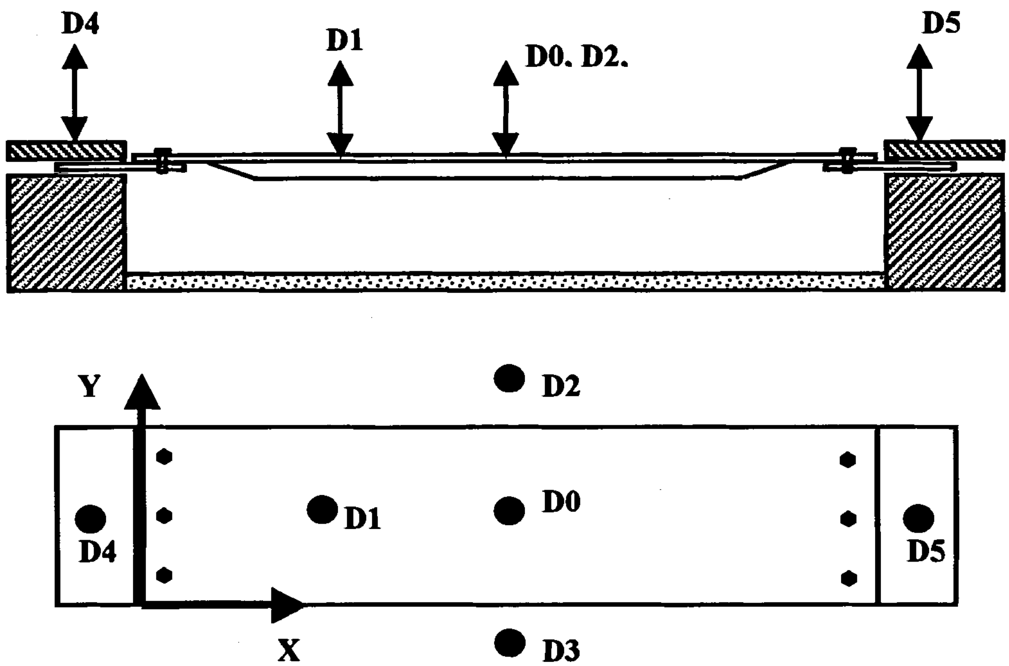

Figure 2.27 – LVDT Locations (Specimens HSHT-01 through HSHT-03, HSRT-01 through HSRT-03)

Table 2.15 – LVDT Coordinates (Specimens HSHT-01 through HSHT-03, HSRT-01 through HSRT-03)

Description	X	Y
D0 – MTS LVDT	13.0 in	3.375 in
D1 – Quarter-Length	6.5 in	3.375 in
D2 – Left Centerline	13.0 in	11.625 in
D3 – Right Centerline	13.0 in	-4.875 in
D4 – Front-Clamped Edge	-0.75 in	3.375 in
D5 – Rear Clamped Edge	26.75 in	3.375 in

2.5.3.6 Composite Sandwich Panel Strain Gages

All of the composite sandwich panels were instrumented with six strain gages. Figure 2.28 and Table 2.16 give the locations of the strain gages bonded to the 24-inch composite sandwich panels. These include panels: FI-ET-D5B, FI-RT-D5C, FI-RT-D5A.

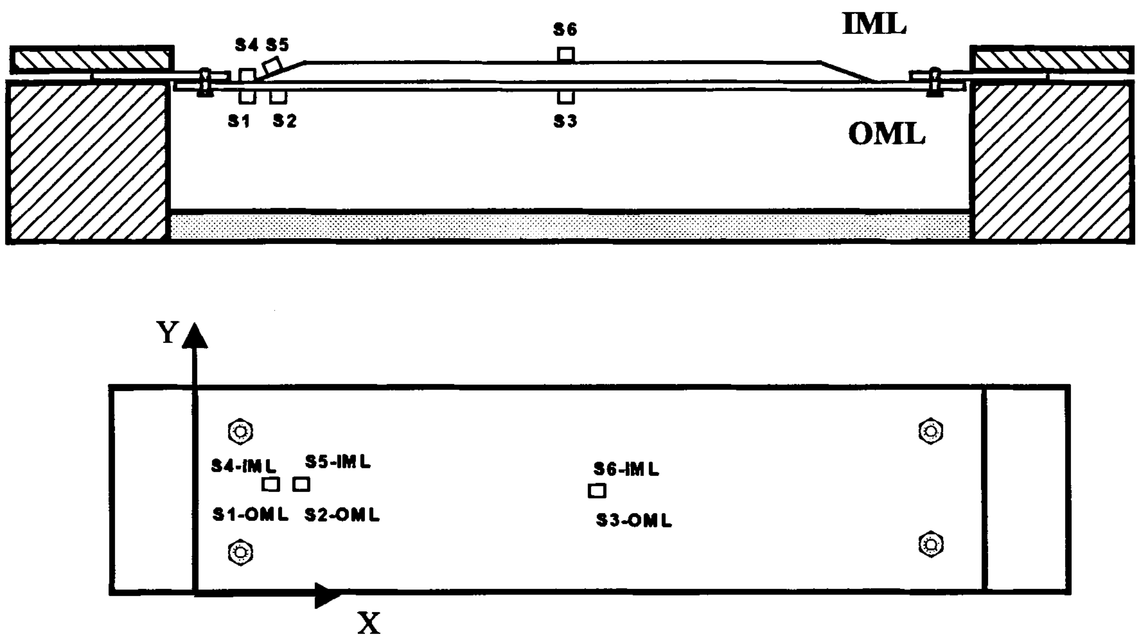

Figure 2.28 – Location of Strain Gages for Composite Sandwich Panels

Table 2.16 – Strain Gage Coordinates for 30° Taper Sandwich Panels

Designation	Device	X (in)	Y (in)	Facesheet
S1*	Uniaxial Strain Gage	1.9 in	2.25 in	OML
S2*	Uniaxial Strain Gage	2.3 in	2.25 in	OML
S3*	Uniaxial Strain Gage	12 in	2.25 in	OML
S4*	Uniaxial Strain Gage	1.9 in	2.25 in	IML
S5*	Uniaxial Strain Gage	2.3 in	2.25 in	IML
S6*	Uniaxial Strain Gage	12 in	2.25 in	IML
*CEA-00-125UW-350				

Table 2.17 lists the coordinates for the strain gages bonded to the 26-inch composite sandwich panels. These include: FI-ET-D3B, FI-RT-P03D, FI-RT-P01C, FI-RT-P05D, FI-RT-D3C, FI-RT-D3A.

Table 2.17 – Strain Gage Coordinates for 20° Taper Composite Sandwich Panels

Designation	Device	X (in)	Y (in)	Facesheet
S1*	Uniaxial Strain Gage	1.9 in	2.25 in	OML
S2*	Uniaxial Strain Gage	2.5 in	2.25 in	OML
S3*	Uniaxial Strain Gage	13 in	2.25 in	OML
S4*	Uniaxial Strain Gage	1.9 in	2.25 in	IML
S5*	Uniaxial Strain Gage	2.5 in	2.25 in	IML
S6*	Uniaxial Strain Gage	13 in	2.25 in	IML
*CEA-00-125UW-350				

2.5.3.7 Composite Sandwich Panel LVDTs

Figure 2.29 and Table 2.18 give the locations of the LVDTs for the 30° taper composite sandwich panels, which included: FI-ET-D5B, FI-RT-D5C, FI-RT-D5A. D0 represents the MTS LVDT and D1 through D6 represent Macro Sensor LVDTs mounted on the exterior of the chamber with steel and aluminum rods extending into the interior contacting the test specimens. D1 and D2 are the LVDTs used with the centerline clamp.

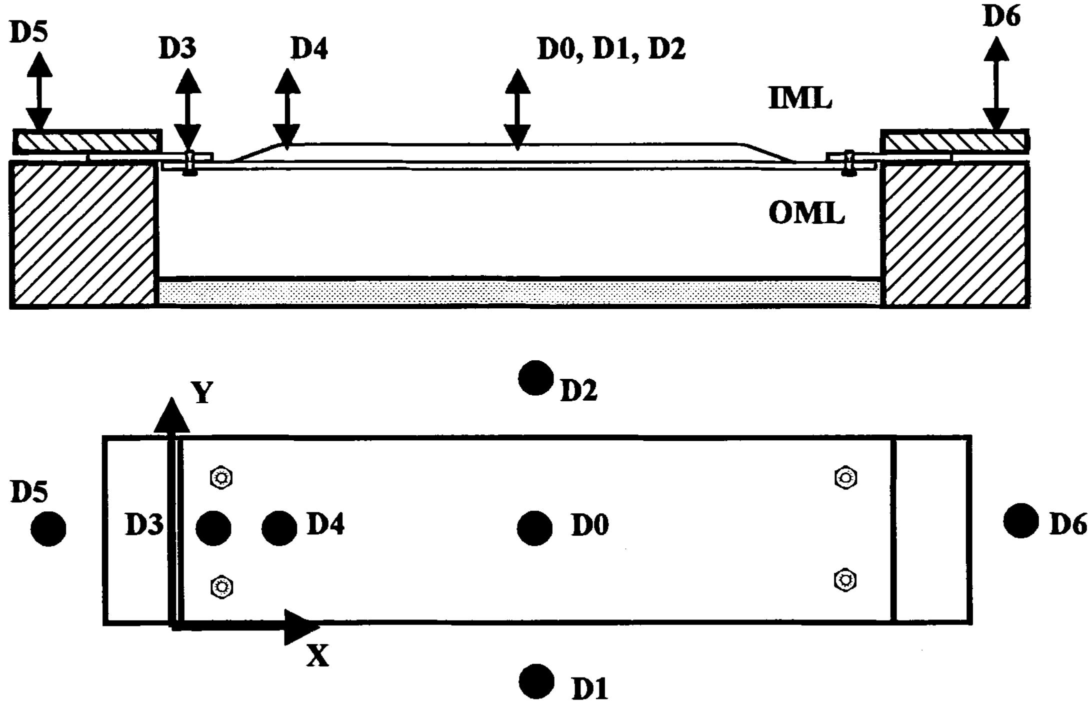

Figure 2.29 – Location of LVDT's for Composite Sandwich Panels

Table 2.18 – LVDT Coordinates for 30° Taper Composite Sandwich Panels

Designation	Device	X (in)	Y (in)	Facesheet
D0	MTS LVDT	12 in	2.25 in	OML
D1	LVDT	12 in	-6.25 in	IML
D2	LVDT	12 in	10.75 in	IML
D3	LVDT	3.75 in	2.25 in	IML
D4	LVDT	1.0 in	2.25 in	IML
D5	LVDT	-1.25 in	2.25 in	-
D6	LVDT	25.25 in	2.25 in	-

Table 2.19 lists the coordinates of the LVDTs for the 20° tapered composite sandwich panels. D0 represents the MTS LVDT and D1 through D6 represent Macro Sensor LVDTs mounted on the exterior of the chamber with steel and aluminum rods extending into the interior contacting the test specimens. These included: FI-ET-D3B, FI-RT-P03D, FI-RT-P01C, FI-RT-P05D, FI-RT-D3C, FI-RT-D3A.

Table 2.19 – LVDT Coordinates for 20° Taper Composite Sandwich Panels

Designation	Device	X (in)	Y (in)	Facesheet
D0	MTS LVDT	13 in	2.25 in	OML
D1	LVDT	13 in	-6.25 in	IML
D2	LVDT	13 in	10.75 in	IML
D3	LVDT	4.25 in	2.25 in	IML
D4	LVDT	1.0 in	2.25 in	IML
D5	LVDT	-1.25 in	2.25 in	-
D6	LVDT	27.25 in	2.25 in	-

2.5.4 Elevated Temperature Test Procedure

The first step in the elevated temperature testing procedure is to ensure that the entire oven is centered within the MTS load frame. The steel I-beam is set loosely into the bottom grips of the MTS load frame. The steel channel is then bolted to the I-beam, and the base of the chamber is bolted to the channel. To center the base of the oven in the grips, a plumb bob and string is hung from the centerline mark etched onto the top

grips of the MTS. When centered, the lower grips of the MTS are closed around the support I-beam. The steel blocks are then placed into position on the chamber base, and the cartridge heaters are inserted into the blocks and plugged into the junction box. Then the infrared heating lamps are spaced evenly around the base of the chamber and plugged into the junction box. The titanium bolts attaching the aluminum end plates to the test panel are torqued to 75 in-lbf, and then the specimen is placed into the chamber on the steel blocks, ensuring that the aluminum endplates are centered on the steel blocks and that there is a 0.25 in gap between the end of the panel and the edge of the steel blocks. Then the top steel plates are clamped down on the endplates of the test article. The bolts clamping around the panel are torqued to 30 ft-lbf. The top of the test chamber is then placed on top of the base, and the pivoting load contact head, with its steel extension arm, is inserted in the top grips of the MTS. Rope is passed through the rings on top of the chamber and the steel rings atop the MTS crosshead. This allows the top of the chamber to be raised and lowered with the crosshead of the MTS. The spring-loaded DCDT followers are then brought into contact with the article and the strain gages are connected to the strain amplifier. For the elevated temperature tests, it is necessary to use high temperature strain gage wire within the chamber, and standard three-wire strain gage wire outside of the chamber. The oven door is clamped into place, and the HeatChamber program is launched to begin heating to the desired temperature. Once at temperature, the bottom load head of the MTS is brought up until it just contacts the surface of the panel. The MTS is switched to “load control” and any pre-load is removed from the panel while still keeping it in contact with the pivoting load head. With the MTS in “load control”, the load is

maintained by allowing the computer to adjust the displacement at will. All of the strain gages are balanced using the controls on the strain amplifier and the DCDTs are adjusted so that they read zero displacement according to the DAQFI software. The data acquisition program is activated, and the MTS TestStar program is launched in "displacement control". With the MTS in "displacement control", the load head moves at a constant rate once the test commences. The rate of displacement for the test depends on the type of panel being tested. In this study, 0.00167 in/sec was used for the hat-stiffened laminates, 0.0025 in/sec was used for the flat laminates, and 0.00067 in/sec was used for testing of the composite sandwich panels. A greater displacement rate was used for the flat laminates due to their greater flexibility. The elevated temperature procedure is summarized below:

1. Assemble the chamber base and center it in the bottom grips of the MTS 810 load frame.
2. Place the steel end blocks, with cartridge heaters inserted, onto the chamber base.
3. Arrange infrared heating lamps on base.
4. Assemble the test article. The titanium bolts attaching the aluminum endplates to the panel are torqued to 75 in-lbf.
5. Center the assembled panel on the steel blocks.
6. Clamp the panel down with the steel plates. The bolts are torqued to 30 ft-lbf.
7. Connect strain gages to strain amplifier.
8. Place chamber top onto base.

9. Position the LVDTs on top of the chamber, with extension rods contacting the specimen.

10. Balance the strain gages on the strain amplifier and zero the LVDTs using the DAQFI software

11. Close the chamber door and launch HeatChamber program to heat the chamber to desired temperature.

12. Once at temperature, raise bottom MTS grip in "displacement control" until the panel contacts the load head.

13. Switch to "load control" and remove any pre-load on the panel.

14. Balance the strain gages using the strain amplifier and zero the LVDTs using the DAQFI software.

15. Activate the data acquisition system, and commence testing.

2.5.5 Room Temperature Test Procedure

The procedure for the room temperature tests (conducted on specimens HSRT-01, HSRT-02, HSRT-03) is identical to the elevated temperature test with the exception that the chamber heating system is not active and the chamber door is left off for better viewing of the tests. The chamber itself was still lowered down onto the test set-up because the LVDTs are mounted to the exterior of the chamber.

The room temperature sandwich panels (specimens FI-RT-P03D, FI-RT-P01C, FI-RT-P05D, FI-RT-D5C, FI-RT-D5A, FI-RT-D3C, and FI-RT-D3A) were tested as part of a previous study (Caccese and Malm 1999). The test procedure was identical to the

room temperature tests conducted in this study with the exception that the test chamber, steel channel, heating system, and steel extension arm in the MTS upper grips were all omitted. The test specimens spanned the steel blocks, which rested on the I-beam. Different fixtures were also used to mount the LVDTs. For more information, consult the aforementioned reference.

3. Test Results

This section presents the test results at elevated and room temperatures of the three configurations of panels presented in Section 2. Peak loads, maximum displacements, and modes of failure will be discussed. In addition, plots of the load-deflection data, plots of the load-strain data, and photographs of the failures will be presented.

3.1 Results from the Flat Laminate Test Articles

Two problems arose with the testing of the flat laminates. The flat laminates deflected more per unit load than the hat-stiffened laminates due to their lower stiffness values. Because of this, the maximum displacement allowed by the test chamber was reached before either laminate could fail. Two flexure tests were performed on both laminate specimens. During the first test on each laminate, the ends of each specimen were clamped using threaded steel rods that passed through the Marinite base of the chamber and clamped. This condition resulted in excessive support rotation. This condition was mitigated during the second test, where the ends of each specimen were clamped with threaded steel rods that passed through the base of the chamber and the steel channel beneath the chamber, thereby creating an inherently stiffer boundary condition. In addition, during the second test on FLHT-01, the centerline LVDT clamp was removed to allow for a greater centerline deflection.

The results from the elevated temperature flexure tests on the flat laminates are summarized below in Tables 3.1 through 3.5. Peak loads and peak displacements at test termination are given for each specimen in Table 3.1, while Tables 3.2 and 3.5

give panel stiffness values measured at the LVDT sensor locations and strains per unit load measured at the strain gage locations.

Table 3.1 – Summary of Flat Laminate Results

Panel	Peak Load (lbs)	Crosshead Disp. (in)
FLHT-01-test1*	1,583	2.67
FLHT-01-test2	5,793	3.10
FLHT-02-test1	1,726	3.08
FLHT-02-test2	7,491	3.54
*test1 refers to the test before end support stiffening, test2 refers to the test after end support stiffening		

Table 3.2 – Flat Laminate Stiffness Values – Test 1 (lbf/in)

	MTS LVDT	Centerline Displ.	Quarter-Length	Front Clamped Edge	Rear Clamped Edge
FLHT-01-test1	593.92	612.15	927.90	-84375.08	-98903.23
FLHT-02-test1	565.41	N/A	866.71	-92435.33	-1554.55
Average	579.66	612.15	897.30	-88405.20	-50228.89

Table 3.3 – Flat Laminate Stiffness Values – Test 2 (lbf/in)

	MTS LVDT	Centerline Displ.	Front Clamped Edge	Rear Clamped Edge
FLHT-01-test2	2003.89	2248.36	-636565.96	137406.44
FLHT-02-test2	2175.17	1755.49	64153.19	128781.04
Average	2089.53	2001.93	-286206.39	133093.74

Table 3.4 – Flat Laminate Strains per Unit Load – Test 1 (με/lbf)

	Centerline Top	Centerline Bottom	Clamped Edge Top	Clamped Edge Bottom
FLHT-01-test1	-0.0006	0.2671	0.3730	-0.3974
FLHT-02-test1	-0.0005	0.2575	0.4136	-0.3508
Average	-0.0005	0.2623	0.3933	-0.3741

Table 3.5 – Flat Laminate Strains per Unit Load – Test 2 (με/lbf)

	Centerline Top	Centerline Bottom	Clamped Edge Top	Clamped Edge Bottom
FLHT-01-test2	-0.0032	1.0181	1.7009	-0.1182
FLHT-02-test2	-0.4493	1.1860	1.4294	0.8835
Average	-0.2263	1.1021	1.5652	0.3826

Strengthening the end supports greatly increased the measured stiffness values of the flat laminates. This is summarized in Table 3.6, which lists the average stiffness values before and after the alteration was made to the supports and the percentage change from test 1 to test 2.

Table 3.6 – Effects of End Support Stiffening (lbf/in)

	MTS LVDT	Quarter-Length	Front Clamped Edge	Rear Clamped Edge
Test 1	579.66	897.30	-88405.20	-50228.89
Test 2	2089.53	2001.93	-286206.39	133093.74
% Change	360.47	223.10	323.74	-264.97

3.1.1 Specimen FLHT-01

Specimen FLHT-01 was the first flat laminate tested. Figures 3.1 and 3.2 give the load-displacement and load-strain curves from the first test run on FLHT-01, respectively. The load-displacement plots are fairly linear, as are the load-strain plots until a load of approximately 1,150 lbf, where the load-strain plots at the clamped end locations jump up suddenly. The first test on FLHT-01 was terminated at a load of 1,583 lbf (7.08 kN) and a crosshead displacement of 2.67 inches (6.78 cm) because the specimen reached the deflection limit of the chamber. Figures 3.3 and 3.4 are pictures taken after the test was completed. Both show the extent of the curvature of the laminates.

Figures 3.5 and 3.6 give the load-deflection and load-strain curves for the second test run on FLHT-01, respectively. From the load-displacement curves, it appears that the laminate underwent stress stiffening due to the large displacement effect. The load-strain plots are extremely non-linear. This is probably due to an increased amount of in-plane loading experienced at the sensor locations. Figures 3.7 and 3.8 are pictures taken after the test was completed at a load of 5,793 lbs (25.8 kN) and a crosshead displacement of 3.10 inches (7.87 cm). Specimen FLHT-01 experienced damage to the outer ply (see Figure 3.9). As can be seen in Figure 3.8, there was still a degree of end support rotation during the second test on FLHT-01.

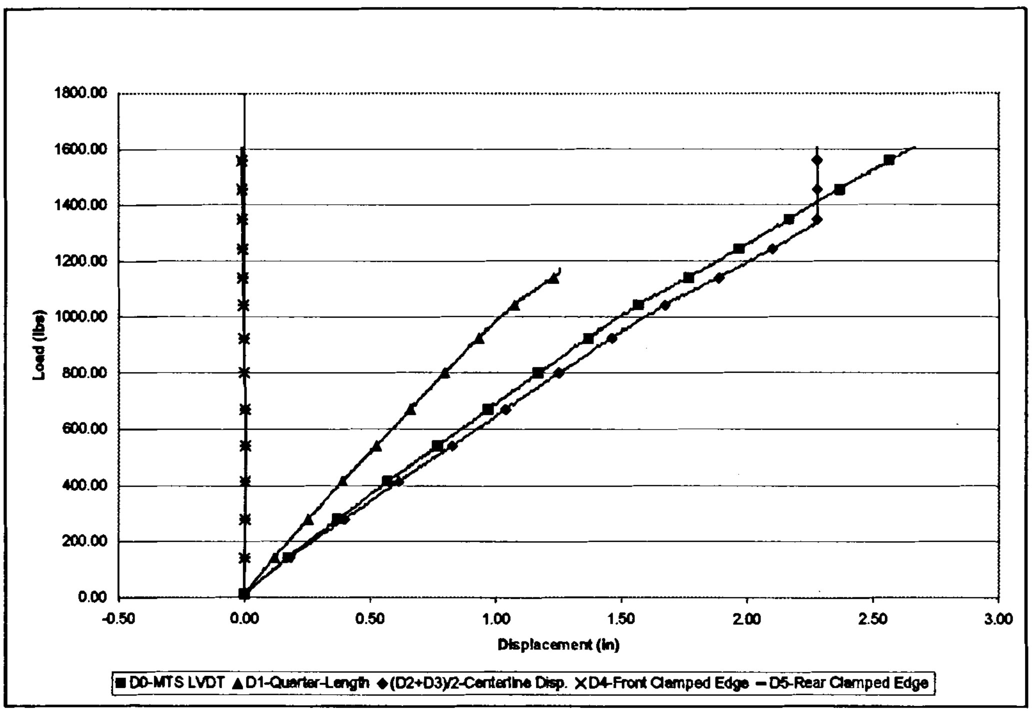

Figure 3.1 – Load-Displacement Curve for FLHT-01 (test 1)

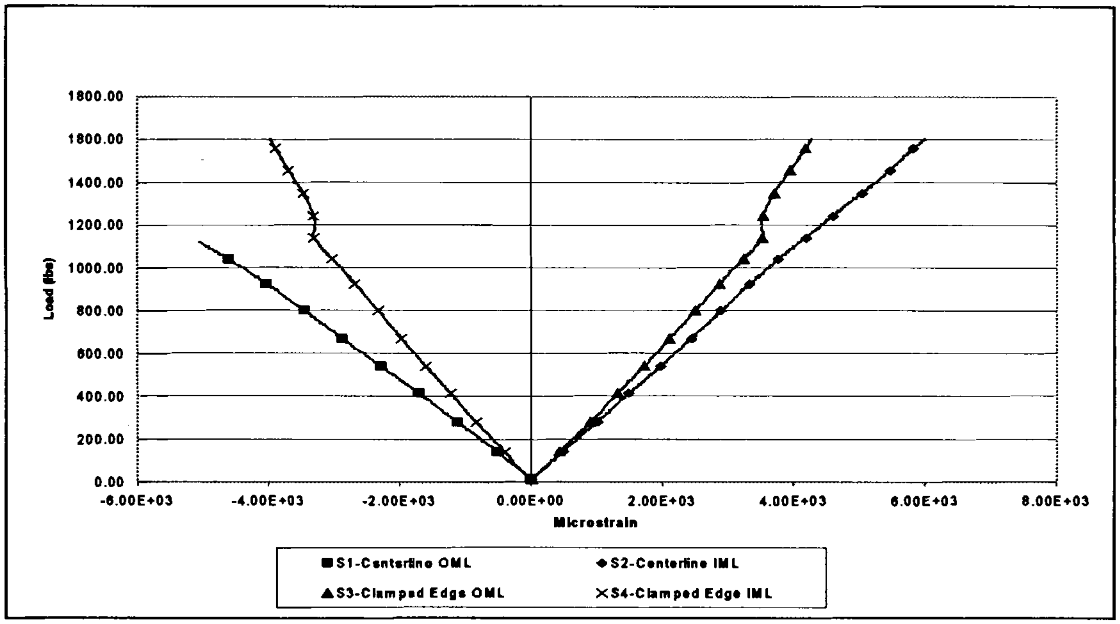

Figure 3.2 – Load-Strain Curve for FLHT-01 (test 1)

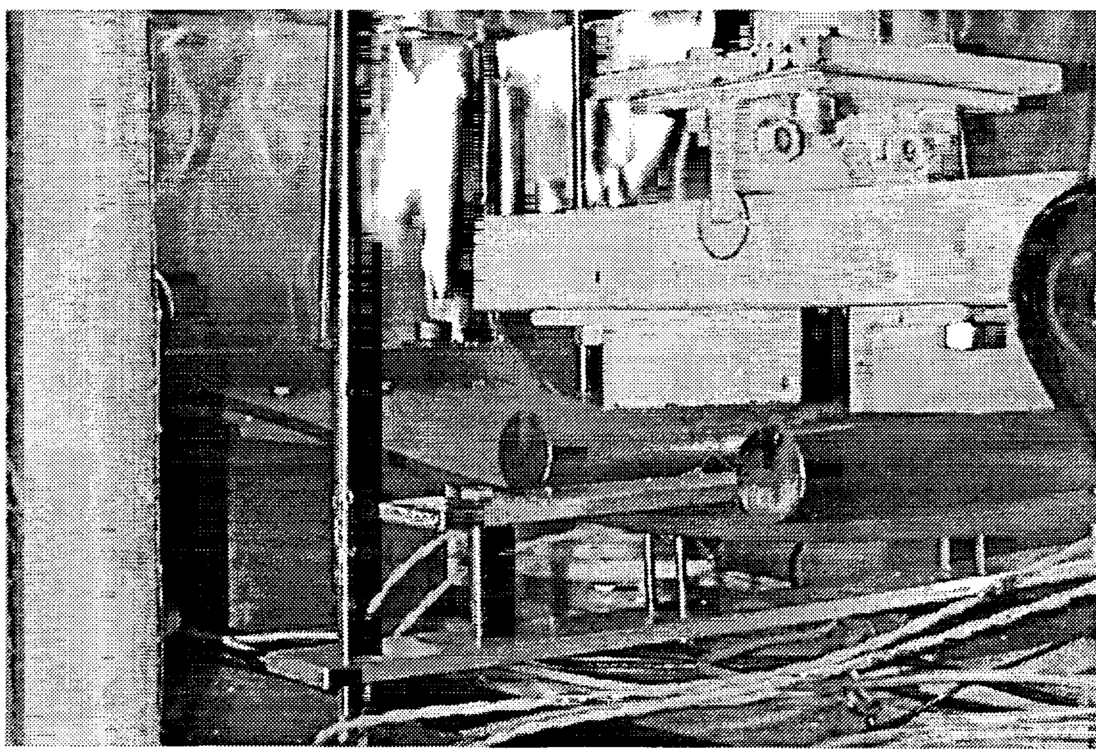

Figure 3.3 – Specimen FLHT-01 (test 1)

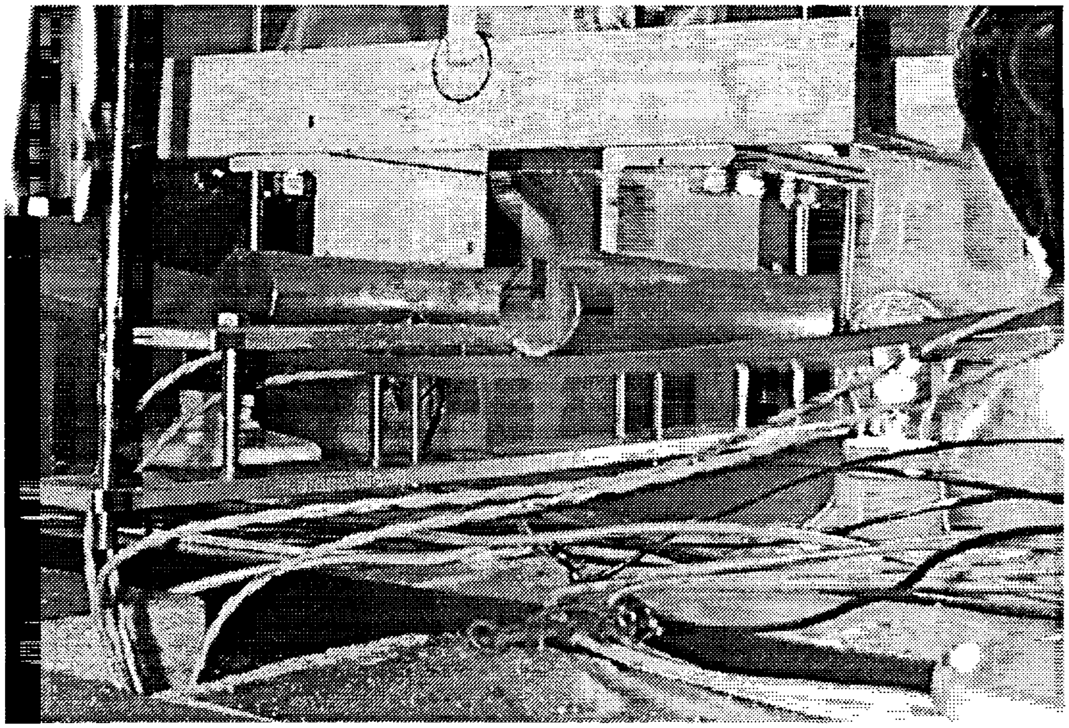

Figure 3.4 – Specimen FLHT-01 (test 1)

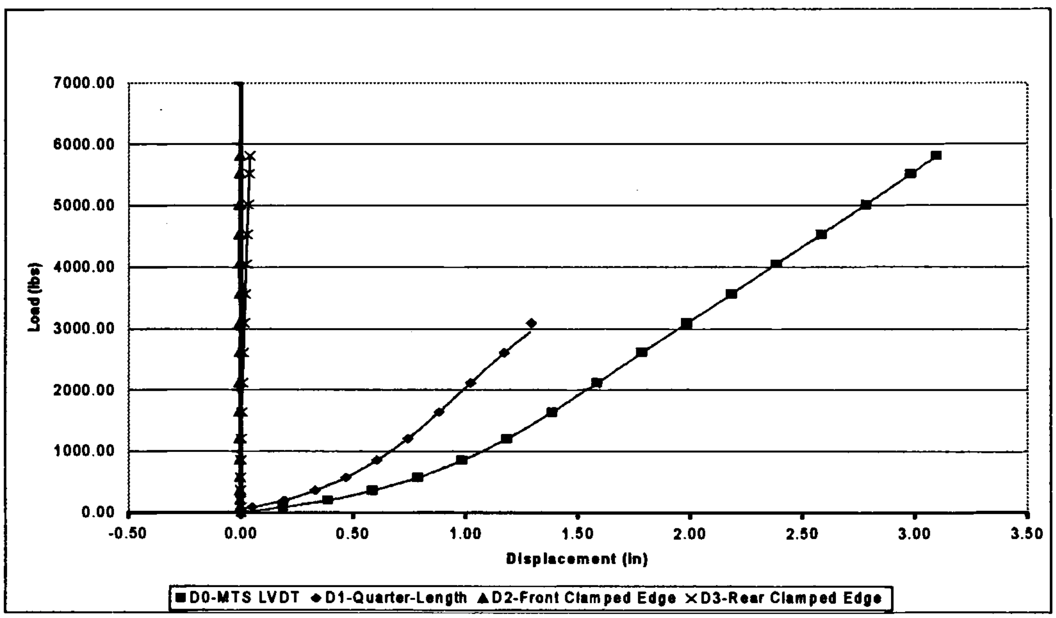

Figure 3.5 – Load-Displacement Curve for FLHT-01 (test 2)

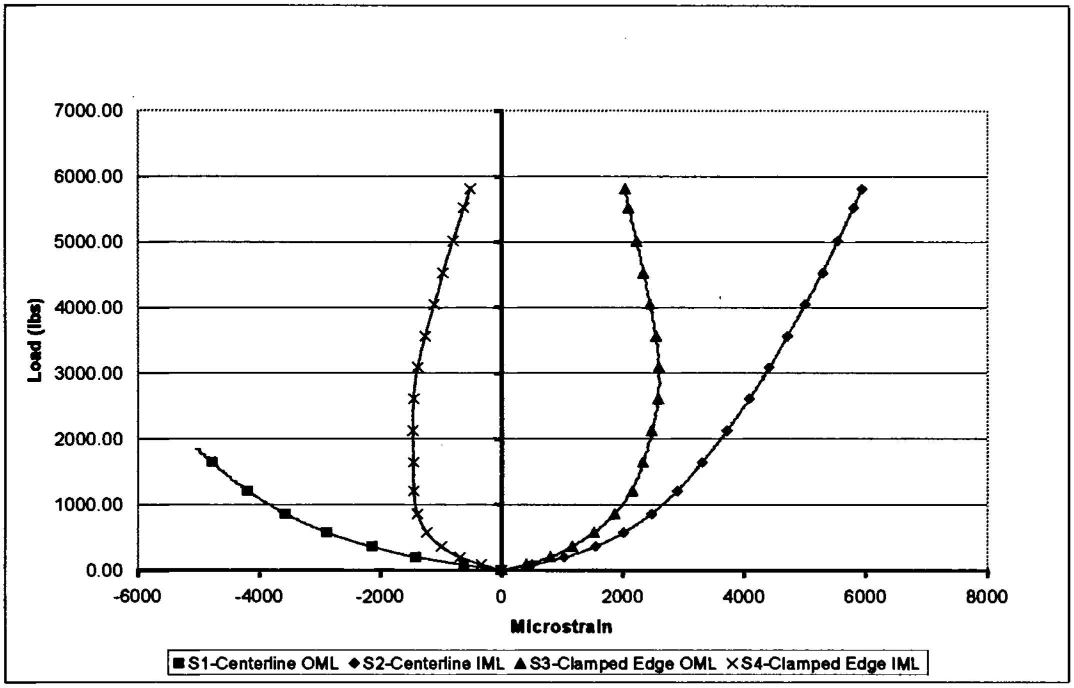

Figure 3.6 – Load-Strain Curve for FLHT-01 (test 2)

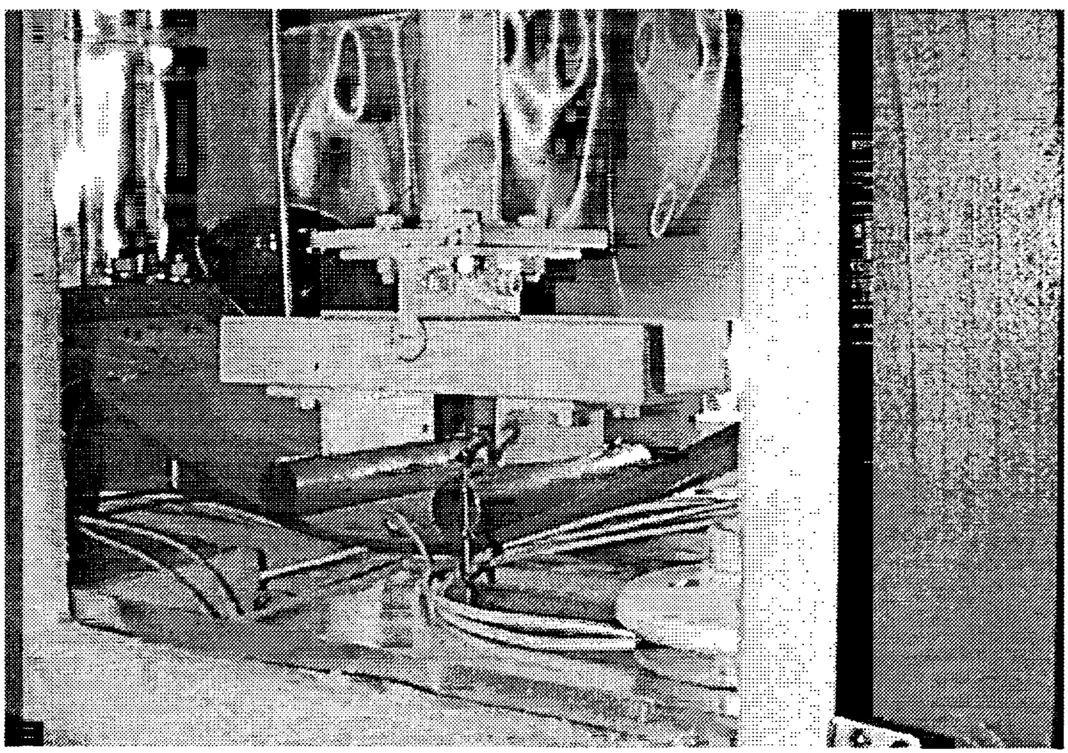

Figure 3.7 – Specimen FLHT-01 (test 2)

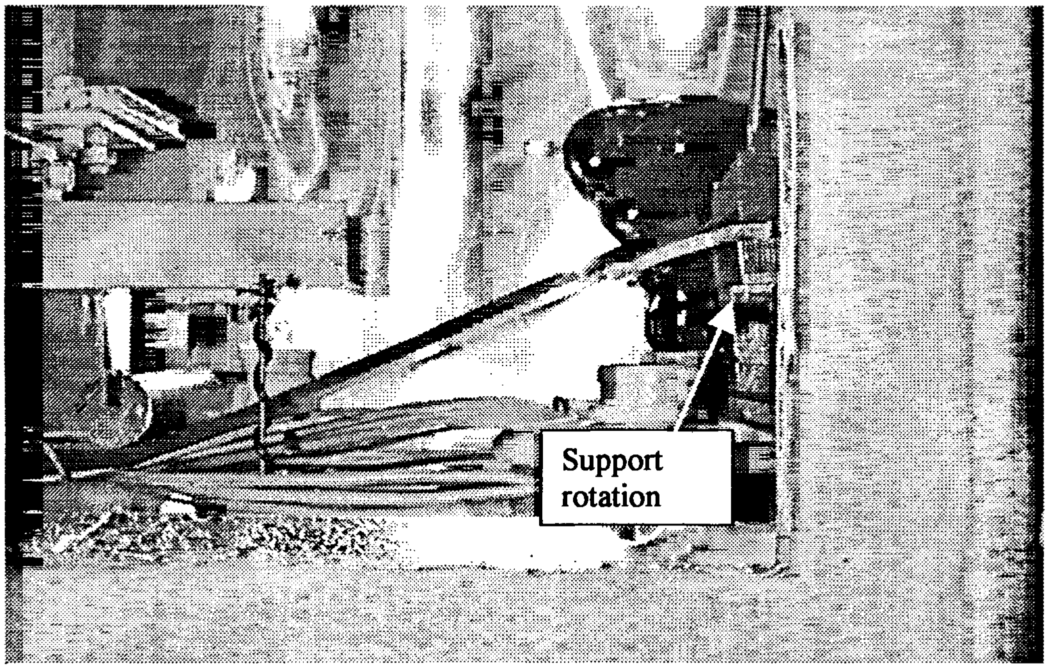

Figure 3.8 – Specimen FLHT-01 (test 2)

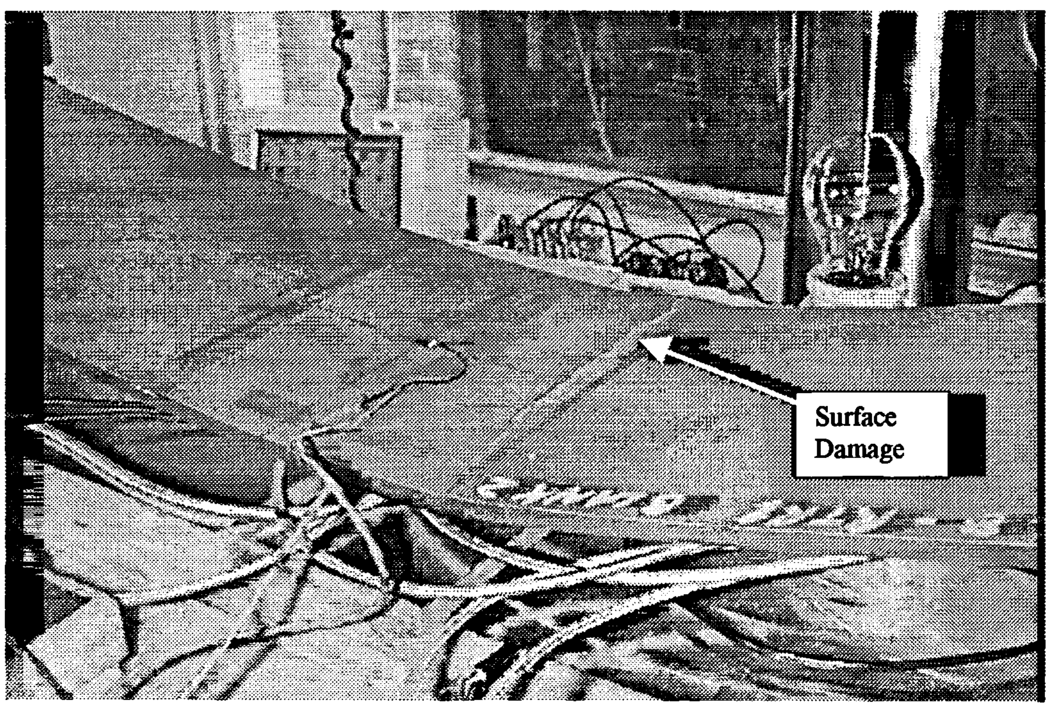

Figure 3.9 – Specimen FLHT-01 (test 2)

3.1.2 Specimen FLHT-02

Specimen FLHT-02 did not fail during the first test or the second test conducted. The centerline clamp was not used during either the first or second test on FLHT-02 in order to allow the laminate to deflect more (approximately 1 inch more). Test 1 on specimen FLHT-02 was terminated at a load of 1,726 lbs (7.68 kN) and a deflection of 3.08 in (7.82 cm). Figures 3.10 and 3.11 are the load-displacement and load-strain curves for FLHT-02 in test 1, respectively. Both the load-displacement and load-strain plots are fairly linear, with a few irregularities that may be attributed to the threaded clamping rods beginning to yield. Figure 3.12 is a photograph taken after test 1 was completed, i.e. when the maximum allowable deflection was reached.

Figures 3.13 and 3.14 are the load-deflection and load-strain curves for test 2 on FLHT-02, respectively. As with specimen FLHT-01, the load-displacement and load-strain plots are highly non-linear. This may be attributed to an increasing amount of in-plane loading from large deformation effects experienced by the laminate as the test progressed. Figures 3.15 through 3.16 are photographs taken after the maximum deflection was reached during test 2. Test 2 was completed at a load 7,491 lbf (33.3 kN) and a deflection of 3.54 in (8.99 cm). The only visible damage was yielding of the aluminum endplates, as shown in Figure 3.17.

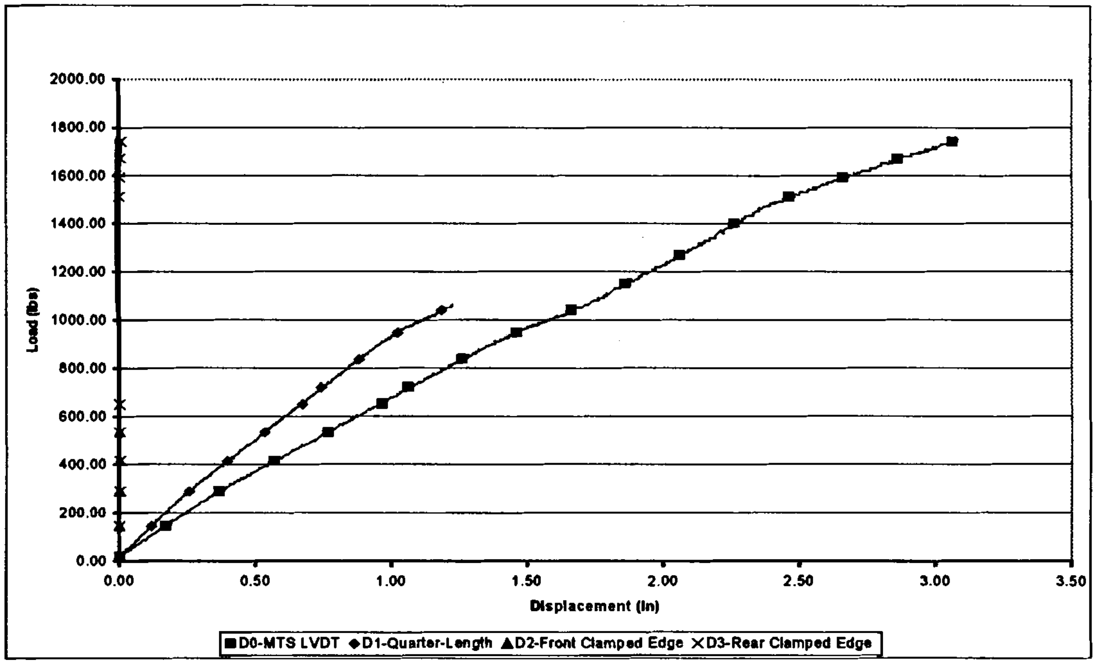

Figure 3.10 – Load-Displacement Curve for FLHT-02 (test 1)

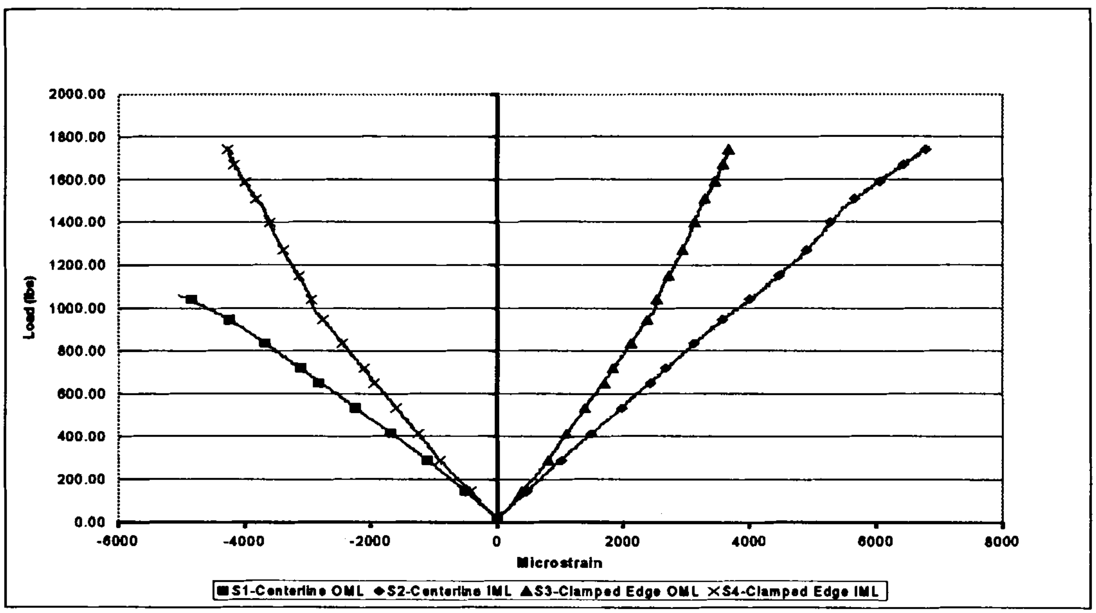

Figure 3.11 – Load-Strain Curve for FLHT-02 (test 1)

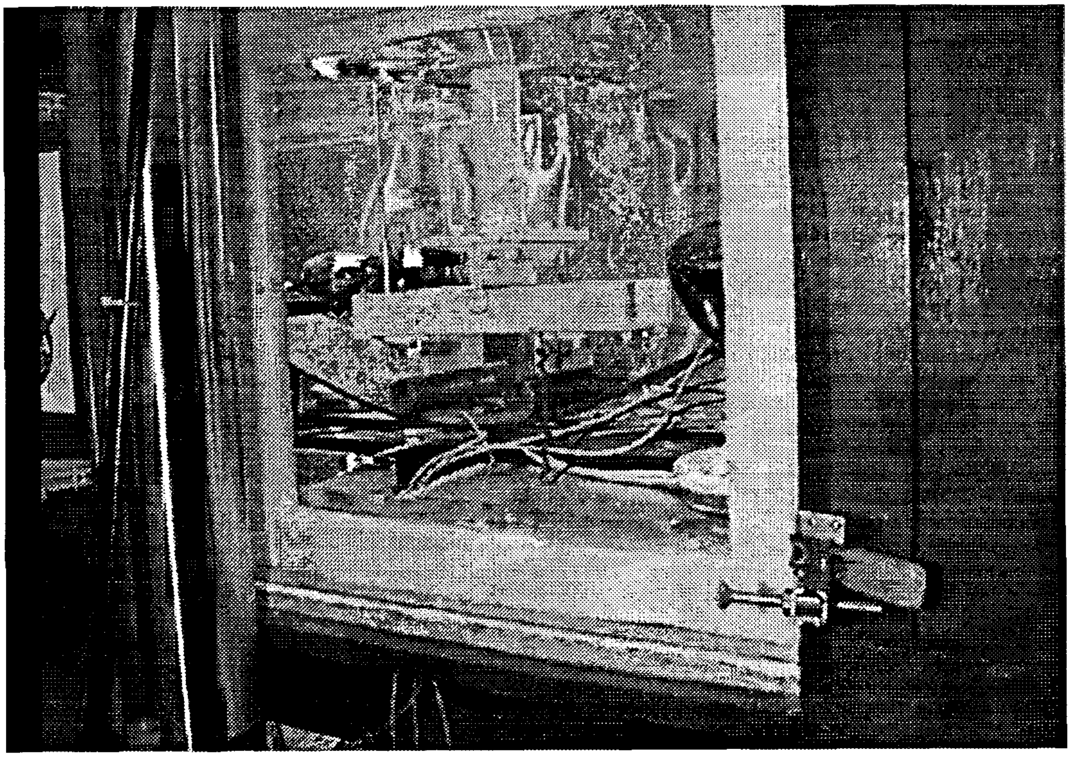

Figure 3.12 – Specimen FLHT-02 (test 1)

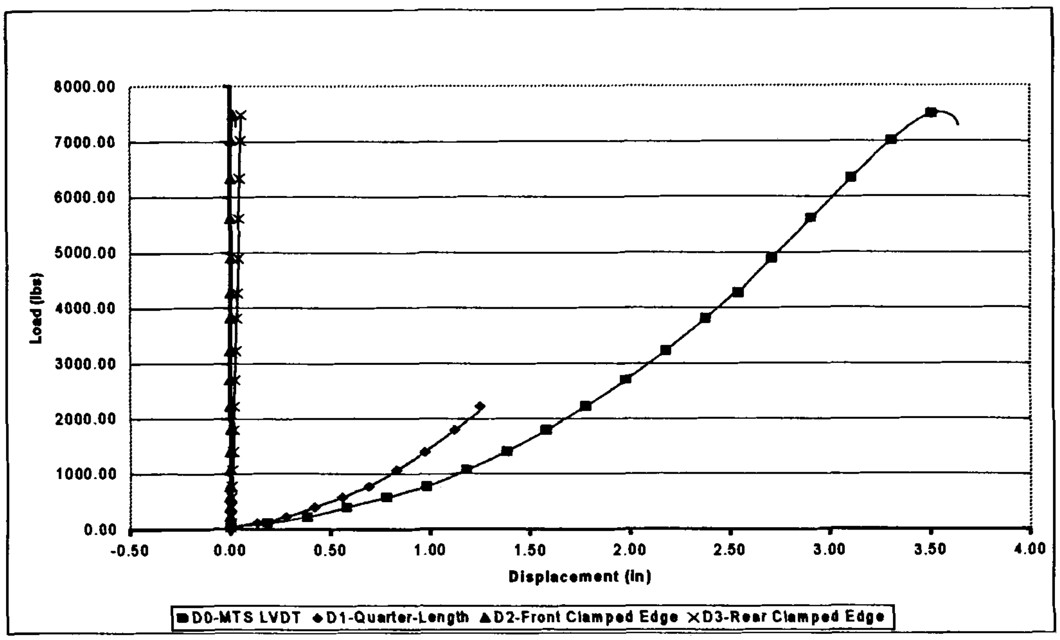

Figure 3.13 – Load Displacement Curve for FLHT-02 (test 2)

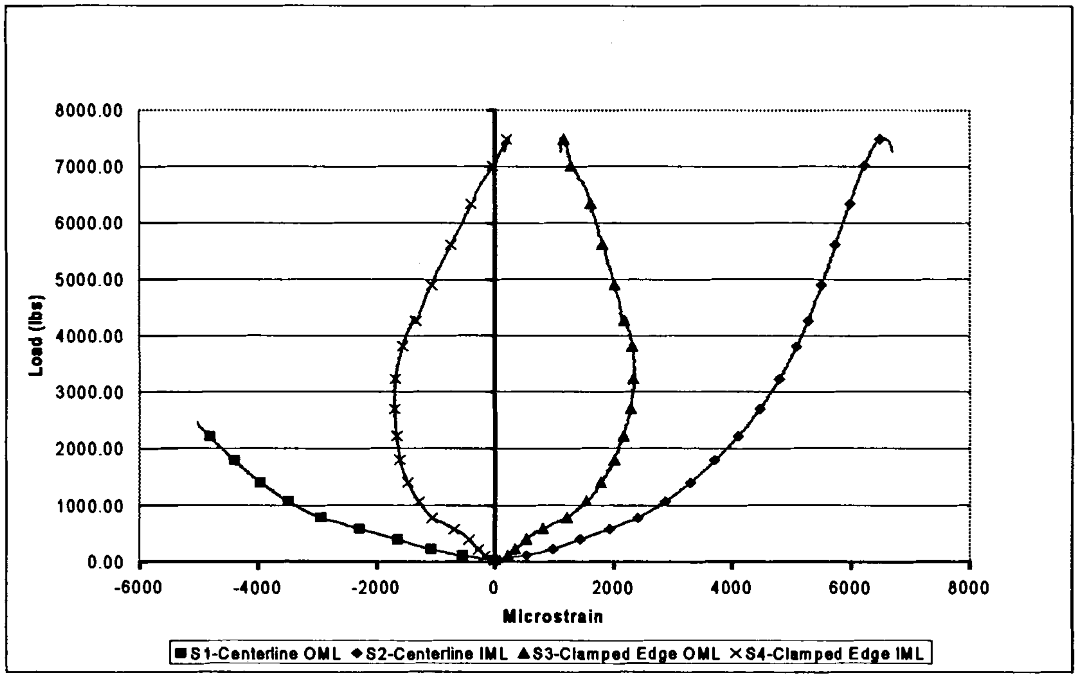

Figure 3.14 – Load-Strain Curve for FLHT-02 (test 2)

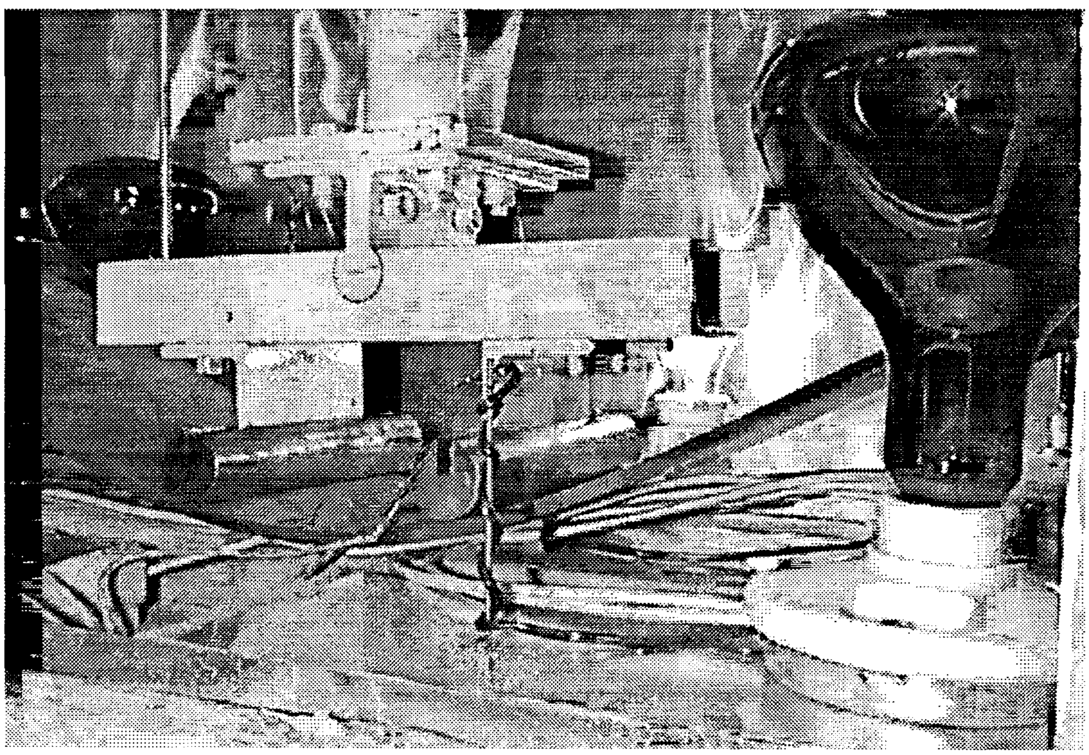

Figure 3.15 – Specimen FLHT-02 (test 2)

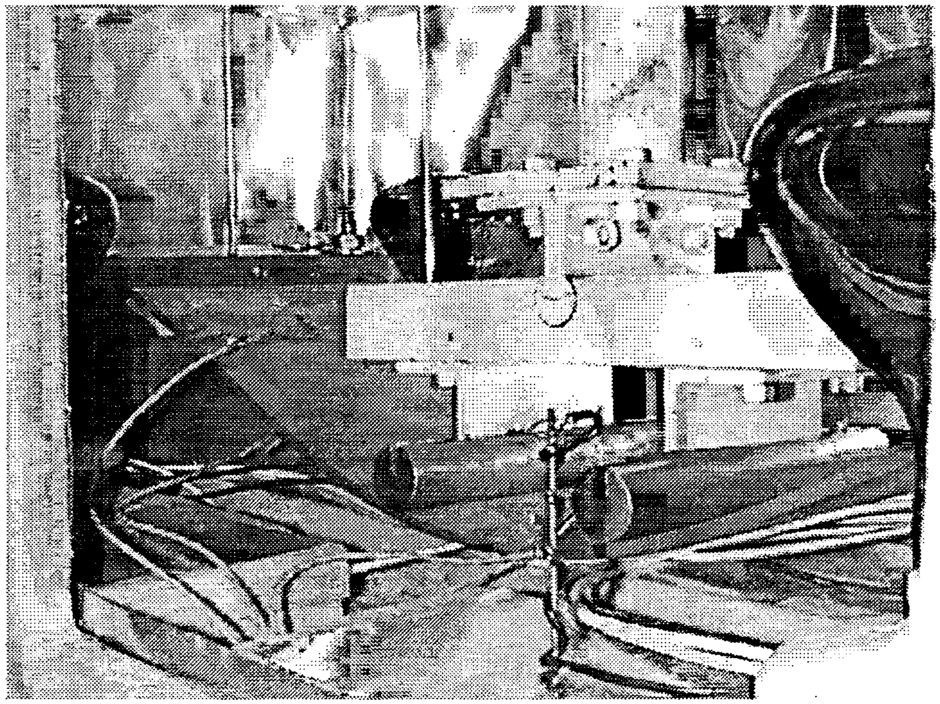

Figure 3.16 – Specimen FLHT-02 (test 2)

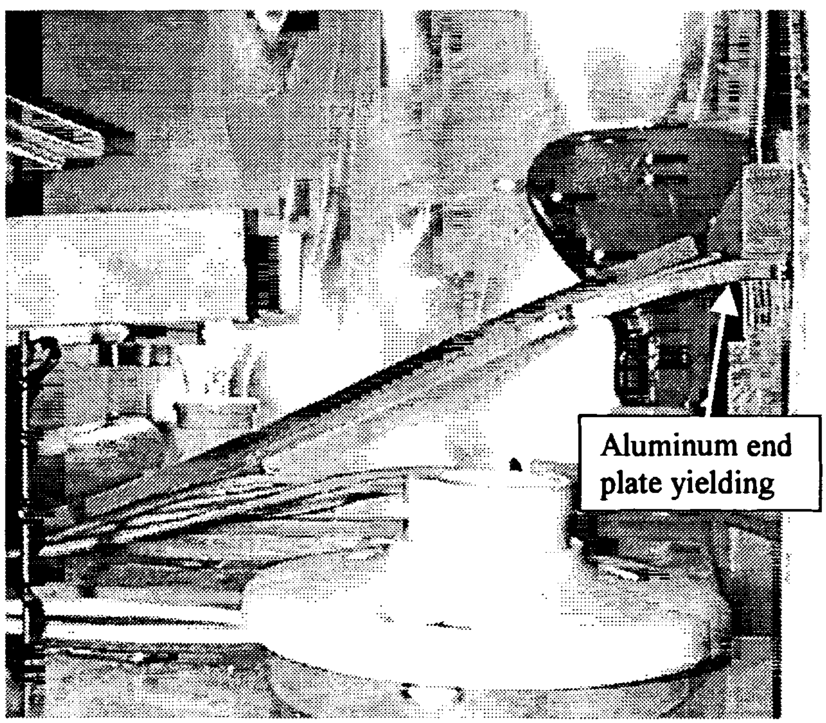

Figure 3.17 – Specimen FLHT-02 (test 2)

3.2 Results from the Hat-Stiffened Test Articles

The results of the tests conducted on the hat-stiffened test specimens are summarized in Table 3.7. This table lists the peak load, crosshead displacement at time of failure, and mode of failure.

Table 3.7 – Summary of Hat-Stiffened Test Articles

Panel	Peak Load at Failure (lbs)	Crosshead Displacement at Failure (in)	Failure Mode
HSHT-01	3,173	1.20	Debond along stiffener bond
HSHT-02	2,784	1.08	Debond along stiffener bond
HSHT-03	3,162	1.25	Debond along stiffener bond
HSRT-01	5,268	1.63	Debond along stiffener bond
HSRT-02	5,239	1.56	Flex. Failure in hat stiffener at centerline
HSRT-03	5,510	1.45	Flex. Failure in hat stiffener at centerline

Table 3.8 is a summary of the initial stiffness values of the hat-stiffened panels, measured at the locations of the LVDT sensors. Values are taken as the initial slope of the load deflection curve and are given in units of pounds force per inch of deflection.

Table 3.8 – Initial Stiffnesses at LVDT-sensor locations (lbf/in)

Panel	MTS LVDT	Centerline LVDT	Quarter-Length LVDT	Front Clamped Edge LVDT	Rear Clamped Edge LVDT
HSHT-01	2670.49	2664.83	3314.26	-74795.68	-48466.77
HSHT-02	2812.93	2811.16	3644.93	75332.44	13639.70
HSHT-03	2739.28	2731.09	3909.32	-132786.07	-41444.90
HSRT-01	3297.83	3295.07	4584.69	-166480.91	-183599.33
HSRT-02	3341.39	3318.57	4673.80	-91700.18	-201150.99
HSRT-03	3808.65	3758.33	5005.52	-697796.38	365345.33

Tables 3.9 through 3.11 are initial strains per unit load for the hat-stiffened panels, as measured at the locations of the strain gages. Values are given in units of microstrain per pound force.

Table 3.9 – Initial Strains per Unit Load (με/lbf)

Panel	Centerline Top – S1	Centerline Bottom – S2	Center Top Edge – S5
HSHT-01	-0.81	3.31	N/A
HSHT-02	-0.68	3.46	N/A
HSHT-03	-0.73	3.24	-0.87
HSRT-01	-0.76	3.03	-0.78
HSRT-02	-0.80	3.06	N/A
HSRT-03	-0.69	3.13	-0.75

Table 3.10 – Initial Strains per Unit Load Continued (με/lbf)

Panel	Center Bottom Edge – S6	Center Clamped End Top – S3	Center Clamped End Bottom – S4
HSHT-01	N/A	N/A	N/A
HSHT-02	N/A	N/A	N/A
HSHT-03	0.04	0.26	-0.28
HSRT-01	-0.02	0.20	-0.20
HSRT-02	N/A	N/A	N/A
HSRT-03	0.01	-0.29	-0.29

Table 3.11 – Additional Initial Strains per Unit Load for HSRT-03 (με/lbf)

HSRT-03	Quarter-Length Center Top - S7	Quarter-Length Center Bottom – S8	Quarter-Length Side Top – S9
	-0.62	1.40	-0.53
	Quarter-Length Side Bottom – S10	**Clamped Side Top – S11**	**Clamped Side Bottom – S12**
	1.40	0.34	-0.39

3.2.1 Specimen HSHT-01

Specimen HSHT0-01 failed under a load of 3,173 lbs. and a crosshead displacement of 1.43 inches. The failure mode was a debonding of the adhesive between the flat laminate and the hat stiffener. This was the same mode of failure experienced by all of the high temperature hat-stiffened panels. Figures 3.18 and 3.19 show the load-displacement curve and load-strain curve, respectively. Figures 3.20 through 3.22 are photographs taken after the panel failed. Figure 3.20 is a wide view of the failed specimen, Figure 3.21 is a close-up of the adhesive debond, and Figure 3.22 is a close-up view showing the condition of the end support after failure.

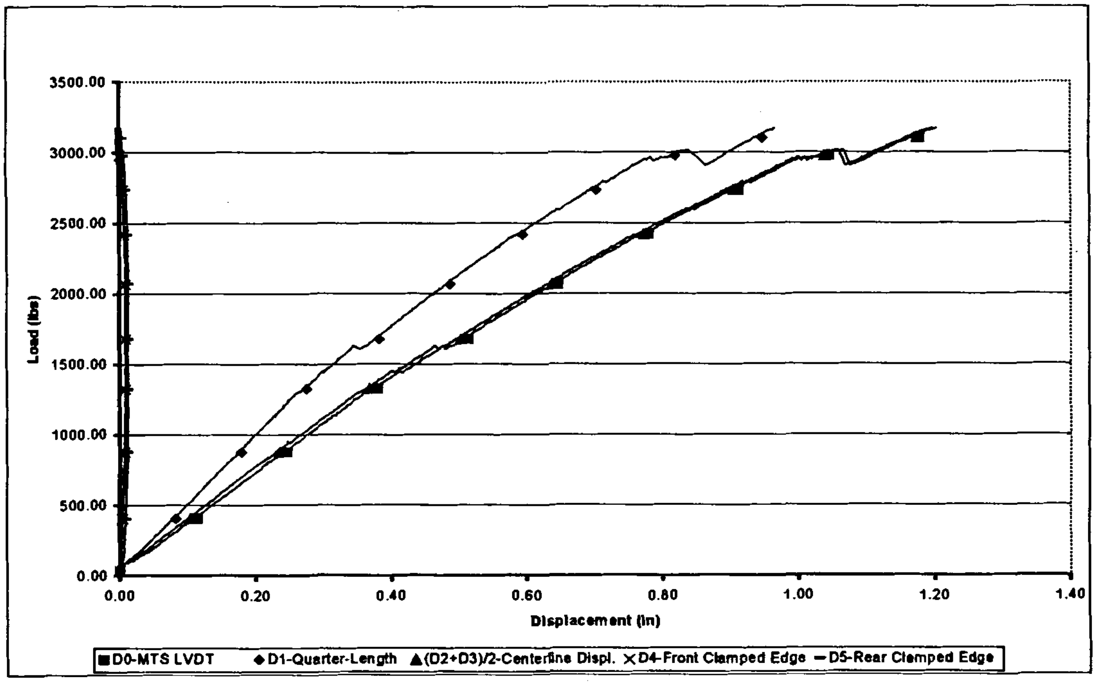

Figure 3.18 – Load-Displacement Curve for HSHT-01

The load-strain plots in Figure 3.19 are highly linear, while the load-deflection plot in Figure 3.18 exhibits a non-linear viscoplastic response for the stiffness values at the centerline and quarter-length locations. Polymers typically exhibit a viscoplastic response under high stress levels and elevated temperatures. A drop in the load capacity is noticed at approximately 1,700 and 3,000 pounds. These indicate damage mechanisms accumulating in the panel, possibly ply damage in the hat stiffener, or cracks propagating in the adhesive bond between the laminate and hat-stiffener. The load capacity drop at 3,000 pounds seems to correlate to a similar drop in the centerline IML load-strain plot near 10,000 microstrain.

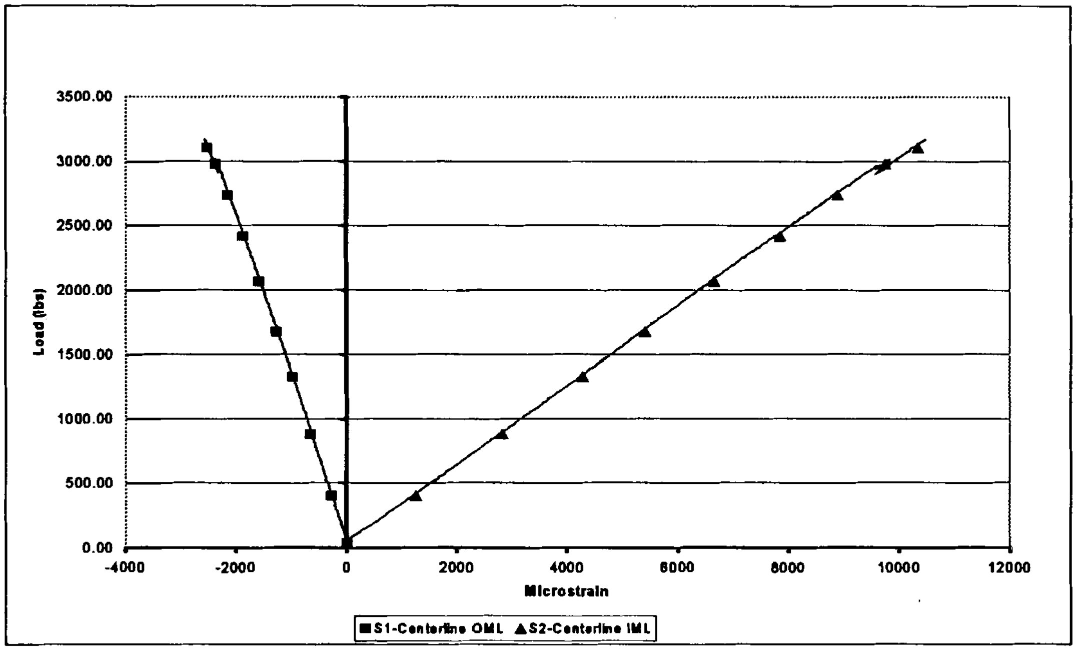

Figure 3.19 – Load-Strain Curve for HSHT-01

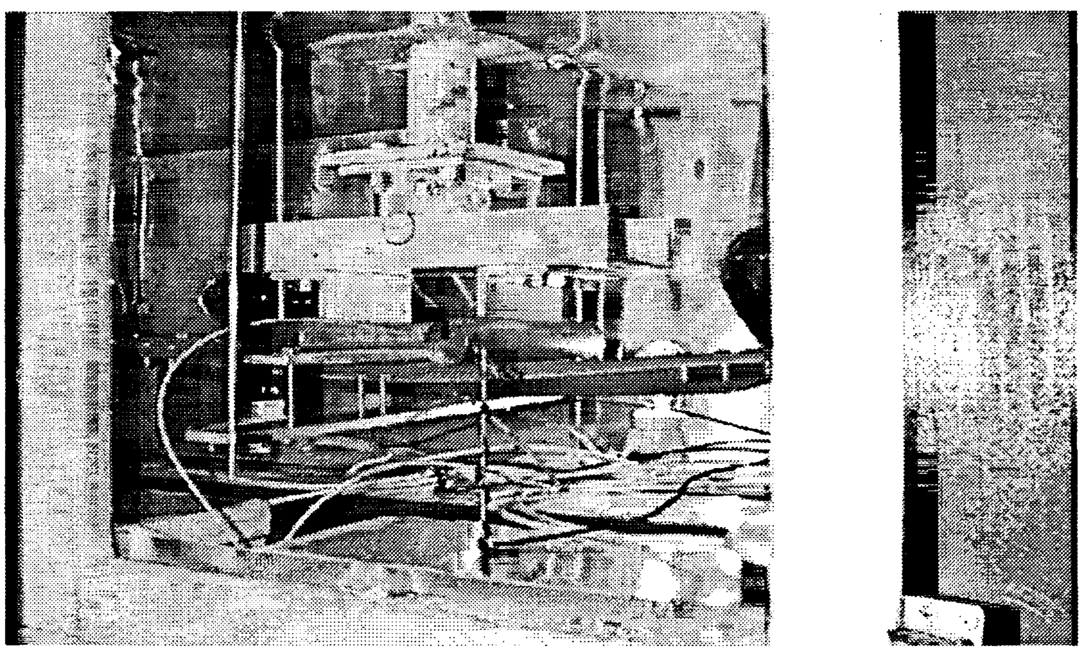

Figure 3.20 – Specimen HSHT-01

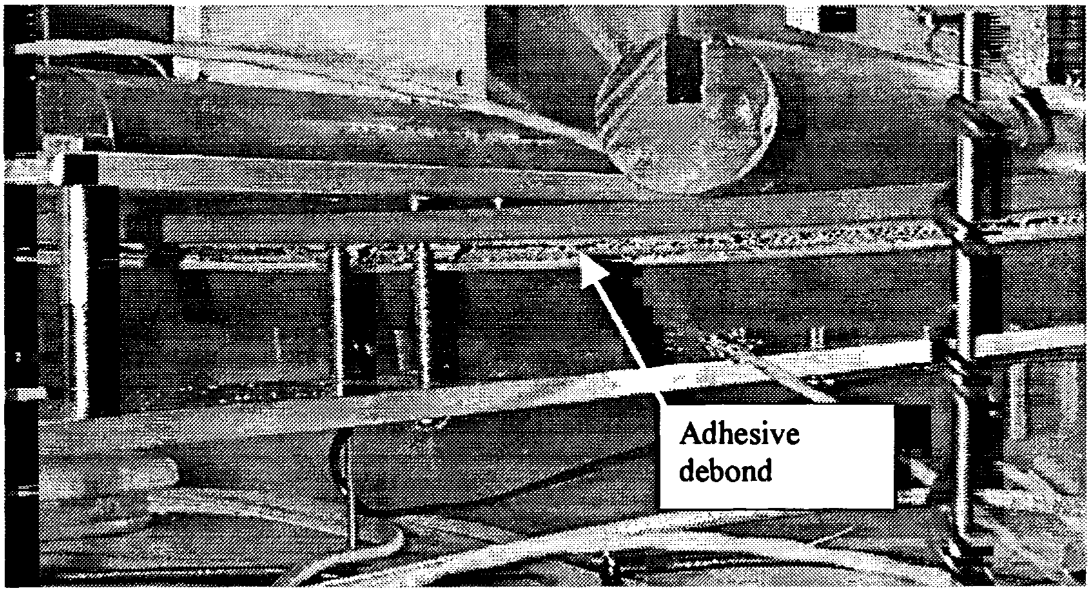

Figure 3.21 – Specimen HSHT-01

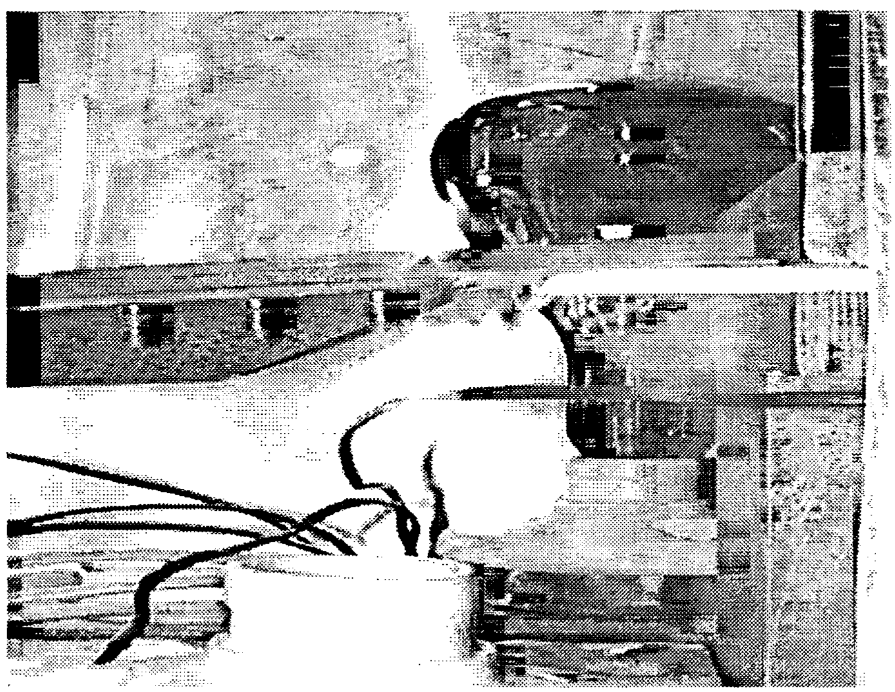

Figure 3.22 – Specimen HSHT-01

3.2.2 Specimen HSHT-02

Specimen HSHT-02 failed under a load of 2,784 lbs. and a crosshead displacement of 1.08 inches. As with the other high temperature hat-stiffened panels, this one failed as a result of a debonding of the adhesive between the flat laminate and the hat-stiffener. Figures 3.23 and 3.24 show the load-displacement and load-strain curves, respectively. The load-strain plots are highly linear, while the load-deflection plots exhibit a non-linear behavior. At a load near 2,250 pounds, the stiffness leveled off dramatically at the quarter-length location. This can be attributed to accumulation of damage in the panel, possibly ply damage in the hat-stiffener or cracks propagating in the adhesive bond. Also, the load-deflection plots from the clamped ends seems to indicate that the end supports rotated in and then changed direction, rotating in the opposite direction. This is could have been caused by minute crushing of the end blocks into the base of the oven. The top centerline strain gage ceased to function after approximately 4.8 minutes into the test, at a load of 1,454 lbs. Figures 3.25 is a wide angle view of the failed specimen, while Figure 3.26 is a close-up view of the debonded adhesive. Finally, Figure 3.27 is a photo showing the condition of the end support after failure.

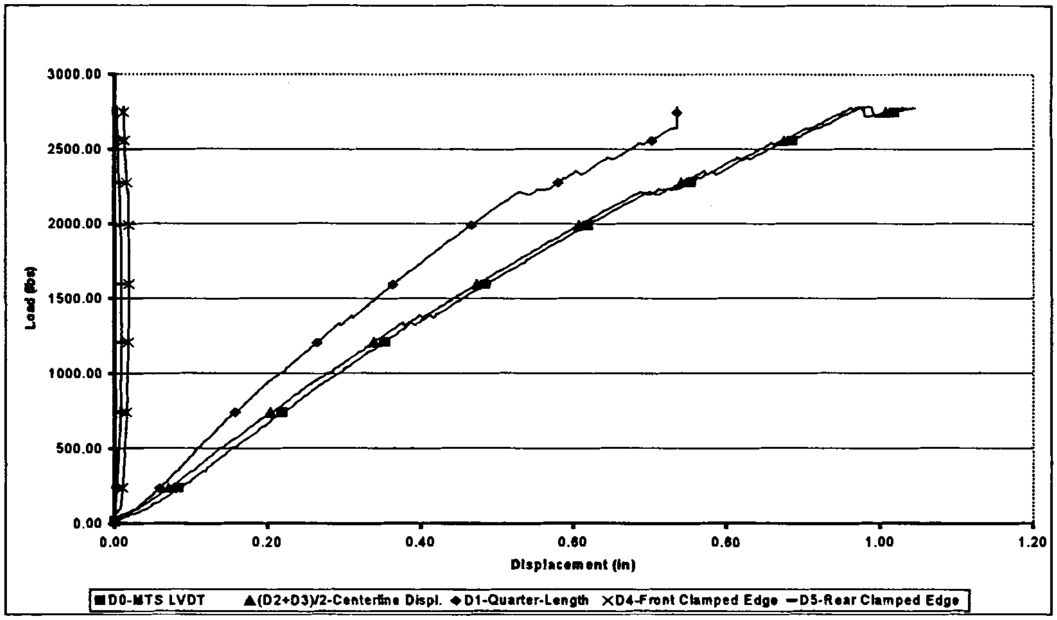

Figure 3.23 – Load-Displacement Curve for HSHT-02

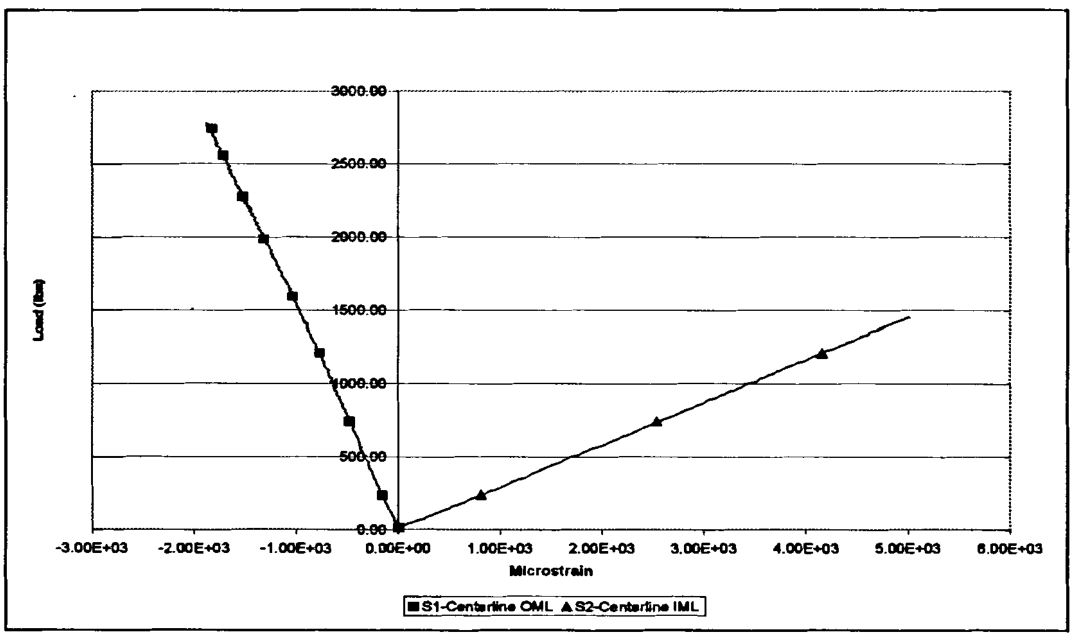

Figure 3.24 – Load-Strain Curve for HSHT-02

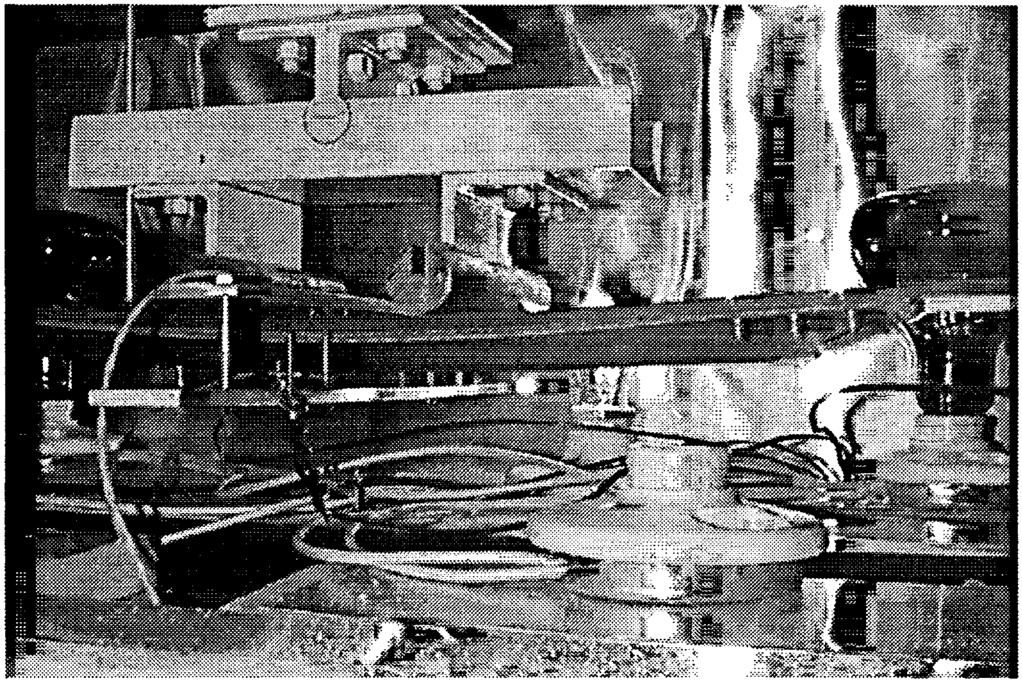

Figure 3.25 – Specimen HSHT-02

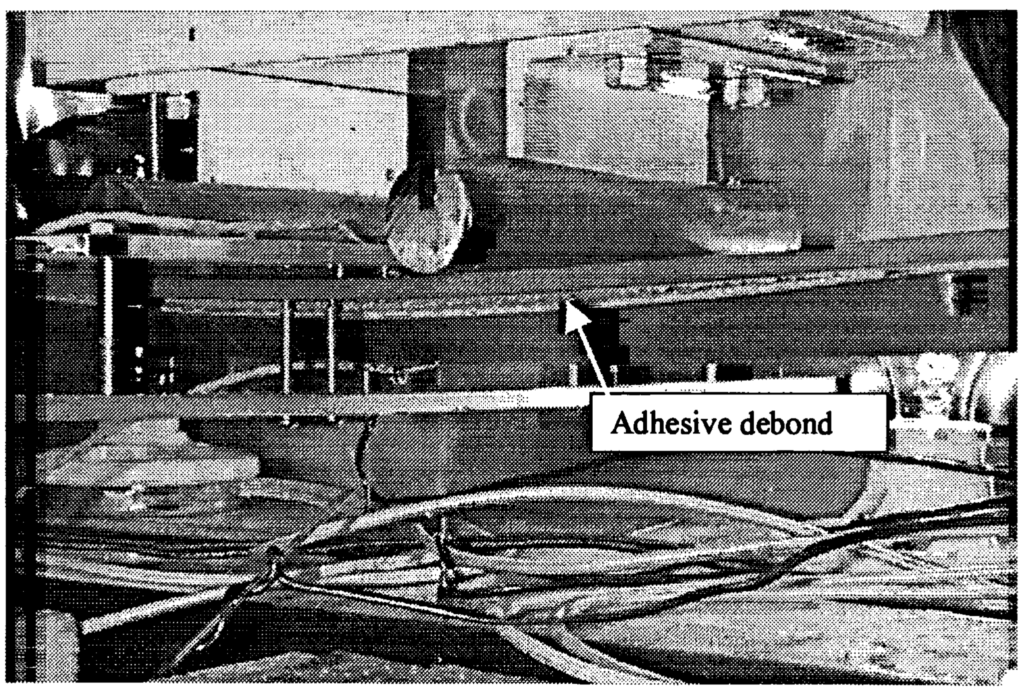

Figure 3.26 – Specimen HSHT-02

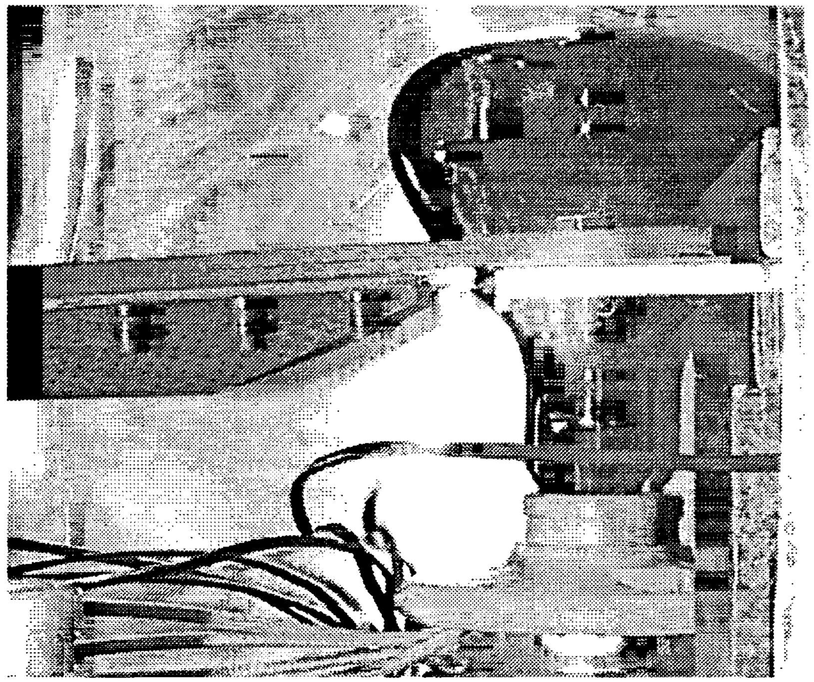

Figure 3.27 – Specimen HSHT-02

3.2.3 Specimen HSHT-03

Specimen HSHT-03 failed under a load of 3,162 lbs. and a crosshead displacement of 1.25 inches. The failure was a debonding of the adhesive between the flat laminate and the hat-stiffener. Figures 3.28 and 3.29 show the load-displacement and load-strain curves. The load-strain plots are highly linear. The clamped end strain gages failed to respond until a load of approximately 1000 pounds. The load-deflection plots were very non-linear in nature. A drop in load capacity was noted near a load of 2,250 pounds. This could be explained by first ply damage in the hat-stiffener or cracks propagating through the adhesive bond. The quarter-length DCDT ceased to operate at approximately 2,600 lbs. This was due to the physical interference of the top crosshead. Figure 3.30 is a wide view of the panel following failure. Figure 3.32 is a

close-up photo of the debond between the laminate and hat-stiffener, and Figure 2.33 is another close-up photo of the debond.

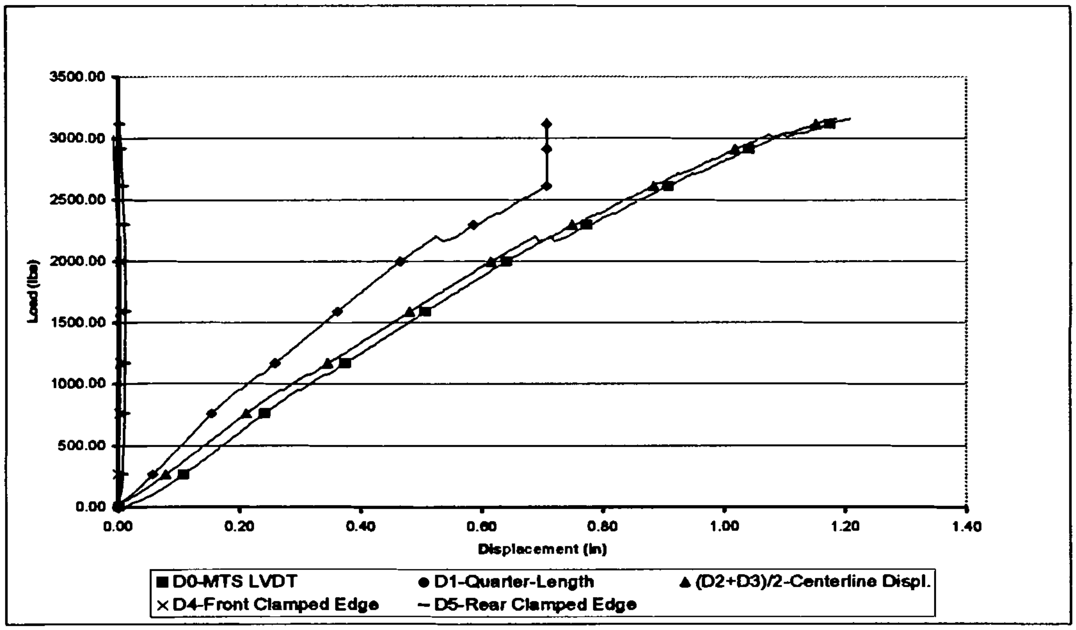

Figure 3.28 – Load-Displacement Curve for HSHT-03

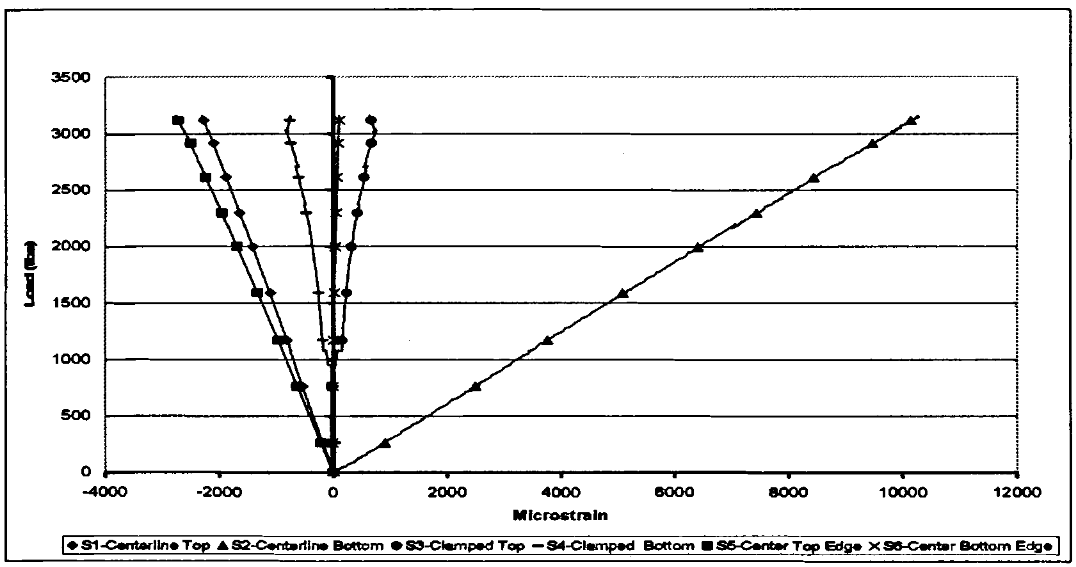

Figure 3.29 – Load-Strain Curve for HSHT-03

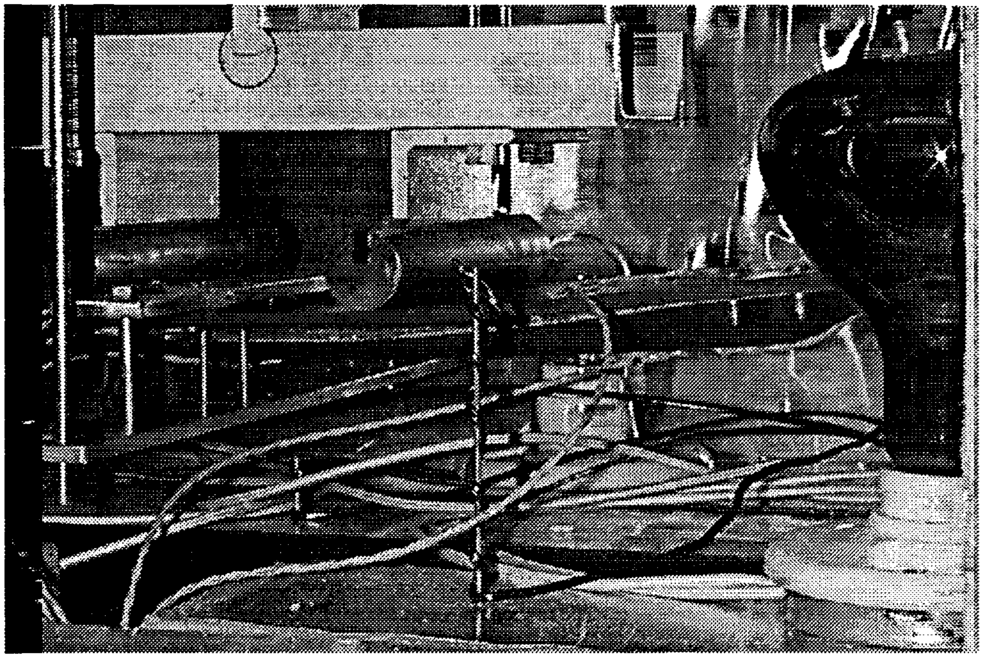

Figure 3.30 – Specimen HSHT-03

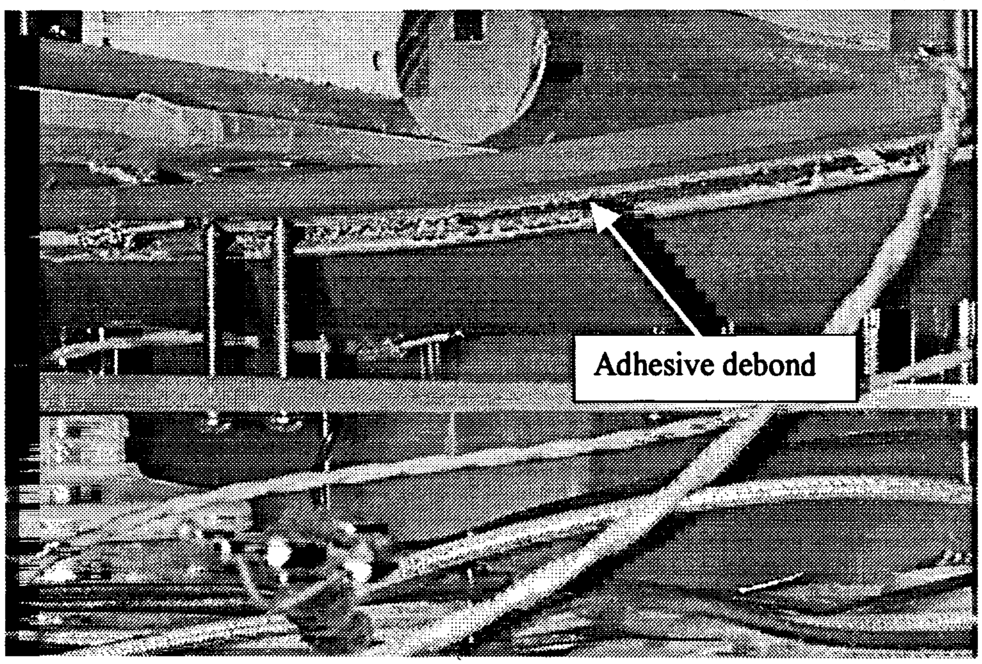

Figure 3.31 – Specimen HSHT-03

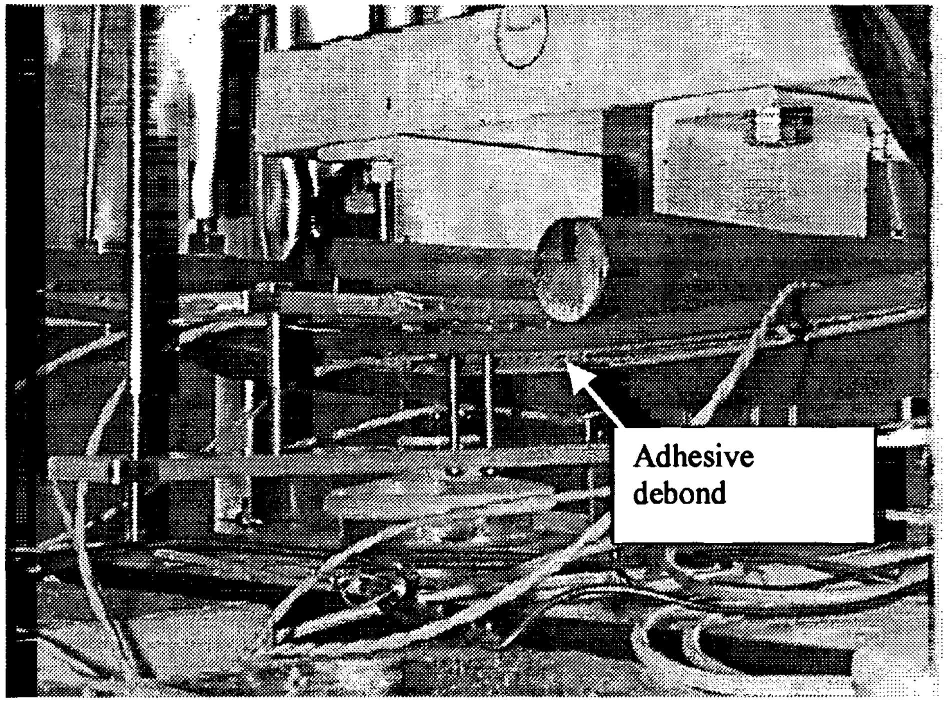

Figure 3.32 – Specimen HSHT-03

3.2.4 Specimen HSRT-01

Specimen HSRT-01 failed under a load of 5,268 lbs. and a crosshead displacement of 1.63 inches. The failure loads for the room temperature panels were higher than the failure loads for the high temperature panels because, as expected, the hat-stiffened panels were stiffer at room temperature than at 325°F. The failure mode for this panel was a debonding of the adhesive between the flat laminate and the hat stiffener. Of the three hat-stiffened panels tested at room temperature, this was the only one to fail in this manner. Both HSRT-02 and HSRT-03 failed as a result of a flexural failure at the center of the hat stiffener. In the room temperature tests, it was much easier to hear the beginnings of failure, i.e. sounds of the fibers cracking and breaking. Figures 3.33 and 3.34 show the load-displacement and load-strain curves for HSRT-01,

respectively. The load-strain plots are linear with the exception of the plots of the load vs. strain at the clamped ends. A relaxation of strain was noted at both clamped end strain gages near a load of 4,200 pounds. This corresponds to a drop in stiffness on the load-deflection plots near the same load. This could be due to the onset of ply damage in the hat stiffener or possibly cracks propagating through the adhesive bond. Figures 3.35 is a wide view of the panel after failure, Figure 3.36 is a close-up photo of the debonded adhesive, and Figure 3.37 is a photograph showing the condition of the end support after failure. Figure 3.37 shows a visible amount of end support rotation inward.

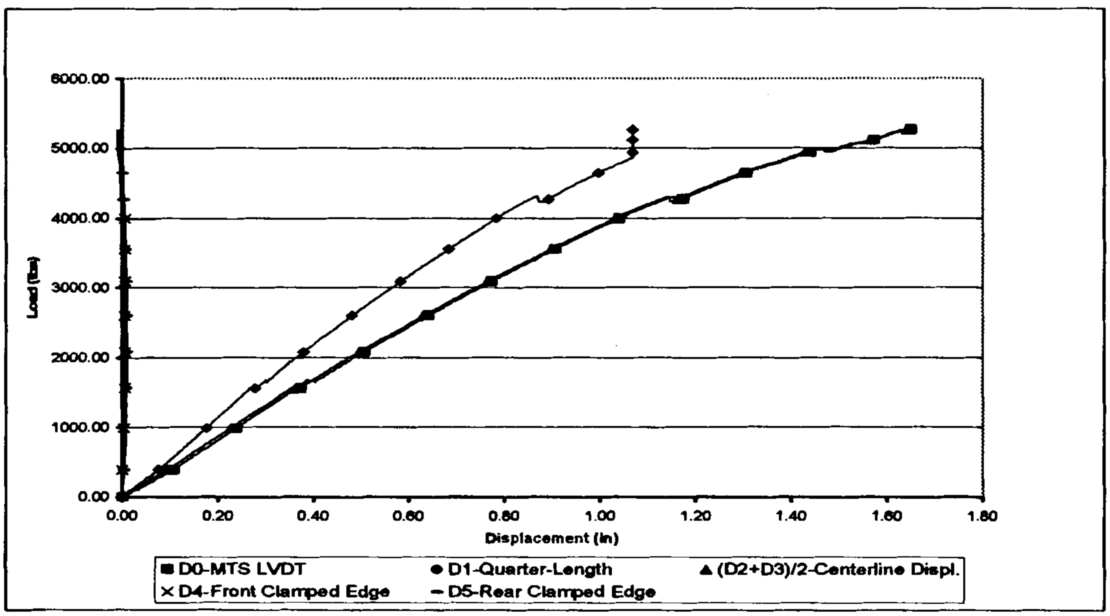

Figure 3.33 – Load-Displacement Curve for HSRT-01

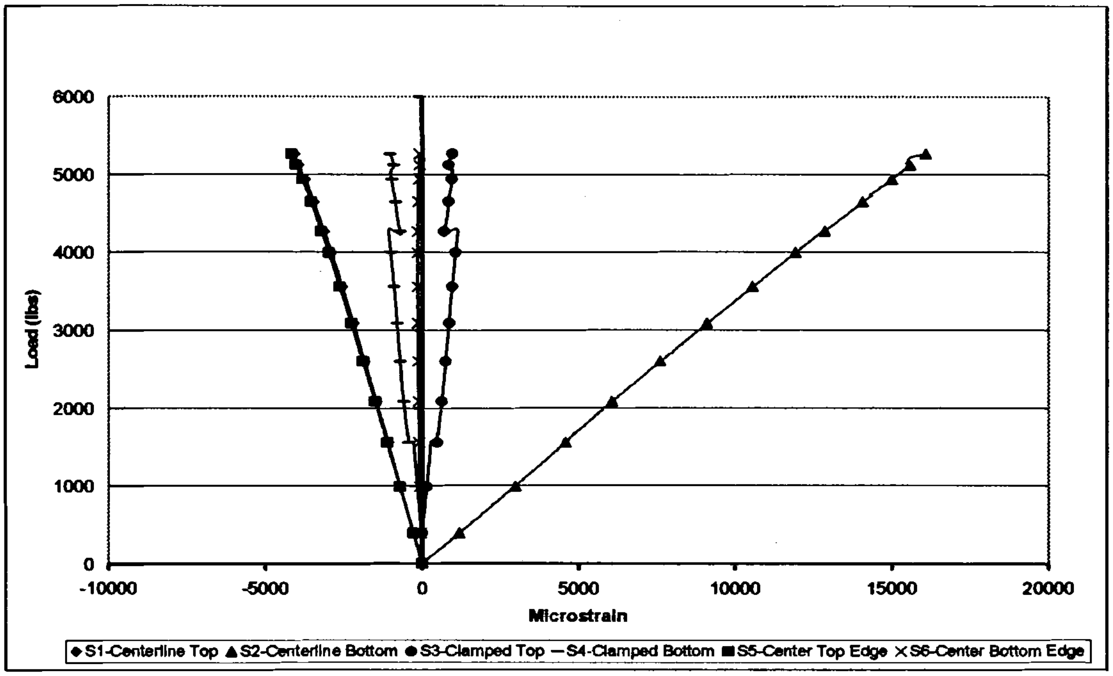

Figure 3.34 – Load-Strain Curve for HSRT-01

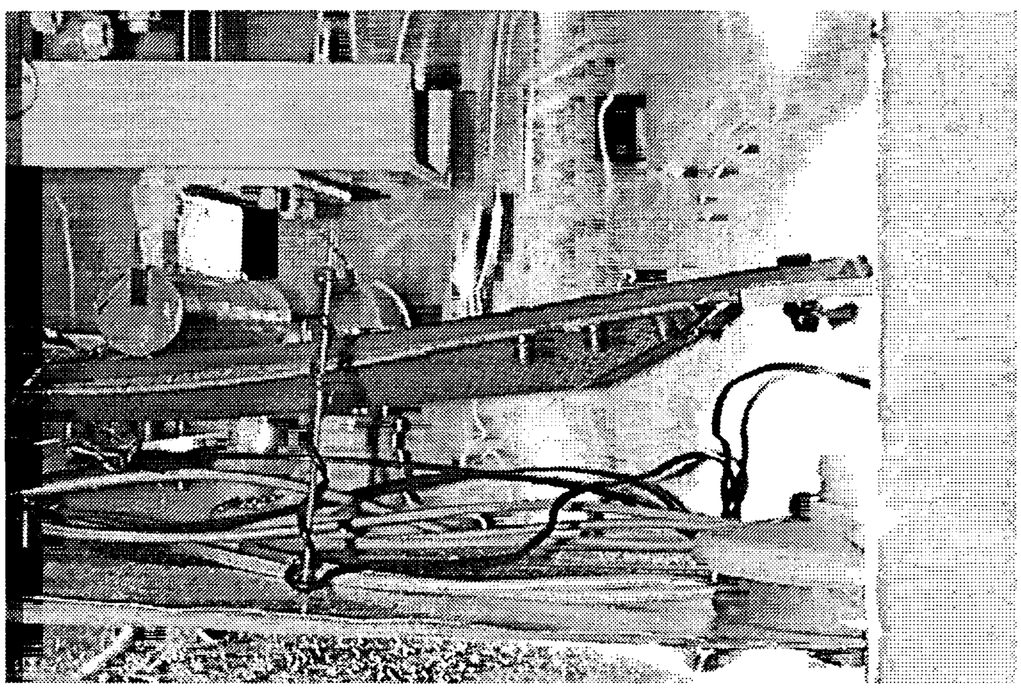

Figure 3.35 – Specimen HSRT-01

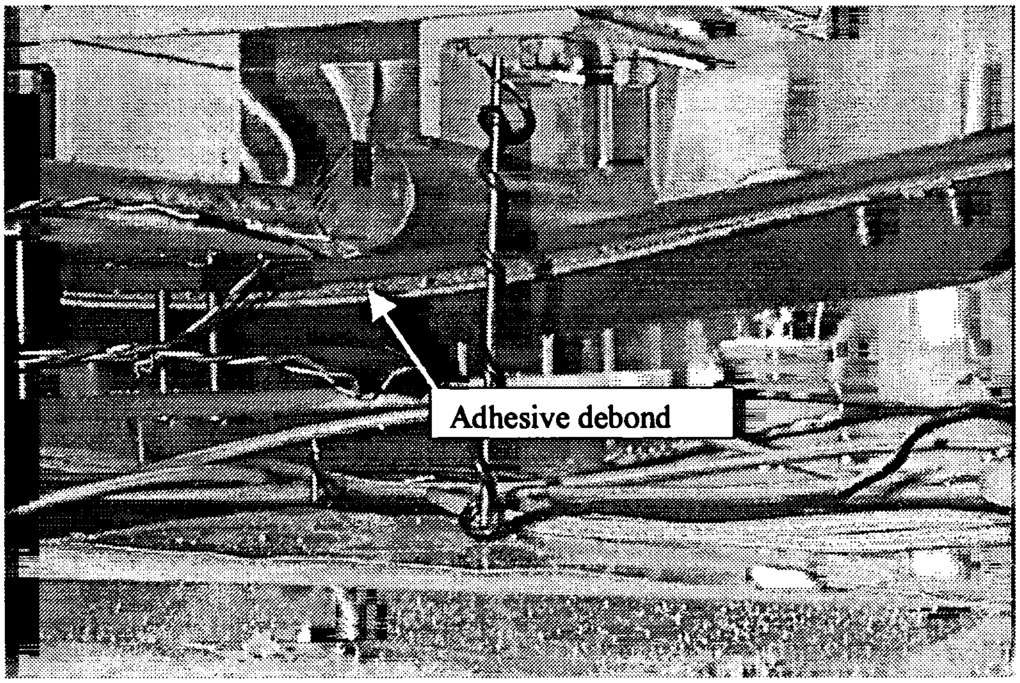

Figure 3.36 – Specimen HSRT-01

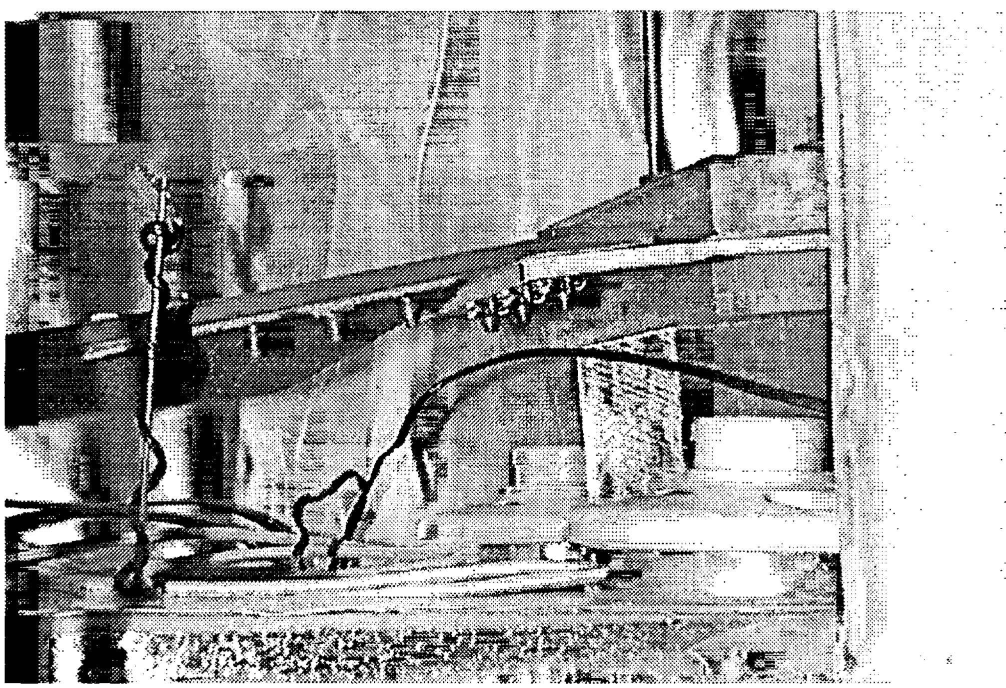

Figure 3.37 – Specimen HSRT-01

3.2.5 Specimen HSRT-02

Specimen HSRT-02 failed under a load of 5,239 lbs. and a crosshead displacement of 1.56 inches. The mode of failure was a flexural failure of the hat-stiffener near the centerline. Figures 3.38 and 3.39 give the load-displacement and load-strain curves for HSRT-02, respectively. The load-strain plots are highly linear, while the load-deflection plots are slightly non-linear. A drop in load capacity is noted at a load of 2,250 pounds, indicating a damage mechanism. This could possibly be fiber damage in the hat-stiffener, or crack propagation through the adhesive. Figures 3.40 is a wide view of the failed specimen, Figure 3.41 is a photo of the condition of the end support after failure, and Figure 3.42 is a close-up photograph of the hat stiffener rupture.

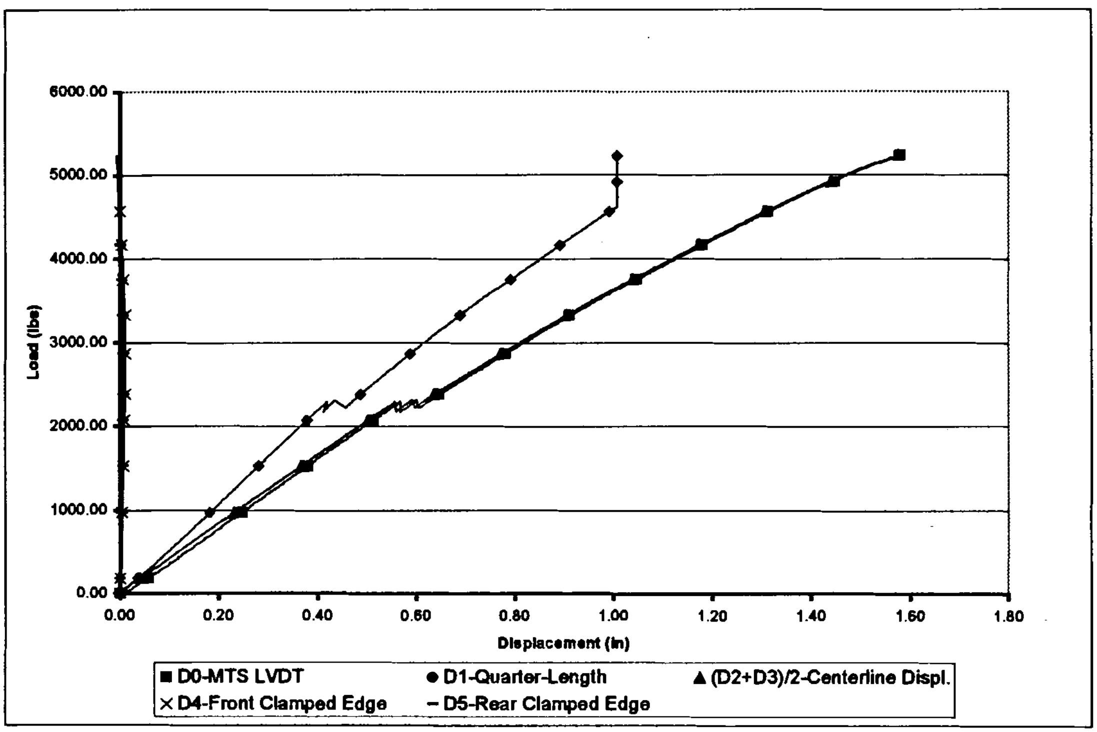

Figure 3.38 – Load-Displacement Curve for HSRT-02

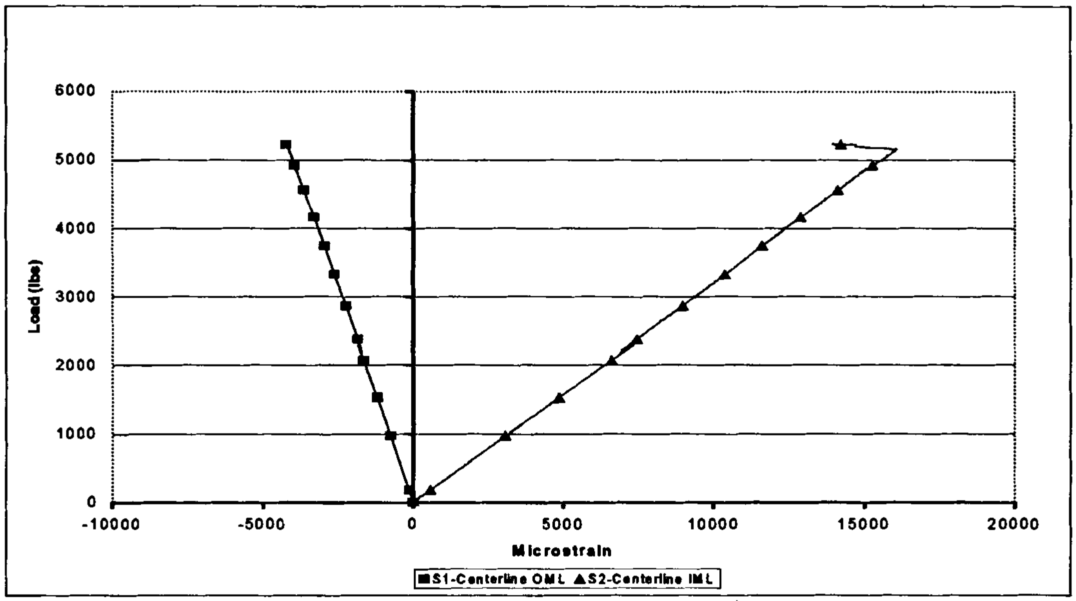

Figure 3.39 – Load-Strain Curve for HSRT-02

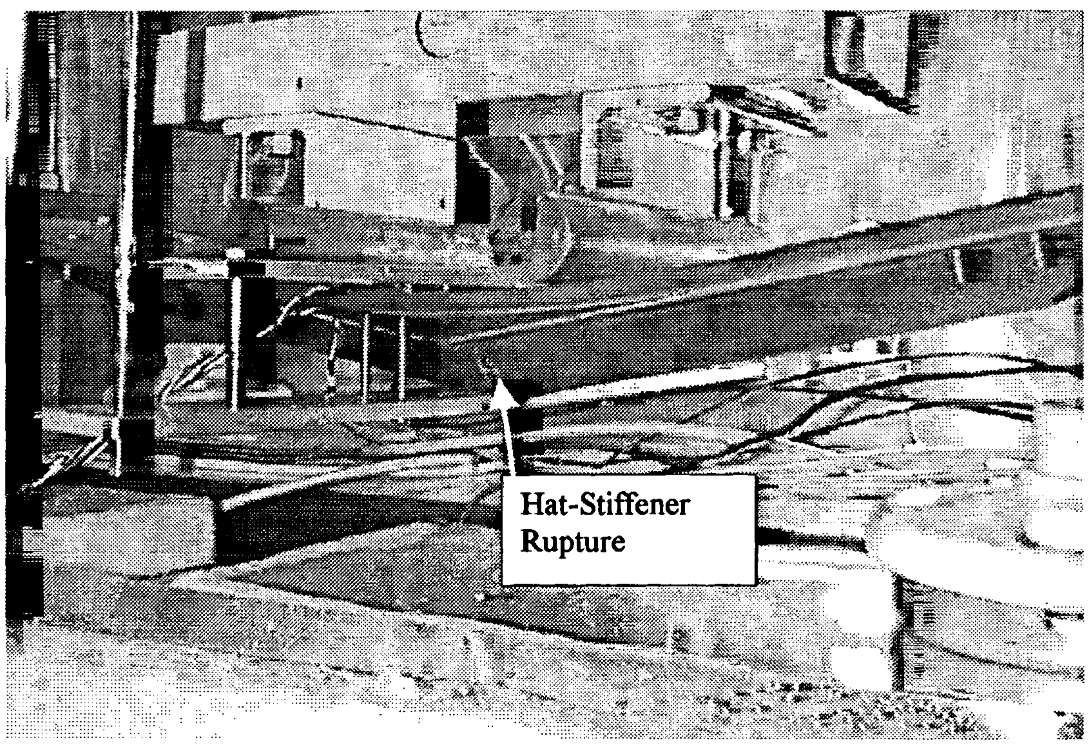

Figure 3.40 – Specimen HSRT-02

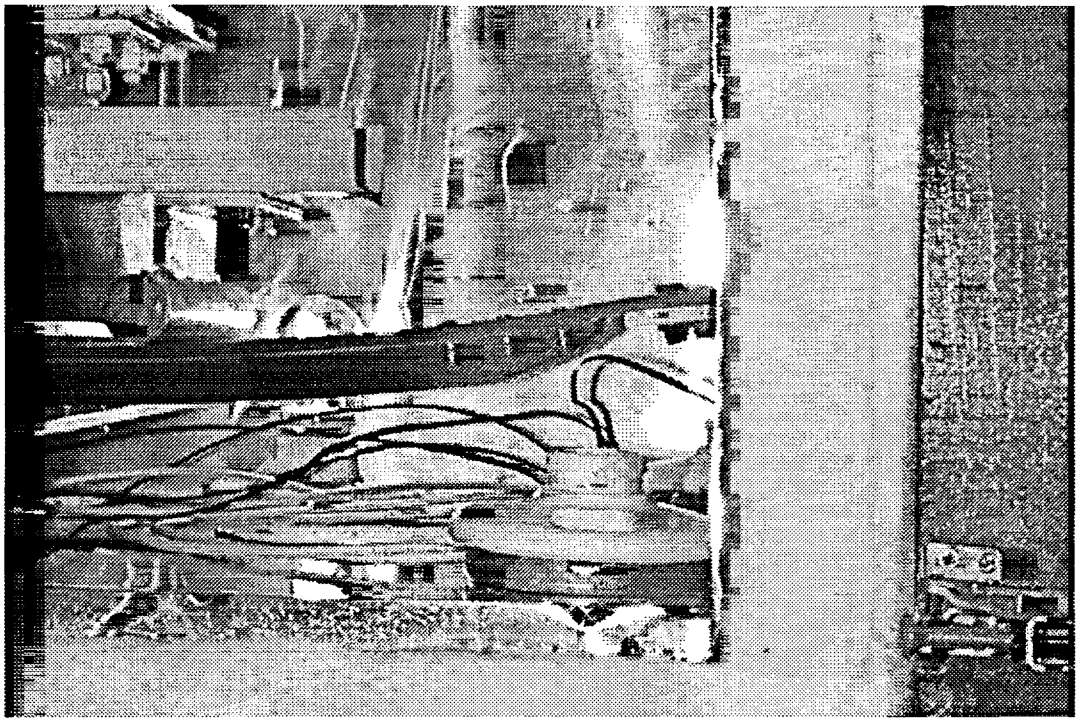

Figure 3.41 – Specimen HSRT-02

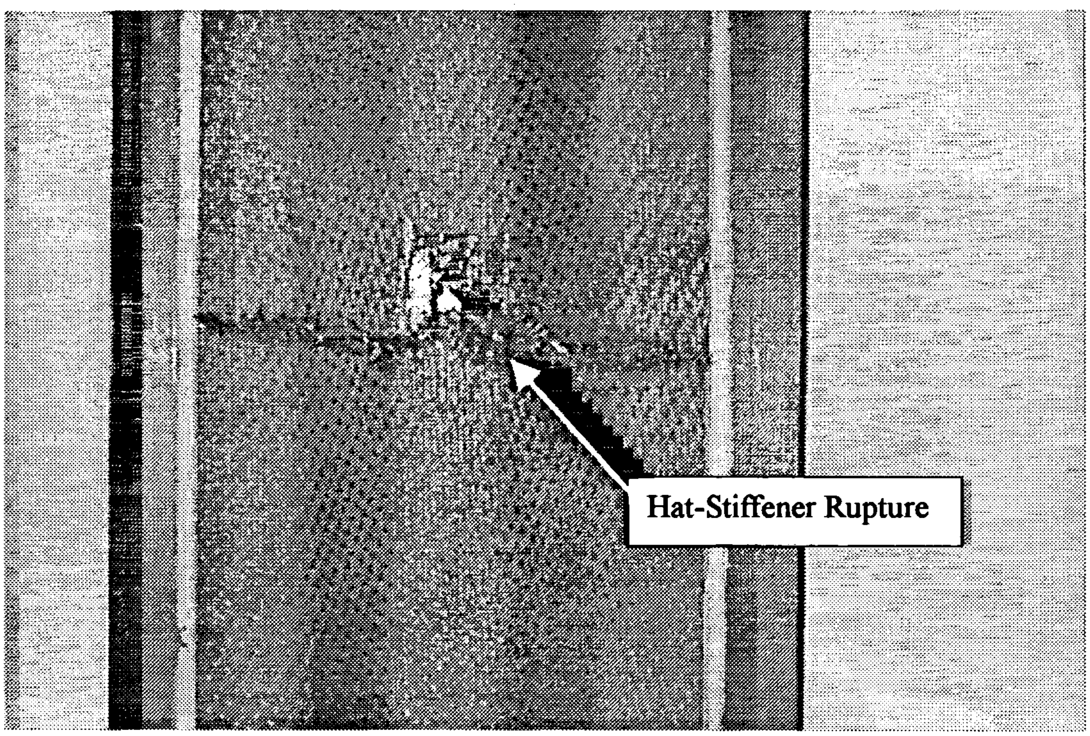

Figure 3.42 – Specimen HSRT-02

3.2.6 Specimen HSRT-03

Specimen HSRT-03 failed under a load of 5,510 lbs. and a crosshead displacement of 1.45 inches. The failure mode was a flexural failure of the hat-stiffener near the center. Figures 3.43 and 3.44 show the load-displacement and load-strain curves for HSRT-03, respectively. Both the load-strain plots and the load-deflection plots are fairly linear. A slight reduction in load capacity is noted near a load of 1,700 pounds on both plots, indicating a damage mechanism. This could have taken the form as fiber damage in the hat-stiffener or cracks propagating through the adhesive bond between the laminate and the hat-stiffener. Figures 3.45 is a wide view photo of the failed specimen. Figure 3.46 is a close-up photo of the ruptured hat-stiffener, and Figure 3.47 is a photo showing how the rupture spread across the stiffener.

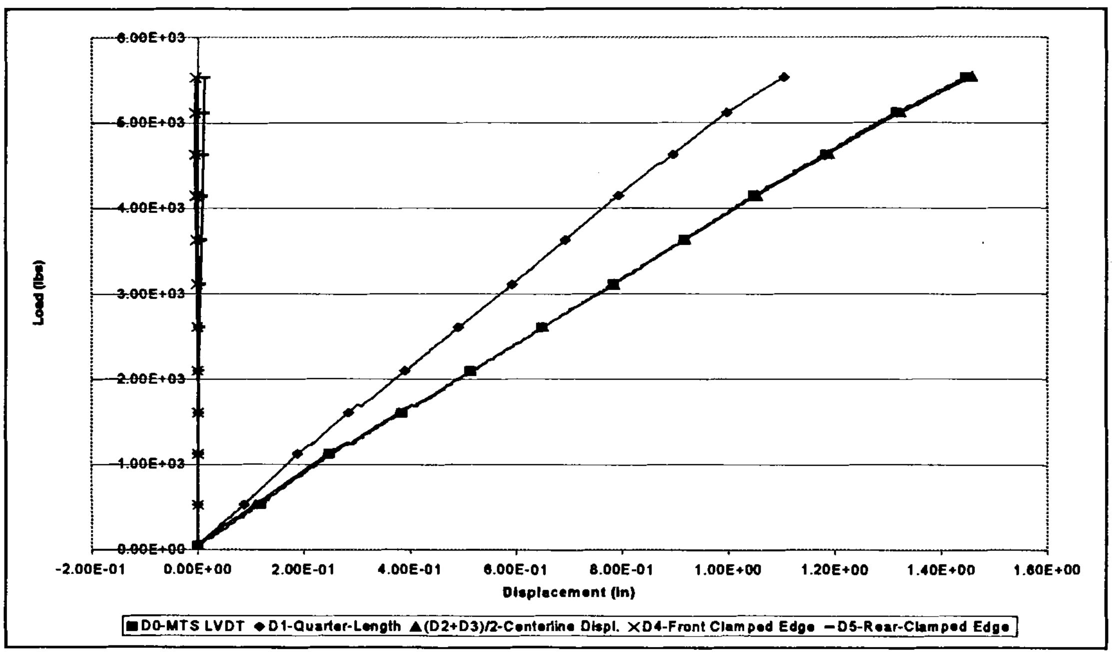

Figure 3.43 – Load-Displacement Curve for HSRT-03

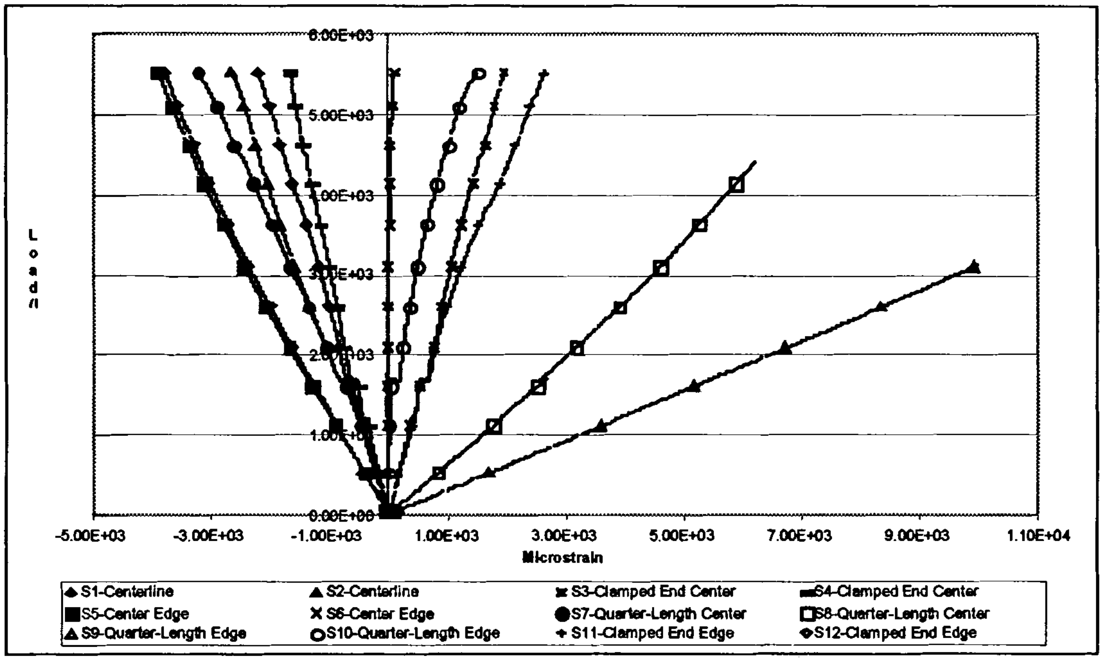

Figure 3.44 – Load-Strain Curve for HSRT-03

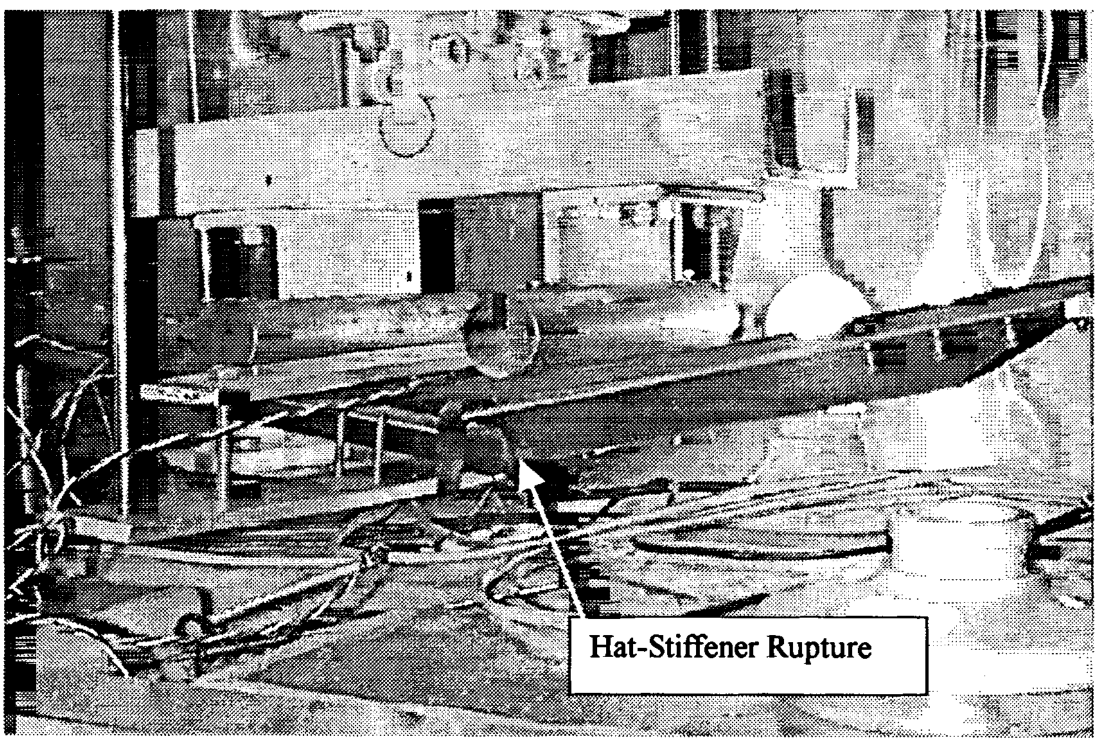

Figure 3.45 – Specimen HSRT-03

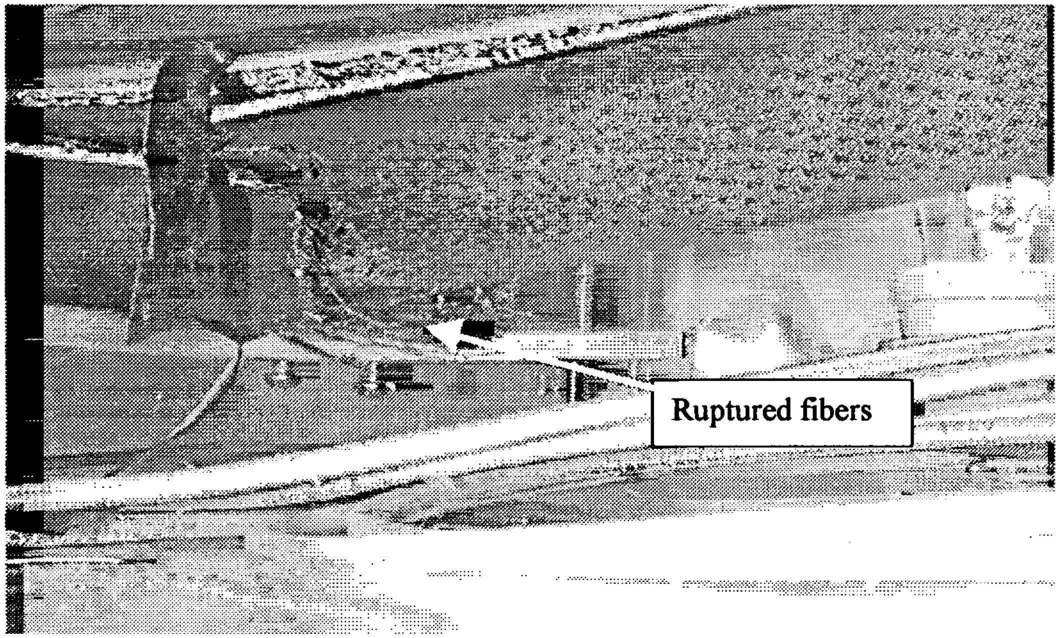

Figure 3.46 – Specimen HSRT-03

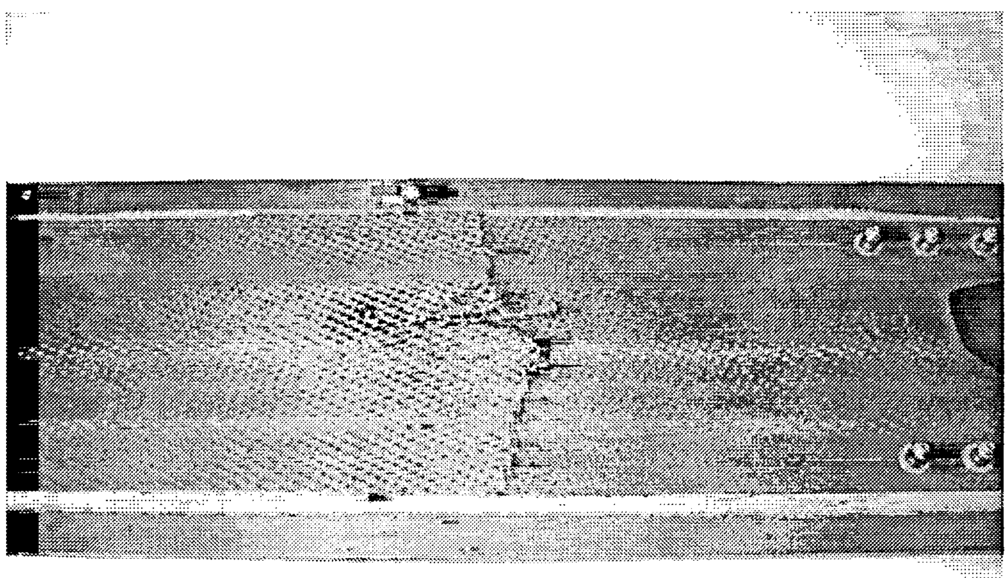

Figure 3.47 – Specimen HSRT-03

3.2.7 Room Temperature Vs. Elevated Temperature Hat-Stiffened Test Results

Table 3.12 lists the average initial stiffness and strength values for the elevated temperature hat-stiffened panels, and the percentage drop from room temperature to elevated temperature. The centerline stiffness of the panels dropped an average of 21 percent as a result of the elevated temperature environment. Figure 3.48 is a centerline load-deflection plot of the results from all of the hat-stiffened laminates. Graphically, there appears to be a correlation between test temperature and stiffness, as can be seen by the grouping of the room temperature and high temperature plots. The high temperature articles appear to respond in a non-linear fashion, as opposed to the room temperature articles, which are more linear.

Table 3.12 – Hat-Stiffened Panel Knockdown Factors

Average Room Temp Stiffness (lbf/in):	3,483
Average Elevated Temp Stiffness (lbf/in):	2,741
Knockdown Factor:	0.79
Average Room Temp Peak Load (lbf):	5,339
Average Elevated Temp Peak Load (lbf):	3,040
Knockdown Factor:	0.57

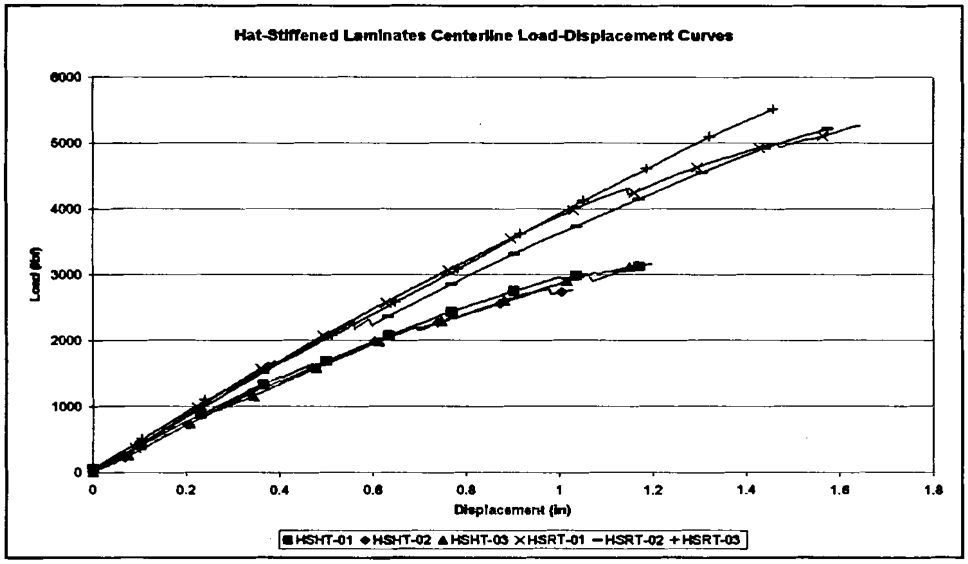

Figure 3.48 – Hat-Stiffened Centerline Load-Deflection Plot

Figure 3.49 is a plot of the centerline strains recorded on the OML side versus applied load for all of the hat-stiffened test articles. It is less clear from this plot which plots are the high temperature specimens and which are the room temperature articles.

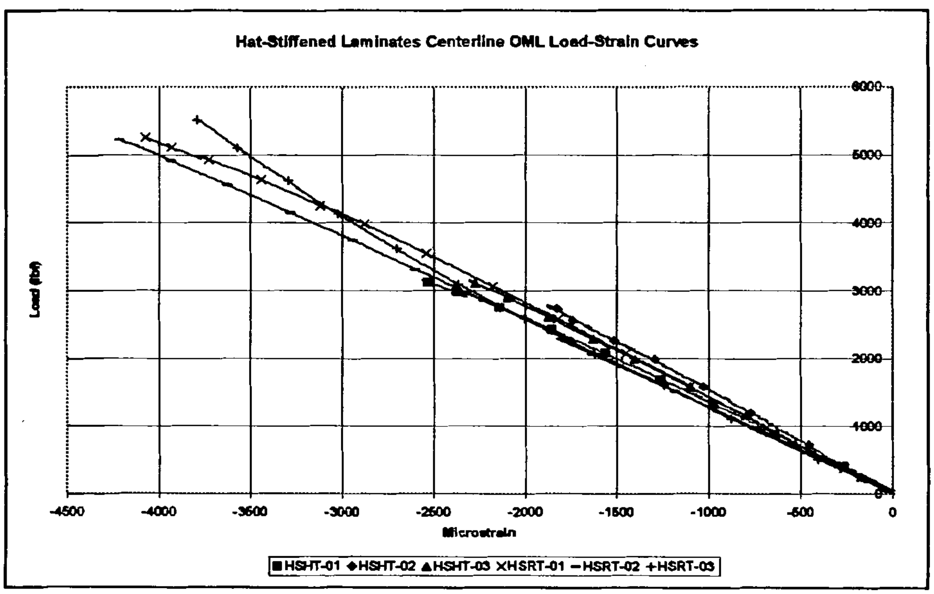

Figure 3.49 – Hat-Stiffened Centerline OML Load-Strain Plot

3.3 Test Results from Elevated Temperature Composite Sandwich Panels

The test results for the composite sandwich panels tested at 325°F (163°C) are summarized in Table 3.13. This table gives the peak load, failure mode, crosshead travel at the time of failure, and stiffness factors at each of the DCDT locations. Tables 3.14 and 3.15 compare the stiffness factors at the sensor locations. Table 3.14 lists stiffness factors recorded at the LVDT points in units of pounds per inch of deflection. Table 3.15 lists stiffness factors recorded at the strain gage locations in units of strain per unit load.

Table 3.13 – Summary of IML Sandwich Panel Room and Elevated Temp. Tests

Panel	Temperature	Peak Load at Failure (lbs/kN)	Centerline Disp. at Failure (in/cm)	Failure Mode
FI-RT-D5C	Room Temp.	1,881/8.37	0.45/1.14	Core Shear
FI-RT-D5A	Room Temp.	1,908/8.49	0.45/1.14	Core Shear
FI-RT-D3C	Room Temp.	1,729/7.69	0.51/1.30	Core Shear/Crushing
FI-RT-D3A	Room Temp.	1,647/7.33	0.50/1.27	Core Shear/Crushing
FI-ET-D3B	325°F/163°C	1,432/6.37	0.51/1.30	IML Debond
FI-ET-D5B	325°F/163°C	1,492/6.64	0.47/1.19	Core Shear

Table 3.14 - Stiffness Factors at LVDT Locations (lbs per inch of deflection)

	MTS (D0)	Center (D1+D2)/2	Boltline (D3)	Taper End (D4)
FI-ET-D3B	2,850	3,172	50,037	7,190
FI-ET-D5B	3,300	3,824	30,779	8,147

Table 3.15 – Strains per Unit Load at Sensor Locations (με/lb)

	S1	S2	S3	S4	S5	S6
FI-ET-D3B	-2.26	2.14	-0.699	0.521	0.115	-0.0725
FI-ET-D5B	-1.81	1.88	-0.935	0.800	0.207	-0.400

The maximum failure load percentage drop from room temperature to 325°F (163°C) is 26.1%. This is calculated by dividing the minimum room temperature failure load (panel FI-ET-D3B) by the maximum elevated temperature failure load (panel FI-RT-D5A).

3.3.1 Specimen FI-ET-D3B

Panel FI-ET-D3B failed under a load of 1,432 lbs (6.37 kN). The failure was a sudden catastrophic debonding of the IML facesheets from the center of the panel to the start of the taper. Figures 3.50 and 3.51 show the load-displacement and load-strain curves, respectively. The LVDT at the taper did not respond until approximately 3.7 minutes into the test (~400 pounds load). This was most probably due to the transducer being incorrectly zeroed before the test started. Both the load-strain plots and the load-deflection plots are highly linear. Figures 3.52 through 3.54 are close-up photos of the IML facesheets debonding. Figure 3.55 is a view of the tapered region after failure.

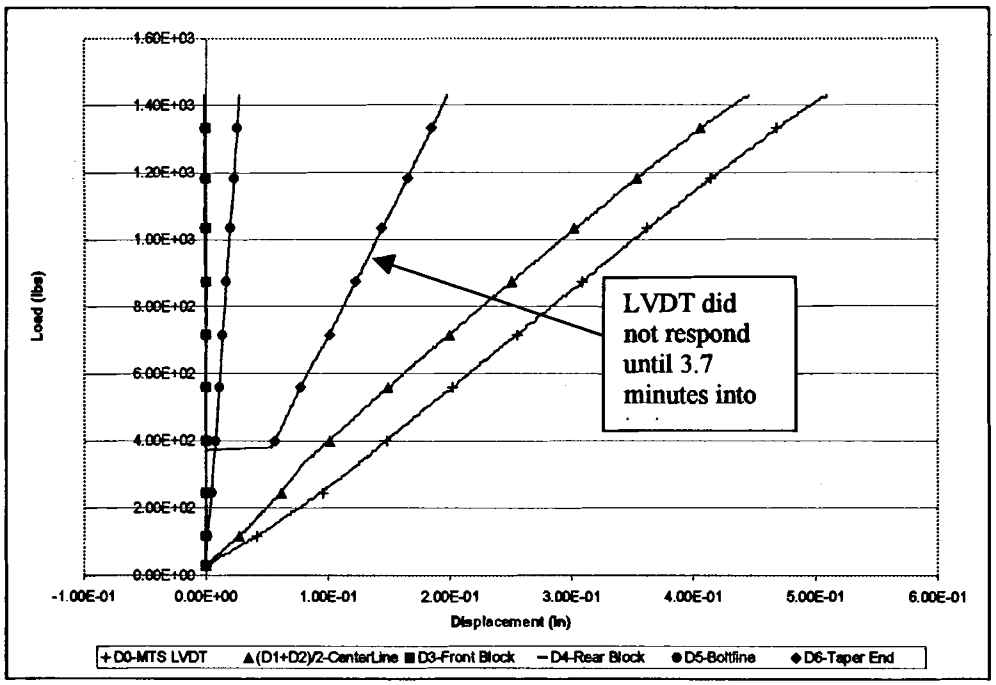

Figure 3.50 – Load-Displacement Curve for FI-ET-D3B

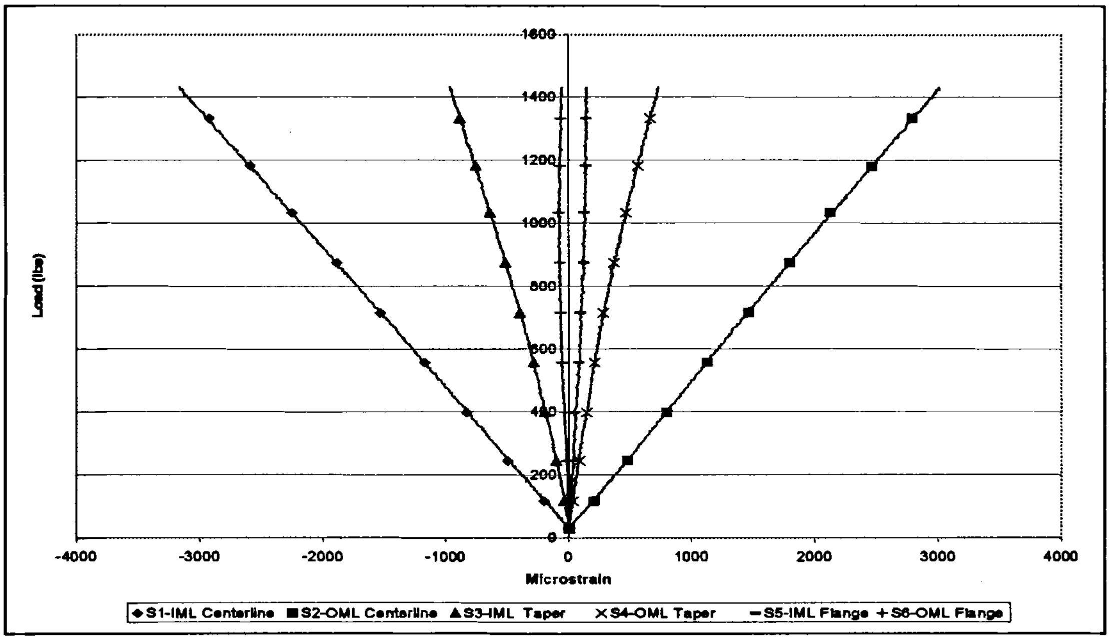

Figure 3.51 – Load-Strain Curve for FI-ET-D3B

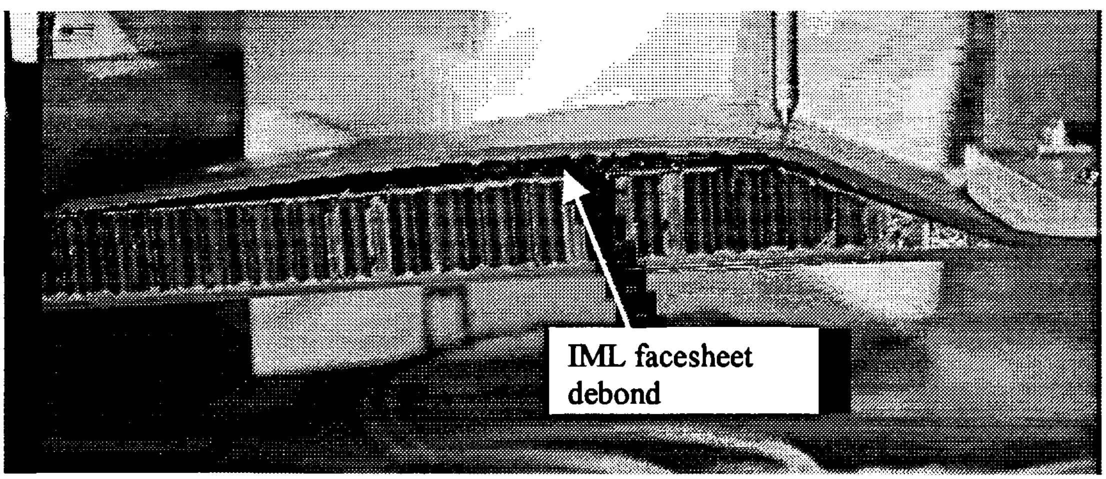

Figure 3.52 – Specimen FI-ET-D3B (photo courtesy of Bangor Daily News)

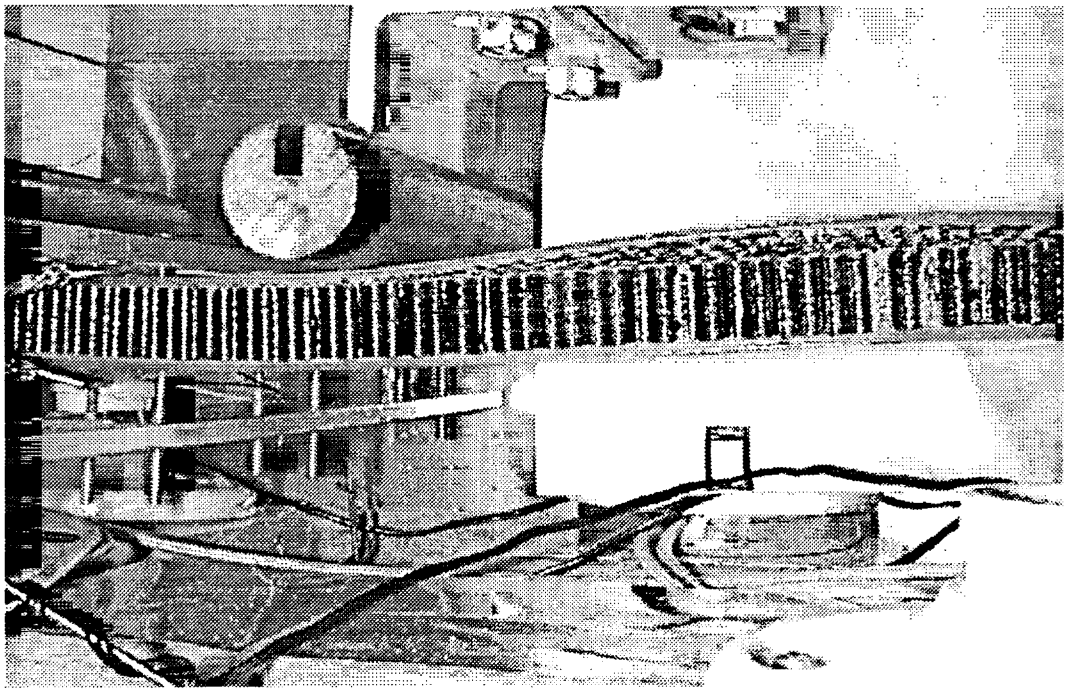

Figure 3.53 – Specimen FI-ET-D3B

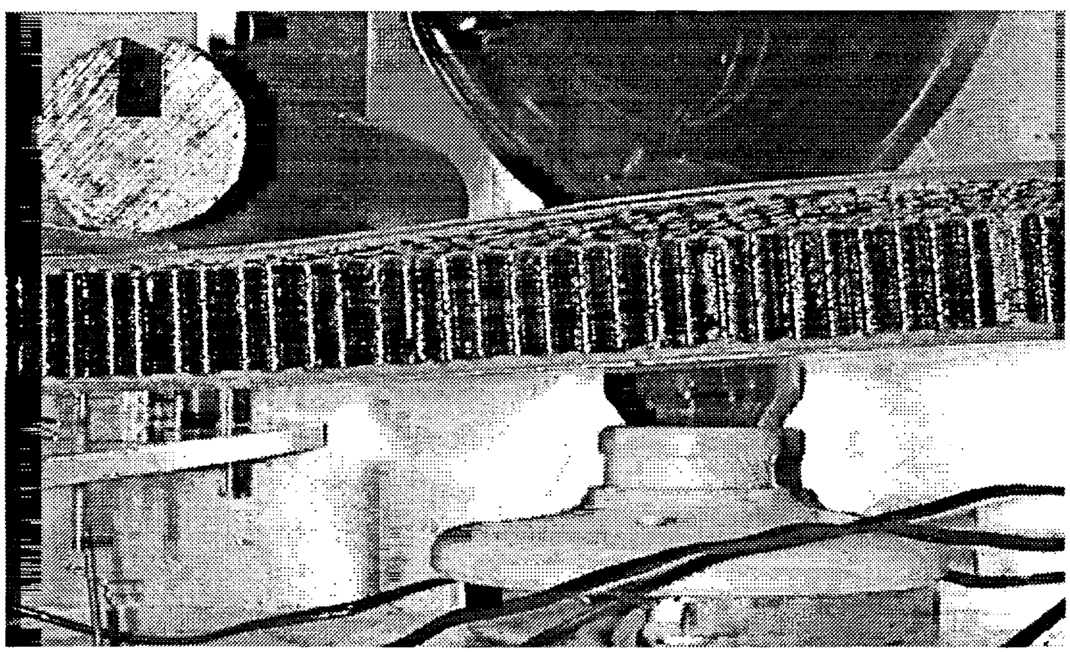

Figure 3.54 – Specimen FI-ET-D3B

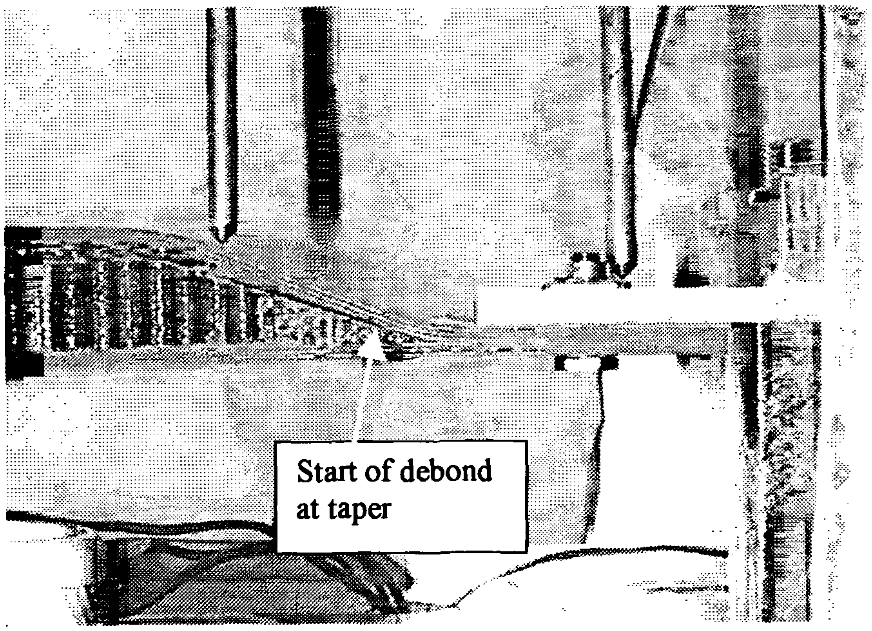

Figure 3.55 – Specimen FI-ET-D3B

3.3.2 Specimen FI-ET-D5B

Specimen FI-ET-D5B failed under a slightly greater load of 1,492 lbs (6.64 kN). The panel failed when the core failed under shearing. Figures 3.56 and 3.57 are graphs of the load-displacement curve and load-strain curve, respectively. Both the load-strain plots and the load-deflection plots are highly linear. Figures 3.58 and 3.59 are photos that were taken after the panel failed. They are both close-up views of the core shear failure.

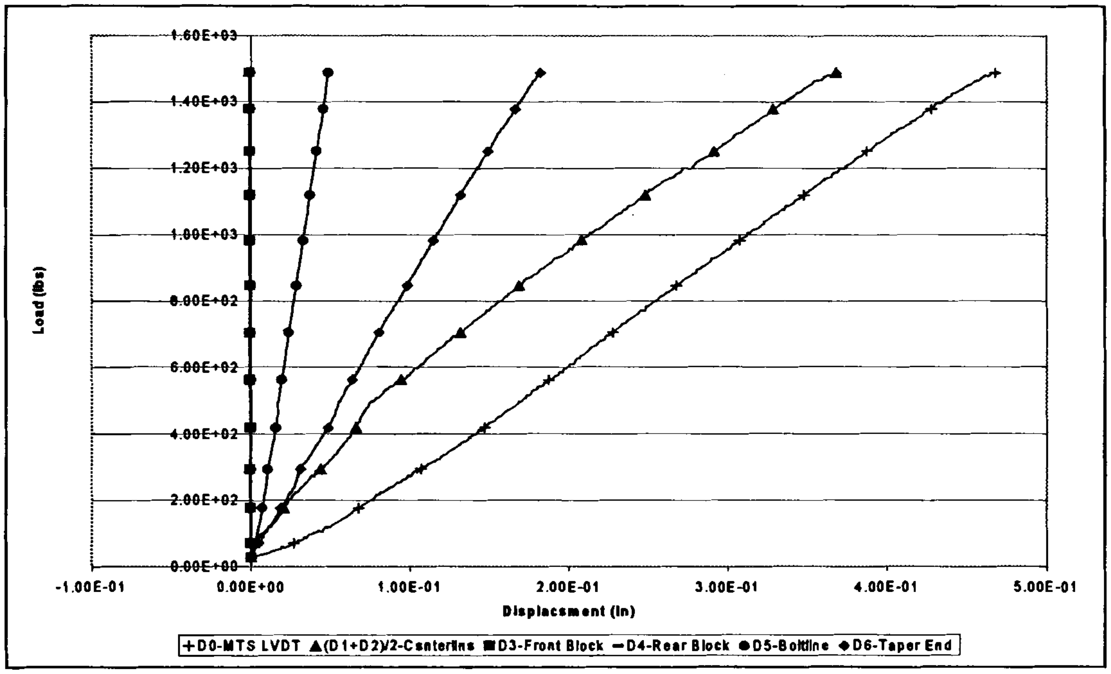

Figure 3.56 – Load-Displacement Curve for FI-ET-D5B

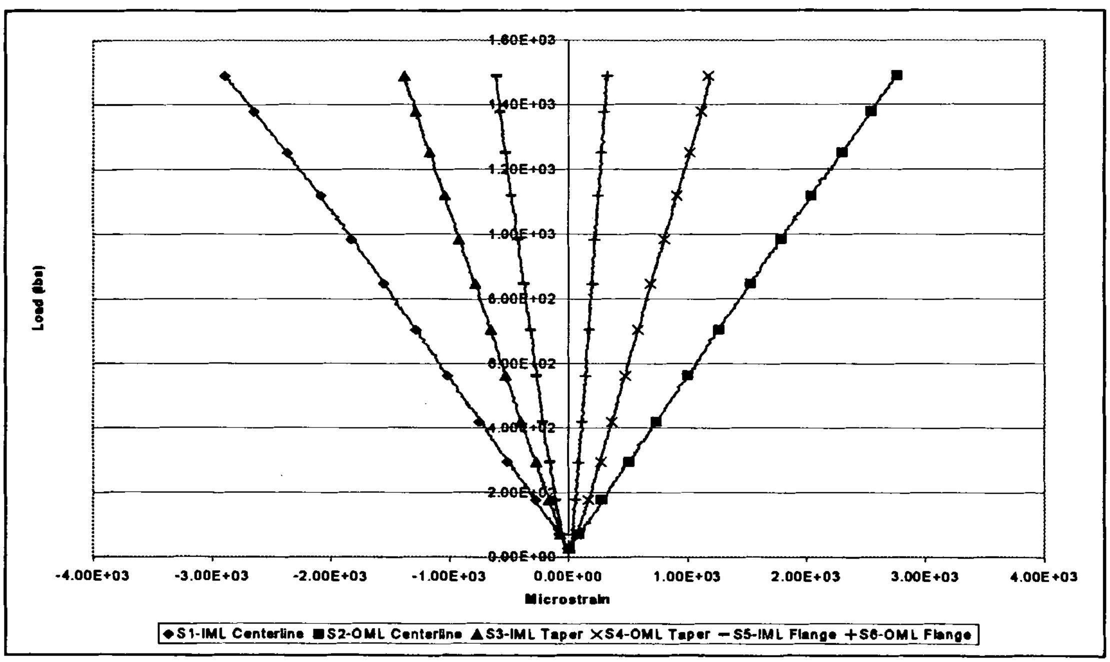

Figure 3.57 – Load-Strain Curve for FI-ET-D5B

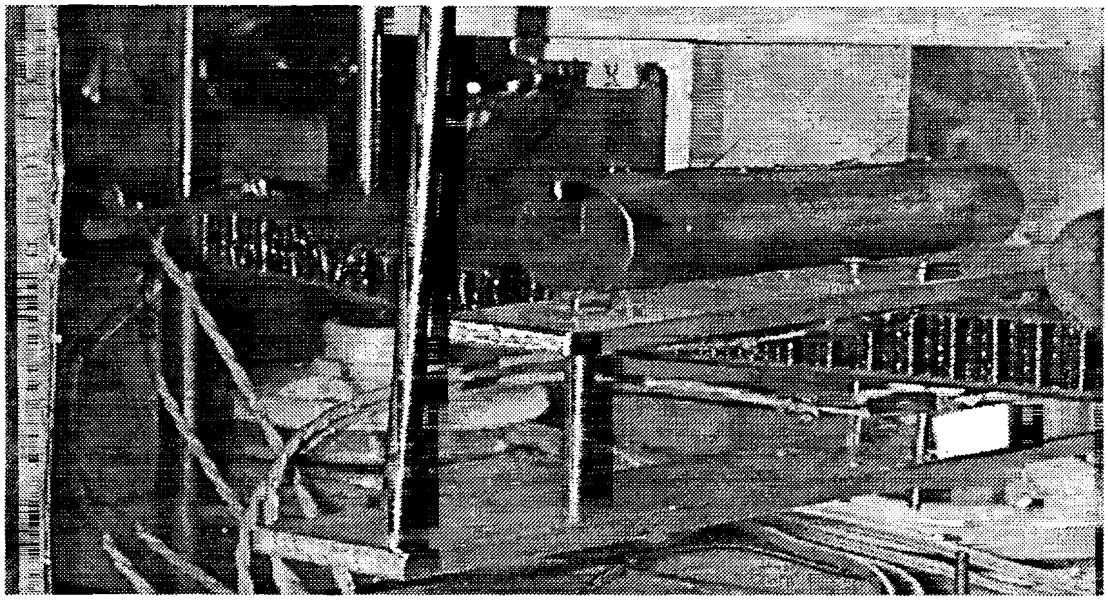

Figure 3.58 – Specimen FI-ET-D5B

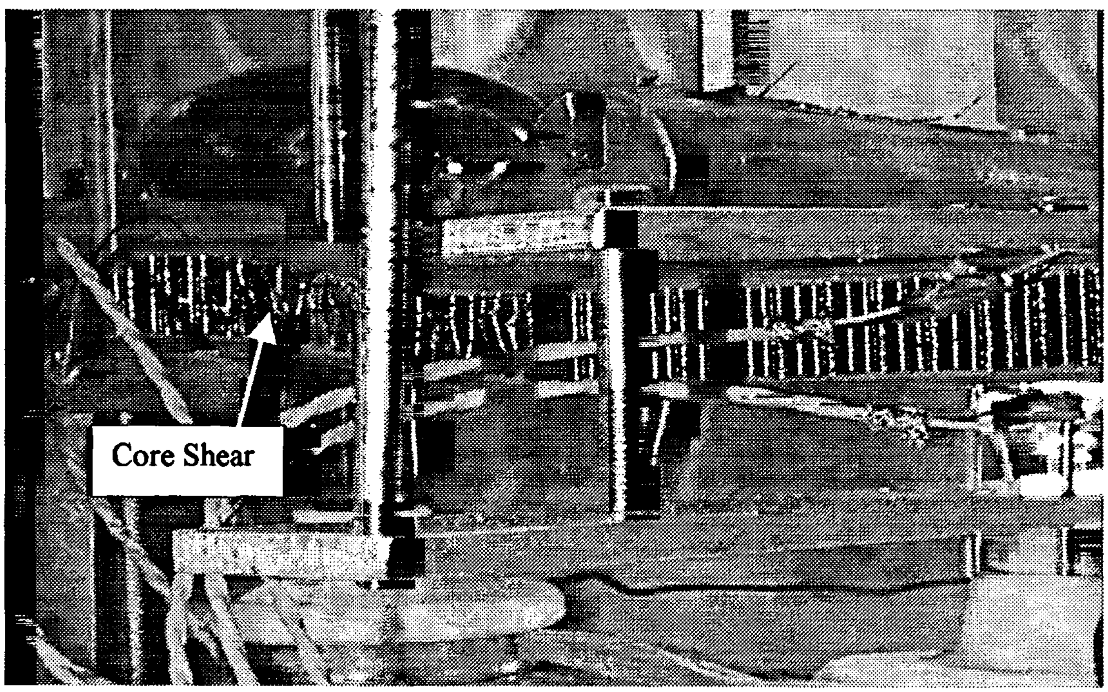

Figure 3.59 – Specimen FI-ET-D5B

3.3.3 Elevated Temperature Vs Room Temperature Sandwich Panels

The elevated temperature caused a substantial reduction in panel stiffness. This effect is quantified in Tables 3.16 and 3.17 below, listing the average centerline stiffness and strength values for both lengths of sandwich panels, and the percentage change in stiffness from room temperature to elevated temperature. The 24-inch panels with the 20° taper experienced an average drop in stiffness of 12 percent as a result of the elevated temperature environment. The 26-inch panels with the 30° taper experienced an average drop in stiffness of 8 percent. Figure 3.60 is a composite plot of the centerline load-deflection curves for the 30° tapered specimens. Figure 3.61 is a compilation of the centerline OML load-strain plots for the 30° tapered specimens. Figures 3.62 and 3.63 are compilations of the centerline load-deflection curves and centerline OML load-strain curves for the 20° tapered specimens, respectively.

Table 3.16 – Sandwich Panel Stiffness Knockdown Factors

24" Panels	
Average Room Temp Stiffness (lbf/in):	**4,332**
Average Elevated Temp Stiffness (lbf/in):	**3,825**
Knockdown Factor:	**0.88**
26" Panels	
Average Room Temp Stiffness (lbf/in):	**3,456**
Average Elevated Temp Stiffness (lbf/in):	**3,173**
Knockdown Factor:	**0.92**

Table 3.17 – Sandwich Panel Strength Knockdown Factors

24" Panels	
Average Room Temp Peak Load (lbf/in):	1,895
Average Elevated Temp Peak Load (lbf/in):	1,492
Knockdown Factor:	0.79
26" Panels	
Average Room Temp Peak Load (lbf/in):	1,688
Average Elevated Temp Peak Load (lbf/in):	1,432
Knockdown Factor:	0.85

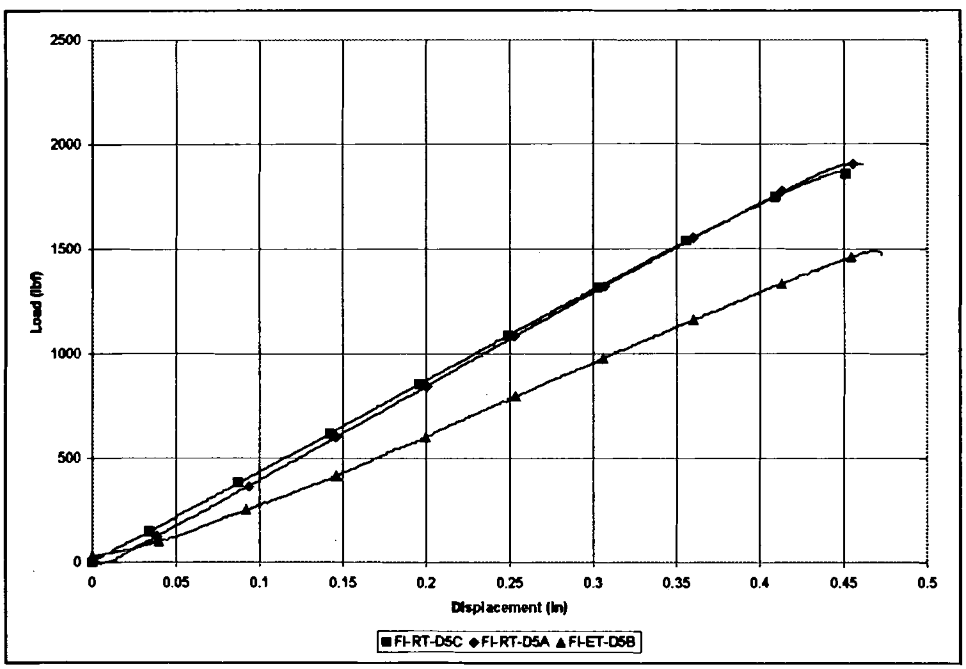

Figure 3.60 – Load vs Centerline Deflection of Room Temp/Elevated Temp 30° Taper Sandwich Panels

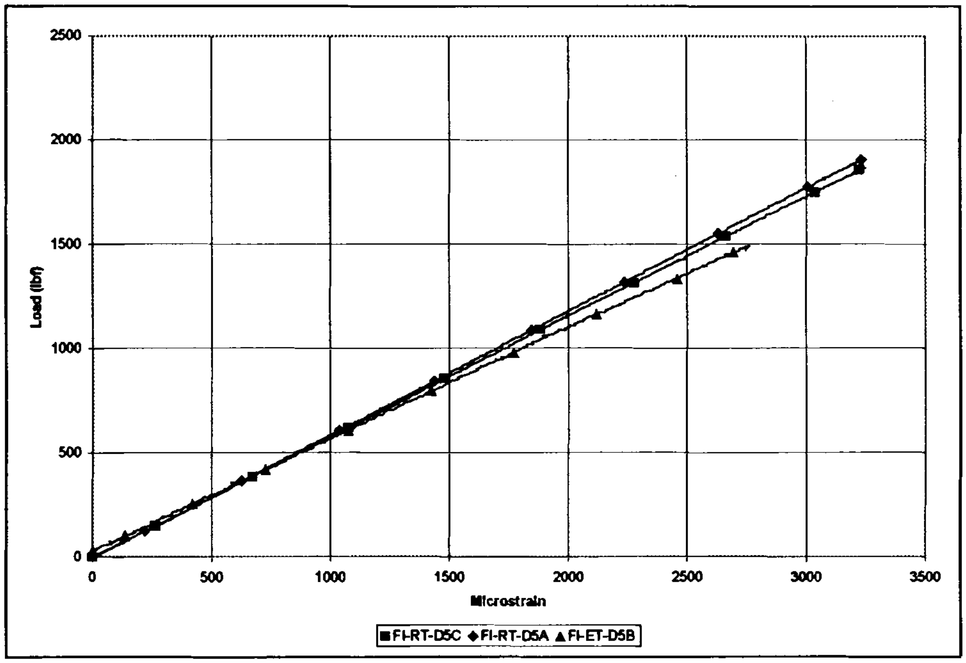

Figure 3.61 – Load vs Centerline OML Strain of Room Temp/Elevated Temp 30° Taper Sandwich Panels

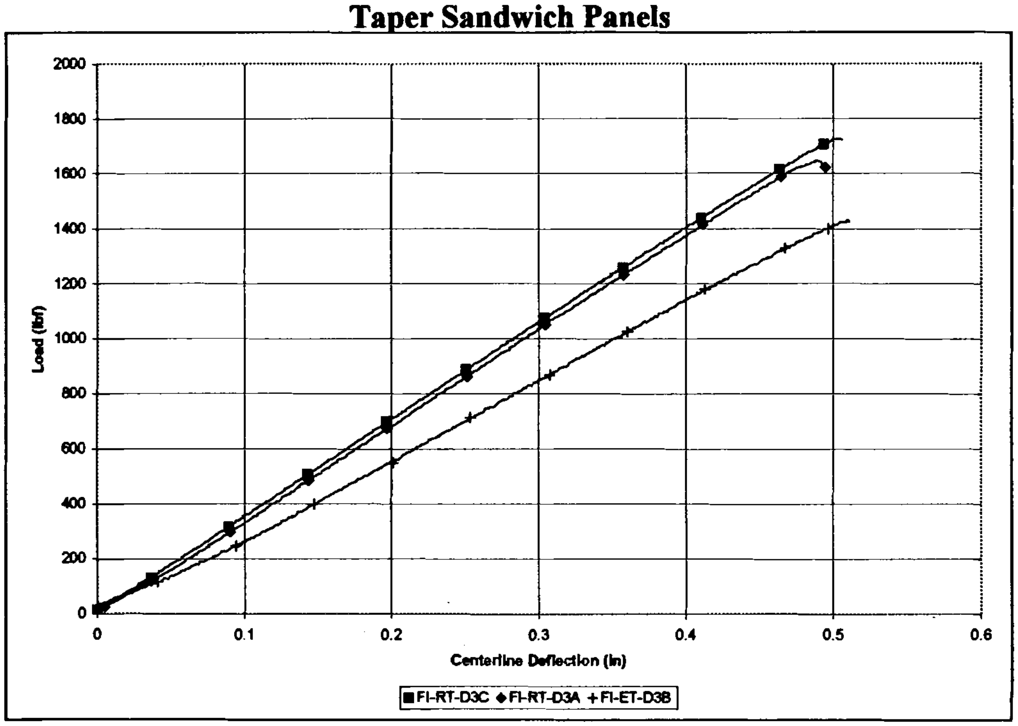

Figure 3.62 – Load vs Centerline Deflection of Room Temp/Elevated Temp 20° Taper Sandwich Panels

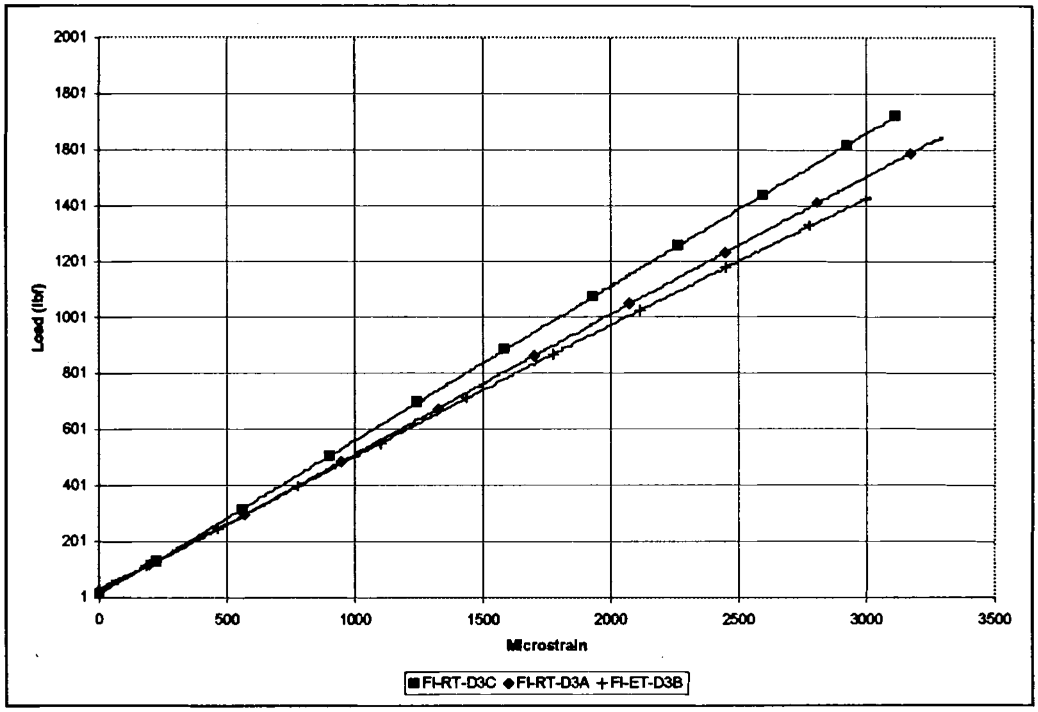

Figure 3.63 – Load vs Centerline OML Strain of Room Temp/Elevated Temp 20° Taper Sandwich Panels

4. Simplified Beam Analysis

Classical beam theory from strength of materials can be used to predict the behavior of the test articles described in Section 3. Each panel is modeled (see Figure 4.1) as the summation of the solution to a simply supported beam loaded with two line loads offset from the center and the solution to a simply supported beam loaded with restoring moments at the ends to simulate the restraint of the joints. A flexibility based analysis was chosen for this purpose. The critical parameters in this analysis are the behavior of the joint at either end of the panel, and the magnitude of the restoring moments.

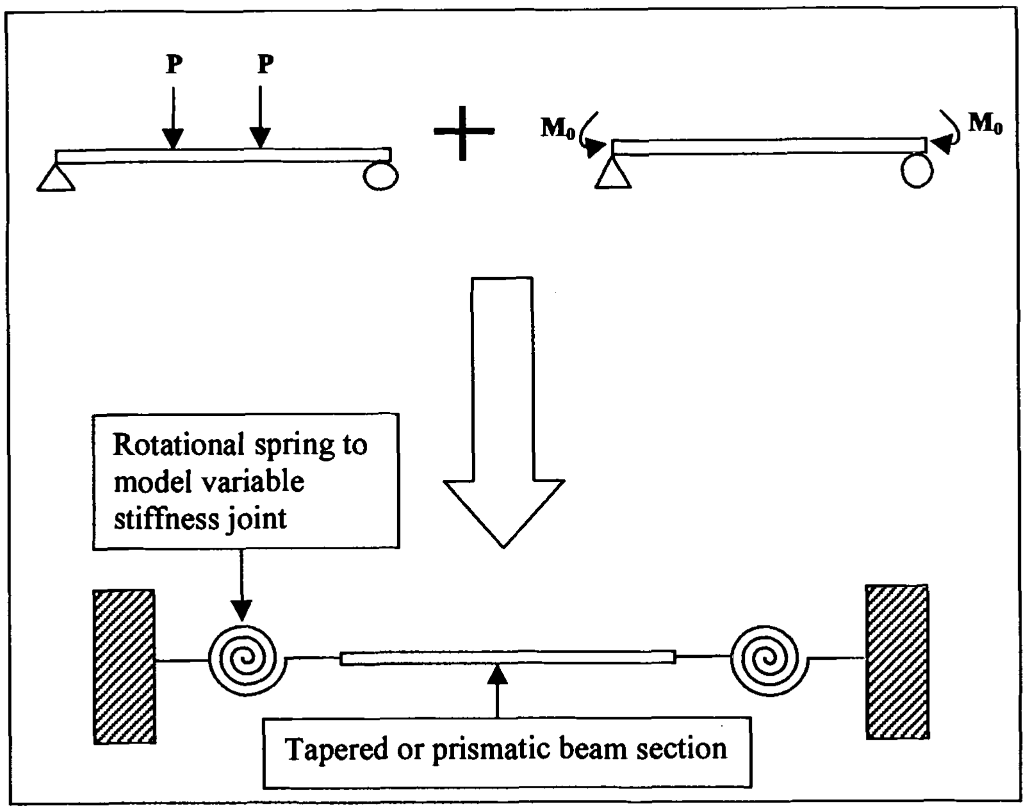

Figure 4.1 – Beam Analysis Summary

Simply supported beams loaded in flexure deflect as a result of both bending and shear deformations. The deflection of a beam can be calculated by multiple integration of the beam's curvature. The curvature of a beam due to bending effects alone is given by Equation 4.1:

$$\frac{d^2}{ds^2}v_b = \frac{-M(x)}{E \cdot I(x)} \qquad \textbf{(4.1)}$$

where:

v_b is the deflection of the beam due to bending effects

M(x) is the moment applied to the beam (in*lbf)

E is effective Young's modulus in flexure for the beam (psi)

I(x) is the cross-sectional moment of inertia (in^4) varying with length x

The curvature of a beam due to the effects of shear is given by equation 4.2.

$$\frac{d^2}{ds^2}v_s = -\frac{d}{dx}\frac{\alpha_s \cdot V(x)}{G \cdot A(x)} \qquad \textbf{(4.2)}$$

where:

v_s is the deflection of the beam due to shear effects (in)

V(x) is the shear force applied to the beam (lbf)

G is the effective shear modulus (psi)

A(x) is the cross-sectional area (in^2)

α_s is the shear coefficient of the cross-section (1.0 in this case)

Addition of equations 4.1 and 4.2 results in the total curvature of the beam, due to both bending and shear effects. This is given is equation 4.3.

$$\frac{d^2}{ds^2}v = \frac{-M(x)}{E \cdot I(x)} - \frac{d}{dx}\frac{\alpha_s \cdot V(x)}{G \cdot A(x)} \qquad \textbf{(4.3)}$$

where:

v is the total deflection of the beam due to bending and shear

Successive integration of equation 4.3 will result in the total deflection of the beam. Deflections due to shear are usually discounted in isotropic beams that have a large length to depth (L/D) ratio, typically greater than ten. In this study, the shear deflection terms will be discounted for the thin flat laminates and the hat-stiffened laminates because the deformations due to shear are small compared to the deformations due to bending. However, the shear deformations will be included in the analysis of the sandwich construction panels because shear deformations are significant in sandwich panels even with large L/D ratios.

4.1 Flat Laminates

In developing a simplified modeling approach, it is convenient to assume that the flat laminates behave as a prismatic beam with end connectors. Using laminate theory, an effective Young's modulus is obtained using properties presented in Section 2.3.1. The material model is given in Table 4.1. The laminate properties and effective properties are listed.

Table 4.1 – Laminate Properties

E_1	23.3E6 psi (160.65 GPa)
E_2	1.12E6 psi (7.7224 GPa)
ν_{12}	0.30
G_{12}	0.50E6 psi (3.4475 GPa)
Effective E	24.58E6 psi (169.46 GPa)
Effective ν	0.322

The effective bending modulus for the laminate was calculated using Equation 4.4, from laminate theory (Barbero 1998) as follows.

$$E_b := 12\cdot\frac{\left[D_{1,1}\cdot D_{2,2}-\left(D_{1,2}\right)^2\right]}{h^3\cdot D_{2,2}} \qquad \textbf{(4.4)}$$

where:

h is the thickness of the laminate (in)

and $D_{1,1}$, $D_{2,2}$, and $D_{1,2}$ are terms from the laminate stiffness matrix, as given by equation 4.5:

$$D_{i,j} := \sum_{k=1}^{N}\left(Qbar_{i,j}\right)_k\cdot\left[t_k\cdot\left(zbar_k\right)^2+\frac{\left(t_k\right)^3}{12}\right] \qquad \textbf{(4.5)}$$

$i,j := 1,2,6$

where:

Qbar is the off-axis reduced stiffness matrix (psi)

t_k is the thickness of each ply of the laminate (in)

zbar is the location of the center of each ply (in)

Shear deflections are discounted because of the large length to depth ratio (104) of the flat laminates. Therefore, the deflection of the flat laminate becomes a function of moment, modulus, moment of inertia, and connection properties. The modulus and cross-sectional moment of inertia are constants, but the moment is a function of position down the length of the beam, due to the location of the line loads offset from the center of the beam. Figure 4.2 illustrates how the moment changes down the length of the laminate. The moment is zero at the ends of the beam, and graduates up to a final value of P*a/L at the location of the line loads, which are treated as point loads in the beam equations.

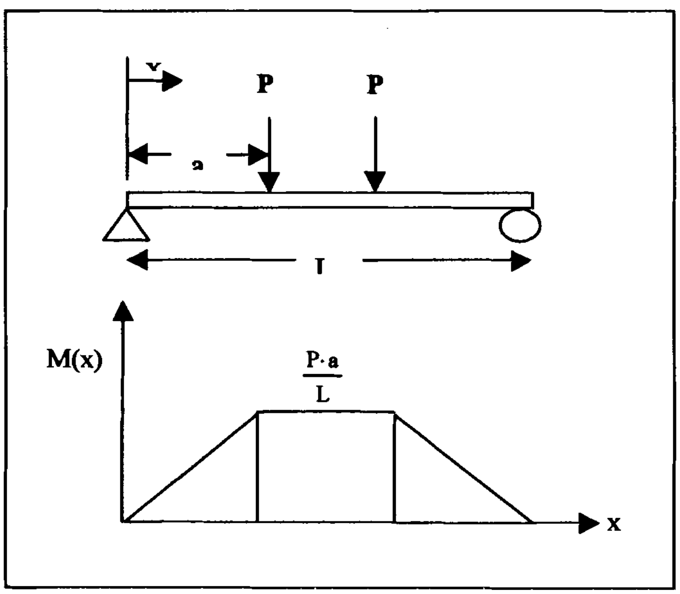

Figure 4.2 – Moment Diagram for Point Loading Solution

Double integration of Equation 4.3 for the beam shown in Figure 4.2 results in Equation 4.6, which is piecewise continuous.

$$\delta_{ss}(x) := \begin{cases} \dfrac{P\cdot x}{6\cdot E\cdot I}\cdot\left(3\cdot L\cdot a - 3\cdot a^2 - x^2\right) & \text{if } x \le a \\ \dfrac{P\cdot a}{6\cdot E\cdot I}\cdot\left(3\cdot L\cdot x - 3\cdot x^2 - a^2\right) & \text{if } x \le (L-a), \text{and}, (x \ge a) \\ \dfrac{-P\cdot(x-L)}{6\cdot E\cdot I}\cdot\left[3\cdot L\cdot a - 3\cdot a^2 - (x-L)^2\right] & \text{if } x \ge (L-a) \end{cases} \tag{4.6}$$

where:

P is the magnitude of the load

L is the length of the beam

a is the distance from the end of the beam to the load

x is the position along the beam

A restoring moment exists at the end of the beam due to the partial restraint of the connection. The restoring moment load case is illustrated in Figure 4.3, where the moment is a constant value down the length of the beam.

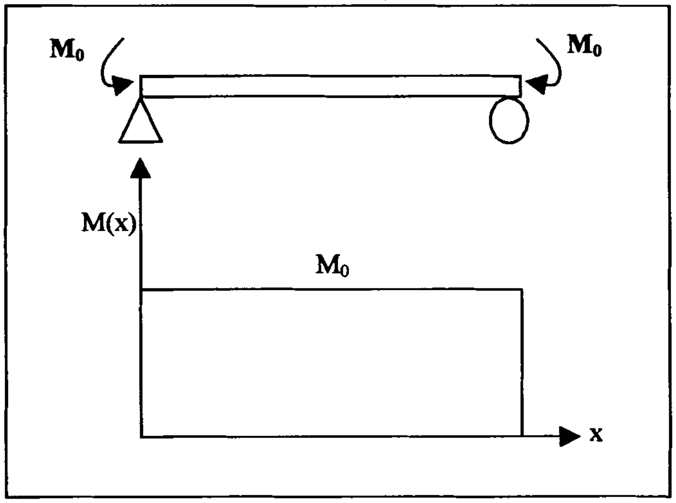

Figure 4.3 – Moment Diagram for End Moment Loading Case

Double integration of Equation 4.3, in this case yields Equation 4.7, given below:

$$\delta_m(x) := \frac{-M_0 \cdot x}{2 \cdot E \cdot I} \cdot (L - x) \qquad \textbf{(4.7)}$$

where:

M_0 is the magnitude of the restoring end moments

The magnitude of the restoring end moment (M_0) is assumed to depend on the joint rotational stiffness. The joint rotational stiffness, J, is a function of the net change in angular deflection, θ, at the ends of the beam. The angular deflection at the end of the beam is taken as the slope at the ends of the beam from the simply supported solution, and the resulting end moment is given by Equation 4.8:

$$M_0 := J \cdot \theta_{endtotal} \qquad \textbf{(4.8)}$$

where:

$\theta_{endtotal}$ is the angular rotation at the end of the point loaded beam (radians)

J is the joint rotational stiffness (in*lbf)

Originally, the panels were clamped between a steel plate on top and the base of the test chamber on the bottom. Due to the flexibility of the unstiffened laminates, no failure was recorded for either laminate during its first flexure test. Load was applied until the displacement limit of the test chamber was reached (~3.5 inches). After these two tests were conducted, it was noted that the end supports were rotating inward due to insufficient stiffness at the clamped ends. To stiffen the clamped ends, holes were drilled through the base of the oven and the steel channel beneath. The flat laminates were then clamped between the steel plate above and the steel channel beneath the test chamber. This results in a modification to the end joint restraint.

Because of this inability to achieve perfect boundary conditions, the flexural behavior of the flat laminates, in both tests, was in between that of a simply supported beam and a fully clamped beam. This is illustrated graphically in Figures 4.3 and 4.4, which compare the deflected shape of the actual beam (dotted line) to the deflected shape of a simply supported beam (dashed line) and a totally clamped beam (solid line) with the same properties. Figures 4.3 and 4.5 represent the response in flat laminates FLHT-01 and FLHT-02 before the end supports were stiffened, and Figures 4.4 and 4.6 represent the response after the end supports were stiffened. A sample MathCAD worksheet is shown in Appendix B, Section 7.1.

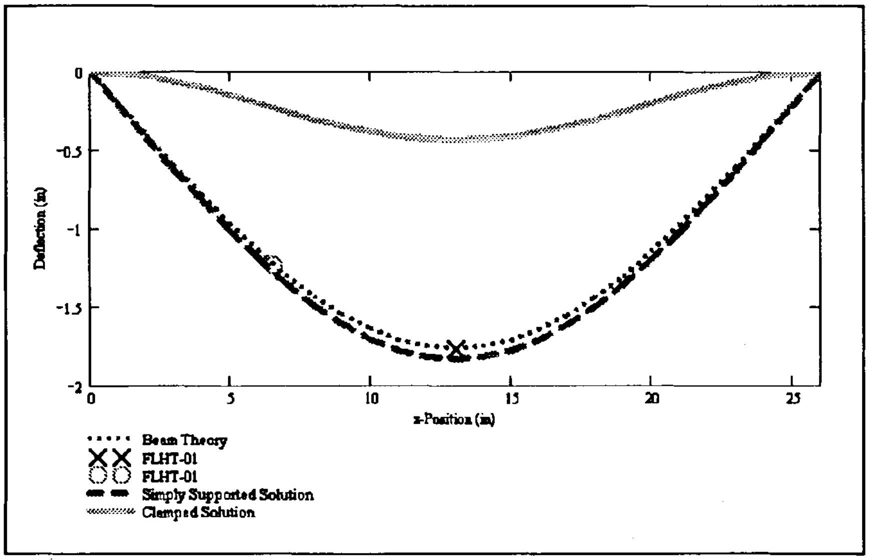

Figure 4.4 – Response of FLHT-01 Before Support Stiffening

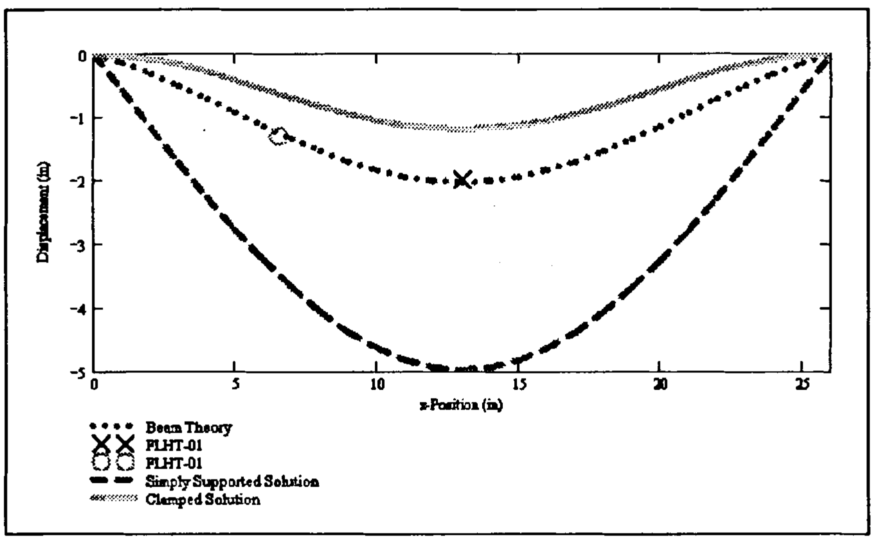

Figure 4.5 – Response of FLHT-01 After Support Stiffening

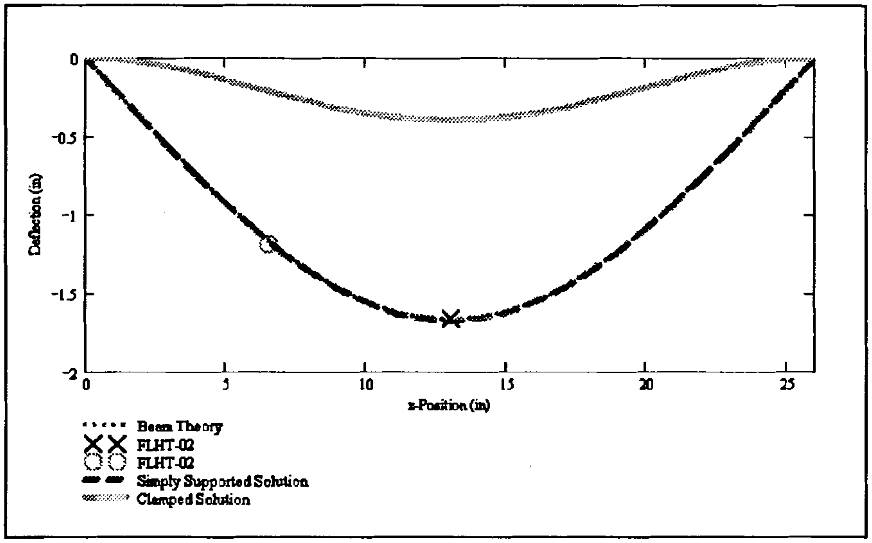

Figure 4.6 – Response of FLHT-02 Before Support Stiffening

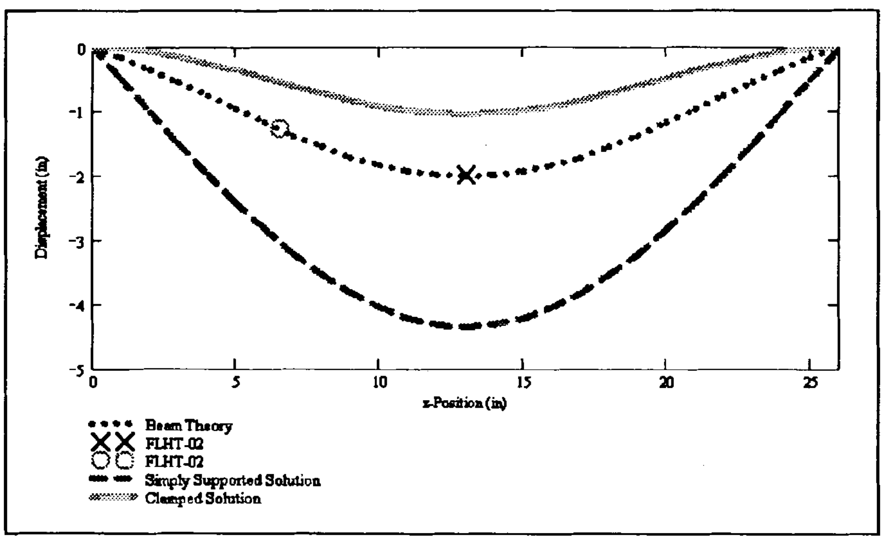

Figure 4.7 – Response of FLHT-02 After Support Stiffening

It is noted that the rotation at the end of the member in the first case causes the response of to be very close to that of a simply supported member. In the second case with the stiffer boundary condition, it is concluded that the stiffness of the end restraints is close to that of a fixed condition. The actual connection condition is partially restrained. The results are summarized in Table 4.2, which lists the joint stiffness factors and the percent rigidity, or the percentage of the totally clamped solution. A percentage close to zero indicates a near-simply supported case.

Table 4.2 – Summary of Flat Laminate Beam Models

Panel #	Joint Stiffness (lbf*in)	% Rigidity
FLHT-01-test1	885	5.1
FLHT-02-test1	100	0.60
FLHT-01-test2	59,280	78.1
FLHT-02-test2	30000	64.4

4.2 Hat-Stiffened Panels

For both the tapered hat-stiffened and tapered sandwich panels, the cross-section of the panel changes as a function of position down the length of the beam. Both are analyzed in a similar fashion to the flat laminates. The total beam solution is the sum of the solution to a simply supported beam loaded with concentrated point loads offset from the center plus the solution to a simply supported beam loaded with restoring end moments. The difference between the analysis of the flat laminates and the hat-stiffened and sandwich panels is the tapered portion. The tapered portion of the hat-

stiffened panels and the tapered sandwich panels was modeled using two different approaches for this study. The first approach is to model the entire panel with the prismatic part, the taper and a joint stiffness factor J, at the ends of the panel. The second approach is to incorporate the tapered portion of the panel into the joint and model the entire panel as a prismatic beam with flexible ends. This is shown in Figure 4.7.

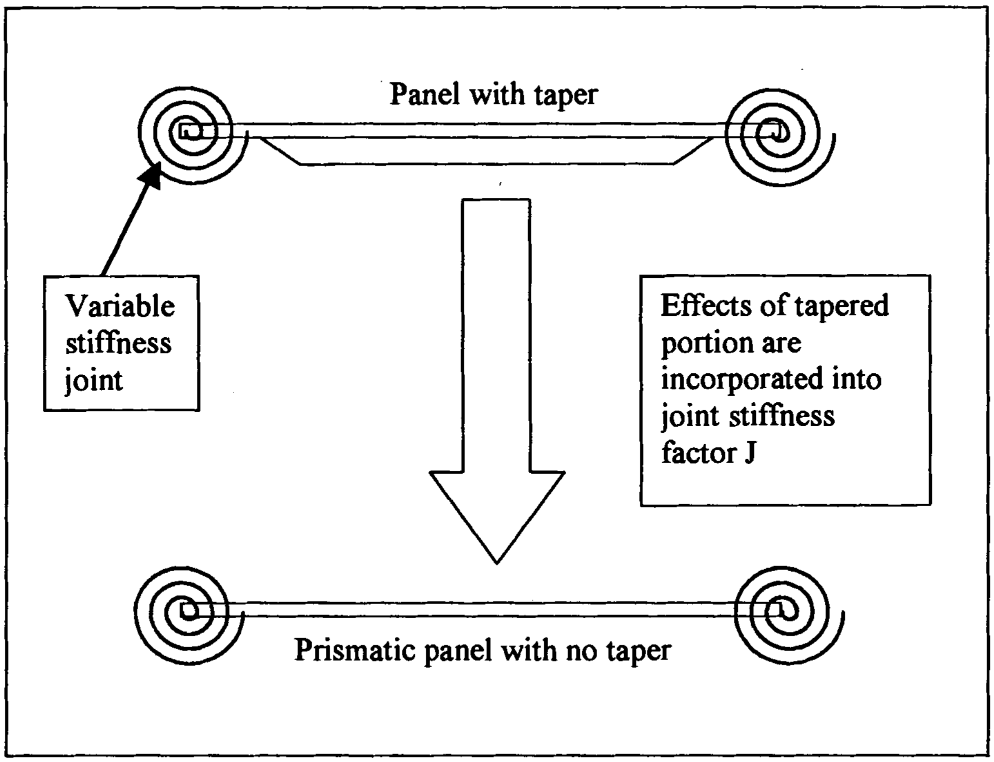

Figure 4.8 – Analysis of Tapered Hat-Stiffened and Sandwich Panels

For a non-prismatic beam, as in the case of the hat-stiffened or sandwich panels, the previous equations need to be modified since the moment of inertia is now a function of position down the length of the beam. The first 2.5 inches of the beam have a moment of inertia identical to the flat laminates. The next 2 inches is a tapered

section, where the hat-shaped stiffener graduates up to its final height of 1 inch. Equation 4.3 is again integrated twice over the length of the beam.

Another important issue is the fact that the hat-stiffened laminates are made of two different materials. The laminate and the hat-shaped stiffener have different composite lay-ups and therefore different properties. To make the analysis more convenient, the flat laminate portion of the panel cross-section can be transformed into an equivalent cross-section with the properties of the stiffener material by changing the width of the beam, as shown below in Equation 4.9:

$$b_{lamtransformed} := b_{lam} \cdot \left(\frac{E_{lam}}{E_{stiffener}} \right) \qquad \textbf{(4.9)}$$

This creates a cross-section for the hat-stiffened laminate that is, virtually speaking, made of one material having a different geometry than the original, but having the same flexural properties. Only the room temperature hat-stiffened panels are modeled, since the elevated temperature lamina properties were unavailable.

In this instance, the elements of the cross-section can be treated as thin plates and the effective modulus is given by Equation 4.10.

$$E := \frac{A_{1,1} \cdot A_{2,2} - \left(A_{1,2}\right)^2}{t \cdot A_{2,2}} \qquad \textbf{(4.10)}$$

Where $A_{1,1}$, $A_{2,2}$, and $A_{1,2}$ are terms from the laminate stiffness matrix given by Equation 4.13.

$$A_{i,j} := \sum_{k=1}^{N} \left(Qbar_{i,j}\right)_k \cdot t_k \qquad \textbf{(4.13)}$$

$i,j := 1,2,6$

As with the flat laminates, the problem of modeling the panels is broken down into the solution of a simply supported beam loaded with two point loads offset from the center, added with the solution from a simply supported beam loaded with restoring end moments. Due to the symmetry and complexity of this problem, only half of the beam needs to be modeled. Integrating the equation 4.3 results in several integration constants. The equation has to be integrated over four sections of the beam model, as shown below in Figure 4.9.

The moment of inertia changes with position down the length of the panel. For simplicity, the average moments of inertia was used in the tapered section. This was approximated using a constant moment of inertia across each section. This is summarized in Table 4.3 and shown graphically in Figure 4.10.

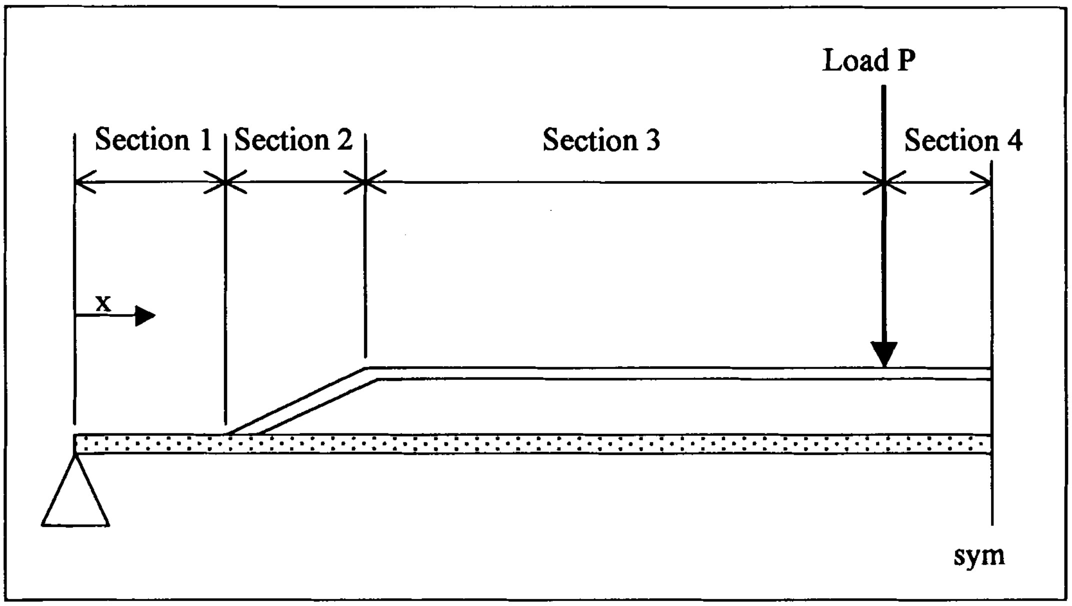

Figure 4.9 – Stiffened Panel Problem Breakdown

Table 4.3 – Hat-Stiffened Section Moments of Inertia

Section 1	0.008789 in^4
Section 2	0.020224 in^4
Section 3	0.11005 in^4
Section 4	0.11005 in^4

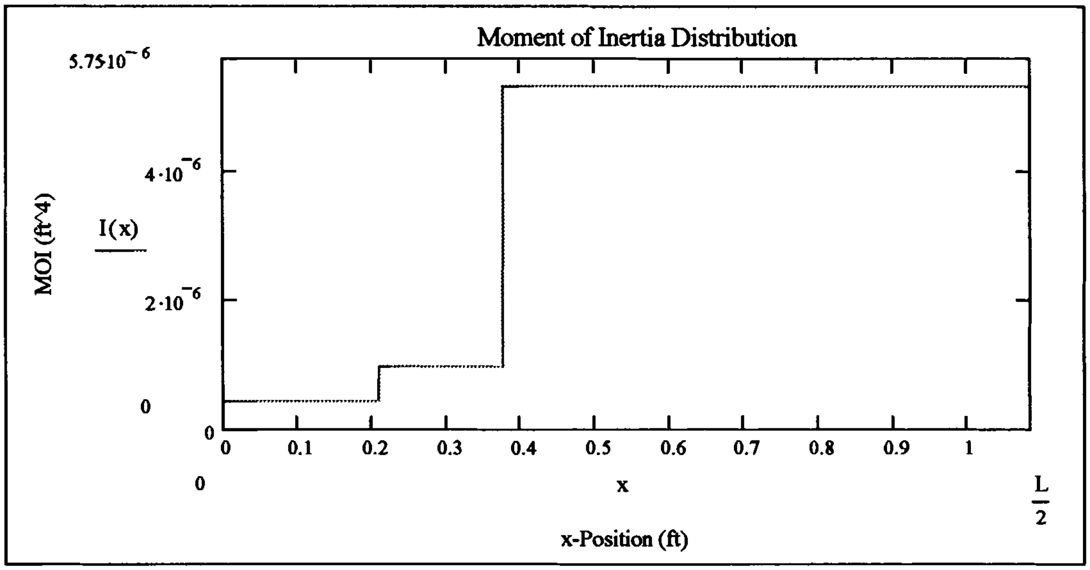

Figure 4.10 – Moment of Inertia Distribution for Hat-Stiffened Panels

Figures 4.11 through 4.16 are plots of the deflected shapes of the hat-stiffened panels under their peak experimental loads. In Figures 4.11, 4.13, and 4.15 the panels are modeled with a tapered section at the ends, and compared to actual data points, simply supported tapered models, and totally clamped tapered models. In Figures 4.12, 4.14, and 4.16, the panels are modeled as prismatic, and compared to actual data points, simply supported prismatic models, and totally clamped prismatic models. The results are also summarized in Table 4.4. This table lists the peak load, joint stiffness, and the percent rigidity of the joint (as compared to the simply supported and clamped prismatic solutions). It is noted that when using the simple prismatic model the connection tends to behave as a pin joint. A sample MathCAD worksheet is shown in Appendix B, Section 7.2.

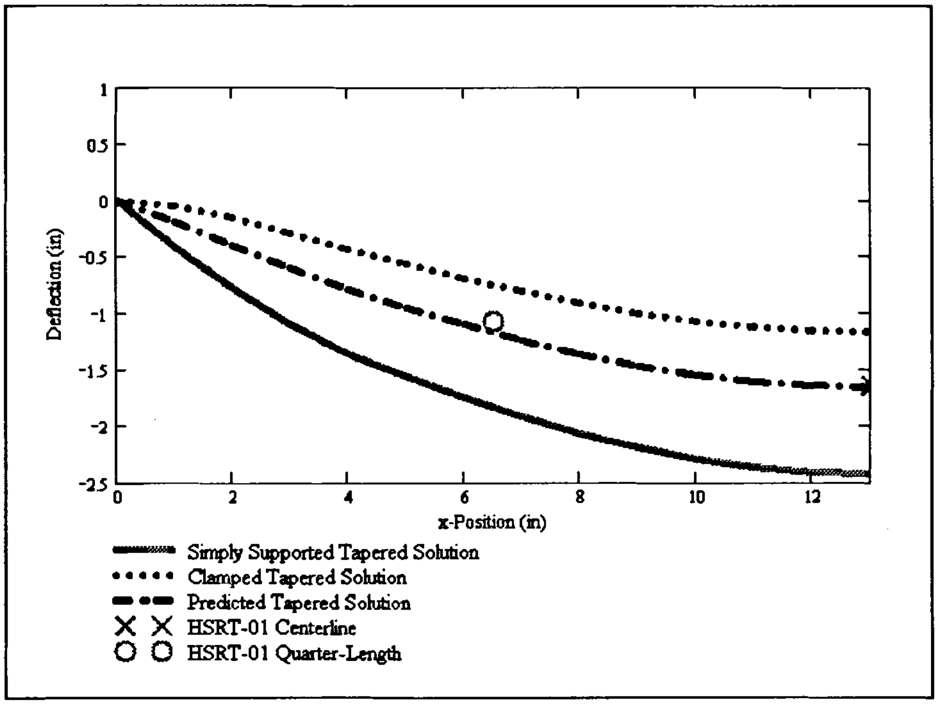

Figure 4.11 – HSRT-01 Using Tapered Beam Model

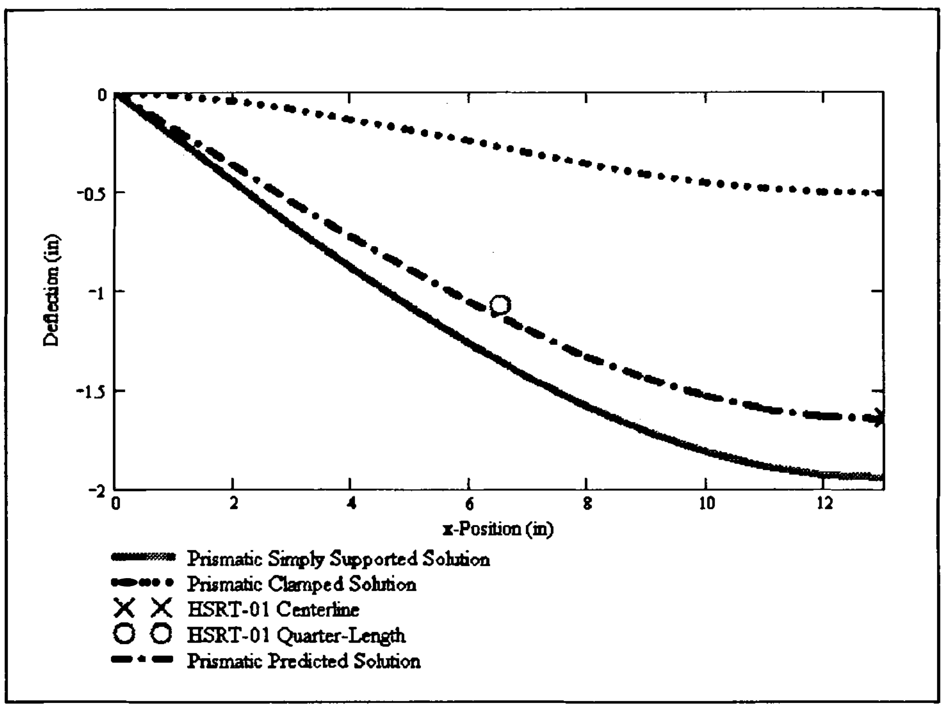

Figure 4.12 – HSRT-01 Using Prismatic Beam Model

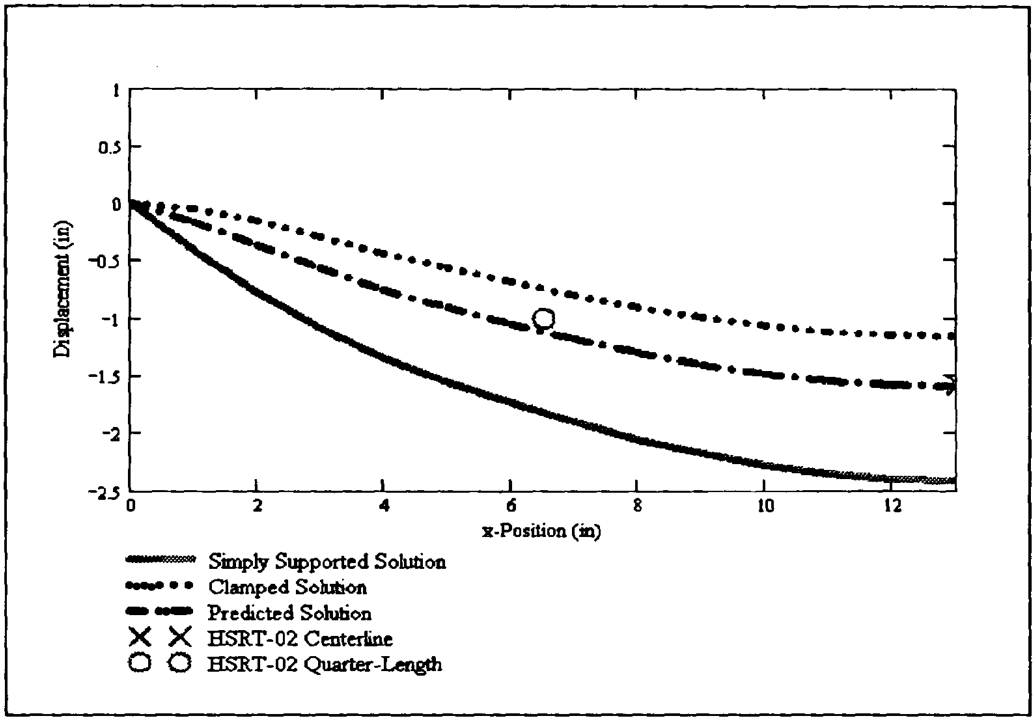

Figure 4.13 – HSRT-02 Using Tapered Beam Model

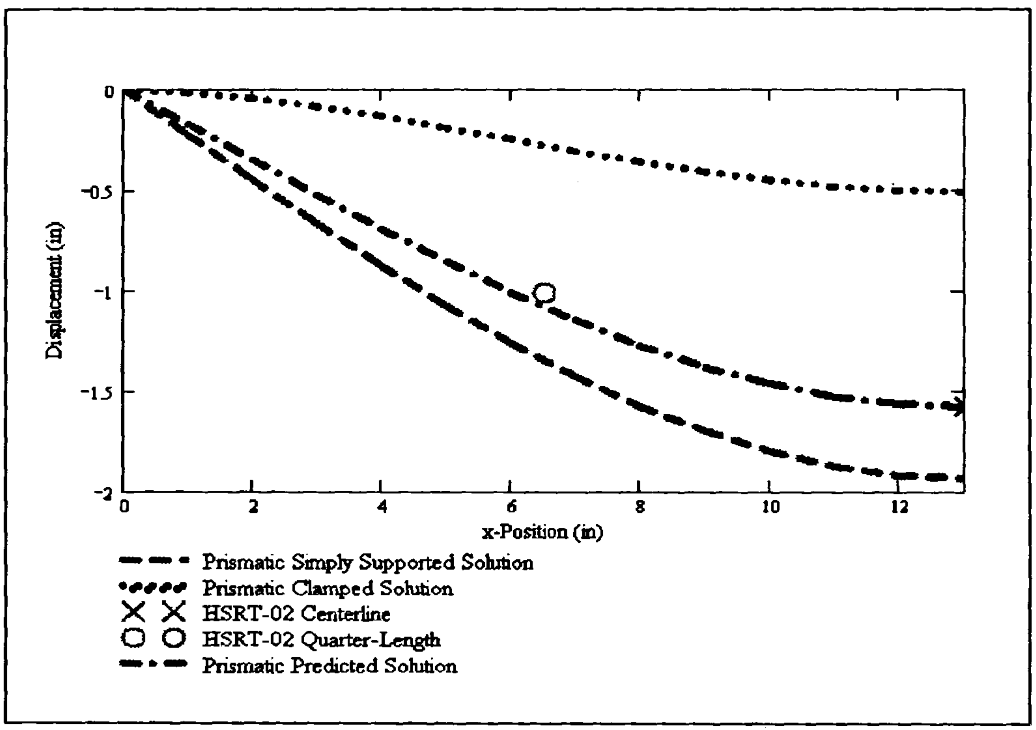

Figure 4.14 – HSRT-02 Using Prismatic Beam Model

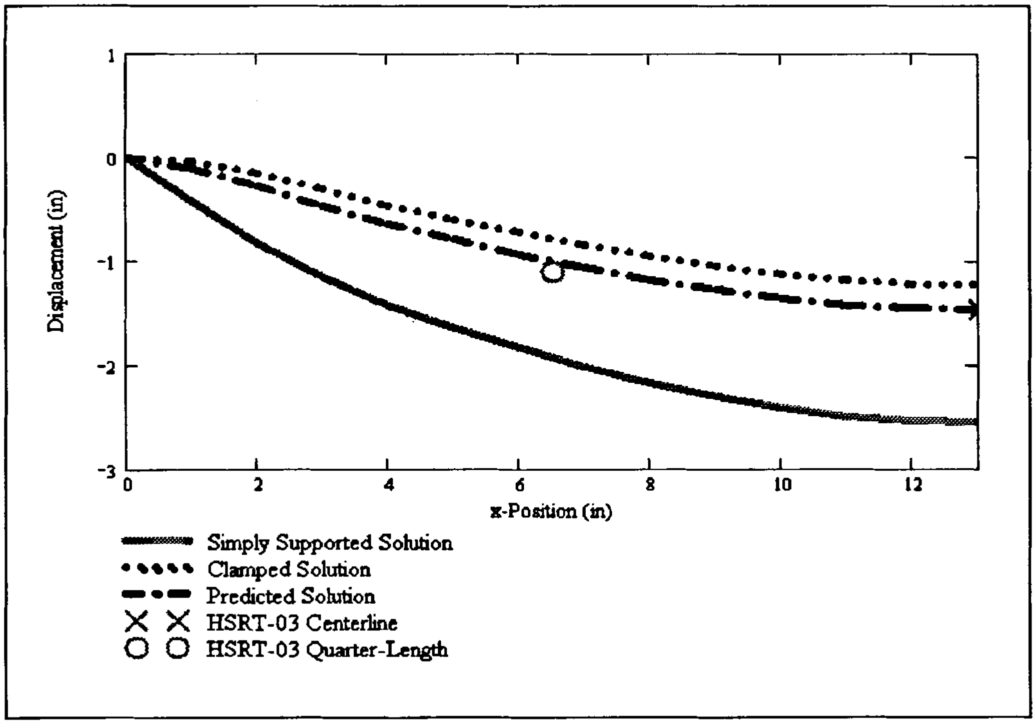

Figure 4.15 – HSRT-03 Using Tapered Beam Model

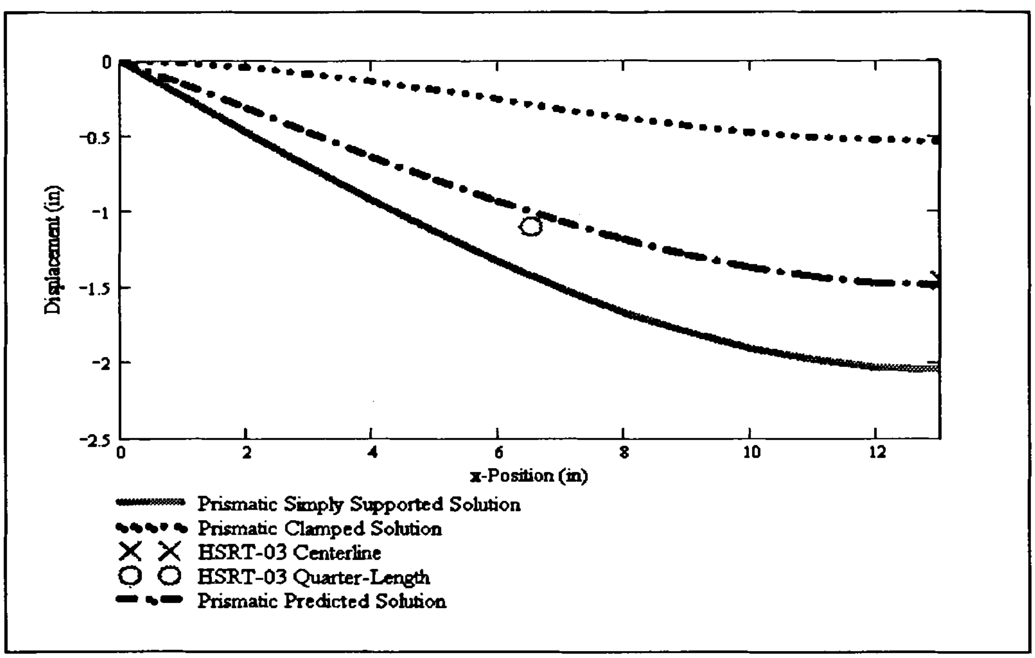

Figure 4.16 – HSRT-03 Using Prismatic Beam Model

Table 4.4 – Summary of Hat-Stiffened Panel Simplified Beam Theory Models

Panel #	Tapered Joint Stiffness (in*lbf)	% Rigidity (Tapered Solution)	Prismatic Joint Stiffness (in*lbf)	% Rigidity (Prismatic Solution)
HSRT-01	11,500	61.3	14,500	20.7
HSRT-02	12,300	65.6	17,500	25
HSRT-03	15,300	81.6	26,000	37.1

4.3 Sandwich Composite Panels

As with the hat-stiffened panels, the moment of inertia changes down the length of the tapered section in the sandwich construction panels. Because of this, it is necessary to integrate the general form of the beam deflection equation. Also, it is also necessary to include terms in the equation that account for shear deflections. In simplified sandwich panel theory, it is assumed that the shear stress is transferred through the thickness of the core and is a constant. Therefore, in equation 4.3, G is the shear modulus of the core and A(x) is the cross-sectional area of the core. Also, E is the effective modulus of the facesheets about the bending axis, as given by Equation 4.10, and I(x) is the moment of inertia of the facesheet cross-section given below in Equation 4.14.

$$I = \frac{b \cdot \left(d^3 - c^3\right)}{12} \qquad \textbf{(4.14)}$$

where:

b is the width of the panel

d is the total thickness of the panel

c is the thickness of the core, varying with position x

The theory behind the bending of composite sandwich panels is explained in more detail in Gauthier and Caccese (1998).

As with the hat-stiffened panels and flat composite laminates, the simplified model of the composite sandwich panels is the sum of the solution to a simply supported beam loaded with to point loads offset from the centerline, and the solution to a simply supported beam loaded with restoring moments at both ends of the panel.

To solve the first half of the solution, the sandwich panels are split into 4 different sections. Section 1 is the flat laminate at the flange end of the sandwich panel. Section 2 is the region of the taper. Section 3 is the prismatic middle section of the panel between the end of the taper and the point load, and Section 4 is the prismatic middle section of the panel between the centerline and the point load. This is shown in Figure 4.9, and the moments of inertia for each section are summarized in Table 4.5. After integration, constants are solved by applying the same continuity constraints as with the hat-stiffened panels.

Figures 4.17 through 4.24 are plots of the deflected shapes of the sandwich panels under their peak experimental loads. In Figures 4.17, 4.19, 4.21, and 4.23, the panels are modeled with a tapered section at the ends, and compared to actual data points, simply supported tapered models, and totally clamped tapered models. In Figures 4.18, 4.20, 4.22,and 4.24, the panels are modeled as prismatic, and compared to actual data points, simply supported prismatic models, and totally clamped prismatic models. The results are also summarized in Table 4.6. This table lists the peak load, joint stiffness, and the percent rigidity of the joint (as compared to the simply supported and clamped prismatic solutions). A sample MathCAD worksheet is given in Appendix B, Section 7.3.

Table 4.5 – Sandwich Panel Section Moments of Inertia

Section 1	0.003993 in^4
Section 2	0.059216 in^4
Section 3	0.124386 in^4
Section 4	0.124386 in^4

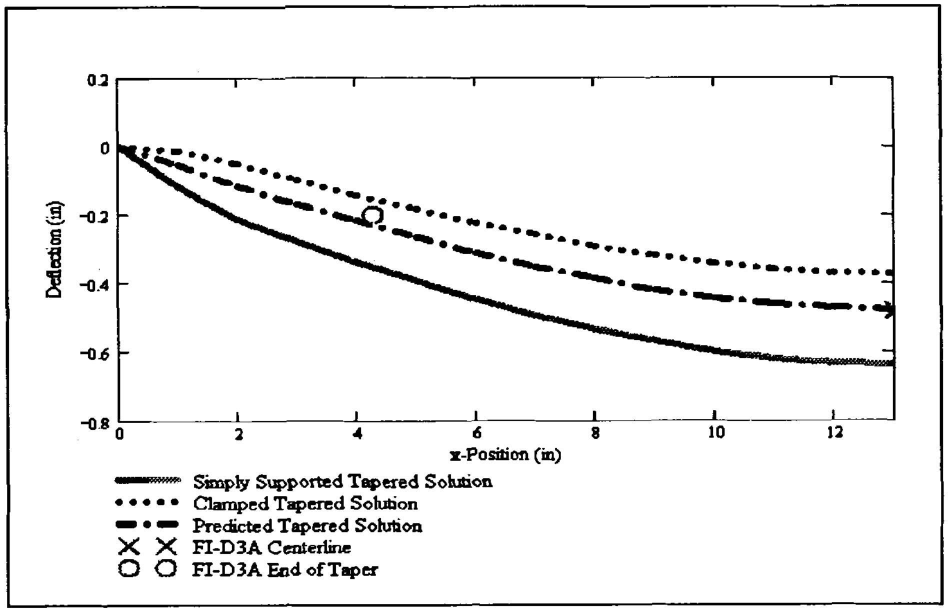

Figure 4.17 – Sandwich Panel FI-D3A Tapered Beam Model

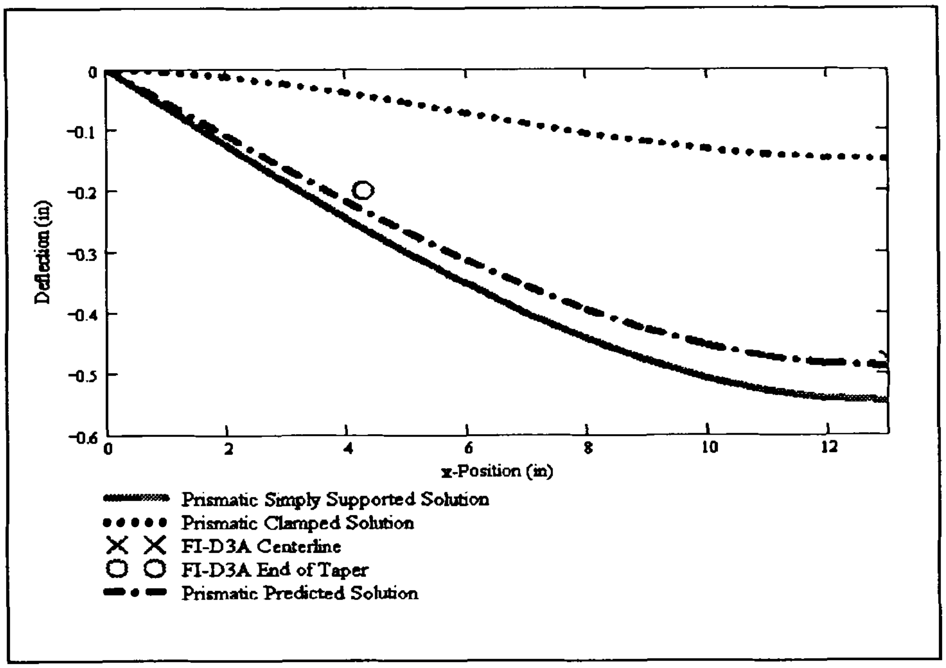

Figure 4.18 – Sandwich Panel FI-D3A Prismatic Beam Model

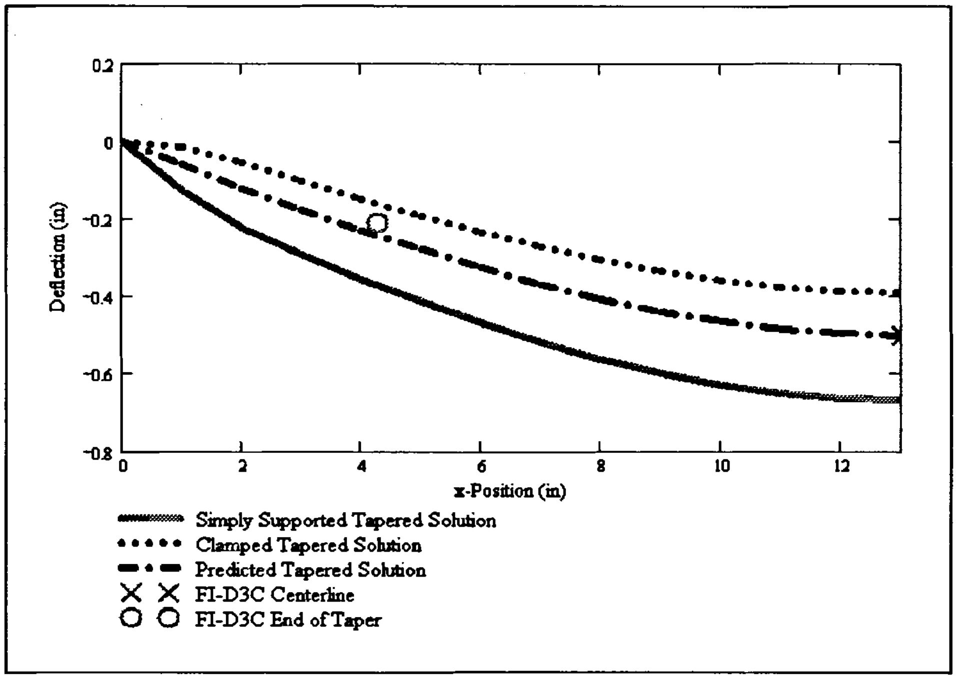

Figure 4.19 – Sandwich Panel FI-D3C Tapered Beam Model

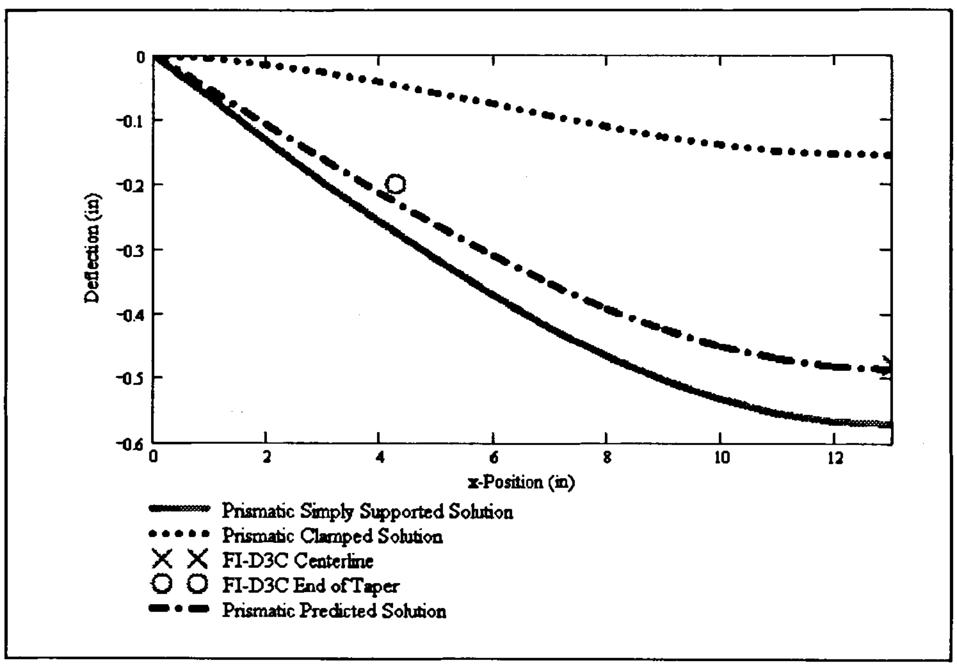

Figure 4.20 – Sandwich Panel FI-D3C Prismatic Beam Model

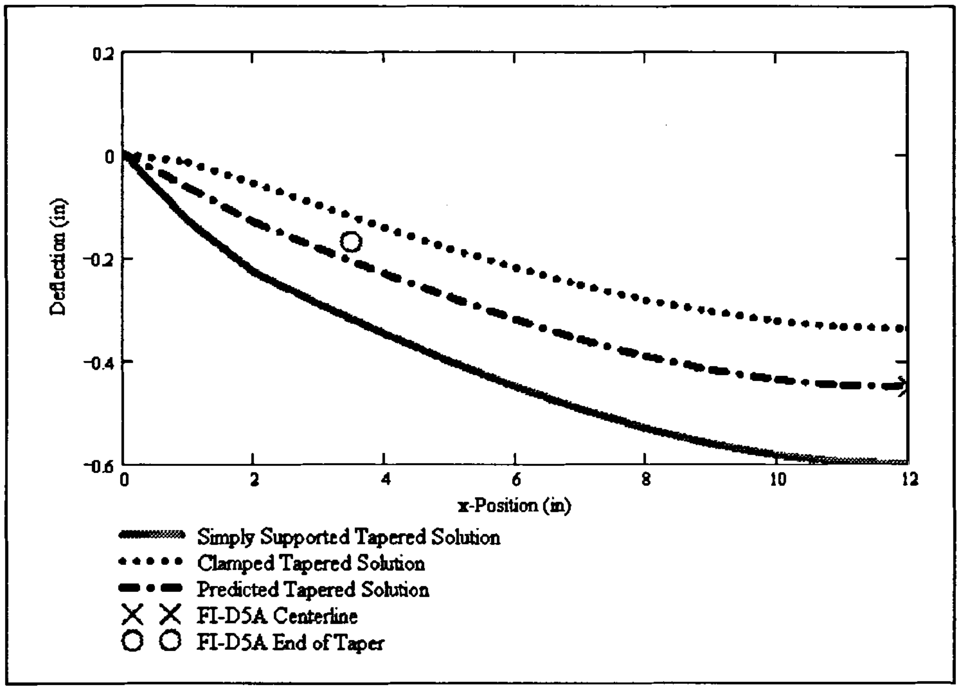

Figure 4.21 – Sandwich Panel FI-D5A Tapered Beam Model

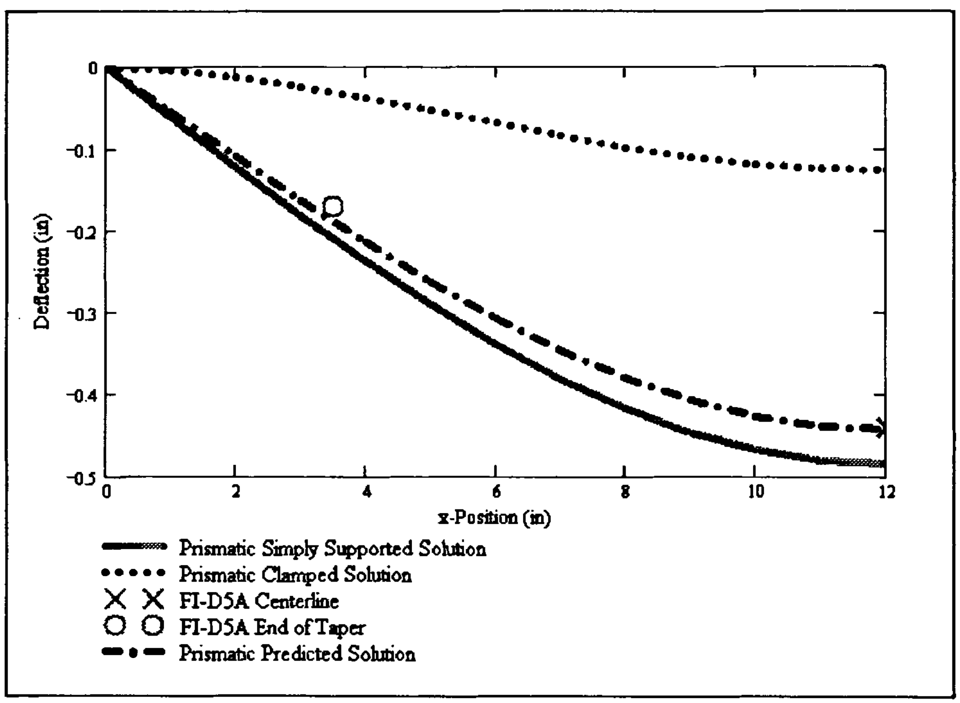

Figure 4.22 – Sandwich Panel FI-D5A Prismatic Beam Model

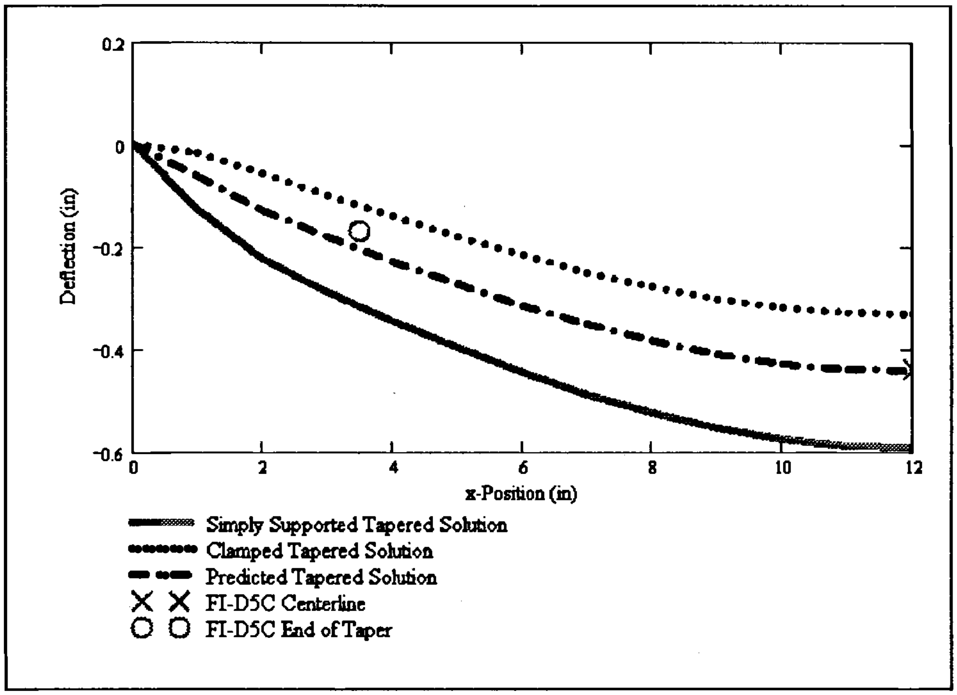

Figure 4.23 – Sandwich Panel FI-D5C Tapered Beam Model

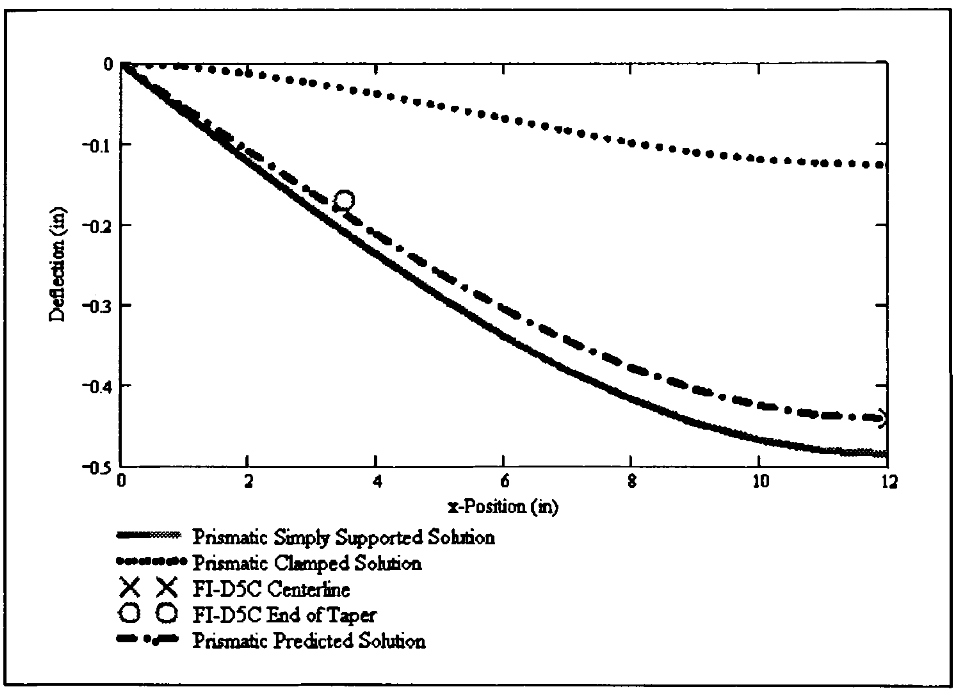

Figure 4.24 – Sandwich Panel FI-D5C Prismatic Beam Model

Table 4.6 – Summary of Sandwich Panel Simplified Beam Theory Models

Panel #	Tapered Joint Stiffness (in*lbf)	% Rigidity (Tapered Solution)	Prismatic Joint Stiffness (in*lbf)	% Rigidity (Prismatic Solution)
FI-D3A	8,500	60.7	11,000	14.3
FI-D3C	8,500	60.7	16,000	20.7
FI-D5A	7,900	56.4	10,000	11.8
FI-D5C	8,000	57.1	10,500	12.4

5. Conclusions and Recommendations

5.1 Conclusions

Hat-stiffened composite laminates and composite sandwich panels were tested in four-point bending at both elevated and room temperatures. Flat composite laminates were also tested in four-point bending at elevated temperature. Of the test articles tested at room and elevated temperatures, all specimens experienced a reduction of stiffness and strength in the elevated temperature environment. The hat-stiffened laminates exhibited an average reduction in stiffness of 21 percent and an average reduction in flexure strength of 43 percent. The composite sandwich panels with the thirty-degree taper exhibited an average reduction in stiffness of 12 percent and an average reduction in flexure strength of 24 percent. The composite sandwich panels with the twenty-degree taper experienced an average reduction in stiffness of 8 percent and an average reduction in strength of 12 percent. Engineers at NASA's Johnson Space Center included a strength knockdown factor of 0.50 into their preliminary design of the X-38 to account for the detrimental effects of an elevated temperature environment to the composite aeroshell. Knockdown factors for strength generated from data gathered in this study range from 0.57 to 0.85. Knockdown factors for stiffness ranged from 0.79 to a high of 0.92. It is noted that all of the data in this study was derived from a limited number of test specimens.

Ease of fabrication and more predictable modes of failure have led the engineers at NASA to utilize the hat-stiffened laminates instead of the sandwich panels. One disadvantage to using the hat-stiffened laminates is the added weight from the

mechanical fasteners. The composite sandwich panels do not have the added weight from the fasteners, but fabrication of sandwich structures tends to be more labor intensive than fastening together two laminates. Great care must be taken to ensure proper bonding between the outer facesheets and the core material. This becomes an even greater concern near tapered edges, because premature failures can be produced near stress concentrations such as these. The more desired mode of failure for composite sandwich structures is a core shear failure. The desired mode of failure for the hat-stiffened laminates is a rupture of the hat-stiffener.

Much was learned in this study about the importance of boundary conditions during testing, especially regarding the flat composite laminates. The measured joint stiffness from the flat laminates increased by 238 percent due to reinforcing each clamped end with two extra threaded steel rods. This was a ramification of the test set-up only. The tests of the sandwich panels with robust end restraints show that the connection response can be conservatively modeled as a simply supported member. The same can be applied to the hat-stiffened laminates. The flat laminate response is partially restrained.

The elevated temperature environment has a deleterious effect on the failure modes, also. Primarily, this involves the failure of an adhesive. The hat-stiffened laminates tested at elevated temperature failed primarily because of the adhesive, which in conjunction with the mechanical fasteners held the stiffener to the laminate, failing and thus causing a dramatic drop in load capacity. The sandwich panels tested at

elevated temperature failed primarily as a result of a debonding occurring between the honeycomb core and the laminate facesheets. This debonding was most likely to start at the beginning of the taper.

5.2 Recommendations

Based on the data from this study, it is clear that proper design of joints is a critical parameter in the X-38 composite aeroshell. To better ascertain the joint stiffness, an independent investigation is recommended. One possible method would be to use a double cantilever beam to study the joint stiffness. Applying loads at both ends of the beam and monitoring the deflection at discrete intervals down the beam's length would provide information about the exact joint response and mitigate the effects of an asymmetric moment going through the boundary. Also, further studies are recommended to investigate the effects of varying the joint geometry and the geometry of the close-out at the connections.

The hat-stiffened laminates tested at elevated temperature failed predominantly as a result of a failure of the adhesive attaching the stiffener to the laminate. Further studies into the type of adhesive would be valuable, as a more durable adhesive might require less mechanical fasteners and hence, save weight.

A study of the dynamic characteristics of the panels at elevated temperature is also recommended. A modal analysis of the panels and joints at room and elevated temperatures would provide valuable information on the effects of the elevated

temperature environment on the frequency response of the material. Parameters measured during such a study could include the effect of temperature on damping constant. An independent verification of the stiffness change would also be measured.

Works Cited

Babero, E.J., "Introduction to Composite Materials Design", (1998), Taylor & Francis

Caccese, V., and Malm, C., (1999), "Flexure, Compression and Tension Testing of Bolted Composite Sandwich Panels in Support of LMMSS X-38 V201 Panel #13 Subcomponent Test Program", Department of Mechanical Engineering, University of Maine, Orono, Maine

Caccese, V., and Gauthier, R., (1998), "Strength and Stability of Composite Sandwich Panels for the NASA X-38", Maine Science and Technology Foundation Grant MSTF 96-48, Department of Mechanical Engineering, University of Maine, Orono, Maine

Gafka, T., and Baccus, R., (2000), "X-38 Aeroshell Panel Design Reference Data Book", Lyndon B. Johnson Space Center, Houston, Texas

Measurements Group, (1992), "Student Manual for Strain Gage Technology", Bulletin 309D

Mewer, R., (2000), "Test Plan for the Design and Construction of a High Temperature Test Chamber"Department of Mechanical Engineering, University of Maine, Orono, Maine

6. Appendix A - Heat Chamber Computer Code (Delphi 3)

6.1 Daqfi32Main Form

This is the main control code for the elevated temperature test chamber. The temperatures from the chamber are evaluated, compared to the control parameters, and the heaters are turned off or on.

```
unit Daqfi32Main;

interface

uses
  Windows, Messages, SysUtils, Classes, Graphics, Controls, Forms, Dialogs,Menus,
Daqcomp, Errex, DAQ32Interface, StdCtrls, HeatChamberC, ExtCtrls, Spin, Buttons,
ToolWin, ComCtrls;

type
  THeatChamberMainFrm = class(TForm)
    MainMenu1: TMainMenu;
    File1: TMenuItem;
    Exit1: TMenuItem;
    N1: TMenuItem;
    PrintSetup1: TMenuItem;
    Print1: TMenuItem;
    N2: TMenuItem;
    SaveAs1: TMenuItem;
    Save1: TMenuItem;
    Open1: TMenuItem;
    New1: TMenuItem;
    Help1: TMenuItem;
    About1: TMenuItem;
    HowtoUseHelp1: TMenuItem;
    SearchforHelpOn1: TMenuItem;
    Contents1: TMenuItem;
    Test1: TMenuItem;
    Test2: TMenuItem;
    Memo1: TMemo;
    DefaultErrBtn: TCheckBox;
    DaqBoardBtn: TCheckBox;
    Setup1: TMenuItem;
    Configure1: TMenuItem;
    N3: TMenuItem;
```

```
DirectAD1: TMenuItem;
StrainAmp1: TMenuItem;
LVDTAtten1: TMenuItem;
N4: TMenuItem;
N5: TMenuItem;
OpenCFGFileDialog: TOpenDialog;
SaveCFGFileDialog: TSaveDialog;
AcquireControl1: TMenuItem;
HeatOn1: TMenuItem;
View1: TMenuItem;
GraphNo11: TMenuItem;
HeatOff1: TMenuItem;
Calibrate1: TMenuItem;
GroupBox1: TGroupBox;
Label1: TLabel;
Label2: TLabel;
Label3: TLabel;
Edit1: TEdit;
Edit2: TEdit;
Edit3: TEdit;
Edit4: TEdit;
Label4: TLabel;
Label5: TLabel;
Edit5: TEdit;
Timer1: TTimer;
Label6: TLabel;
Edit6: TEdit;
Edit7: TEdit;
Edit8: TEdit;
Edit9: TEdit;
Edit10: TEdit;
Label7: TLabel;
Label8: TLabel;
ControlCombo: TComboBox;
Edit11: TEdit;
HeatMsgED: TEdit;
Timer2: TTimer;
Edit12: TEdit;
CheckBox1: TCheckBox;
Label11: TLabel;
DataRateSpin: TSpinEdit;
CoolBar1: TCoolBar;
OutFileBTN: TSpeedButton;
SaveDialog1: TSaveDialog;
FileNameED: TEdit;
```

```
SpeedButton2: TSpeedButton;
Label12: TLabel;
Label13: TLabel;
SpeedButton3: TSpeedButton;
SpeedButton4: TSpeedButton;
Label9: TLabel;
WarmUpBTN: TSpeedButton;
Label10: TLabel;
Label14: TLabel;
Label15: TLabel;
Label16: TLabel;
Edit13: TEdit;
Edit14: TEdit;
LogWarmup: TCheckBox;
procedure Test2Click(Sender: TObject);
procedure DirectAD1Click(Sender: TObject);
procedure Exit1Click(Sender: TObject);
procedure Configure1Click(Sender: TObject);
procedure N4Click(Sender: TObject);
function FileExists(FileName: string): Boolean;
procedure Open1Click(Sender: TObject);
procedure Save1Click(Sender: TObject);
procedure SaveAs1Click(Sender: TObject);
procedure SaveCFGFile(Sender: TObject);
procedure OpenCFGFile(Sender: TObject);
procedure FormCreate(Sender: TObject);
procedure HeatOn1Click(Sender: TObject);
procedure HeatOff1Click(Sender: TObject);
procedure Calibrate1Click(Sender: TObject);

procedure ShowTempData;
procedure ReadTempData;
procedure CheckHeaters;
procedure WarmupOven;
procedure Timer1Timer(Sender: TObject);
procedure ControlComboChange(Sender: TObject);
procedure Timer2Timer(Sender: TObject);
procedure OutFileBTNClick(Sender: TObject);
procedure DataRateSpinChange(Sender: TObject);
procedure SpeedButton3Click(Sender: TObject);
procedure SpeedButton2Click(Sender: TObject);
procedure SpeedButton4Click(Sender: TObject);
procedure WarmUpBTNClick(Sender: TObject);

private
```

```
  { Private declarations }
 public
  { Public declarations }
  CFGFileName  : string;
 end;

var
 HeatChamberMainFrm: THeatChamberMainFrm;

implementation

uses DirectADfrmU, ConfigureFrmU, SelectThermo;


{$R *.DFM}

 function THeatChamberMainFrm.FileExists(FileName: string): Boolean;

{ Boolean function that returns True if the file exists; otherwise,it returns False. Closes
the file if it exists. }

var
 F: file;

begin
 {$I-}
 AssignFile(F, FileName);
 FileMode := 0;  { Set file access to read only }
 Reset(F);
 CloseFile(F);
 {$I+}
 FileExists := (IOResult = 0) and (FileName <> '');
end;  { FileExists }

procedure THeatChamberMainFrm.Test2Click(Sender: TObject);
var
BlockHeaters, HeatLamp : Integer;


begin

 Switch := not Switch;

 BlockHeaters := Heat_Ch2;
 HeatLamp     := Heat_Ch1;
```

```
{Check the Current Temperatures}
if switch then
 begin
  TempControl.TurnHeatOn(HeatLamp);
  showmessage('on');
 end
 else
 begin
  TempControl.TurnHeatOff(HeatLamp);
  showmessage('off');
 end;
end;

procedure THeatChamberMainFrm.DirectAD1Click(Sender: TObject);
begin
 DirectADFirst16frm.ShowModal;
end;

procedure THeatChamberMainFrm.Exit1Click(Sender: TObject);
begin
 Close;
end;

procedure THeatChamberMainFrm.Configure1Click(Sender: TObject);
begin
  ConfigureFrm.ShowModal;
  if ConfigureFrm.CheckingFileName = true then
   ConfigureFrm.ShowModal;
end;

procedure THeatChamberMainFrm.N4Click(Sender: TObject);
begin
 Configure1Click(Sender);
end;

procedure THeatChamberMainFrm.Open1Click(Sender: TObject);
var
result : integer;
begin
   if OpenCFGFileDialog.Execute then
   begin
    CFGFileName :=  OpenCFGFileDialog.FileName;
    if FileExists(CFGFileName) then
     begin
```

```
      result := MessageDlg('Overwrite existing file?', mtConfirmation,
mbYesNoCancel, 0);
     end
     else
      ShowMessage('File OK');;
   end;
end;

procedure THeatChamberMainFrm.Save1Click(Sender: TObject);
begin
  SaveCFGFile(Sender);
end;

procedure THeatChamberMainFrm.SaveAs1Click(Sender: TObject);
var
result : integer;
begin
   if SaveCFGFileDialog.Execute then
   begin
    CFGFileName :=  SaveCFGFileDialog.FileName;
    if FileExists(CFGFileName) then
     begin
      result := MessageDlg('Overwrite existing file?', mtConfirmation,
mbYesNoCancel, 0);
     end
     else
      SaveCFGFile(Sender);
      ShowMessage('File OK');
   end;
end;

procedure THeatChamberMainFrm.SaveCFGFile(Sender: TObject);
begin
  {  }
end;

procedure THeatChamberMainFrm.OpenCFGFile(Sender: TObject);
begin
  {   }
end;


procedure THeatChamberMainFrm.FormCreate(Sender: TObject);
begin
  RampUp          := true;
```

```
 Warmup          := false;
 CanGo           := false;
 TakeThermo      := false;
 LogWarmup.checked :=false;
 ControlCombo.ItemIndex :=4;
 TempFileName    := DefaultTempFileName;
 FileNameEd.Text := TempFileName;
 daqPort         := 0;
 OpenTheDaq;
 CreateTempControlObject(0,1,0);
 CreateScanDataObject(0,0,100000,10000.0,0);
 Overshoot       := Overshoot_val;
 HeatUp_Margin   := HU_Margin_val;
 ControlTemp     := StrToInt(ControlCombo.Text);
 TempFileOpen    := false;
 Timer2.Interval := DataRateSpin.Value*1000;
end;

procedure THeatChamberMainFrm.HeatOn1Click(Sender: TObject);
begin
 TempControl.TurnHeatOn(Heat_All);
{ TempControl.ReadTemp(3); }
end;

procedure THeatChamberMainFrm.HeatOff1Click(Sender: TObject);
begin
 TempControl.TurnHeatOff(Heat_All);
end;

procedure THeatChamberMainFrm.Calibrate1Click(Sender: TObject);
begin
 SelectThermoFRM.Show;
end;

procedure THeatChamberMainFrm.ShowTempData;
begin
 Edit1.Text := FloatToStr(9/5*Temperature[1]+32);
 Edit2.Text := FloatToStr(9/5*Temperature[2]+32);
 Edit3.Text := FloatToStr(9/5*Temperature[3]+32);
 Edit4.Text := FloatToStr(9/5*Temperature[4]+32);
 Edit5.Text := FloatToStr(9/5*Temperature[5]+32);
 Edit6.Text := FloatToStr(Temperature[1]);
 Edit7.Text := FloatToStr(Temperature[2]);
 Edit8.Text := FloatToStr(Temperature[3]);
 Edit9.Text := FloatToStr(Temperature[4]);
```

```
 Edit10.Text := FloatToStr(Temperature[5]);
end;

procedure THeatChamberMainFrm.ReadTempData;
var
i   : integer;
Temp : real;
begin
for i:=1 to 5 do
begin
Temp := TempControl.ReadTemp(i+1,TC_J);
Temperature[i] := TEMP;
end;
end;

procedure THeatChamberMainFrm.Timer1Timer(Sender: TObject);
begin
  {read temp Data}
  {Check to see if we are warmed up???}
  If TakeThermo and CanGo then
  begin
    ReadTempData;
    ShowTempData;
    if not warmup then CheckHeaters else WarmupOven;
  end
  else
    if TakeThermo then
    begin
      ReadTempData;
      ShowTempData;
      HeatMsgEd.Text := 'Reading Temp Only';
  end;
 end;
{**********************************************************
            Check the Current Temperatures
**********************************************************}
procedure THeatChamberMainFrm.CheckHeaters;
var
BlockHeaters, HeatLamp : Integer;
begin
BlockHeaters  := Heat_Ch2;
HeatLamp      := Heat_Ch1;
AirTemp       := 9/5*((Temperature[1]+Temperature[2]+Temperature[3])/3) + 32;
BlockTemp     := 9/5*((Temperature[4]+Temperature[5])/2) + 32;
Edit11.Text   := FloatToStr(AirTemp);
```

```
Edit12.Text   := FloatToStr((Temperature[1]+Temperature[2]+Temperature[3])/3);
Edit13.Text   := FloatToStr(BlockTemp);
Edit14.Text   := FloatToStr((Temperature[4]+Temperature[5])/2);


If WarmUp then RampUp := false else
 begin
 If RampUp and (AirTemp<(ControlTemp + Overshoot)) then
  begin
   TempControl.TurnHeatOn(HeatLamp);
   HeatMsgEd.Text := 'Heat Lamps On';
  end
 else
  begin
    TempControl.TurnHeatOff(Heat_All);
    HeatMsgEd.Text := 'All Heaters Off';
    RampUp := false;
  end;

 If Rampup and (BlockTemp<(ControlTemp - Overshoot)) then
  begin
   TempControl.TurnHeatOn(BlockHeaters);
   HeatMsgEd.Text := 'Block Heaters On';
  end
 else
  begin
   TempControl.TurnHeatOff(BlockHeaters);
   {HeatMsgEd.Text := 'Block Heaters Off';}
  end;


  If not RampUp and (AirTemp<(ControlTemp)) then
   begin
    TempControl.TurnHeatOn(HeatLamp);
    HeatMsgEd.Text := 'Heat Lamps On';
    RampUp := true;
  end
  else
  {begin
    TempControl.TurnHeatOff(Heat_All);
    HeatMsgEd.Text := 'All Heaters Off';
  end; }
 end;
end;
{**********************************************************
```

Warm-Up Oven Routine

```
*******************************************************}
procedure THeatChamberMainFrm.WarmupOven;
var
BlockHeaters, HeatLamp : Integer;

begin
 BlockHeaters := Heat_Ch2;
 HeatLamp     := Heat_Ch1;
 {Check the Current Temperatures}
 AirTemp      := 9/5*((Temperature[1]+Temperature[2]+Temperature[3])/3) + 32;
 BlockTemp    := 9/5*((Temperature[4]+Temperature[5])/2) + 32;
 Edit11.Text  := FloatToStr(AirTemp);
 Edit12.Text  := FloatToStr((Temperature[1]+Temperature[2]+Temperature[3])/3);
 Edit13.Text  := FloatToStr(BlockTemp);
 Edit14.Text  := FloatToStr((Temperature[4]+Temperature[5])/2);

  TempControl.TurnHeatOn(BlockHeaters);

  If ((AirTemp - HeatUp_Margin) > BlockTemp)
  then
  begin
   TempControl.TurnHeatOff(HeatLamp);
   HeatMsgEd.Text := 'Block Heaters On';
  end
  else
  begin
    TempControl.TurnHeatOn(HeatLamp);
    HeatMsgEd.Text := 'All Heaters On';
  end;

 If (AirTemp >= ControlTemp - HeatUp_Margin*2)
 then HeatUP_Margin := Overshoot;

 If BlockTemp >= ControlTemp - 3 then
  begin
    TempControl.TurnHeatOff(Heat_All);
    HeatMsgEd.Text := 'All Heaters Off';
    WarmUp     := false;
    Cango      := true;
    TakeThermo := true;
  end
  else
 If (AirTemp >= ControlTemp + Overshoot) then
  begin
```

```
    TempControl.TurnHeatOff(Heat_All);
    HeatMsgEd.Text := 'All Heaters Off';
    WarmUp     := false;
    Cango      := true;
    TakeThermo := true;
  end;

end;
{*****************************************************}

procedure THeatChamberMainFrm.ControlComboChange(Sender: TObject);
begin
 ControlTemp := StrToInt(ControlCombo.Text);
end;

procedure THeatChamberMainFrm.Timer2Timer(Sender: TObject);
var
F : TextFile;
i : integer;
begin
if CanGo or (LogWarmup.Checked and Warmup) then
begin
 if TempFileOpen then
  begin
   AssignFile(F,TempFileName);
   Append(F);
  end
  else
  begin
   AssignFile(F,TempFileName);
   Rewrite(F);
  end;
 for i:=1 to MaxThermo-1 do
 begin
  Write(F,(9/5*Temperature[i])+32);
 end;
  Writeln(F,(9/5*Temperature[MaxThermo]+32));
  TempFileOpen := true;
  CloseFile(F);
end; {if CanGo}
end;
{*****************************************************}
{              OutFileBTNClick              }
{*****************************************************}
 procedure THeatChamberMainFrm.OutFileBTNClick(Sender: TObject);
```

```
begin
 if SaveDialog1.execute then
 begin
   TempFileName := SaveDialog1.FileName;
   FileNameED.Text :=  TempFileName;
 end;

end;

procedure THeatChamberMainFrm.DataRateSpinChange(Sender: TObject);
begin
  Timer2.Interval := DataRateSpin.Value*1000;
end;

procedure THeatChamberMainFrm.SpeedButton3Click(Sender: TObject);
begin
 if (CanGo=false) then
   TakeThermo := not TakeThermo
 else TakeThermo := true;
end;

procedure THeatChamberMainFrm.SpeedButton2Click(Sender: TObject);
begin
  TempReadError := false;
  TakeThermo    := true;
  CanGo         := true;
  Warmup        := false;
end;

procedure THeatChamberMainFrm.SpeedButton4Click(Sender: TObject);
begin
  TempControl.TurnHeatOff(Heat_All);
  HeatMsgEd.Text := 'All Heaters Off';
  rampUp := false;
  CanGo  := false;
  Warmup := false;
end;
procedure THeatChamberMainFrm.WarmUpBTNClick(Sender: TObject);
begin
  TempReadError := false;
  TakeThermo    := true;
  CanGo         := true;
  Warmup        := true;
end;
```

end.

6.2 HeatChamberC Form

This form declares all of the global variables used in the other forms.

```
unit HeatChamberC;

interface

const
MaxThermo        = 5;
Overshoot_Val     = 1.0;
HU_Margin_Val     = 5.0;
DefaultTempFileName = 'D:\TempChamberData\Test.dat';

var
Temperature    : Array[1..MaxThermo] of real;
ControlTemp    : real;
AirTemp        : real;
BlockTemp      : real;
TempFileOpen   : boolean;
TempFileName   : String;
CanGo          : boolean;
TakeThermo     : boolean;
TempReadError  : boolean;
Overshoot      : real;
HeatUp_Margin  : real;
Rampup         : boolean;
Warmup         : boolean;
LogWarmup      : boolean;
switch         : boolean;


implementation

end.
```

6.3 DAQ32Interface Form

This form reads in temperature data from the Daqbook and outputs to the Daqbook a signal to initialize the heaters.

```
unit DAQ32Interface;

interface

uses SysUtils,Windows, Messages, Dialogs, DaqComp, HeatChamberC;
const
NAVG        = 10;

MaxChannels  = 16;
debug       = true;
Heat_All     = 127;
Heat_Ch1     = 0;
Heat_Ch2     = 1;
Heat_Ch3     = 2;
Heat_Ch4     = 3;
Heat_Ch5     = 4;
Heat_CH6     = 5;
Heat_Ch7     = 6;
Heat_Ch8     = 7;

Cal_Fac      = 0.093;

TCCARD       = 14;

DIO_Write    = 0;
DIO_Read     = 1;

TC_J        = 0;
TC_T        = 1;

var
DaqPort      : word;
err         : DaqError;

procedure CreateTempControlObject(StartChan,EndChan:DWORD; DIOport:byte);
procedure CreateScanDataObject(StartChan,EndChan:DWORD; pts:longint;
                Freq:Single; Ga : byte);
```

```
type
 PScanData = ^TScanData;
 TScanData = array [0..1] of Word;

 PScanTags = ^TScanTags;
 TScanTags = array [0..1] of Byte;

 PRealData = ^TRealData;
 TRealData = array [1..MaxChannels,0..1] of Single;

type
 PReadScanObject = ^TReadScanObject;
 TReadScanObject = object
      NoOfChannels    : Integer;
    StartChannel,
    EndChannel      : DWORD;
    PointsToAcquire : longint;
    Frequency       : single;
    Gain            : byte;
    OneShot         : byte;
    Trigger         : word;
    Level           : byte;
    CalFactor       : array [1..MaxChannels] of Single;
      constructor Init(StartChan,EndChan:DWORD; pts:longint;
               Freq:Single; Ga : byte);
      destructor Done;
    procedure ScanN;
    procedure ScanOnce;
    procedure Sort;

  protected
    TotalData       : longint;
end;


{********************************************************}
{TEMP CONTROL OBJECT INTERFACE **************************}
{********************************************************}
type
 PTempControlObject = ^TTempControlObject;
 TTempControlObject = object
      NoOfChannels    : Integer;
    StartChannel,
    EndChannel      : DWORD;
```

```
    Port            : byte;
    CalFactor       : array [1..MaxChannels] of Single;
    DIOConfig       : byte;
    TC_Card         : byte;
    TC_Channel      : byte;
    TC_SoftChan     : Dword;
    CurrentCounts   : Integer;
    CurrentTemp     : real;
    TC_Type         : integer;


      constructor Init(StartChan,EndChan:DWORD; DIOport:byte);
      destructor  Done;
    procedure  TurnHeatOn (HeatChannel: DWORD);
    procedure  TurnHeatOff(HeatChannel: DWORD);
    function   ReadTemp(ChNo,TType: integer): real;
    function   SelectChannel(TCCard,ChNo: Integer): DWOrd;

  protected
    TotalData       : longint;
end;

var
 ScanData     : PReadScanObject;
 RawData      : PScanData;
 Buffer       : PScanData;
 Tags         : PScanTags;
 RealData     : PRealData;
 TempControl  : PTempControlObject;

implementation


procedure CreateTempControlObject(StartChan,EndChan:DWORD; DIOport:byte);
begin
 New(TempControl, Init(StartChan,EndChan,DIOport));
end;


procedure CreateScanDataObject(StartChan,EndChan:DWORD; pts:longint;
                 Freq:Single; Ga : byte);

begin
 New(ScanData, Init(StartChan,EndChan,pts,Freq,Ga));
end;
```

```
constructor TReadScanObject.Init(StartChan,EndChan:DWORD; pts:longint;
                         Freq:Single; Ga : byte);
begin

 StartChannel    := StartChan;
 EndChannel      := EndChan;
 NoOfChannels    := EndChannel-StartChannel+1;
 PointsToAcquire := pts;
 Frequency       := Freq;
 Gain            := Ga;
 OneShot         := 0;
 Level           := 0;
 Trigger         := 0;
 TotalData       := NoOfChannels*PointsToAcquire;
 GetMem(RawData,  TotalData*SizeOf(Word));
 GetMem(Buffer,   TotalData*SizeOf(Word));
 GetMem(Tags,     TotalData*SizeOf(Byte));
 GetMem(RealData, TotalData*SizeOf(Single)*MaxChannels);
end;

destructor TReadScanObject.Done;
begin
end;

procedure TReadScanObject.ScanN;
var
i: integer;
begin

 daqAdcRdScanN(StartChannel,EndChannel,@RawData^,PointsToAcquire,Trigger,
         OneShot,Level,Frequency,Gain);
 Sort;

end;

procedure TReadScanObject.ScanOnce;
var
i: integer;
begin
 PointsToAcquire :=1;
 daqAdcRdScan(StartChannel,EndChannel,@RawData^,Gain);
 Sort;
end;
```

```
procedure TReadScanObject.Sort;
var
i:integer;
begin
 daqAdcConvertTagged( @RawData^, @buffer^, @tags^,
              NoOfChannels*PointsToAcquire);

 For i:=0 to PointsToAcquire-1 do
 begin
 RealData^[1,i] := (Buffer^[i]-2048)*5/2048;
 if (debug = true) and (i<10) then
 showMessage('scan  ' + inttostr(i) + '   ' + floattostr(RealData^[1,i]));
 end;


end;

{*********************************************************}
{TEMP CONTROL OBJECT METHODS *****************************}
{*********************************************************}

constructor TTempControlObject.Init(StartChan,EndChan:DWORD; DIOport:byte);
var
cfg : byte;
begin
  {Config Port A & B for Output C for Input}
  daqDigGetConf(DIO_Write,DIO_Write,DIO_Read,DIO_Read,cfg);
  DIOConfig      := cfg;
  StartChannel   := StartChan;
  EndChannel     := EndChan;
  NoOfChannels    := EndChannel-StartChannel+1;

  TC_Card        := TCCARD;
  TC_Channel      := 3;
  daqAdcExpToChan(TC_Card,TC_Channel,TC_SoftChan);
 {  showmessage(inttostr(TC_SoftChan));   }

  daqDigGetConf(0,1,0,1,DIOConfig);
  daqDigConf(DdcLocal,DIOConfig);

  if DIOPort =0 then Port := DdPLocalA;
  if DIOPort =1 then Port := DdPLocalB;

  TC_Type:=TC_J;
```

```
{ ShowMessage(Inttostr(DdPLocalA) + '    ' +  Inttostr(Port)); }

 end;

destructor TTempControlObject.Done;
begin
end;

function TTempControlObject.SelectChannel(TCCard,ChNo: integer): DWord;
var
ThisChannel : DWord;
begin
 TC_Card        := TCCard;
 TC_Channel     := ChNo;
{  showmessage('TCCARD  ' + inttostr(TC_CARD)+ '    ' + inttostr(TC_Channel));  }
 daqAdcExpToChan(TC_Card,TC_Channel,ThisChannel);
 Result := ThisChannel;
{  showmessage(inttostr(Result)); }
end;

procedure TTempControlObject.TurnHeatOn(HeatChannel: DWORD);
var
byteval : byte;
error   : DaqError;

begin

  if HeatChannel= Heat_All then
   begin
          byteval :=$FF;
          error := daqDigWtByte(Port,byteval);
   end
   else
   begin
          byteval :=$1;
          error := daqDigWtBit(Port,HeatChannel,byteval);
   end;

 { if Error=DerrNoError then Showmessage('Heat On'); }

end;

procedure TTempControlObject.TurnHeatOff(HeatChannel: DWORD);
var
```

```
byteval : byte;
error   : DaqError;

begin
  if HeatChannel= Heat_All then
   begin
          byteval :=$0;
          error := daqDigWtByte(Port,byteval);
   end
   else
   begin
          byteval :=$0;
          error := daqDigWtBit(Port,HeatChannel,byteval);
   end;
{ if Error=DerrNoError then Showmessage('Heat Off'); }
end;

function TTempControlObject.ReadTemp(ChNo,TType: integer): real;
var
sample    : WORD;
Chans     : array[0..5] of DWord;
gains     : array[0..3] of byte;
nscan     : DWord;
bp        : byte;
Avg       : DWord;
Counts    : array[0..40] of Word;
WTemp     : DWord;
scans     : DWord;
Ntc       : DWord;
i,n       : integer;
TempR     : real;
TGain     : DWord;
DataSum   : longint;
NoError   : boolean;

begin
  nscan    := 4;
  bp       :=1;
  Avg      :=1;
  Scans    :=1;
  Ntc      :=1;
  TGain    := 3;
  TC_Type  := TType;
```

```
DataSum :=0;
for n:=1 to NAVG do
begin
NoError  := not TempReadError;
If NoError then
begin
  TC_SoftChan := SelectChannel(TCCard,0);
  daqAdcRd(TC_SoftChan,sample,TGain);
  TC_Channel := ChNo;

  Chans[0] := TC_SoftChan + 1;
  Chans[1] := TC_SoftChan + 1;
  Chans[2] := TC_SoftChan;
  Chans[3] := TC_SoftChan + TC_Channel;
  gains[0] := dbk19BiCJC;
  gains[2] := dbk19BiCJC;
  case TC_type of
   TC_T :
    begin
     gains[3] := dbk19BiTypeT;
     gains[1] := dbk19BiTypeT;
    end;
   TC_J :
    begin
     gains[3] := dbk19BiTypeJ;
     gains[1] := dbk19BiTypeJ;
    end;
  end; {case}

  daqAdcSetScan(@chans,@gains,nscan);
  daqAdcSetTag(1);
  daqAdcSetClk(100,10);
  daqTCSetup(nscan,2,1,Dbk19TCTypeT,bp,Avg);
  daqAdcSetTrig(DtsSoftware,0,0,0,10);

 {READ COUNT SEPARATELY}
   daqAdcRd(Chans[3],sample,Dbk19BiTypeT);
   sample := sample and $0FF;

   For i:= 0 to nscan-1 do
   begin
   daqAdcRd(Chans[i],sample,Dbk19BiTypeT);
   Counts[i] := Sample;
   end;
```

```
daqCalSetupConvert(nscan,2,1,DcalTypeCJC,Dbk19BiTypeT,16,1,1,@Counts,scans);
   daqTCConvert(@counts,Scans,@WTemp,ntc);

   WTemp :=WTemp and $0FFF;
   DataSum := DataSum + WTemp;
 end; {if NoError}
 end; {For n}
if NoError then
begin
   DataSum := round(DataSum/NAVG);
   CurrentCounts := DataSum;
   TempR := DataSum*Cal_Fac-22.0;
   CurrentTemp := TempR;
   Result := TempR;
end
else
begin
   Result := -99999;
end;

end;

end.
```

6.4 Errex Form

This form prevents the program from terminating is there are any hardware problems, such as a thermocouple not connected to the Daqbook or the Daqbook not turned on. It also notifies the user of the problem encountered.

```
unit Errex;

interface

uses Daqcomp, DAQ32Interface, HeatChamberC;

procedure TestError;
procedure SetTheErrorHandler;
procedure OpenTheDaq;
```

```
// Daqx error handler prototypes
procedure ErrorHandler( errCode: DaqError ); stdcall;

implementation

uses Daqfi32Main, SysUtils, Dialogs;


//**********************************************************************
*
// This unit demonstrates how to initialize a daqx device and
//   how to select and error handler
//
// Functions used:
//   daqOpen( daqName )
//   daqOnline( handle, online )
//   daqSetDefaultErrorHandler( errHandler )
//   daqSetErrorHandler( handle, errHandler )
//   daqAdcSetTrig( handle, triggerSource, rising, level, hysteresis, channel );
//   daqClose( handle )
//
procedure TestError;
var
  online:   longbool;
  drVersion: DWORD;     // Use to receive driver version
  hwVersion: DWORD;     // Use to receive hardware version
begin

  with HeatChamberMainFrm do
  begin
   // Write to status memo control.
   Memo1.Clear;
   Memo1.Lines.Add('Initialization and Error Handling Example'+ Chr(13));

   // Use default error handler (daqx) or user error handler depending on the state
   // of radio buttons 1 and 2.
   if DefaultErrBtn.Checked then
   begin

    //*****************************************************
    //       Driver default error handling selected
    //*****************************************************

    // Initialize using the procedure implemented in Errex.pas.
```

```
  OpenTheDaq;

  // Confirm the device is on line.
  online:= daqOnline;
  if online then
    Memo1.Lines.Add('The device is on line')
  else
    Memo1.Lines.Add('The device is off line');

  // Get the hardware and driver versions
  daqDriverVersion( drVersion );
  daqVersion( hwVersion );
  Memo1.Lines.Add( Format('Driver version: %d', [drVersion]) );
  Memo1.Lines.Add( Format('Hardware version is %d', [hwVersion]) );

  // Cause intentional error (non device-specific).
  Memo1.Lines.Add('Causing intentional Invalid Channel error...');
  daqAdcSetMux( 511, 0, DgainX1);
end
else
  //********************************************************
  //      User-defined error handling selected
  //********************************************************
begin

  // Set the user-defined error handler.
  daqSetErrHandler( addr(ErrorHandler) );

  // Initialize using the procedure implemented in Errex.pas.
  OpenTheDaq;

  // Confirm the device is on line.
  online:= daqOnline;
  if online then
    Memo1.Lines.Add('The device is not on line')
  else
    Memo1.Lines.Add('The device is on line');

  // Get the hardware and driver versions
  daqDriverVersion( drVersion );
  daqVersion( hwVersion );
  Memo1.Lines.Add( Format('Driver version: %d', [drVersion]) );
  Memo1.Lines.Add( Format('Hardware version is %d', [hwVersion]) );

  // Once a user-specified error handler has been set, the driver default error
```

```
    // handler cannot be used.  Disable the "Default Error Handler" radio button.
    DefaultErrBtn.Enabled:= False;

    // Cause an intentional error (non device-specific).
    Memo1.Lines.Add('Causing intentional Invalid Channel error...');
    daqAdcSetMux( 511, 0, DgainX1);
   end;

  // Close the device.
  daqClose;
  Memo1.Lines.Add( 'Device Closed' );
 end;

end;

//*******************************************************************
*************
// Error handler for daq errors.
//
procedure ErrorHandler( errCode: DaqError ); stdcall;
var
 msg: string;
begin
 if ord(errCode)=39 then
 begin
  ShowMessage('ERROR - Thermocouple Malfunction');
  TempReadError := True;
 end
 else
 begin
  msg:= 'Message from procedure ErrorHandler' + Chr(13) + Chr(10);
  msg:= msg + 'DaqComp error number ' + IntToStr(ord(errCode)) + ' occurred.';
  MessageDlg(msg , mtError, [mbOk], 0);
 end;

end;


//*******************************************************************
*************
// Procedure to set the error handler. Complains and stops if unable.
//
procedure SetTheErrorHandler;
begin
 if (daqSetErrHandler(addr(ErrorHandler)) <> DerrNoError ) then
```

```
 begin
   MessageDlg('Unable to set default error handler. Exiting program', mtError,
[mbOk], 0);
   Halt;
 end;
 HeatChamberMainFrm.Memo1.Lines.Add( 'Error handler set to procedure
"ErrorHandler"');
 // Disable the choice for the driver built-in error handler since it isn't available
 // after setting another handler until the DAQX.DLL is reloaded.
 HeatChamberMainFrm.DefaultErrBtn.Enabled:= False;

end;

//**********************************************************************
*************
// Procedure to open a DaqBook or DaqBoard depending on which is selected on
Form1.
//
procedure OpenTheDaq;
var
  err:    DaqError;
begin
 with HeatChamberMainFrm do
 begin
    daqSetErrHandler( addr(ErrorHandler) );
    err:= daqInit( daqPort, 10 );

    // Quit the program if the device could not be opened
    If err <> DerrNoError then Halt;

    Memo1.Lines.Add( 'DaqBook opened successfully' );
  end; // with Form1 do
end;
end.
```

7. Appendix B - MathCAD Worksheets

7.1 Flat Laminate Worksheet

Input Variables:

$b_s := 6.75$ $h := .25$ $J := 884.72$

$P := \frac{-1160}{2}$ $I := \frac{b_s \cdot h^3}{12}$

$L := 26$ $a := 10.5$ $b := a$

$E := 2.458 \times 10^7$ $\delta_{totalactual} := 3.1$

$x := 0, 1 .. L$

Point Loading Case:

$$\delta_{ss}(x) := \begin{cases} \frac{P \cdot x}{6 \cdot E \cdot I} \cdot \left(3 \cdot L \cdot a - 3 \cdot a^2 - x^2\right) & \text{if } x \le a \\ \frac{P \cdot a}{6 \cdot E \cdot I} \cdot \left(3 \cdot L \cdot x - 3 \cdot x^2 - a^2\right) & \text{if } [x \le (L - a)] \cdot (x \ge a) \\ \frac{-P \cdot (x - L)}{6 \cdot E \cdot I} \cdot \left[3 \cdot L \cdot a - 3 \cdot a^2 - (x - L)^2\right] & \text{if } x \ge (L - a) \end{cases}$$

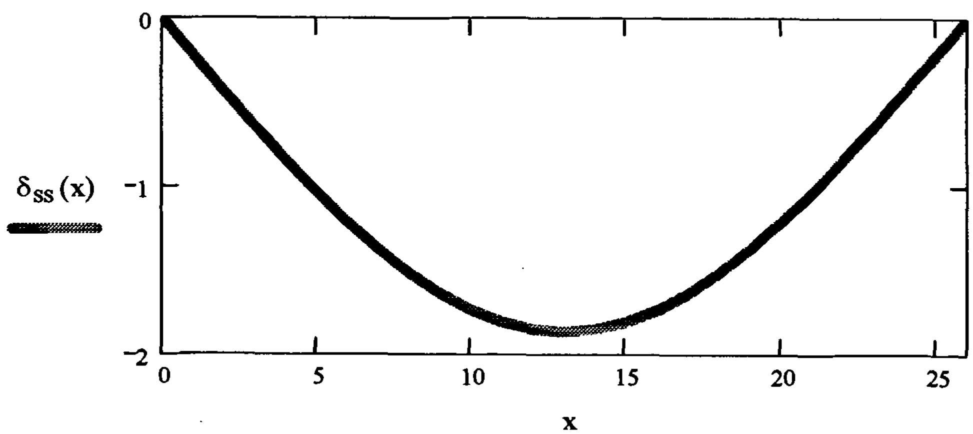

$$\theta_{ss}(x) := \begin{cases} \dfrac{P}{2\cdot E\cdot I}\cdot\left(L\cdot a - a^2 - x^2\right) & \text{if } x \le a \\ \dfrac{P\cdot a}{2\cdot E\cdot I}\cdot(L - 2\cdot x) & \text{if } [x \le (L-a)]\cdot(x \ge a) \\ \dfrac{-P}{2\cdot E\cdot I}\cdot\left[L\cdot a - a^2 - (x-L)^2\right] & \text{if } x \ge (L-a) \end{cases}$$

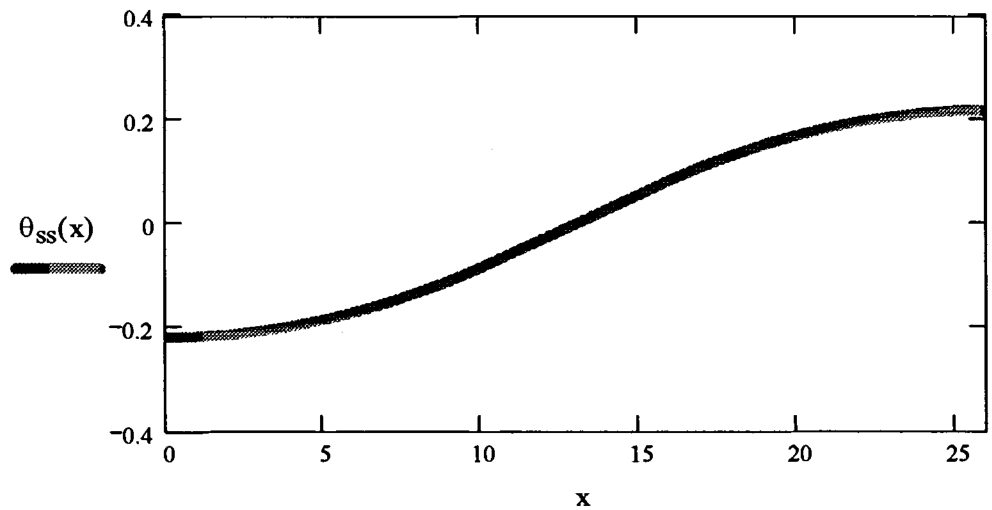

$$\theta_{ssmax} := \frac{P\cdot a\cdot(L-1)}{2\cdot E\cdot I}$$

$$\theta_{ssmax} = -0.352$$

End Moment Loading Case:

$$\theta_{endtotal} := \frac{P\cdot a\cdot(L-a)}{2\cdot E\cdot I + J\cdot L}$$

$$M_0 := J\cdot\theta_{endtotal}$$

$$M_0 = -183.516$$

$$\theta_{endtotal} := \frac{[P \cdot a \cdot (L - a)] + M_0 \cdot L}{2 \cdot E \cdot I}$$

$$\theta_{endtotal} = -0.23$$

$$\delta_m(x) := \frac{-M_0 \cdot x}{2 \cdot E \cdot I} \cdot (L - x)$$

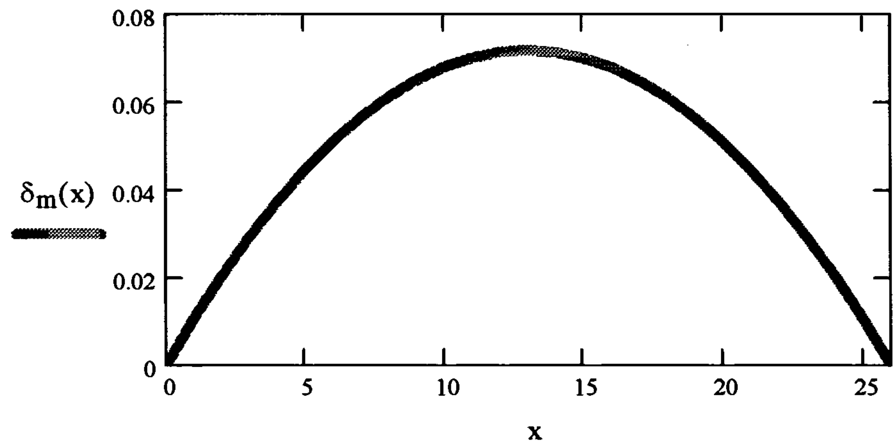

$$\theta_m(x) := \frac{-M_0}{2 \cdot E \cdot I} \cdot (L - 2 \cdot x)$$

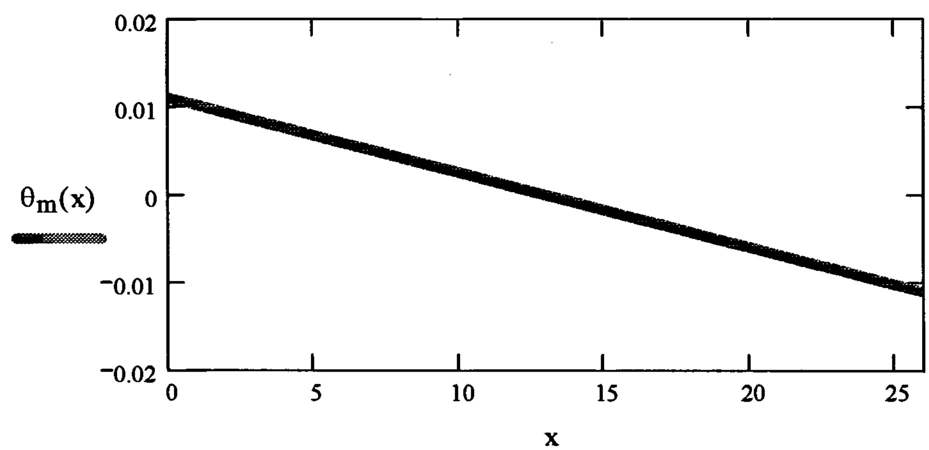

Clamped Case:

$$\delta_{ss}(x) := \begin{cases} \dfrac{P \cdot x}{6 \cdot E \cdot I} \cdot \left(3 \cdot L \cdot a - 3 \cdot a^2 - x^2\right) & \text{if } x \le a \\ \dfrac{P \cdot a}{6 \cdot E \cdot I} \cdot \left(3 \cdot L \cdot x - 3 \cdot x^2 - a^2\right) & \text{if } [x \le (L - a)] \cdot (x \ge a) \\ \dfrac{-P \cdot (x - L)}{6 \cdot E \cdot I} \cdot \left[3 \cdot L \cdot a - 3 \cdot a^2 - (x - L)^2\right] & \text{if } x \ge (L - a) \end{cases}$$

$$M_{clamped} := \frac{-P \cdot a \cdot (L - a)}{L}$$

$$\delta_{m1}(x) := \frac{M_{clamped} \cdot x}{2 \cdot E \cdot I} \cdot (L - x)$$

$$\delta_{clamped}(x) := \delta_{ss}(x) + \delta_{m1}(x)$$

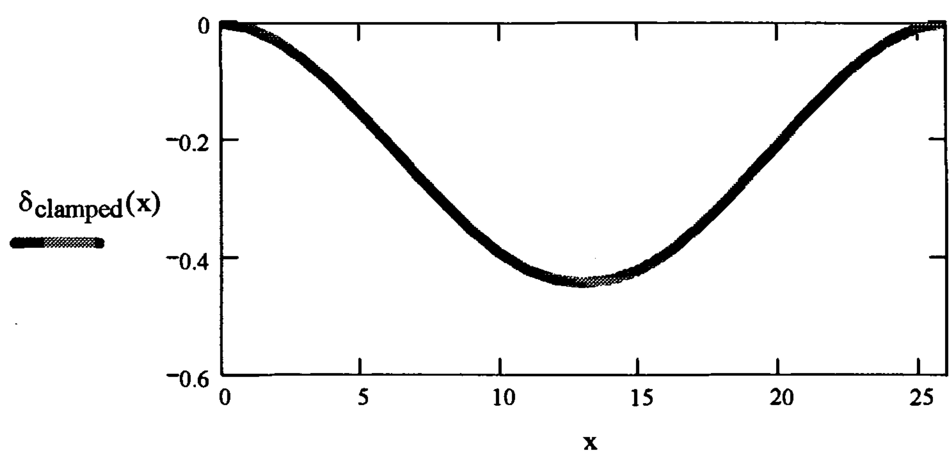

Combined Solution:

$$\delta_{maxtotal} := \delta_{ss}\left(\frac{L}{2}\right) + \delta_{m}\left(\frac{L}{2}\right)$$

centerlinex := 13·in quaterlengthx := 6.5·in

centerliney := −1.80·in quaterlengthy := −1.26·in

$$\delta_{maxtotal} = -70.562 \frac{1}{m} \text{in}$$

$$\theta_{endtotal} \cdot \left(\frac{180}{\pi}\right) = -13.15$$

$\delta_{combined}(x) := \delta_{ss}(x) + \delta_m(x)\ \theta_{combined}(x) := \theta_{ss}(x) + \theta_m(x)$

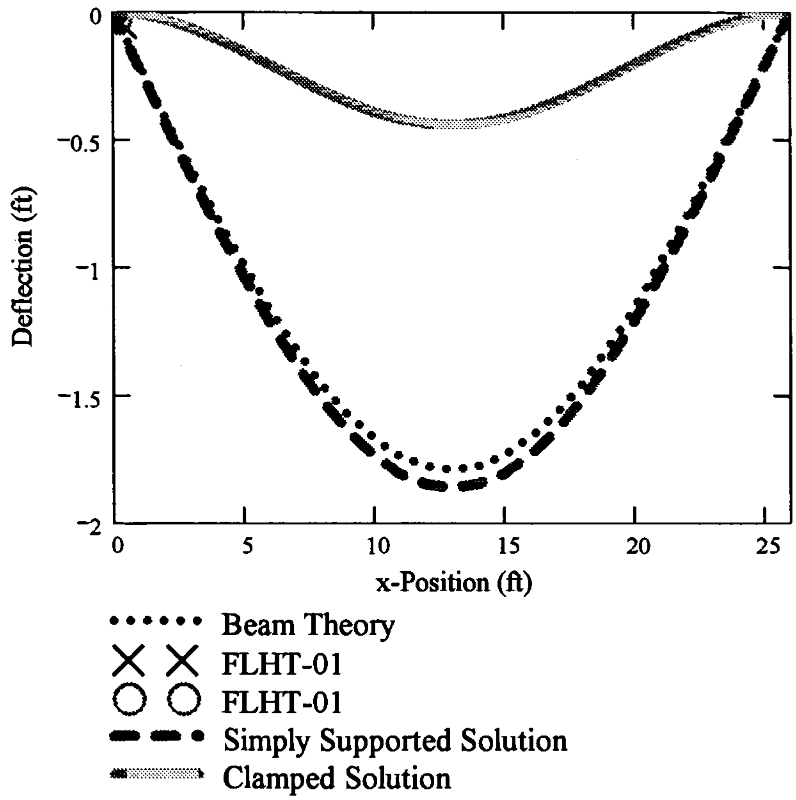

Measuring the relative stiffness of the beam:

$$\frac{\delta_{clamped}\left(\frac{L}{2}\right)}{\delta_{combined}\left(\frac{L}{2}\right)} = 0.248 \qquad \frac{\delta_{ss}\left(\frac{L}{2}\right)}{\delta_{combined}\left(\frac{L}{2}\right)} = 1.04$$

7.2 Hat-Stiffened Laminate Worksheet

Input Variables:

$P := \frac{-5268}{2}$

$L := 26$

$a := 10.5$ $\quad b := a$

$E_{lam} := 8.544 \cdot 10^6$ $\quad L_1 := 2.50$ $\quad L_2 := 4.50$ $\quad x := 0, 1 .. L$

$E_{stiffener} := 8.544 \cdot 10^6$

$J := 11500$ $\quad h := 0.25$ $\quad J_1 := 18750$

Transformed laminate cross-section:

$b_{lam} := 6.75$

$b_{lamtransformed} := b_{lam} \cdot \left(\frac{E_{lam}}{E_{stiffener}} \right)$ $\quad b_{lamtransformed} = 6.75$

$I_{lamtransformed} := \frac{b_{lamtransformed} \cdot h^3}{12}$

$I_{lamtransformed} = 8.789 \times 10^{-3}$ $\quad I_{stiffened} := 0.11005$ $\quad I_2 := 0.020224$

$$M_{ss}(x) := \begin{vmatrix} -P \cdot x \ \text{ if } x \le a \\ -P \cdot a \ \text{ if } [x \le (L - a)] \cdot (x \ge a) \\ P \cdot x - P \cdot L \ \text{ if } x \ge (L - a) \end{vmatrix}$$

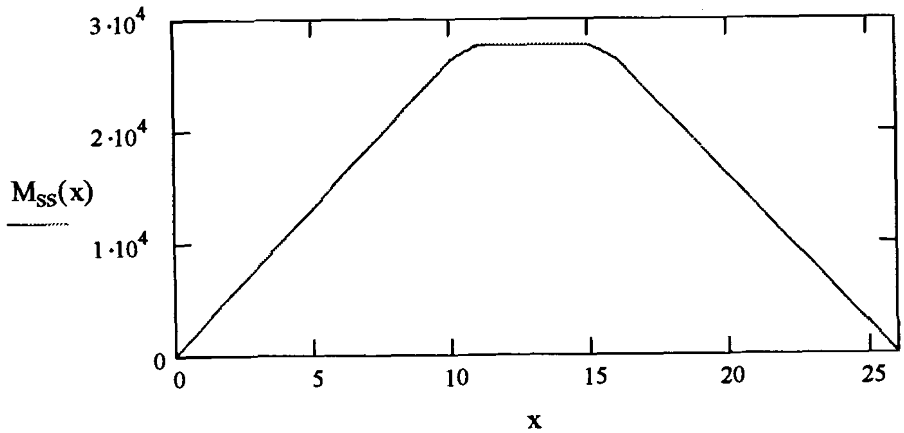

Integration Constants for Point Loading Solution:

$$C_2 := 0$$

$$C_7 := \frac{-P \cdot a \cdot L}{2 \cdot E_{stiffener} \cdot I_{stiffened}}$$

$$C_5 := \frac{P \cdot a^2 - P \cdot a \cdot L}{2 \cdot E_{stiffener} \cdot I_{stiffened}}$$

$$C_3 := \frac{P \cdot a^2 - P \cdot a \cdot L + P \cdot L_2^{\,2}}{2 \cdot E_{stiffener} \cdot I_{stiffened}} - \frac{P \cdot L_2^{\,2}}{2 \cdot E_{stiffener} \cdot I_2}$$

$$C_1 := \left(\frac{P \cdot L_1^{\,2}}{2 \cdot E_{stiffener} \cdot I_2} - \frac{P \cdot L_1^{\,2}}{2 \cdot E_{stiffener} \cdot I_{lamtransformed}} + \frac{P \cdot a^2 - P \cdot a \cdot L + P \cdot L_2^{\,2}}{2 \cdot E_{stiffener} \cdot I_{stiffened}} \right) \cdot\cdot$$
$$+ \frac{-P \cdot L_2^{\,2}}{2 \cdot E_{stiffener} \cdot I_2}$$

$$C_4 := \frac{P \cdot L_1^3}{6 \cdot E_{stiffener} \cdot I_{lamtransformed}} + L_1 \cdot \left(\frac{-P \cdot L_1^2}{2 \cdot E_{stiffener} \cdot I_{lamtransformed}} \ldots \\ + \frac{P \cdot a^2 - P \cdot a \cdot L + P \cdot L_2^2}{2 \cdot E_{stiffener} \cdot I_{stiffened}} \ldots \\ + \frac{P \cdot L_1^2}{2 \cdot E_{stiffener} \cdot I_2} - \frac{P \cdot L_2^2}{2 \cdot E_{stiffener} \cdot I_2} \right) \ldots$$

$$+ \frac{-P \cdot L_1^3}{6 \cdot E_{stiffener} \cdot I_2} - L_1 \cdot \left(\frac{P \cdot a^2 - P \cdot a \cdot L + P \cdot L_2^2}{2 \cdot E_{stiffener} \cdot I_{stiffened}} - \frac{P \cdot L_2^2}{2 \cdot E_{stiffener} \cdot I_2} \right)$$

$$C_6 := \frac{P \cdot L_2^3}{6 \cdot E_{stiffener} \cdot I_2} + C_3 \cdot L_2 + C_4 - \frac{P \cdot L_2^3}{6 \cdot E_{stiffener} \cdot I_{stiffened}} - C_5 \cdot L_2$$

$$C_8 := \frac{P \cdot a^3}{6 \cdot E_{stiffener} \cdot I_{stiffened}} + C_5 \cdot a + C_6 - \frac{P \cdot a^3}{2 \cdot E_{stiffener} \cdot I_{stiffened}} - C_7 \cdot a$$

$C_1 = 0.416$ $C_5 = 0.228$

$C_2 = 0$ $C_6 = 0.481$

$C_3 = 0.354$ $C_7 = 0.382$

$C_4 = 0.103$ $C_8 = -0.059$

$$\delta_{1ss}(x) := \frac{P \cdot x^3}{6 \cdot E_{stiffener} \cdot I_{lamtransformed}} + C_1 \cdot x + C_2$$

$$\delta_{2ss}(x) := \frac{P \cdot x^3}{6 \cdot E_{stiffener} \cdot I_2} + C_3 \cdot x + C_4$$

$$\delta_{3ss}(x) := \frac{P \cdot x^3}{6 \cdot E_{stiffener} \cdot I_{stiffened}} + C_5 \cdot x + C_6$$

$$\delta_{4ss}(x) := \frac{P \cdot a \cdot x^2}{2 \cdot E_{stiffener} \cdot I_{stiffened}} + C_7 \cdot x + C_8$$

$$\delta_{ss}(x) := \left| \begin{array}{ll} -\delta_{1ss}(x) & \text{if } (x < L_1) \\ -\delta_{2ss}(x) & \text{if } (x \geq L_1) \cdot (x < L_2) \\ -\delta_{3ss}(x) & \text{if } (x \geq L_2) \cdot (x < a) \\ -\delta_{4ss}(x) & \text{if } (x \geq a) \end{array} \right.$$

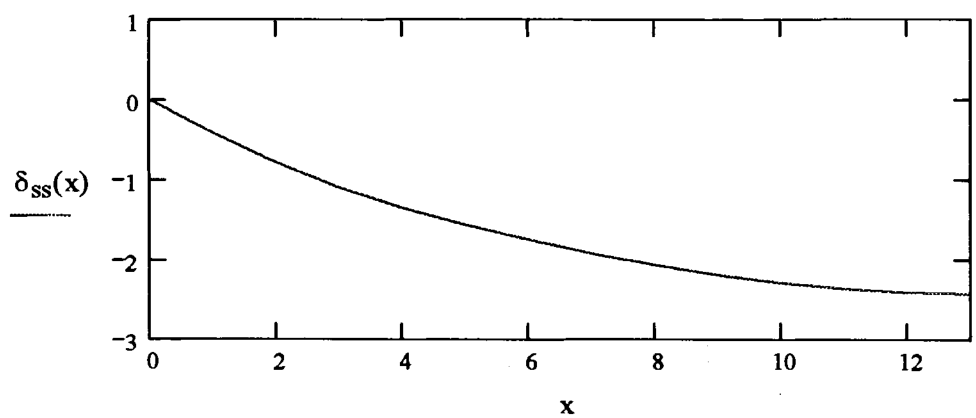

$$Q(x) := \frac{d}{dx}\delta_{ss}(x)$$

$$Q(0) = -0.416$$

$$\theta_{endtotal} := Q(0)$$

$$M_0 := -J \cdot \theta_{endtotal}$$

$$M_0 = 4.783 \times 10^3$$

Integration Constants for End Moment Loading Solution:

$$C_{2m} := 0$$

$$C_{5m} := \frac{-M_0 \cdot L}{2 \cdot E_{stiffener} \cdot I_{stiffened}}$$

$$C_{3m} := \frac{M_0 \cdot L_2}{E_{stiffener} \cdot I_{stiffened}} - \frac{M_0 \cdot L_2}{E_{stiffener} \cdot I_2} - \frac{M_0 \cdot L}{2 \cdot E_{stiffener} \cdot I_{stiffened}}$$

$$C_{1m} := \frac{M_0 \cdot L_1}{E_{stiffener} \cdot I_2} + C_{3m} - \frac{M_0 \cdot L_1}{E_{stiffener} \cdot I_{lamtransformed}}$$

$$C_{4m} := \frac{M_0 \cdot L_1^{\,2}}{2 \cdot E_{stiffener} \cdot I_{lamtransformed}} + C_{1m} \cdot L_1 - \frac{M_0 \cdot L_1^{\,2}}{2 \cdot E_{stiffener} \cdot I_2} - C_{3m} \cdot L_1$$

$$C_{6m} := \frac{M_0 \cdot L_2^{\,2}}{2 \cdot E_{stiffener} \cdot I_2} + C_{3m} \cdot L_2 + C_{4m} - \frac{M_0 \cdot L_2^{\,2}}{2 \cdot E_{stiffener} \cdot I_{stiffened}} - C_{5m} \cdot L_2$$

$$\delta_{1m}(x) := \frac{M_0 \cdot x^2}{2 \cdot E_{stiffener} \cdot I_{lamtransformed}} + C_{1m} \cdot x + C_{2m}$$

$$\delta_{2m}(x) := \frac{M_0 \cdot x^2}{2 \cdot E_{stiffener} \cdot I_2} + C_{3m} \cdot x + C_{4m}$$

$$\delta_{3m}(x) := \frac{M_0 \cdot x^2}{2 \cdot E_{stiffener} \cdot I_{stiffened}} + C_{5m} \cdot x + C_{6m}$$

$$\delta_m(x) := \left| \begin{array}{l} -\delta_{1m}(x) \ \text{ if } \ x < L_1 \\ -\delta_{2m}(x) \ \text{ if } \ (x \geq L_1) \cdot (x < L_2) \\ -\delta_{3m}(x) \ \text{ if } \ x \geq L_2 \end{array} \right.$$

$$\delta_{total}(x) := \delta_{ss}(x) + \delta_m(x)$$

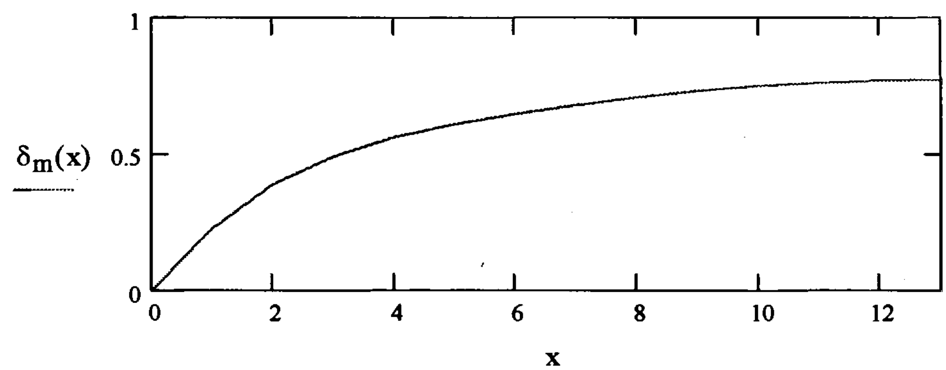

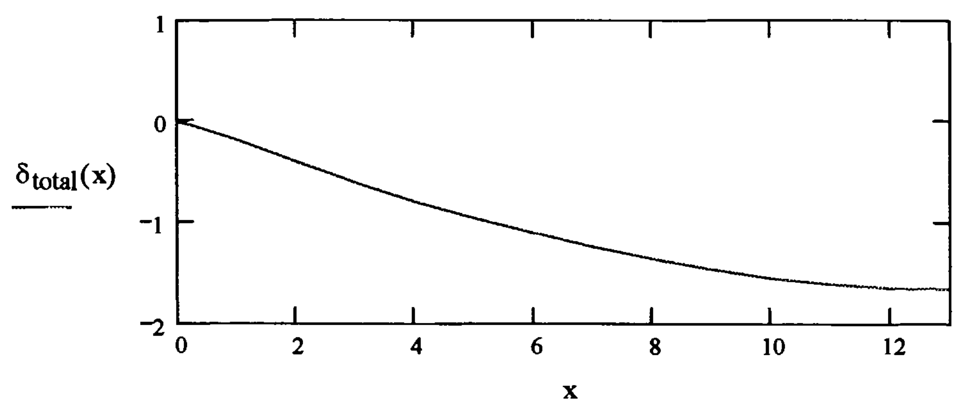

$$\delta_{sspris}(x) := \begin{cases} \dfrac{P \cdot x}{6 \cdot E_{stiffener} \cdot I_{stiffened}} \cdot \left(3 \cdot L \cdot a - 3 \cdot a^2 - x^2\right) & \text{if } x \le a \\ \dfrac{P \cdot a}{6 \cdot E_{stiffener} \cdot I_{stiffened}} \cdot \left(3 \cdot L \cdot x - 3 \cdot x^2 - a^2\right) & \text{if } [x \le (L - a)] \cdot (x \ge a \\ \dfrac{-P \cdot (x - L)}{6 \cdot E_{stiffener} \cdot I_{stiffened}} \cdot \left[3 \cdot L \cdot a - 3 \cdot a^2 - (x - L)^2\right] & \text{if } x \ge (L - a) \end{cases}$$

$$\theta_{pris}(x) := \frac{d}{dx}\delta_{sspris}(x)$$

$$M_{pris} := J \cdot \theta_{pris}(0)$$

$$\theta_{pris}(0) = -0.228$$

$$\delta_{mpris}(x) := \frac{-M_{pris} \cdot x}{2 \cdot E_{stiffener} \cdot I_{stiffened}} \cdot (L - x)$$

$$\theta_{endtotal} = -0.416$$

$$\delta_{mpris}(13) = 0.236$$

$$\delta_{totalpris}(x) := \delta_{sspris}(x) + \delta_{mpris}(x)$$

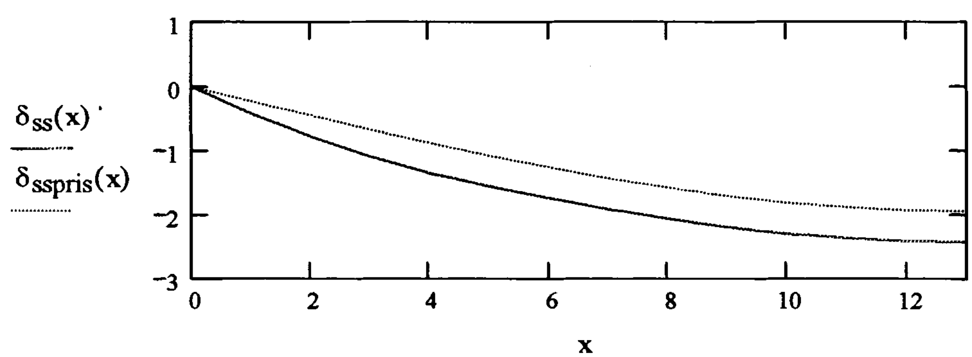

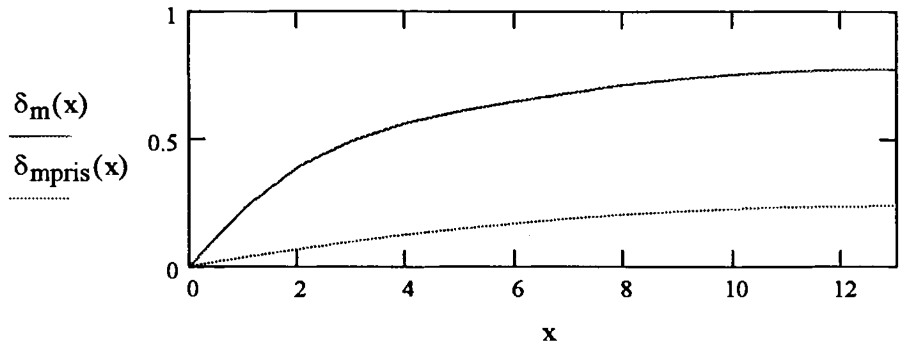

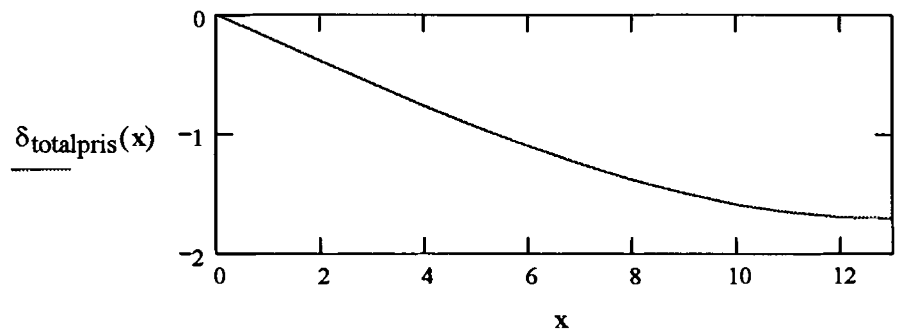

$$M_l := J_l \cdot \theta_{endtotal}$$

$$C_{2ml} := 0$$

$$C_{5ml} := \frac{-M_l \cdot L}{2 \cdot E_{stiffener} \cdot I_{stiffened}}$$

$$C_{3ml} := \frac{M_l \cdot L_2}{E_{stiffener} \cdot I_{stiffened}} - \frac{M_l \cdot L_2}{E_{stiffener} \cdot I_2} - \frac{M_l \cdot L}{2 \cdot E_{stiffener} \cdot I_{stiffened}}$$

$$C_{1ml} := \frac{M_l \cdot L_1}{E_{stiffener} \cdot I_2} + C_{3ml} - \frac{M_l \cdot L_1}{E_{stiffener} \cdot I_{lamtransformed}}$$

$$C_{4ml} := \frac{M_l \cdot L_1^{\,2}}{2 \cdot E_{stiffener} \cdot I_{lamtransformed}} + C_{1ml} \cdot L_1 - \frac{M_l \cdot L_1^{\,2}}{2 \cdot E_{stiffener} \cdot I_2} - C_{3ml} \cdot L_1$$

$$C_{6m1} := \frac{M_1 \cdot L_2^{\,2}}{2 \cdot E_{stiffener} \cdot I_2} + C_{3m1} \cdot L_2 + C_{4m1} - \frac{M_1 \cdot L_2^{\,2}}{2 \cdot E_{stiffener} \cdot I_{stiffened}} - C_{5m1} \cdot L_2$$

$$\delta_{1m1}(x) := \frac{M_1 \cdot x^2}{2 \cdot E_{stiffener} \cdot I_{lamtransformed}} + C_{1m1} \cdot x + C_{2m1}$$

$$\delta_{2m1}(x) := \frac{M_1 \cdot x^2}{2 \cdot E_{stiffener} \cdot I_2} + C_{3m1} \cdot x + C_{4m1}$$

$$\delta_{3m1}(x) := \frac{M_1 \cdot x^2}{2 \cdot E_{stiffener} \cdot I_{stiffened}} + C_{5m1} \cdot x + C_{6m1}$$

$$\delta_{m1}(x) := \left| \begin{array}{l} -\delta_{1m1}(x) \text{ if } x < L_1 \\ -\delta_{2m1}(x) \text{ if } (x \ge L_1) \cdot (x < L_2) \\ -\delta_{3m1}(x) \text{ if } x \ge L_2 \end{array} \right.$$

$$\delta_{clamped}(x) := -\delta_{m1}(x) + \delta_{ss}(x)$$

$\text{centerx} := 13$

$\text{centery} := -1.64$

$\text{quarterx} := 6.5$

$\text{quartery} := -1.07$

$\delta_{totalpris}(13) = -1.709$

$\delta_{total}(13) = -1.655$

$\delta_{total}(6.5) = -1.171$

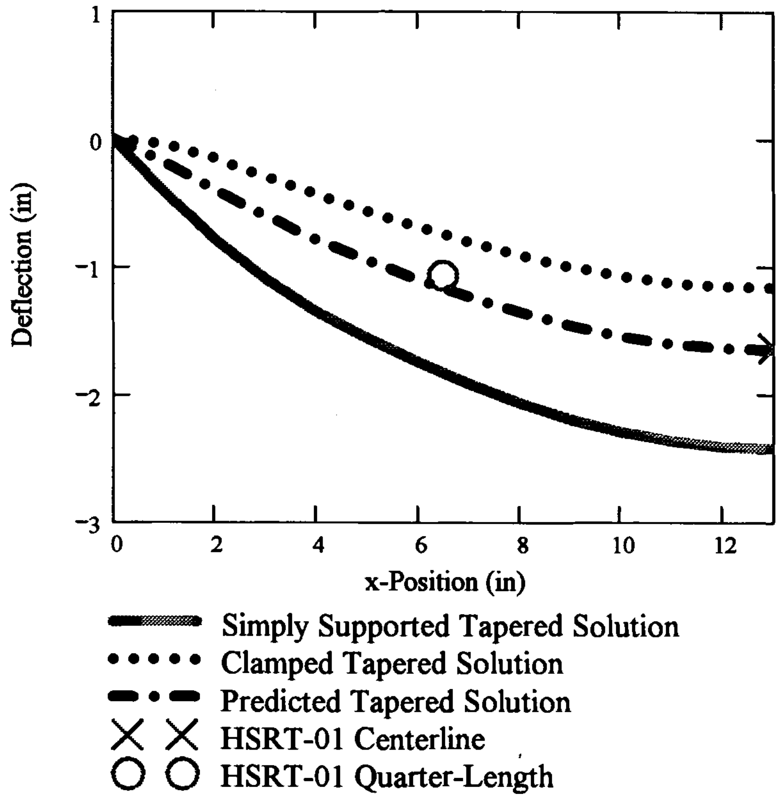

$$\%R := \frac{\delta_{ss}\left(\frac{L}{2}\right) - \delta_{total}\left(\frac{L}{2}\right)}{\delta_{ss}\left(\frac{L}{2}\right) - \delta_{clamped}\left(\frac{L}{2}\right)}$$

$\%R = 0.613$

7.3 Composite Sandwich Worksheet

Input Variables:

$P := \frac{-1881}{2}$

$L := 24$ $\quad L_1 := 2.2$ $\quad L_2 := 3.499$ $\quad a := 9.5$ $\quad A := 0.75 \cdot 4.5$

$I_1 := 0.003993$ $\quad I_2 := 0.059216$ $\quad I_3 := 0.124386$

$E := 8.442 \cdot 10^6$ $\quad G := 25 \cdot 10^3$ $\quad J := 8000$ $\quad J_1 := 14000$

$x := 0, 1 .. L$

Integration Constants for Point Loading Solution:

$C_2 := 0$

$$C_7 := \frac{-P \cdot a \cdot L}{2 \cdot E \cdot I_3}$$

$$C_5 := C_7 + \frac{P \cdot a^2}{E \cdot I_3} - \frac{P \cdot a^2}{2 \cdot E \cdot I_3} - \frac{P}{G \cdot A}$$

$$C_3 := C_5 + \frac{P \cdot L_2^2}{2 \cdot E \cdot I_3} + \frac{P}{G \cdot A} - \frac{P \cdot L_2^2}{2 \cdot E \cdot I_2}$$

$$C_1 := C_3 + \frac{P \cdot L_1^2}{2 \cdot E \cdot I_2} - \frac{P \cdot L_1^2}{2 \cdot E \cdot I_1}$$

$$C_4 := C_1 \cdot L_1 + \frac{P \cdot L_1^{\,3}}{6 \cdot E \cdot I_1} - C_3 \cdot L_1 - \frac{P \cdot L_1^{\,3}}{6 \cdot E \cdot I_2}$$

$$C_6 := C_4 + C_3 \cdot L_2 + \frac{P \cdot L_2^{\,3}}{6 \cdot E \cdot I_2} - \frac{P \cdot L_2^{\,3}}{6 \cdot E \cdot I_3} - \frac{P \cdot L_2}{G \cdot A} - C_5 \cdot L_2$$

$$C_8 := C_6 + C_5 \cdot a + \frac{P \cdot a}{G \cdot A} + \frac{P \cdot a^3}{6 \cdot E \cdot I_3} - \frac{P \cdot a^3}{2 \cdot E \cdot I_3} - C_7 \cdot a$$

$C_1 = 0.131$	$C_5 = 0.073$
$C_2 = 0$	$C_6 = 0.106$
$C_3 = 0.068$	$C_7 = 0.102$
$C_4 = 0.092$	$C_8 = -0.022$

$$\delta_{1ss}(x) := \frac{P \cdot x^3}{6 \cdot E \cdot I_1} + C_1 \cdot x$$

$$\delta_{2ss}(x) := \frac{P \cdot x^3}{6 \cdot E \cdot I_2} + C_3 \cdot x + C_4$$

$$\delta_{3ss}(x) := \frac{P \cdot x^3}{6 \cdot E \cdot I_3} + \frac{P \cdot x}{G \cdot A} + C_5 \cdot x + C_6$$

$$\delta_{4ss}(x) := \frac{P \cdot a \cdot x^2}{2 \cdot E \cdot I_3} + C_7 \cdot x + C_8$$

$$\delta_{ss}(x) := \begin{vmatrix} -\delta_{1ss}(x) \text{ if } (x < L_1) \\ -\delta_{2ss}(x) \text{ if } (x \geq L_1) \cdot (x < L_2) \\ -\delta_{3ss}(x) \text{ if } (x \geq L_2) \cdot (x < a) \\ -\delta_{4ss}(x) \text{ if } (x \geq a) \end{vmatrix}$$

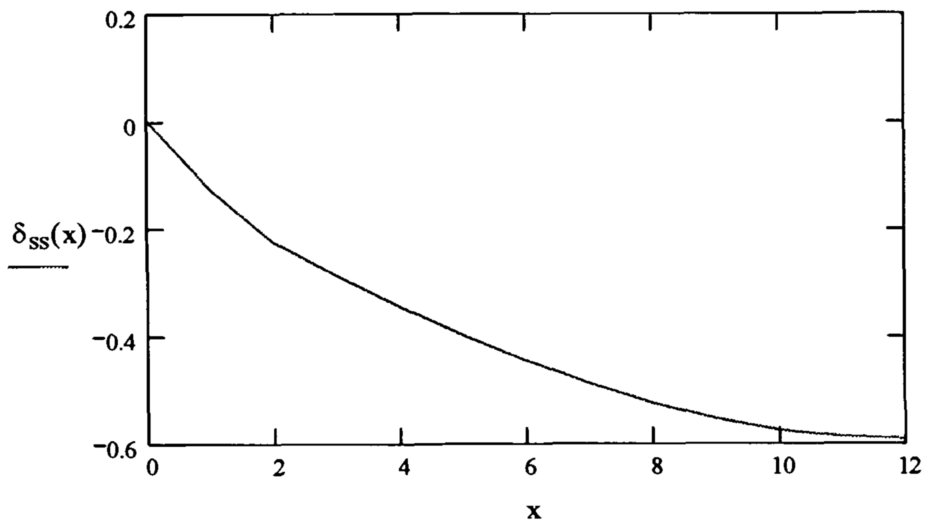

$$Q(x) := \frac{d}{dx}\delta_{ss}(x)$$

$$Q(0) = -0.131$$

$$\theta_{endtotal} := Q(0)$$

$$M_0 := -J \cdot \theta_{endtotal} \qquad M_0 = 1.046 \times 10^3$$

Integration Constants for End Moment Loading Solution:

$$C_{2m} := 0$$

$$C_{5m} := \frac{-M_0 \cdot L}{2 \cdot E \cdot I_3}$$

$$C_{3m} := C_{5m} + \frac{M_0 \cdot L_2}{E \cdot I_3} - \frac{M_0 \cdot L_2}{E \cdot I_2}$$

$$C_{1m} := C_{3m} + \frac{M_0 \cdot L_1}{E \cdot I_2} - \frac{M_0 \cdot L_1}{E \cdot I_1}$$

$$C_{4m} := C_{1m} \cdot L_1 + \frac{M_0 \cdot L_1^2}{2 \cdot E \cdot I_1} - \frac{M_0 \cdot L_1^2}{2 \cdot E \cdot I_2} - C_{3m} \cdot L_1$$

$$C_{6m} := C_{4m} + C_{3m} \cdot L_2 + \frac{M_0 \cdot L_2^2}{2 \cdot E \cdot I_2} - C_{5m} \cdot L_2 - \frac{M_0 \cdot L_2^2}{2 \cdot E \cdot I_3}$$

$$\delta_{1m}(x) := \frac{M_0 \cdot x^2}{2 \cdot E \cdot I_1} + C_{1m} \cdot x + C_{2m}$$

$$\delta_{2m}(x) := \frac{M_0 \cdot x^2}{2 \cdot E \cdot I_2} + C_{3m} \cdot x + C_{4m}$$

$$\delta_{3m}(x) := \frac{M_0 \cdot x^2}{2 \cdot E \cdot I_3} + C_{5m} \cdot x + C_{6m}$$

$$\delta_m(x) := \left| \begin{array}{l} -\delta_{1m}(x) \ \text{ if } \ x < L_1 \\ -\delta_{2m}(x) \ \text{ if } \ (x \ge L_1) \cdot (x < L_2) \\ -\delta_{3m}(x) \ \text{ if } \ x \ge L_2 \end{array} \right.$$

$$\delta_{total}(x) := \delta_{ss}(x) + \delta_m(x)$$

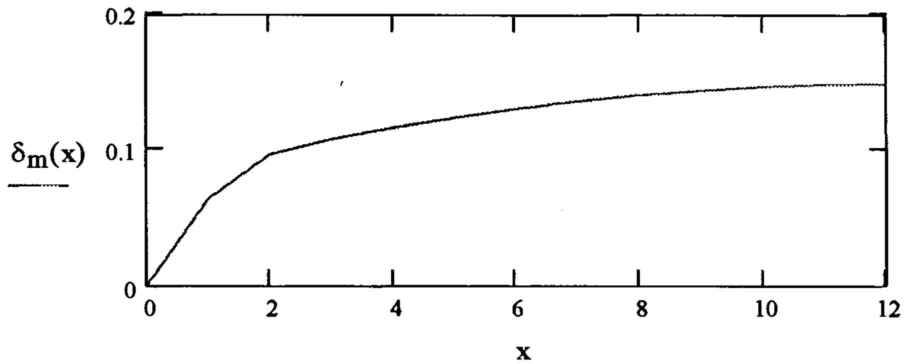

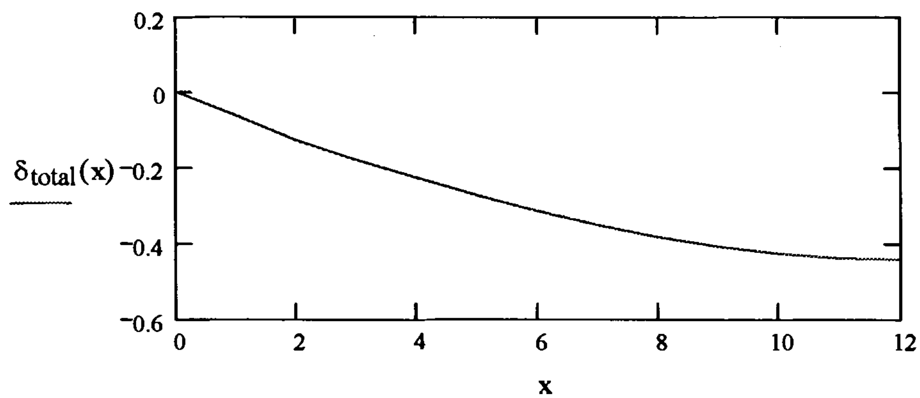

$$\delta_{sspris}(x) := \begin{vmatrix} \dfrac{P \cdot x}{6 \cdot E \cdot I_3} \cdot \left(3 \cdot L \cdot a - 3 \cdot a^2 - x^2\right) \text{ if } x \le a \\ \dfrac{P \cdot a}{6 \cdot E \cdot I_3} \cdot \left(3 \cdot L \cdot x - 3 \cdot x^2 - a^2\right) \text{ if } [x \le (L - a)] \cdot (x \ge a) \\ \dfrac{-P \cdot (x - L)}{6 \cdot E \cdot I_3} \cdot \left[3 \cdot L \cdot a - 3 \cdot a^2 - (x - L)^2\right] \text{ if } x \ge (L - a) \end{vmatrix}$$

$$\theta_{pris}(x) := \frac{d}{dx}\delta_{sspris}(x)$$

$M_{pris} := J \cdot \theta_{pris}(0)$

$\theta_{pris}(0) = -0.062$

$$\delta_{mpris}(x) := \frac{-M_{pris} \cdot x}{2 \cdot E \cdot I_3} \cdot (L - x)$$

$\theta_{endtotal} = -0.131$

$\delta_{mpris}(13) = 0.034$

$\delta_{totalpris}(x) := \delta_{sspris}(x) + \delta_{mpris}(x)$

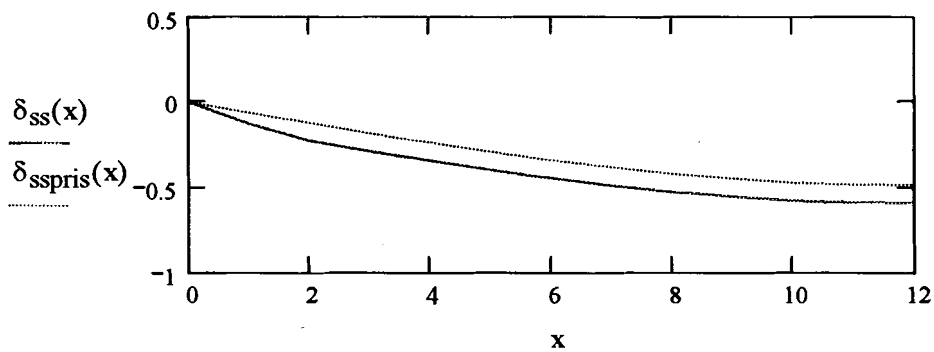

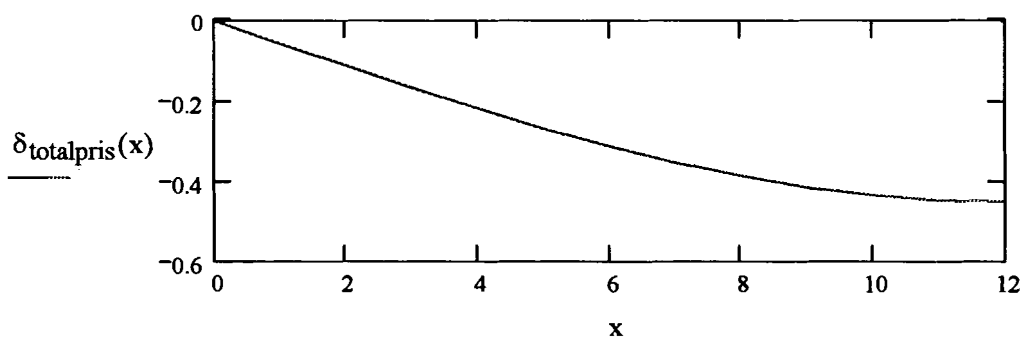

$M_1 := -J_1 \cdot \theta_{endtotal}$ $\quad$ $M_1 = 1.83 \times 10^3$

$C_{2m1} := 0$

$$C_{5m1} := \frac{-M_1 \cdot L}{2 \cdot E \cdot I_3}$$

$$C_{3m1} := C_{5m1} + \frac{M_1 \cdot L_2}{E \cdot I_3} - \frac{M_1 \cdot L_2}{E \cdot I_2}$$

$$C_{1m1} := C_{3m1} + \frac{M_1 \cdot L_1}{E \cdot I_2} - \frac{M_1 \cdot L_1}{E \cdot I_1}$$

$$C_{4m1} := C_{1m1} \cdot L_1 + \frac{M_1 \cdot L_1^2}{2 \cdot E \cdot I_1} - \frac{M_1 \cdot L_1^2}{2 \cdot E \cdot I_2} - C_{3m1} \cdot L_1$$

$$C_{6m1} := C_{4m1} + C_{3m1} \cdot L_2 + \frac{M_1 \cdot L_2^2}{2 \cdot E \cdot I_2} - C_{5m1} \cdot L_2 - \frac{M_1 \cdot L_2^2}{2 \cdot E \cdot I_3}$$

$$\delta_{1m1}(x) := \frac{M_1 \cdot x^2}{2 \cdot E \cdot I_1} + C_{1m1} \cdot x + C_{2m1}$$

$$\delta_{2m1}(x) := \frac{M_1 \cdot x^2}{2 \cdot E \cdot I_2} + C_{3m1} \cdot x + C_{4m1}$$

$$\delta_{3m1}(x) := \frac{M_1 \cdot x^2}{2 \cdot E \cdot I_3} + C_{5m1} \cdot x + C_{6m1}$$

$$\delta_{m1}(x) := \left| \begin{array}{l} -\delta_{1m1}(x) \ \text{ if } \ x < L_1 \\ -\delta_{2m1}(x) \ \text{ if } \ (x \ge L_1) \cdot (x < L_2) \\ -\delta_{3m1}(x) \ \text{ if } \ x \ge L_2 \end{array} \right.$$

$$\delta_{clamped}(x) := \delta_{m1}(x) + \delta_{ss}(x)$$

centerx := 12

centery := −0.44

taperx := 3.499

tapery := −0.17

$\delta_{totalpris}(13) = -0.447$

$\delta_{total}(13) = -0.439$

$\delta_{total}(4.2606) = -0.239$

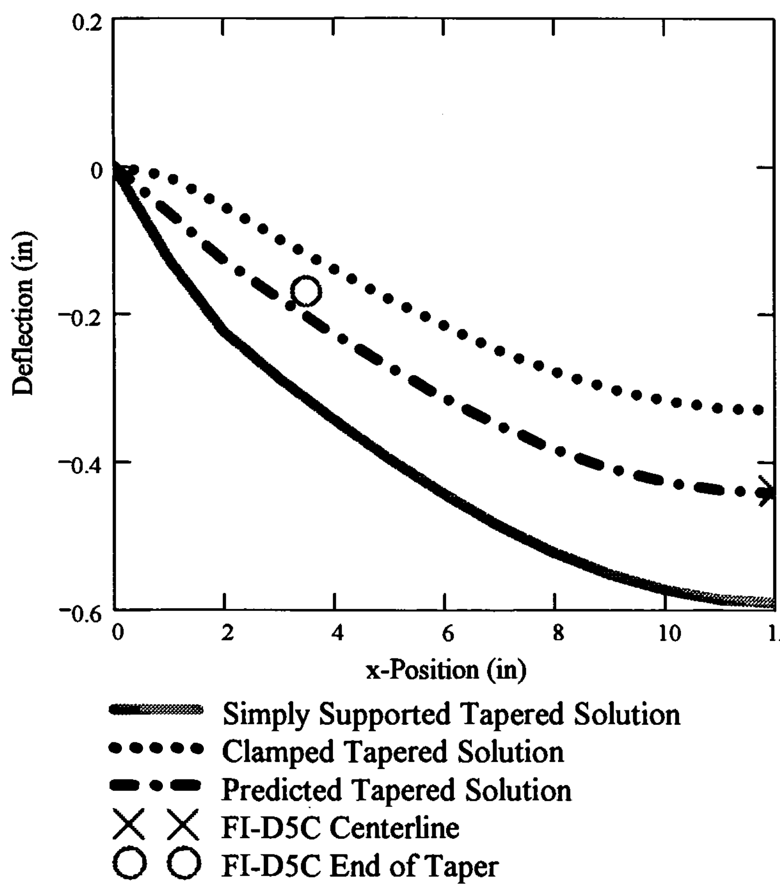

$$\%R := \frac{\delta_{ss}\left(\frac{L}{2}\right) - \delta_{total}\left(\frac{L}{2}\right)}{\delta_{ss}\left(\frac{L}{2}\right) - \delta_{clamped}\left(\frac{L}{2}\right)}$$

$\%R = 0.571$

Biography of the Author

Christopher Gary Malm was born in Caribou, Maine, on July 26, 1977. He attended Caribou High School from 1991-1995, and then went on to attend the University of Maine. While in college, he was a member of the American Society of Mechanical Engineers and Pi Tau Sigma, the mechanical engineering national honor society. He was also a member of the University of Maine Jazz Ensemble, Jazz Combo, Symphonic Band, Orchestra, and Pep Band. He graduated with a Bachelor's degree in Mechanical Engineering in May, 1999. Christopher is a candidate for the Master of Science degree in Mechanical Engineering from The University of Maine in May, 2001.